Characterisation of the molecular and functional changes exerted on human bone marrow mesenchymal stem cells by prostate cancer cells

A thesis submitted to the National University of Ireland in fulfilment of the requirements for the degree of:

Doctor of Philosophy

By

Sarah Ridge

Prostate Cancer Institute,

School of Medicine,

National University of Ireland, Galway

PhD Supervisors:

Sharon Glynn PhD, MPH

Prof. Frank Sullivan MB MRCPI FFR RCSI

February 2016

Index

Table of Contents

Acknowledgements

Most importantly I'd like to thank my parents – Deirdre and Martin Ridge – for their unwavering support throughout this long academic journey.

I would like to express my gratitude to my supervisors – Dr. Sharon Glynn and Prof. Frank Sullivan – for their guidance, patience and understanding.

I was very lucky to have colleagues that I now call friends so a big thank you to Amy, Ali, Carol, Ronan, Karen and Pablo for creating a supportive and entertaining work environment.

In any research facility it is important to have great tea buddies. I'd like to thank Steph and Martin for the chats, laughs and friendship.

I would like to acknowledge all those I have worked alongside over the past four years, Alessandro Natoni in particular, for their scientific expertise. Great ideas are born out of great discussion.

To my family and friends, I am deeply grateful for all the love and support. You were behind me every step of the way.

Declaration

I, Sarah Ridge, hereby declare that this is entirely my own work and that it has not been submitted as an exercise for the award of a degree at this or any other university.

Signed:_____ Date: _____

List of Figures

List of Tables

Abbreviations

αSMA	α smooth muscle actin
BMP	Bone morphogenetic protein
bFGFR	Basic fibroblast growth factor receptor
CAF	Cancer associated fibroblast
CCL	Chemokine ligand
CCR	Chemokine receptor
CD	Cluster of differentiation
CM	Conditioned media
COL1A1	Collagen type I alpha I
COL5A1	Collagen type V alpha I
DKK-1	Dickkopf WNT signalling pathway inhibitor
DMEM	Dulbecco's Modified Eagle Medium
DMSO	Dimethyl sulfoxide
D-PBS	Duulbecco's phosphate-buffered saline
EC	Endothelial cell
ECM	Extracellular matrix
EDTA	Ethylenediaminetetraacetic acid
EGF	Epidermal growth factor
EMMPRIN	Extracellular matrix metalloproteinase inducer
EMT	Epithelial-mesenchymal transition
FAP	Fibroblast activation protein
FGF-2	Fibroblast growth factor-2
FSP1	Fibroblast specific protein 1
GDF-15	Growth differentiation factor-15
GM-CSF	Granulocyte colony stimulating factor

HGF	Hepatocyte growth factor
HSC	Haematopoietic stem cell
IFNγ	Interferon γ
IGFBP-2	Insulin-like growth factor binding protein-2
IGF-1R	Insulin-like growth factor-1 receptor
IL	Interleukin
LPS	Lipopolysaccharide
MCP-1	Monocyte chemotactic protein
MIF	Macrophage migration inhibitory factor
MMP	Matrix metalloproteinase
MSC	Mesenchymal stem cell
NGF	Nerve growth factor receptor
NO	Nitric oxide
OPN	Osteopontin
PAI-1	Plasminogen activator inhibitor-1
PDGF	Platelet-derived growth factor
PDGFR	Platelet-derived growth factor receptor
PlGF	Placental growth factor
PSA	Prostate specific antigen
RANKL	Receptor activator of nuclear factor kappa-B ligand
RTCA	Real-time Cell Analyse
SASP	Senescence associated secretory phenotype
SDF-1α	Stromal cell-derived factor 1α
SDS	Sodium dodecyl sulphate
sFlt-1	Soluble fms-like tyrosine kinase-1

SHH	Sonic hedghog
STAT5	Signal transducer and activator of transcription 5
TAM	Tumour associated macrophages
TGFβ	Transforming growth factor β
TIMP-1	TIMP metallopeptidase-1
TLR	Toll-like receptor
TN-C	Tenascin-C
TNF-α	Tumour necrosis factor-α
TRAIL	TNF-related apoptosis-inducing ligand
uPA	Urokinase-type plasminogen activator
uPAR	Urokinase-type plasminogen activator receptor
VEGF	Vascular endothelial growth factor
XIAP	X-linked inhibitor of apoptosis protein

Abstract

Mesenchymal stem cells (MSCs) are a heterogenous population of multipotent cells that are capable of differentiating into osteocytes, chondrocytes and adipocytes. MSCs reside in various areas such as the bone marrow, fat and dental pulp. Recently, MSCs have been found to home to the tumour site and engraft in the tumour stroma. However, it is not yet known whether they have a tumour promoting or suppressive function. We investigated the interaction between prostate cancer cell lines - 22Rv1, DU145 and PC3 - and bone marrow derived MSCs. MSCs were 'educated' for extended periods in prostate cancer cell conditioned media and analysed for molecular and functional phenotypic changes. MSCs conditioned with the bone metastatic cell line, PC3, were found to be the most responsive with a secretory profile rich in pro-inflammatory cytokines. PC3 educated MSCs secreted increased MCP-1, osteopontin, IL-8 and FGF-2 and decreased sFlt-1 in comparison to untreated MSCs, which was sustained following prolonged growth in complete medium post-conditioning. PC3 educated MSCs are larger in size and have a reduced migration and invasion capacity that is dependent on exposure to PC3 conditioned medium. Vimentin and αSMA expression is decreased in PC3 educated MSCs in comparison to untreated MSCs, however they do retain the capacity to differentiate to osteocytes and adipocytes. Interestingly, the migration of PC3 cells was increased towards PC3 educated MSCs in comparison to untreated MSCs and of the three cells lines examined (22Rv1, DU145 and PC3), the effect was specific only to PC3 cells. Taken together, MSCs develop an altered phenotype in response to PC3 conditioned medium which results in increased secretion of pro-inflammatory cytokines, modified functional activity and the chemoattraction of PC3 cells.

Chapter 1

General Introduction

1.1 Prostate Cancer

Prostate cancer is the fourth most common cancer worldwide and the second most common cancer diagnosed in men. An estimated 307,000 deaths were recorded globally in 2012, with 519 occurring in Ireland (NCRI, 2014, IARC, 2012). Incidence rates are known to be higher in Western and Northern Europe, North America and Oceania (IARC, 2012). This increased detection rate is at least partly due to greater use of the biomarker prostate specific antigen (PSA) and patient biopsies, though data collected from migrant populations to western countries also suggest environmental and lifestyle factors play a role (IARC, 2012). Although use of PSA as a biomarker for prostate cancer has led to over-diagnosis and over-treatment, the screening is associated with reduced mortality in men who would not otherwise be screened (Attard et al., 2015, Schroder et al., 2012). Worldwide, 75% of cases are recorded in men over the age of 65 therefore PSA screening typically begins with men over the age of 50 (Cook et al., 1969). Depending on tumour grade and stage of invasiveness, patients may not choose immediate treatment and partake in active surveillance, or they may be recommended radiation therapy, androgen deprivation therapy or a radical prostatectomy (Attard et al., 2015).

1.2 Prostate Cancer Bone Metastasis

While prostate cancer can metastasise to tissues such as the lung, liver, pleura and adrenals, the most frequent site of metastasis is the bone (Bubendorf et al., 2000). Patients suffering from prostate cancer, when treated, have a 5-year survival rate of >99% in the USA (Siegel et al., 2015) and >90% in Ireland (NCRI, 2014). However, when the cancer advances and metastasises to the bone the 5-year survival rate drops to around 25% in the USA (Coleman, 1997).

What makes the bone microenvironment favourable to the metastasis and proliferation of prostate cancer cells however, is still largely unknown. The likelihood of a cancer cell reaching and invading the bone depends on its ability to pass through the endothelium, migrate through the circulatory system and extravasate from the blood vessel to the metastatic site (Clarke et al., 2009).

1.3 Molecular Mechanisms of Bone Metastasis

Most cancer cells in a primary tumour do not metastasise but can however be reprogrammed to gain metastatic function. During this process the cell must downregulate its epithelial characteristics by reducing the expression of cell-cell and cell-matrix adhesion molecules and gain mesenchymal properties such as motility and the capacity to breakdown the extracellular matrix (ECM) (Behrens et al., 1989, Liotta, 1986) (figure 1.1). This process is known as the epithelial-to-mesenchymal transition (EMT).

1.3.1 Loss of Cell-to-cell Adhesion

Cell-to-cell contact in prostate cancer cells occurs through the binding of adhesion molecules such as cadherins and selectins. The role of E-cadherin in cell-to-cell adhesion and its involvement in the transition of a resident tumour cell to an invasive cell type has been well studied (Behrens et al., 1992, Birchmeier and Behrens, 1994, Bussemakers et al., 1992, Perl et al., 1998). E-cadherin is a transmembrane glycoprotein that binds catenins intracellularly allowing it to bind cadherins on neighbouring cells. Changes in the binding of E-cadherin to β-catenin or in the expression levels of either component can lead to a loss of cellular adhesion, a crucial step in the EMT (Takeichi, 1991, Bussemakers et al., 1992, Bryden et al., 1999, Birchmeier and Behrens, 1994). A study by Bryden and colleagues suggests that the level of E-cadherin is reflective of local tumour grade, where well differentiated tumours expressed the highest level of E-cadherin (Bryden et al., 1999).

1.3.2 ECM Degradation

The capacity of prostate cancer cells to migrate and enter the bone marrow is dependent on the cellular secretion of enzymes that degrade the ECM. Matrix metalloproteinases (MMPs) and serine proteinases, particularly urokinase-type plasminogen activator (uPA), play a role in the breakdown of the ECM (Hart et al., 2002). MMPs are zinc-binding proenzymes, regulated by tissue inhibitor of metalloproteinases-1 (TIMP-1). MMP-9 is activated by MMP-2 and high expression of both molecules, coupled with low expression of TIMP-1, has been associated with

metastatic prostate cancer (Morgia et al., 2005, Brehmer et al., 2003). Prostate cancer cell secretion of MMPs is an important step in the metastatic process both at the endothelium and at entry to the bone marrow stroma (Montague et al., 2004, Hart et al., 2002).

uPA is a serine protease that binds to its receptor resulting in the conversion of plasminogen to plasmin, which is involved in the activation of pro-collagenases, an important factor in the degradation of the ECM (Hart et al., 2002). The molecule is also involved in the activation of MMPs and it has been shown that by decreasing the expression of uPA, the level of bone degradation due to prostate cancer metastasis is reduced (Festuccia et al., 1998, Dong et al., 2008).

1.3.3 Passage through the Endothelium

Metastatic cells can migrate via the lymphatic and vascular systems. Metastatic prostate cancer cells must pass through the endothelium to enter the blood vessel by intravasation at the primary tumour site and exit by extravasation at the secondary metastatic site. Passage through the endothelium requires interaction with and adherence to the endothelium in what is referred to as a 'dock and lock' mechanism (Honn and Tang, 1992). Key proteins involved in the binding of prostate cancer cells to endothelial cells include P-selectin, E-selectin and integrins $\alpha v\beta 3$, $\alpha_5\beta_1$ and $\alpha_3\beta_1$ (Romanov and Goligorsky, 1999, Tang et al., 1993).

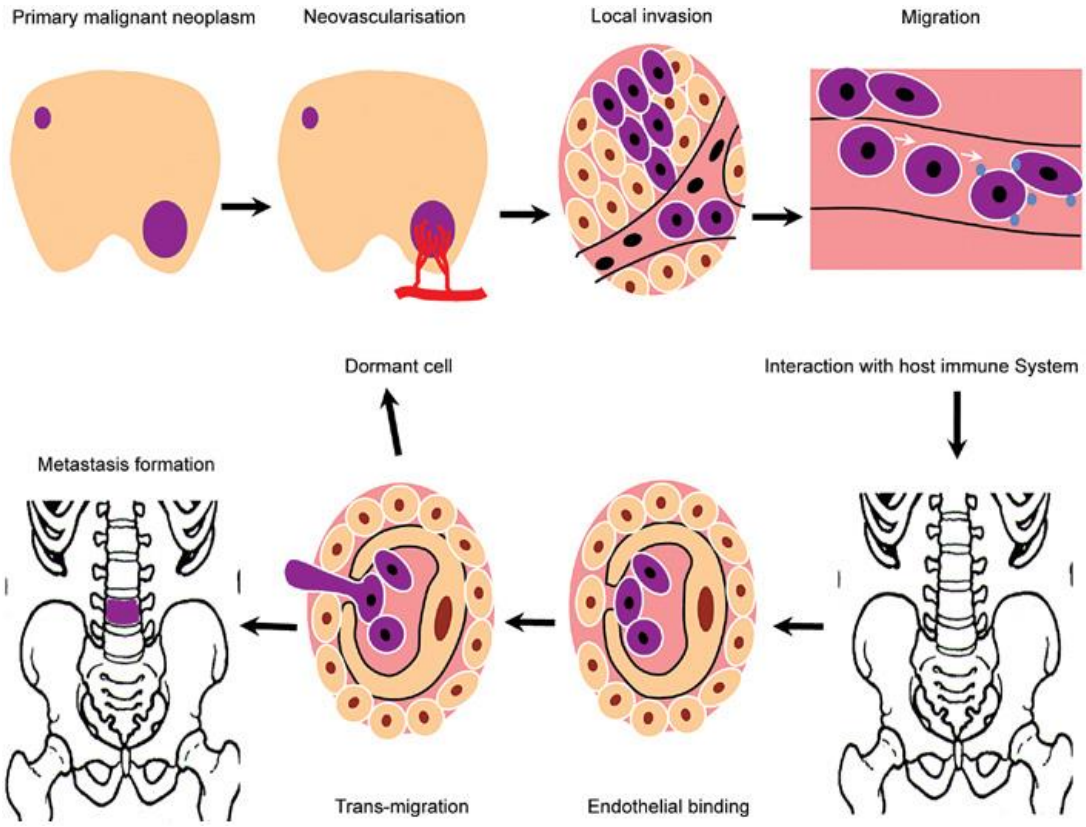

Figure 1.1. Metastasis to the Bone. Metastasis to the bone from the primary tumour site occurs by a series of steps including detachment of the tumour cell from adjacent cells and the cell matrix, intravasation into the vascular system, immune system evasion, migration, extravasation through the endothelium and trans-migration into the site of metastasis. Image taken from Clarke *et al.* 2009 (Clarke et al., 2009)

1.3.4 Homing of Metastatic Cells to the Bone through Chemotaxis

The 'seed and soil' hypothesis was originally described by Stephen Paget in 1889 whereby cancer cells act as the 'seed' and the metastatic site, the 'soil' (Paget, 1989). Subsequent research has further developed this theory which suggests that the secondary site provides a microenvironment preferential and complementary to certain tumour cells. Another aspect to this theory is that chemoattractant factors are released from the secondary microenvironment that bind to corresponding receptors on the circulating tumour cells allowing the cells to home towards that specific organ.

Metastatic prostate cancer cells are attracted to the bone by factors, namely chemokines, which are released from the bone marrow. The chemokine, stromal

derived factor-1 (SDF-1), is expressed by endothelial cells at the bone marrow, which binds to its receptor, CXCR4, which is expressed on prostate cancer cells. Both factors have been shown to be increased in prostate cancer bone metastasis, where the more aggressive the metastasis, the more CXCR4 is expressed (Taichman et al., 2002, Sun et al., 2003).

More recently, other factors have been shown to attract prostate cancer cells to the bone including monocyte chemoattractant protein 1 (MCP-1), osteonectin and osteopontin (Loberg et al., 2006, Jacob et al., 1999, Thalmann et al., 1999, Angelucci et al., 2002). MCP-1 is a member of the C-C chemokine family, originally found to be a potent chemoattractant of monocytes to inflammatory sites (Deshmane et al., 2009). Recent studies have found that MCP-1 is expressed within the bone marrow microenvironment and promotes the migration and invasion of prostate cancer cells (Loberg et al., 2006, Lu et al., 2006).

1.3.5 Osteolytic and Osteoblastic Bone Metastasis

Bone remodelling is a process that occurs continuously in order to maintain the structure and function of the skeleton. This is achieved by bone resorption and formation, with osteoclasts, osteocytes and osteoblasts being the principal cells involved in these two processes. Breast cancer bone metastasis is considered to be predominantly osteolytic and prostate cancer - osteoblastic, although, both bone resorption and formation are increased in patients with prostate cancer bone metastasis in comparison to healthy patients and patients with benign prostatic hyperplasia (Garnero et al., 2000).

Osteoblasts are derived from mesenchymal stem cells (MSCs) and play a major role in bone formation through the synthesis of bone matrix and further differentiation to osteocytes (Pittenger et al., 1999). Osteoclasts are multinucleated cells differentiated from monocytes following the binding of their receptor RANK with NF-κB ligand (RANKL) on the osteoblast cell surface (Suda et al., 1999). Osteoclasts break down the bone tissue by secreting acid and lysosomes containing acid phosphatase along with their binding to $\alpha_v\beta_3$, $\alpha_v\beta_5$ and $\alpha_v\beta_1$ integrins on the membrane surface (Suda et al., 1999). Therefore, the production and function of osteoblasts, osteocytes

and osteoclasts are linked and disruption of any of these processes, as occurs in bone metastatic cancer, leads to disruption in bone homeostasis.

To investigate whether osteoclast activity creates a hospitable environment for invasive breast cancer cells, studies have used bisphosphonates to inhibit bone resorption (Mundy and Yoneda, 1998). Bisphosphonates inhibit the function of osteoclasts and have been found to reduce the incidence of metastases and rate of death in breast cancer patients (Diel et al., 1998).

Osteolytic activity is also elevated in osteoblastic metastasis and so bisphosphonates have also been used to treat prostate cancer patients and the treatment was successful in reducing skeletal related events and bone pain (Saad et al., 2002). Endothelin-1 is a protein produced by breast and prostate cancer cells that binds to the endothelin-A receptor, expressed by osteoblasts. This interaction stimulates an increase in bone formation and osteoblastic metastases. Treatment with an endothelin-A receptor antagonist was found to decrease bone metastases and tumour burden in mice (Yin et al., 2003, Guise et al., 2003). Although these are not yet curative therapies, they do confirm the significance of cancer cell/bone marrow cell cross-talk to achieve an optimal environment for tumour growth.

1.4 The Tumour Microenvironment

It is now understood that tumour cells do not act alone. Cancer cells interact with their surrounding stroma and these interactions lead to an ‘activated state’ resulting in increased release of pro-inflammatory cytokines and growth factors (Pietras and Ostman, 2010). The tumour is in a chronic state of inflammation and has been described as a ‘wound that never heals’ (Dvorak, 2015). This inflammatory state drives the recruitment of responsive cell types such as macrophages, myeloid derived suppressor cells and MSCs (Pollard, 2004, Hall et al., 2007, Young and Wright, 1992). Cross-talk between cancer cells and cells of the surrounding stroma promotes tumour progression and creates a dynamic ECM, favourable for the invasive tumour cell (Sato et al., 2004, Sung et al., 2008).

Tumour infiltrating macrophages can become activated by the stromal microenvironment and are referred to as tumour associated macrophages (TAMs) (Mantovani et al., 2002, Sica et al., 2002). Depending on the stimuli, macrophages can be polarised toward an M1 or M2 phenotype. The M1 phenotype can be activated by interferon gamma (IFN-γ) and lipopolysaccharides and have been shown to have cytotoxic effects on tumour cells. In contrast M2 macrophages are activated by IL-4, IL-13 and IL-10, promote wound healing and angiogenesis and are phenotypically similar to TAMs (Allavena et al., 2008, Sica et al., 2006, Mantovani et al., 2002, Solinas et al., 2009).

The tumour stroma varies between each cancer type and the heterogenous nature of the tumour makes it complicated to study. It is important to develop an understanding of what drives non-cancerous cells toward an activated state, what that activated state is and what it subsequently means for tumour cell progression.

1.5 Mesenchymal Stem Cells

MSCs are multipotent cells originally found to have the capacity to differentiate into osteoblasts, chondrocytes and adipocytes (Pittenger et al., 1999). They are generally characterised by their tri-lineage differentiation capacity and by surface markers CD73, CD105 and CD90 (Dominici et al., 2006). They can be sourced from the bone marrow, adipose tissue and dental pulp (Gronthos et al., 2000, Huang et al., 2002, Friedenstein et al., 1970, Pittenger et al., 1999). They are also found in circulation and are known to home to inflammatory sites (Chamberlain et al., 2007). Due to their capacity to home to injured tissue, research has suggested a reparative function for MSCs in multiple tissues including the lung (Ortiz et al., 2003), liver (Sato et al., 2005), brain (Ji et al., 2004) and heart (Wu et al., 2003). MSCs can evade the immune system (Ryan et al., 2005) and are also known to have immunomodulatory effects (Fouillard et al., 2003, Horwitz et al., 2002, Pereira et al., 1995).

MSCs reside in the bone marrow stroma alongside haematopoietic stem cells (HSCs), osteoblasts, osteoclasts, adipocytes, endothelial cells (ECs) and monocytes (Serbina and Pamer, 2006, Chitteti et al., 2010). MSCs may play a supportive role for HSCs and

have previously been used to enhance long-term HSC engraftment in human transplantation (Almeida-Porada et al., 2000, Maitra et al., 2004).

Knowledge of these characteristics as well as their differentiation capacity has caused excitement in the field of regenerative medicine and use of MSCs has potential for therapeutics in a range of fields such as cardiology, immunology and neurology. However, in the field of cancer research recent studies suggest that MSC activity may contribute to poorer outcomes (Ame-Thomas et al., 2007, Kansy et al., 2014, Karnoub et al., 2007, Prantl et al., 2010).

1.5.1 Mesenchymal Stem Cell Nomenclature and Potency

A subpopulation of bone marrow cells was initially discovered by Friedenstein and colleagues that had an osteogenic differentiation capacity (Friedenstein et al., 1970). The cells were subsequently found to be clonal and plastic adherent (Friedenstein et al., 1970) and later studies by Pittenger *et al.* demonstrated their multilineage differentiation capacity (Pittenger et al., 1999). However, the non-skeletal differentiation capacity of these cells has not definitively been proven *in vivo* which has led to controversy regarding usage of the term 'mesenchymal stem cells'. Moreover, MSCs are a heterogenous population of cells containing subpopulations with differing differentiation capacities (Horwitz et al., 2005). Alternative terms have been used such as 'multipotent mesenchymal stromal cells' that keep the acronym 'MSC' to maintain a consistency within the literature (Horwitz et al., 2005).

MSCs were found to express embryonic stem cell or pluripotency markers which differed depending on the source. Bone marrow derived MSCs were found to express Oct4, Nanog, alkaline phosphatase and SSEA-4; adipose and dermis derived MSCs were found to express Oct4, Nanog, SOX2, alkaline phosphatase and SSEA-4; while heart MSCs were found to express Oct4, Nanog, SOX2 and SSEA-4. The full differentiation potential of MSCs has not yet been elucidated; however more recent developments have shown a wider range in differentiation potential (aside from a capacity to differentiate into osteocytes, adipocytes and chondrocytes) such as myocyte and neuron induction (Wakitani et al., 1995, Kopen et al., 1999).

1.6 Mesenchymal Stem Cells and Cancer

In recent studies, it has been shown that MSCs can also home to tumour sites and contribute to tumour growth and progression (Prantl et al., 2010, Suzuki et al., 2011, Karnoub et al., 2007, Kucerova et al., 2010). Analysis from human prostatectomies showed that MSCs represented 0.01-1.1% total cells present in the tumour (Brennen et al., 2013). MSCs have been found to increase the metastatic potential of tumour cells by promoting their motility and invasiveness as well as having a role in the creation of a metastatic niche at the secondary site (Karnoub et al., 2007, Nabha et al., 2008, Duda et al., 2010, Corcoran et al., 2008).

As the tumour microenvironment exists as a heterogenous population of cells and each cancer type has its own unique characteristics, it is difficult to establish a universal role for MSCs in tumour development. Research shows conflicting results as to whether MSCs are tumour promoting or suppressing (Klopp et al., 2011). This has led to investigation into whether exposure to tumour cells can alter the MSCs into an activated state with the possibility of a dual role similar to macrophages (Waterman et al., 2010, Waterman et al., 2012).

1.6.1 Mesenchymal Stem Cell Chemotaxis to the Tumour

Ex vivo expanded MSCs were shown to home to gliomas and ovarian and breast tumours using magnetic resonance imaging and bioluminescent imaging (Wu et al., 2008, Kidd et al., 2009). The mechanisms by which MSCs migrate toward the tumour are not yet fully understood, however the interaction between cytokines and chemokines secreted by the tumour and the corresponding MSC surface receptors is currently being explored.

Several studies have attempted to characterise MSCs based on their chemokine receptor expression which could give insight into their chemoattraction towards pro-inflammatory tissues (Sordi et al., 2005, Von Luttichau et al., 2005, Wynn et al., 2004, Honczarenko et al., 2006). Von Lüttichau and colleagues showed the functional expression of chemokine receptors CCR1, CCR4, CCR7, CCR10, and CXCR5 but not CXCR4 on human bone marrow derived MSCs (Von Luttichau et al., 2005), while

Wynn and colleagues found that a small subset of MSCs expressed CXCR4 (Wynn et al., 2004). The interaction between CXCR4 and its receptor ligand, SDF-1α, is known to mediate the migration of HSCs, endothelial progenitor cells and primordial germ cells (Levesque et al., 2003, Petit et al., 2002, Yamaguchi et al., 2003, Doitsidou et al., 2002). The interaction between CXCR4 and SDF-1α in MSC chemotaxis to the tumour was thus considered. Many studies have shown that MSCs migrate toward SDF-1α in a dose dependent manner (Ringe et al., 2007, Sordi et al., 2005, Shi et al., 2007, Stich et al., 2009). Additionally, an upregulation of SDF-1α was found in rat bone marrow derived MSCs in response to colorectal cancer CM, and the MSCs were found to migrate *in vitro* toward the tumour cells in an SDF-1α dependent manner (Menon et al., 2007).

MCP-1 is expressed within the tumour, including the primary prostate cancer tumour (Lu et al., 2006, Dwyer et al., 2007). Although not all studies are in agreement (Ringe et al., 2007), there is a growing body of evidence to suggest that MCP-1 is a key player in the chemotaxis of MSCs to the tumour (Dwyer et al., 2007, Xu et al., 2010, Zhang et al., 2009). Loberg and colleagues found that MCP-1 is a potent chemoattractant for prostate cancer cells in a dose dependent manner which resulted in the activation of the PI3-kinase/Akt signalling pathway (Loberg et al., 2006). MCP-1 has also been implicated in the promotion of invasion and proliferation of prostate cancer cells (Loberg et al., 2007b, Lu et al., 2006).

1.6.2 Mesenchymal Stem Cells at the Primary Tumour Site

MSCs have been implicated in the promotion of tumour growth in numerous cancer types such as follicular lymphoma (Ame-Thomas et al., 2007), head and neck carcinoma (Kansy et al., 2014), glioma (Hossain et al., 2015), breast (Karnoub et al., 2007), gastric (Li et al., 2015), colon (Zhu et al., 2006) and prostate cancer (Prantl et al., 2010).

Karnoub and colleagues showed that co-injection of bone marrow MSCs with one of four breast cancer cell lines (MCF7) led to accelerated tumour growth, yet, co-injection with all cell lines (MDA-MB-231, HMLR, MDA-MB-435 and MCF7) led to increased metastasis (Karnoub et al., 2007). Similarly, in a more recent study it was

found that co-injection of bone marrow MSCs with the triple negative inflammatory breast cancer cell line, SUM149, resulted in inhibited primary tumour growth but increased invasion and metastasis (Lacerda et al., 2015). These findings indicate a role for MSCs at the tumour site in the promotion of metastasis possibly through the induction of EMT in primary tumour cells.

An increase in tumour growth was also found in mice following co-injection of adipose tissue derived MSCs with the prostate cancer cell line MDA-PCa-118b (Prantl et al., 2010). Bone marrow MSCs were also found to stimulate the proliferation, migration and invasion of the prostate cancer cell line PC3. This effect was inhibited by blocking transforming growth factor β (TGFβ) (Ye et al., 2012). In a similar study, TGFβ silencing in adipose tissue derived MSCs reduced the adhesion capacity of PC3 cells (Lee et al., 2013).

Some research groups have investigated the tumour promoting function of MSCs isolated from the tumour, arguably a more realistic approach to understanding the role of MSCs within the tumour microenvironment. Co-injection of MSCs isolated from head and neck carcinoma (Kim et al., 2013), gastric cancer (Kansy et al., 2014) and gliomas (Hossain et al., 2015) with tumour cells into mouse models resulted in an increase in tumour growth and progression. Interestingly, Li and colleagues found that MSCs isolated from gastric cancer stimulated increased proliferation and migration of gastric cancer cell lines (BGC-823 and MKN-28) in comparison to bone marrow derived MSCs or MSCs isolated from non-cancerous adjacent tissue. They also found that they secreted more vascular endothelial growth factor (VEGF), macrophage inflammatory protein-2, TGF-β1, IL-6, and IL-8 while blockade of IL-8 attenuated the tumour promoting function of the gastric cancer MSCs (Li et al., 2015).

1.6.3 Angiogenesis and Vasculogenesis

MSCs can differentiate into pericytes, ECs and cancer associated fibroblasts (CAFs) (Rajantie et al., 2004, Al-Khaldi et al., 2003, Mishra et al., 2008, Spaeth et al., 2009). ECs line the inner vessel wall and pericytes surround the EC layer, and it is thus considered that MSC influx may contribute to the increase in angiogenesis noted at the tumour site (Rajantie et al., 2004, Al-Khaldi et al., 2003). Human bone marrow

MSCs were shown to have the capacity to differentiate into cells expressing endothelial-specific markers - kinase insert domain receptor and fms-like tyrosine kinase-1 (FLT-1) in an *in vitro* study using VEGF in the conditioning medium (Oswald et al., 2004). The differentiation of adipose tissue-derived MSCs to ECs was found at the site of the primary tumour in prostate cancer along with tumour growth (Prantl et al., 2010). In contrast, Rajantie and colleagues found that, at both VEGF and tumour-induced blood vessels, a sub-population of bone marrow stem cells differentiated into vascular mural periendothelial cells that were morphologically indistinguishable to pericytes and engrafted in close contact with ECs, however, bone marrow cell derived ECs were not detected (Rajantie et al., 2004).

Conversely, undifferentiated MSCs may support the tumour vasculature by the release of angiogenic factors. MSCs are known to release proangiogenic factors such as VEGF, platelet derived growth factor (PDGF), IL-6, fibroblast growth factor 2 (FGF-2) and FGF-7 (Kinnaird et al., 2004, Menon et al., 2007, Suzuki et al., 2011). These factors can also increase the proliferation and migration of ECs, leading to further promotion of vasculogenesis and angiogenesis (Kinnaird et al., 2004).

1.6.4 Cytotoxic Resistance

One of the major difficulties in the treatment of cancer is the development of drug resistance. Sensitivity to chemotherapy is decreased as a result of genetic mutations within the cancer cells as well as changes in the gene expression of drug targets. There is now evidence to support that the tumour microenvironment could provide protective mechanisms against cytoxicity (Baguley, 2010, Tomida and Tsuruo, 1999, Meads et al., 2008, Taylor et al., 2000).

In research by Straussman and colleagues an extensive range of cancer cells including head and neck carcinoma, melanoma, breast, pancreatic and colorectal cancer cells were co-cultured with 23 different stromal cell lines. Cytotoxic resistance was found to be frequent in co-culture with stromal cells and particularly to targeted agents (Straussman et al., 2012). Bone marrow MSCs were found to cause increased chemoresistance in leukemia cells. Co-culture of the two cell types resulted in decreased apoptosis and an increase in the expression of c-Myc, a finding only

reproducible when cells were in direct co-culture suggesting cell-to-cell contact as key to the protective mechanism (Ito et al., 2015, Xia et al., 2015). Interestingly, inhibition of SDF-1α/CXCR4 interactions decreased the MSC induced cytotoxic resistance of leukemia cells (Zeng et al., 2009).

1.6.5 Role in Immunomodulation

MSCs have immunosuppressive properties, activation of which would be advantageous to the growing tumour. MSCs inhibit T-cell and B-cell proliferation (Di Nicola et al., 2002, Krampera et al., 2003, Corcione et al., 2006, Bocelli-Tyndall et al., 2007), induce the apoptosis of activated T-cells (Plumas et al., 2005) and have been found to inhibit dendritic cell differentiation and function (Zhang et al., 2004, Nauta et al., 2006).

Although not extensively studied, there is evidence to suggest that MSCs have an immunosuppressive function within the tumour. A study by Djouad and colleagues found that subcutaneous co-injection of B16 melanoma cells with murine bone marrow MSCs into an allogeneic murine melanoma tumour model lead to tumour growth, whereas when the B16 melanoma cells were rejected when injected alone (Djouad et al., 2003).

MSCs have been shown to produce nitric oxide (NO) in the presence of T-cells, which in turn, inhibits T-cell proliferation through suppression of STAT5 phosphorylation (Sato et al., 2007, Ren et al., 2008). It was found that co-injection of the melanoma cell line, B16F0, with MSCs derived from p53 deficient mice formed larger tumours than when using MSCs from a wild-type mouse. Accordingly, the p53 deficient MSCs expressed more inducible nitric oxide synthase and were found to have a greater immunosuppressive capacity than their counterparts through the suppression of T-cell proliferation (Huang et al., 2014).

1.6.6 Role in Tumour Suppression

In contrast to the research described above there is evidence to suggest that MSCs can also have an inhibitory effect on tumour growth. Suppression of tumour growth has been noted in breast cancer (Sun et al., 2009), Kaposi's sarcoma (Khakoo et al.,

2006), hepatoma (Qiao et al., 2008) and melanoma (Otsu et al., 2009) models. MSCs derived from the umbilical cord and adipose tissue were implanted into a breast cancer metastasis mouse model and found to inhibit metastasis to the lung and reduce tumour growth through PARP and caspase-3 cleavage, which could in turn induce apoptosis (Sun et al., 2009). However, MSCs derived from the bone marrow, adipose tissue and dental pulp are not functionally identical (Kern et al., 2006, Huang et al., 2009), therefore the studies using MSCs derived from other sources may not be replicated using bone marrow derived MSCs (Lee et al., 2004, Wagner et al., 2005).

Otsu et al. showed that bone marrow MSCs had a cytotoxic effect on the tumour in a melanoma mouse model through the release of reactive oxygen species when in contact with ECs present at the capillaries. This induced apoptosis of the ECs and reduced tumour growth. However, the cytotoxic effect of the MSC was only observed when implanted at high concentrations. MSCs seeded onto EC derived capillaries in matrigel evoked a cytotoxic effect at a EC:MSC ratio of 1:1 or 1:3. Cytotoxicity decreased when the MSC number was reduced by an order of magnitude (Otsu et al., 2009) and given that in prostate cancer MSCs were only found to represent 0.01-1.1% of the tumour experiments using a high ratio of MSCs may not be reflective of the tumour microenvironment *in vivo* (Brennen et al., 2013). These results may explain the difference in outcome observed in studies showing tumour growth promotion by MSCs. Further investigation on the effect of dose on efficacy is warranted for any conclusions to be made, nonetheless, when examining the impact of MSC on tumour biology, the source and specific ratios of MSC to tumour cells reflective of the natural tumour environment is an important consideration.

Another explanation for the contrasting results is that like macrophages there is a polarisation of MSCs in response to secreted factors from the tumour that either drives the cells toward a tumour promoting or suppressive function. Waterman and colleagues proposed a polarisation of MSCs based on downstream toll-like receptor (TLR) signalling. They found functional differences between MSCs stimulated by either TLR4 or TLR3 and classified them as MSC1 and MSC2 respectively (Waterman et al., 2010). MSC1 cells were found to have an anti-tumour effect while MSC2 cells promoted tumour growth and metastasis (Waterman et al., 2012).

1.7 Mesenchymal Stem Cells and Metastasis

MSCs interact with cancer cells at multiple stages of cancer progression. At the primary tumour MSCs have been shown to drive tumour cells toward an invasive, pro-metastatic state. Human MSCs injected alone into mice with mammary carcinoma xenografts resulted in a 42% occurrence of metastatic lesions, compared with 17% in the control treated mice (Albarenque et al., 2011). Similarly, MSCs injected systemically into mice were found to migrate to the stroma of primary colon tumours as well as metastatic liver tumours (Shinagawa et al., 2010). Furthermore, co-culture of human bone marrow MSCs with MDA-MB-231 or MDA-MB-435 breast cancer cell lines 48 hours preceding injection resulted in enhanced metastasis in a mouse orthotopic implantation model, whereas the MSCs had no effect on metastasis without prior co-culture (Chaturvedi et al., 2013).

Tracking of MSCs using magnetic resonance imaging in a mouse xenograft model has shown that MSCs were more likely to home to the lung metastatic site than to the primary tumour (Loebinger et al., 2009b). A study suggests that tumour cells do not always leave the primary site as single cells but also as 'heterotypic tumour fragments' consisting of the metastatic cancer cells along with tumour stromal cells (Duda et al., 2010). These clusters of cells were found to migrate to the metastatic site and promote tumour growth. Moreover, CAFs were found to migrate from the primary tumour to the lung metastatic site in mice (Duda et al., 2010).

In a study by Klopp *et al.*, it was found that irradiation at 2 Gy could increase the recruitment of murine MSCs in a syngeneic 4T1 murine breast cancer model. The level of MSC engraftment was found to be 34% in tumours 48 hours post-irradiation than in the contralateral unirradiated limb (Klopp et al., 2007). Circulating MSCs have also been shown to migrate to prostate tumour sites but not to the normal prostate and co-culture of the MSCs with prostate cancer cells led to enhanced prostate cancer stem cell populations through the upregulation of CCL5 expression in the MSCs and prostate cancer cells and subsequent downregulation of androgen receptor signalling (Luo et al., 2014). Moreover, circulating $CD45^-$ fibroblast-like cells were found to be present in 58% of men with metastatic prostate cancer but not in

any men with localised prostate cancer or no identified cancer (Jones et al., 2013). An increased presence of circulating fibroblasts or MSCs could therefore provide more prognostic information on the development of prostate cancer.

Additionally, a study by Kaplan and colleagues using mouse models found that VEGFR1 expressing bone marrow derived cells migrated to and formed clusters in pre-metastatic sites before the arrival of tumour cells. Interestingly, blocking VEGFR1 function prevented cluster formation and metastasis (Kaplan et al., 2005). These studies indicate a potential role for bone marrow derived cells in the creation and possibly the maintenance of a metastatic niche.

1.7.1 Role in the Promotion of EMT

The presence of MSCs in the tumour stroma may stimulate EMT of the cancer cells. Research has shown that direct co-culture of breast or gastric cancer cells with bone marrow derived MSCs resulted in the upregulation of EMT markers N-cadherin, vimentin, Twist and Snail and the downregulation of E-cadherin (Martin et al., 2010, Xue et al., 2015). Correspondingly, it was found that MSCs pretreated with tumour necrosis factor-α (TNF-α) and IFN-γ, secreted increased levels of TGF-β. Hepatocellular carcinoma cells grown in CM from the TNF-α and IFN-γ treated cells showed marked changes in molecular markers and functional characteristics associated with EMT, such as increased migration and invasion (Jing et al., 2012).

1.7.2 Role in the Establishment of Distant Metastasis

A study by Karnoub and colleagues investigated the effect of MSCs on breast cancer cell motility and migration to the site of metastasis (Karnoub et al., 2007). Bone marrow derived MSCs were co-injected with breast cancer cell line, MDA-MB-231, into mice. The chemokine CCL5 was secreted by MSCs, which in turn interacted with its receptor CCR5 on the breast cancer cells, resulting in increased metastasis to the lung (Karnoub et al., 2007). Further strengthening these results, studies were published demonstrating the secretion of CCL5 by MSCs in response to osteosarcoma cells (Xu et al., 2009) and breast cancer cells (Mi et al., 2011). Additionally, it was found that the release of osteopontin (OPN) by tumour cells induced the production

of CCL5 by MSCs, which in turn promoted CCR5 mediated breast cancer cell metastasis. Furthermore, MSCs isolated from the site of metastasis (the lung and liver) expressed the CAF markers α-SMA, SDF-1α, tenascin-C (TN-C), MMP-2 and MMP-9 (Mi et al., 2011).

1.7.3 MSCs at the Bone Metastatic Site

Entry of cancer cells into the bone marrow may be facilitated by MSCs through adherence of the metastatic cell to bone marrow ECs (Corcoran et al., 2008). Several studies have found that the chemoattraction of tumour cells to the bone marrow is stimulated by bone marrow stromal cell production of SDF-1α (Cooper et al., 2003, Zhang et al., 2013b, Corcoran et al., 2008). Prostate cancer cells were found to express the receptor CXCR4 and migrate and invade in response to SDF-1α (Taichman et al., 2002, Singh et al., 2004). Bone marrow derived MSCs were found to promote the transmigration of breast cancer cell lines (MCF7 and T47D) across bone marrow ECs (Corcoran et al., 2008). Tac1 expression in the breast cancer cell lines was found to play a key role in bone marrow EC transmigration and the adherence of the metastatic cells to MSCs through the regulation of CXCR4 and SDF-1α production in the breast cancer cells (Corcoran et al., 2008).

Cells of the bone marrow including HSCs, megakaryocytes, macrophages and myeloid-derived suppressor cells have been implicated in developing a hospitable metastatic niche (Park et al., 2011). However, given the plasticity of MSCs and their role in bone remodelling it seems likely that the establishment of tumour cells within the bone marrow would result in cellular cross-talk that would disrupt bone homeostasis. Bone morphogenic protein-4 (BMP-4) within the bone marrow has been shown to stimulate the production of sonic hedgehog (SHH) in prostate cancer LNCaP cells which enhanced BMP-responsive reporter signalling in the mouse stromal cell line, MC3T3-E1, leading to increased osteoblastic differentiation (Nishimori et al., 2012).

An interesting study by Joseph *et al.* investigated the interaction between HSCs derived from the bone marrow of mice implanted with prostate cancer cell lines that formed either osteoblastic or osteolytic metastatic lesions. They found that HSCs

derived from the mice with osteoblastic lesions stimulated osteoblastic differentiation of MSCs through BMP2 signalling while HSCs derived from mice with osteolytic lesions enhanced the differentiation of mixed marrow mononuclear to osteoclasts through IL-6 signalling (Joseph et al., 2012). IL-6 may have an important role in cross-talk within the tumour associated bone marrow microenvironment. Production of IL-6 in multiple myeloma by bone marrow stromal cells induces tumour cell adhesion and osteoclastogenesis (Thomas et al., 1998, Michigami et al., 2000). IL-6 secretion in MSCs was found to be stimulated by neuroblastoma cells within the bone marrow which in turn activated osteoclasts (Ara et al., 2009). IL-6 was also found to act on neuroblastoma and multiple myeloma cells within the bone marrow by increasing cell proliferation and survival through activation of the STAT3 pathway (Ara et al., 2009, Brocke-Heidrich et al., 2004).

1.8 Cancer Associated Fibroblasts

1.8.1 Origins and Characteristics

Cancer associated fibroblasts (CAFs) are a heterogeneous population of fibroblast-like cells with a tumour promoting function. The heterogeneity may be due to varying cell origins and the molecular constitution of tumour stroma from which the cell fate is determined. CAFs have been found to originate from bone marrow MSCs, fibroblasts and by transdifferentiation of epithelial and endothelial cells (Spaeth et al., 2009, Evans et al., 2003, Zeisberg et al., 2007). The mechanisms by which the cells differentiate or become 'activated' are largely unknown, however, exposure to TGF-β has been shown to induce the phenotypic changes regardless of cell origin (Kojima et al., 2010, Shangguan et al., 2012, Zeisberg et al., 2007, Calon et al., 2014).

CAFs are morphologically similar to myofibroblasts with both expressing the marker α-smooth muscle actin (αSMA) which assemble to form contractile stress fibres (Kellermann et al., 2008, Tomasek et al., 2002). To identify CAFs and distinguish them from fibroblasts, MSCs and other cells types, the presence or increase in the markers - αSMA, fibroblast specific protein-1 (FSP1), fibroblast activation protein (FAP), vimentin, type I collagen and platelet-derived growth factor receptors (PDGFR) - are often used (Sugimoto et al., 2006, Spaeth et al., 2009, Mishra et al., 2008, Liu et al.,

2006, Anderberg et al., 2009). In comparison to fibroblasts, CAFs have been shown to have an increased proliferation rate and a greater production of collagens, growth factors, pro-inflammatory cytokines and MMPs (Buganim et al., 2011, Madar et al., 2009, Guo et al., 2008, Erez et al., 2010, Eck et al., 2009, Sternlicht et al., 1999).

1.8.2 Role in Tumour Promotion

One of the defining functions of CAFs is their ability to promote cancer progression. CAFs were found to have a greater influence in the formation of breast and prostate tumours in comparison to normal fibroblasts using *in vivo* models (Orimo et al., 2005, Olumi et al., 1999). Further studies have shown CAFs to increase cancer cell proliferation, invasiveness and adhesion (Jia et al., 2013, Subramaniam et al., 2013, Cai et al., 2012). One of the mechanisms by which CAFs promote the development of the tumour is through the release of growth factors such as hepatocyte growth factor (HGF), TGF-β, epidermal growth factor (EGF) and FGF2 (Tyan et al., 2011, Giri et al., 1999, Kalluri and Zeisberg, 2006). Secretion of HGF by CAFs has been shown to induce the secretion of uPA and uPAR by breast cancer cells, promoting their invasive capacity and inhibition of HGF has led to the resistance of lung cancer cells to tyrosine kinase inhibitors (Wang et al., 2009, Jedeszko et al., 2009).

Studies have shown that CAFs release SDF-1α (Orimo et al., 2005, Sugihara et al., 2015). CAF secreted SDF-1α was found to promote angiogenesis by attracting endothelial progenitor cells to carcinomas, promote tumour growth in carcinomas and increase the invasive potential of pancreatic cells through interaction with chemokine receptor CXCR4 (Orimo et al., 2005, Sugihara et al., 2015). Interestingly, a recent study by Feig and colleagues in pancreatic cancer revealed a potential role for CAF derived SDF-1α in immune evasion, as administration of a CXCR4 inhibitor resulted in rapid T-cell accumulation and cancer regression in a mouse model (Feig et al., 2013).

1.8.3 MSCs as an Origin for CAFs

Evidence to suggest CAFs are derived from MSCs was found in *in vivo* studies whereby genetically tagged bone marrow derived cells, injected into mice, were found at the

tumour with myofibroblast morphology and expressing αSMA and α_1 chain of type I (pro)collagen (Direkze et al., 2004, Ishii et al., 2003, Direkze et al., 2006). A subsequent study in a murine ovarian carcinoma xenograft model, found that bone marrow derived MSCs engrafted at the tumour expressed CAF markers FAP, FSP, a-SMA and TN-C (Spaeth et al., 2009).

Further evidence to support the hypothesis that CAFs can originate from MSCs comes from *in vitro* studies where MSCs are cultured long-term in tumour cell CM. In a study by Mishra *et al.* MSCs were cultured for up to 30 days in the breast cancer cell line (MDA-MB-231) CM (Mishra et al., 2008). The conditioned cells expressed increased levels of αSMA, FSP-1, SDF-1α and vimentin and stimulated tumour cell growth in both *in vitro* and *in vivo* models (Mishra et al., 2008). Long-term culture of 12 - 16 days in CM taken from ovarian cancer cell line, SKOV-3, induced the expression of CAF markers in MSCs and elevated secretion of IL-6, leading to increased tumour cell proliferation (Spaeth et al., 2009). Interestingly, TGF-β may be involved in the transition as bone marrow MSCs transduced with a lentiviral vector which inhibited TGF-β/smad signalling, expressed a decrease in CAF markers when conditioned for 10 days in breast cancer cell CM in comparison to naïve MSCs (Shangguan et al., 2012). Furthermore, treatment of MSCs with the endoplasmic reticulum chaperone, GRP78, activated TGF-β/smad signalling and induced the transition to a CAF like phenotype (Peng et al., 2013). Taken together, it is clear that TGF-β plays a major role in the transition from MSC to CAF, however it is unclear to what degree it affects the secretory profile of the cells and their functional characteristics.

On the other hand, it must be noted that MSCs and CAFs share many similarities. A study has shown that CAFs share many of the same surface markers as MSCs such as CD29, CD44, CD73, CD90, CD106 and CD117, have the capacity to differentiate to osteocytes, chondrocytes and adipocytes, and express vimentin (Paunescu et al., 2011). Nonetheless, CAFs were found to have an increased proliferative capacity and secrete increased VEGF, TGF-β, IL-4, IL-10 and TNFα (Paunescu et al., 2011). Due to the lack of specific CAF markers it will be necessary to define whether MSC derived CAFs are more likely to be MSCs in an activated state in response to tumour cells.

1.9 Mesenchymal Stem Cells and Cancer Therapeutics

Although MSCs can promote tumour growth and progression as described above, their capacity to home to the tumour site raises the possibility of using them as vehicles for novel therapeutic approaches. MSCs that were genetically modified to produce tumour necrosis factor apoptosis-inducing ligand (TRAIL) have been shown to reduce tumour growth following intracranial implantation into an invasive glioblastoma mouse model (Sasportas et al., 2009), and in xenograft pulmonary metastatic mouse models following subcutaneous injection of the transfected MSCs (Loebinger et al., 2009a). When used in combination with targeted inhibition of X-linked inhibitor of apoptosis protein (XIAP), MSCs genetically modified to produce TRAIL resulted in decreased numbers of metastatic lesions in an xenograft pancreatic carcinoma metastatic model following intravenous injection (Mohr et al., 2010). MSCs, engineered to produce IFN-β also prolonged cancer-free survival of glioma mouse models (Nakamizo et al., 2005). Reduced growth and extended survival was also shown in a mouse melanoma model following subcutaneous inoculation of MSCs retrovirally transduced to express the cytokine IL-12 (Elzaouk et al., 2006).

MSCs could potentially be used to deliver active drugs to the site of the tumour, a system which significantly reduces the level of side-effects currently observed in current drug therapies used in the clinic. Adipose tissue-derived MSCs, modified to express cytosine deaminase, which converts the pro-drug 5-fluorocytosine to its active form, were found to inhibit xenograft colon cancer tumour growth following subcutaneous administration of modified MSCs in immunocompromised mice (Kucerova et al., 2007). Research by Pessina et al. used a drug transport method that did not involve genetic manipulation. MSCs were primed with paclitaxel, which was released slowly from the cells (Pessina et al., 2011). While preclinical studies support the potential of MSCs as therapeutic tools, a better understanding of their tumour promoting function could lead to more targets such as IL-6 or SDF-1α, particularly in the treatment of bone metastasis where major progress has not been made.

1.10 Experimental Model

The aim of this study was to investigate the interactions between MSCs and prostate cancer cells. We developed an *in vitro* experimental system to examine the response of human bone marrow derived MSCs to long-term growth in prostate cancer cell conditioned media (CM). We used the non-metastatic cell line – 22Rv1, the brain metastatic cell line – DU145 and the bone metastatic cell line – PC3 to generate the prostate cancer cell CM throughout the duration of the study. The MSCs were initially conditioned for 48 hours in prostate cancer cell CM followed by long-term conditioning experiments for 10, 20 and 30 day durations. We examined the conditioned MSCs for molecular and functional changes and investigated whether the MSCs retained the classical characteristics associated with MSCs such as expression of surface marker – CD73, CD105 and CD90 and the capacity to differentiate to adipocytes and osteocytes (Dominici et al., 2006). We also considered whether the conditioned MSCs could induce a functional response in the prostate cancer cells.

Chapter 2

Materials and Methods

2.1 MSC Isolation and Characterisation

Male human MSCs were provided by the Regenerative Medicine Institute at NUI Galway. Bone marrow was aspirated from the iliac crests of healthy volunteers. MSCs were isolated from the bone marrow aspirates through direct plating and non-adherent haematopoietic cells were depleted following 10-12 days of culture. The MSCs were confirmed to have the capacity to differentiate into osteocytes, chondrocytes and adipocytes. Additionally, the expression of cell surface markers was established using positive markers CD105, CD73, CD90 and the negative haematopoietic markers CD34, CD45 and HLA-DR using flow cytometry. The differentiation and cell surface marker characterisation was performed by Ms. Georgina Shaw (REMEDI, NUI Galway) prior to use.

Cells isolated from four male donors were used throughout the duration of the project at ages 38 (donor 1), 25 (donor 2), 20 (donor 3) and 26 (donor 4) (see appendix table 1). The age of the MSC donors does not represent the age cohort of prostate cancer patients; however MSCs derived from younger healthy donors are useful for preliminary proof-of-concept studies. The MSCS were isolated at passage 0 or 1 and used experimentally up to passage 7.

2.2 Cell Lines

Human prostate cancer cell lines PC3 and DU145 and 22Rv1 were obtained from American tissue culture collection (ATCC, VA, USA). PC3 and DU145 cells were originally derived from the bone and brain metastatic site, respectively. The non-metastatic epithelial cell line, 22Rv1, was originally derived from a xenograft that was serially propagated in mice after castration-induced regression and relapse of the parental, human androgen-dependent CWR22 xenograft.

2.3 Culture Conditions

All cells were cultured in α-Minimum Essential Medium GlutaMAX™ (Gibco, Thermofisher, MA, USA) supplemented with serotyped 10% FBS and contained 100 units/mL of penicillin, 100 µg/mL of streptomycin, and 0.25 µg/mL of Fungizone® Antimycotic (Gibco, Thermofisher, MA, USA). The MSC culture medium was

supplemented with 1ng/mL FGF2 (Peprotech, NJ, USA) and the cells were grown and used experimentally at passages 2–7. Culture medium was changed every 2-3 days, and cells were passaged at 70-80% confluency using 0.25% trypsin-Ethylenediaminetetraacetic acid (EDTA) (Sigma, MO, USA). Cells were washed with Dulbecco's phosphate-buffered saline (D-PBS) (Sigma, MO, USA), and trypsinised at 37°C for 5 minutes or until the monolayer detached. Complete medium was added to the detached cells following trypsinisation and the resulting suspension was centrifuged at 300 x g for 5 minutes at room temperature. Cells were counted using the Countess™ Automated System (ThermoFisher, MA, USA) using Countess® Chamber Counting Slides (ThermoFisher, MA, USA). The pellet was re-suspended and re-seeded in T75 or T175 flasks containing complete medium. The culture flasks were incubated in a humidified 5% CO_2 environment at 37°C throughout growth. MSCs were grown in Nunclon™ certified and Nunclon™ Delta treated (Fisher Scientific, ThermoFisher, MA, USA) cell culture flasks and the prostate cancer cell lines were grown in cell+ cell culture flasks (Sarstedt, Nümbrecht, Germany).

2.4 MSC Growth in Tumour Cell Conditioned Media

PC3, DU145 and 22Rv1 cells were seeded into T175 flasks containing 25ml complete medium. PC3 and DU145 cells were seeded at a concentration of 1.7 x 10^4 cells per cm^2 and 22Rv1 cells were seeded at 2.3 x 10^4 cells per cm^2 due to different growth rates. The cells were grown for 48 hours at 37°C with 5% CO_2 until they were 60-70% confluent. The medium was subsequently removed from the flask and centrifuged at 300 x g for 10 minutes. The supernatant was removed and filtered through a 0.45µm pore syringe filter (Whatman, Maidstone, UK). The filtered supernatant, or CM, was frozen at -20°C and used within 30 days.

MSCs were seeded at 1.1 x 10^3 cells per cm^2 initially and up to 2.8 cells per cm^2 following extended growth in PC3 CM. The MSCs were grown throughout the conditioning period in a 1:1 ratio of complete and conditioned media which was supplemented with 1 ng/ml FGF2. The use of 1 ng/ml of FGF2 in the culture medium allows growth at a low seeding density of 1.1 x 10^3 cells per cm^2. The 1:1 ratio was determined based on early optimisation experiments so that the MSCs were exposed

to a sufficient amount of complete media that would not affect survival. The medium was changed every 2 to 3 days depending on cell confluency. The cells were passaged upon reaching a confluency of 70-80% and were immediately re-seeded in CM. Cells were harvested for experimentation at day 10, 20 and 30. A 30 day conditioning period was used to allow time for cell differentiation to occur. MSCs that were treated for 30 days in PC3 CM were removed from the CM and grown for 12 - 16 days in complete medium prior to experimental use.

2.5 Cell Freezing and Thawing

Prostate cancer cell lines were stored at -80°C and MSCs were frozen in a liquid nitrogen dewar. All cell lines were cryopreserved in medium containing 90% FBS and 10% dimethyl sulfoxide (DMSO) (Sigma, MO, USA). Cells were harvested and re-suspended in 1 mL of freezing medium at a concentration of up to 3 x 10^6 cells/ml and pipetted into cryovials (Nunc, ThermoFisher, MA, USA). The cells were placed in a Mr. Frosty (Nalgene, ThermoFisher, MA, USA) in a -80°C freezer and after 24 hours the MSCs were frozen in a liquid nitrogen dewar. When it was necessary to thaw the cells, the vials were taken from the liquid nitrogen dewar and slowly thawed in a 37°C waterbath. Once thawed, the contents of the cryotube were removed using a p1000 Gilson pipette and placed gently into a sterile 15ml tube (Sarstedt, Nümbrecht, Germany) containing 10ml complete medium at room temperature. In order to remove the DMSO used for cryopreservation, the cells were pelleted by centrifugation at 300 x g for 5 minutes. The supernatant was discarded and the cells were re-suspended in complete medium. The re-suspended cells were placed in a flask containing complete medium and the flask was gently rocked to evenly distribute the cells. The flask was placed in the appropriate incubator at 37°C and 5% CO_2.

2.6 Growth Factor and Cytokine Quantification using the MesoScale Discovery Platform

Secreted cytokine and growth factor levels were quantified using MesoScale Discovery (MSD, MD, USA) technology. MSD (MD, US) is an electro-chemiluminescent based immunoassay that uses 96-well carbon electrode plates pre-coated with

capture antibodies that can detect up 10 targets per well. MSD assays use electrochemiluminescent labels that are conjugated to detection antibodies. The analytes bound to the capture antibodies are detected using antibodies conjugated with an electro-chemilluminescent label. Electricity is applied to the plate electrodes by the MSD platform leading to light emission by SULFO-TAG labels. Light intensity is then measured to detect and quantify individual analytes in the sample. The electricity is decoupled from the light signal allowing only labels near the electrode surface to be detected.

MSCs were cultured for short and long term periods in prostate cancer cell CM prior to use. Short-term experiments involved 48 hours of growth in complete medium followed by a 48 hour conditioning period in 22Rv1, DU145 and PC3 CM followed by 48 hours in fresh complete medium. For long-term conditioning experiments MSCs were treated for 10, 20 and 30 days in PC3 CM. MSCs treated for 30 days in PC3 CM were then grown for 12 - 16 days in complete medium. To collect sample for the long-term studies, the conditions were consistent prior to sample collection. Cells were seeded onto a petri dish containing 10ml complete medium at a concentration of 8.6 x 10^4 cells per cm^2. Supernatant was collected after 24 hours and centrifuged for 10 minutes at 300 x g to remove any remaining cells. The supernatant was then frozen at -80°C until use. Each assay was carried out as per manufacturer's guidelines (MSD, MD, USA). See table 2.1 for the lower limit of detection of the cytokine and growth factor analytes used during this study.

Analyte	IL-6	IL-8	OPN	MCP-1	VEGF	PLGF	sFlt-1	FGF2
Lower Limit of Detection (pg/ml)	0.7	0.7	50	10	6.4	0.96	8.9	2.2

Table 2.1. MesoScale Discovery System Lower Limits of Detection

2.6.1 Cytokine Detection

The assay plates used for cytokine detection include a custom made kit to detect IL-6 and IL-8, the Human Osteopontin Kit (OPN) and the Human MCP-1 Tissue Culture Kit (MCP-1).

Standards were reconstituted in the assay diluent provided with the highest concentration at 10 ng/mL followed by 1:4 serial dilutions. Standards and samples were added at 25 µl per well. The plate was sealed and placed on an orbital shaker set at 700 rpm (orbit: 3 mm) and left for 2 hrs at room temperature. Detection antibody was added at 25 µl per well. The plate was sealed and incubated on the orbital shaker for 2 hrs at room temperature. After the incubation period the plate was washed 3 times using 200 µL D-PBS + 0.05% Tween 20. MSD Read Buffer was added at 150 µl per well and plates were read on the MSD Sector Imager 2400 plate reader (MSD, Maryland). The signal was measured by electro-chemiluminescence and analysed using the Discovery Workbench 3.0 software (MSD, MD, USA).

2.6.2 Growth Factor Detection

The Human Growth Factor Kit I (VEGF, placental growth factor, soluble Flt1 and FGF2) was used for growth factor detection using MSD technology. Standards were reconstituted in the assay diluent provided with the highest concentration at 9ng/ml followed by a 1:4 dilution series. The blocker provided was added to each well at 25µl per well and the plate was incubated at room temperature on the orbital shaker set at 700 rpm (orbit: 3 mm) for 2 hours. After the incubation period, the plate was washed 3 times using 200 µL D-PBS + 0.05% Tween 20. Standard and sample were added at 25µl per well. The plate was sealed and placed on an orbital shaker set at 700 rpm (orbit: 3 mm) and left for 2 hours at room temperature. The plate was washed again 3 times using 200 µL D-PBS + 0.05% Tween 20. Detection antibody was added at 25 µL per well. The plate was sealed and incubated on the orbital shaker for 2 hours at room temperature. After the incubation period the plate was washed 3 times using 200 µL D-PBS + 0.05% Tween 20. MSD Read Buffer was added at 150 µl per well and plates were read on the MSD Sector Imager 2400 plate reader (MSD,

MD, USA). The signal was measured by electro-chemilluminescence and analysed using the Discovery Workbench 3.0 software (MSD, MD, USA).

2.7 Cytokine Screen using Proteome Profilers

The Proteome Profiler Human XL Cytokine Array Kit was used to test for cytokine and chemokine secretion in supernatants from the prostate cancer cell lines PC3, DU145 and 22Rv1 and from MSCs conditioned until day 20 or 30. A proteome profiler (R&D Systems, Minneapolis, USA) is a multiplex membrane-based sandwich immunoassay. Test cells were seeded onto a petri dish containing 10 mL complete medium at a concentration of 8.6×10^4 cells per cm^2. Supernatant was collected after 24 hours and centrifuged for 10 minutes at 300 x g to remove any remaining cells. The supernatant was then frozen at -80°C until use. Each assay was carried out as per manufacturer's guidelines (MSD, MD, USA).

Proteome profiler membranes were placed in blocking buffer for 1 hour, after which 1 ml of sample, diluted with 0.5 ml of blocking buffer, was added and membranes were incubated overnight at 2-8°C. The membranes were washed 3 times for 10 minutes using 20 ml of wash buffer followed by a 1 hour incubation period in 30 µl of detection antibody cocktail on a rocking platform shaker at room temperature. The membranes were then washed 3 times for 10 minutes using 20 ml wash buffer and placed in 2 ml of Streptavadin-HRP for 1 hour on a rocking platform shaker at room temperature. The membranes were then washed 3 times for 10 minutes using 20 ml wash buffer. The membranes were scanned to visualise the bound protein by chemilluminescence detection using WesternSure™ ECL substrate (LI-COR Biotechnology, NE, USA) and the membranes were scanned on the LI-COR C-DiGit Blot Scanner (LI-COR Biotechnology, NE, USA). Histogram profiles were generated by quantifying the mean spot pixel densities from the array membrane using Image Studio software (Image Studio Lite Version 4.0, LI-COR Biotechnology, Cambridge, UK) and fold increase was calculated by comparing the conditioned MSCs to the untreated MSCs.

2.8 Protein Detection by Western Blotting

MSCs that had been treated for 30 days with PC3 CM were tested for αSMA, vimentin and FSP1 expression. Mouse skin fibroblasts were treated with TGFβ (Peprotech, NJ, USA) for 5 days to induce a myofibroblast-like phenotype and were used as a positive control for αSMA and FSP1.

2.8.1 Protein Collection and Measurement

Petri dishes or flasks containing cells between 60-70% confluency were washed twice with D-PBS, cells were then lysed on ice for 15 minutes with an appropriate volume of RIPA buffer (Sigma, MO, USA) containing protease inhibitors (Fisher Scientific, ThermoFisher, MA, USA; cat no. 12831640). Samples were then centrifuged at 12,000 x g for 15 minutes at 4°C. Supernatants were transferred to fresh tubes and stored at -80°C. Protein concentration was determined using the BCA assay (ThermoFisher, MA, USA).

2.8.2 Western Blotting

NuPAGE® Sample Reducing Agent with NuPAGE® LDS Sample Buffer (Life Technologies) was added to 10 µg protein sample at a ratio of 1:3 and made up to the necessary volume using distilled water. The samples were then boiled at 95°C for 5 minutes. Equal concentrations of protein from each sample were placed in the appropriate well of 4-12% pre-cast NuPAGE® Bis-Tris gels (Life Technologies, ThermoFisher, MA, USA). NuPAGE® MES SDS Running Buffer (Life Technologies, ThermoFisher, MA, USA) was prepared at a 1:20 dilution with distilled water and used to run the gel at 120 V for approximately 60 minutes. Proteins were transferred to nitrocellulose membranes using the iBlot® dry blotting system (Life Technologies). Membranes were stained with Ponceau S (Sigma, MO, USA) stain to assess equal protein loading which was subsequently washed off using tris buffered saline containing 0.01% tween, (TBS-T) (25 mM Tris; 3 mM potassium chloride (KCl); 68.5 mM sodium chloride (NaCl) (pH8) (Sigma, MO, USA). Membranes were blocked in 5% milk (Sigma, MO, USA) in TBS-T for 1 hour at room temperature. Membranes were then incubated in primary antibody in 5% milk diluted in TBS-T, overnight at 4°C. See

Table 2.2 below for antibody dilutions and details. Membranes were then washed 3 times for 5 minutes in TBS-T, followed by incubation with either IRDye 800CW goat anti-rabbit or IRDye 680LT goat anti-mouse secondary antibodies (LI-COR Biotechnology, Cambridge, UK) in 5% milk in TBS-T for 60 minutes at room temperature in the dark. See Table 2.3 below for secondary antibody details. The blots were then washed with TBS-T followed by one 5 minute wash with D-PBS. The blots were imaged using the ODYSSEY® CLx Imager (LI-COR Biotechnology, NE, USA).

Antibody	Application	Dilution	Company	Product #
Anti-αSMA, mouse, monoclonal	WB/IF	WB - 1:1000 IF – 1:500	Sigma, MO, USA	A 2547
Anti-Vimentin, rabbit, monoclonal	WB/IF	WB - 1:1000 IF – 1:500	Cell Signalling Technology, MA, USA	5741
Anti-FSP1, rabbit, polyclonal	WB/IF	WB - 1:1000 IF – 1:200	Merck Millipore, MA, USA	ABF32
Anti-FAP, mouse, monoclonal	WB/IF	WB - 1:1000 IF – 1:300	Merck, Millipore, MA, USA	OP188

Table 2.2 Primary Antibody Details

Antibody	Application	Dilution	Company	Product #
IRDye 680LT Anti-Mouse IgG	WB	1:20000	LI-COR Biotechnology, Cambridge, UK	926-68020
IRDye 800CW Anti-Rabbit IgG	WB	1:15000	LI-COR Biotechnology, Cambridge, UK	926-32211
AlexaFluor 488 goat anti-mouse IgG	IF	1:500	Invitrogen, MA, USA	A-11001
Alexa Fluor® 594 goat anti-rabbit IgG	IF	1:500	Invitrogen, MA, USA	A11012

Table 2.3 Secondary Antibody Details

2.9 Immunofluorescence Staining

Immunofluorescence staining was used to test and visualise protein expression levels and localisation within MSCs that had been treated for 30 days with PC3 CM. The cells were tested for the presence of αSMA, vimentin, FSP1 and FAP. Mouse skin fibroblasts were treated with TGFβ (Peprotech, NJ, USA) for 5 days to induce a myofibroblast-like phenotype and were used as a positive control for αSMA, FAP and FSP1.

Cells were seeded in 96-well cell+ plates (Sarstedt, Nümbrecht, Germany) at a concentration of 5 x 10^3 cells per well and cultured 37°C in 5% CO_2 until 60-70% confluency was reached. The wells were washed in D-PBS, and fixed for 20 minutes in 10% formalin (ThermoFisher, MA, USA) at room temperature. The wells were washed 3 times for 5 minutes in D-PBS followed by permeabilisation in D-PBS-Triton X-100 (0.1%) on a shaker twice for 3 minutes. The cells were subsequently blocked for 30 minutes in 1% BSA in D-PBS at room temperature and incubated with the relevant primary antibody, diluted appropriately in 1% BSA in D-PBS, for 1 hour on an orbital shaker. Primary antibody was not added to wells that were designated 'secondary only controls'. See table 2.2 for antibody details. The wells were then washed 3 times for 5 minutes in D-PBS. The corresponding secondary antibody was prepared in D-PBS and the cells were incubated for 30 minutes in the dark on an orbital shaker at room temperature. See table 2.3 for antibody details. The wells were washed three times in D-PBS and the cells were then stained with DAPI (1 μg/mL) (Sigma, MO, USA) in D-PBS for 5 minutes at room temperature, which was subsequently washed off during three 5 minute washes. The plates were scanned and images taken using the Operetta HTS imaging system (PerkinElmer, OH, USA) at 20 times magnification.

2.10 Gene Expression Analysis using Real-time PCR

2.10.1 RNA Extraction

RNA was extracted using an RNeasy Mini Kit (Qiagen, Hilden, Germany) as per manufacturer's guidelines. MSCs were harvested following 30 days of treatment with

PC3 CM and centrifuged for 5 minutes at 300 x g to form a pellet. The pellet was then resuspended in 350 µl of lysis buffer. An equal volume of 70% ethanol was added and the resulting 700 µl was added to an RNeasy spin column placed onto a 2 ml collection tube. The lid was closed and samples were centrifuged for 15 seconds at 8000 x g. The flow-through was discarded and 700 µl of the wash buffer RW1 was added. The samples were centrifuged for 15 seconds at 8000 x g. The flow-through was discarded and 500 µl of the wash buffer RPE was added and the samples were centrifuged for 15 seconds at 8000 x g. The flow-through was discarded and the samples were washed again in 500 µl RPE solution for 2 minutes at 8000 x g. The spin columns were then placed in a new 2 ml collection tube and centrifuged for 1 minute at full speed to dry the membrane. The spin columns were subsequently placed in new 1.5 ml collection tubes and 20-30 µl RNase-free water was added. The samples were then centrifuged at 8000 x g for 1 minute. The samples were quantified using the NanoDrop 2000c spectrophotometer (Thermo Scientific, Delware). Good quality RNA was considered to have a 260/280 nm ratio of ~2.0. Samples were stored at -80°C.

2.10.2 cDNA Synthesis

cDNA was synthesised using the Tetro cDNA Synthesis Kit (Bioline, London, UK). To generate the cDNA synthesis mix, 1 µL oligo (dT)18 primers, 1 µL 10 mM dNTP mix, 4 µL 5X RT buffer and 1 µL Tetro reverse transcriptase (200 u/µL) was made up and added to 1 µg of total RNA. The volume adjusted to 20 µL with DEPC-treated water in sterile 0.2 mL tubes (Eppendorf, Hamburg, Germany). Samples were then incubated at 45°C for 30 minutes and the reaction was then terminated by incubation at 85°C for 5 minutes using the Veriti Gradient Thermal Cycler (Applied Biosystems, ThermoFisher MA, USA). Samples were frozen until use at -80°C.

2.10.3 Real-time PCR

Predesigned KicqStart® SYBR Green Primers (Sigma, MO, USA) were reconstituted in molecular grade dH_2O (Sigma, MO, USA) to a stock concentration of 100 µM and stored at -20 ˚C. Working stocks were made at a concentration of 10 µM and stored at -20 ˚C. Primer sequences are detailed in table 2.4. A master mix was prepared using 5 µL 2X SensiFAST SYBR Hi-ROX Mix, 0.4 µL of 10 µM forward primer, 0.4 µl of 10 µM

reverse primer and 2 µL template cDNA and the final volume was adjusted to 10 µl with nuclease-free water. Samples were added to a 96-well PCR micro-plate (Thermo Scientific ABgene) and each reaction was carried out in triplicate. The cycle conditions for real-time PCR were as follows: 95°C for 2 minutes followed by 40 cycles of 95°C for 5 seconds and 60°C for 20 seconds. The StepOne Plus Real Time PCR System (Applied Biosystems) was used for each run. The house-keeping gene 36b4 was used to analyse the relative expression of the genes of interest. Relative gene expression data was analysed using the ΔΔCT method.

Gene Name	**Forward Sequence**	**Reverse Sequence**
IL6	GCAGAAAAAGGCAAAGAATC	CTACATTTGCCGAAGAGC
IL8	GTTTTTGAAGAGGGCTGAG (batch # HA06611482)	TTTGCTTGAAGTTTCACTGG (batch # HA06611483)
SPP1	GACCAAGGAAAACTCACTAC (batch # HA06611494)	CTGTTTAACTGGTATGGCAC (batch # HA06611495)
Vimentin	GGAAACTAATCTGGATTCACTC (batch # HA06611476)	CATCTCTAGTTTCAACCGTC (batch # HA06611477)
FAP	GAAGAGGAAATGCTTGCTAC (batch # HA07359817)	CTAGGATATTGTTCATCGCC (batch # HA07359818)
TNC	GAATCTTTGCAGAGAAAGGG (batch # HA06611468)	AAGTCTCTTGGAGAATCGAG (batch # HA06611469)
MMP9	AAGGATGGGAAGTACTGG	GCCCAGAGAAGAAGAAAAG
COL1A1	GCTATGATGAGAAATCAACCG (batch # HA06563647)	TCATCTCCATTCTTTCCAGG (batch # HA06563648)
COL5A1	TTGACGAGAACTACTACGAC (batch # HA06611462)	ATCCCTTCATAGATGGTATCC (batch # HA06611462)
RUNX2	AAGCTTGATGACTCTAAACC (batch # HA07359815)	TCTGTAATCTGACTCTGTCC (batch # HA07359816)
PPARγ	AAAGAAGCCAACACTAAACC (batch # HA07359821)	TGGTCATTTCGTTAAAGGC (batch # HA07359822

Table 2.4. Primer Sequences

2.11 Flow Cytometry

Flow cytometry was used to analyse MSCs treated with PC3 CM for 30 days based on the expression of MSC cell surface markers CD90, CD105 and CD73 using the BD Stemflow Human MSC Analysis Kit. Cells were harvested and resuspended in D-PBS with 1% FBS. The cell solution was filtered through a 30 µm nylon mesh (Fisher Scientific, ThermoFisher, MA, USA) to ensure a single cell suspension. The cells were counted and diluted to a concentration of 5 x 10^6 cells/ml. The following antibodies were added to separate tubes: FITC Mouse Anti-Human CD90 (5µl), PerCP-Cy™5.5 Mouse Anti-Human CD105 (5µl), APC Mouse Anti-Human CD73 (5µl), human MSC Positive Cocktail (20µl) and human MSC Positive Isotype Control Cocktail (20µl). Sample was then added at 100ul per tube and left to incubate in the dark for 30 minutes. The tubes were washed twice using D-PBS with 1% FBS to remove the antibody. FITC Mouse Anti-Human CD90, PerCP-Cy™5.5 Mouse Anti-Human CD105 and APC Mouse Anti-Human CD73 were used as compensation controls and a no stain control was used without antibody. Samples were analysed using the BD FACS Canto II, with at least 10,000 events collected per sample. Gates were defined as positive or negative according to the fluorescence intensity of the isotype control. Collected data was analysed with FlowJo v10.0.6 (FlowJo, OR, USA) software.

2.12 Cell Migration

2.12.1 xCELLigence Method

Migration was assessed using the xCELLigence method to test the functional differences between untreated MSCs and MSCs treated with PC3, DU145 and PC3 CM for 10, 20 and 30 days. The xCELLigence system (xCELLigence RTCA DP Instrument) measures cell migration in real-time. The instrument analyses a CIM-plate16 which is comprised of 16 wells each containing a modified Boyden chamber using the xCELLigence analyser platform (ACEA Biosciences, San Diego). The plate consists of two separable sections whereby cells seeded in the upper chamber migrate through the microporous membrane toward the lower chamber that contains a chemoattractant, in this case 10% FBS. The plates can be used to measure cell migration or invasion through 8 µm pores of a polyethylene terephthalate membrane

onto gold electrodes on the underside of the membrane. Cells adherent to the microelectrode sensors are measured by increase in impedance.

Complete medium containing 10% FBS (stimulus) or serum free medium (SFM) (negative control) was added to each well in the lower chamber of a CIM-plate 16 at a volume of 160 µl. The upper chamber was connected and 30 µL of SFM was added to each well. The plate was allowed to equilibrate at 37°C for 1 hour. A background measurement was taken using the RTCA DP Instrument. Cells were harvested and washed in SFM. The cells were then resuspended to a concentration of 2 x 10^5 cells/ml in SFM and 100 µL was added per well in triplicate. The plate was incubated for 30 minutes at room temperature to allow the cell attachment, after which the plate was placed in the RTCA analyser at 37°C in 5% CO_2. Cell impedance was measured every 15 minutes over 24 hours.

2.12.2 Co-culture using the Transwell Migration Method

Untreated MSCs and MSCs that had been treated for 30 days with PC3 CM were seeded in triplicate in a 24-well cell+ plate (Sarstedt, Nümbrecht, Germany) at a concentration of 5 x 10^4 cells per well and allowed form a monolayer. The medium was then removed and replaced with 500 µl SFM, empty wells were filled with 500 µl of either SFM or medium containing 10% FBS (negative and positive controls, respectively). Inserts (8.0 µm pore size, 24-well format; BD Biosciences, Belgium) were placed in each well and PC3, DU145 and 22Rv1 cells were harvested and brought to a concentration of 1 x 10^6 cells/ml, 100 µl of which was added to each insert. Based on previous optimisation studies PC3 cells were allowed to migrate for 30 hours, DU145 for 24 hours and 22Rv1 for 48 hours at 37°C in 5% CO_2. The inserts were then removed and washed in D-PBS. The inside of the insert was swabbed with a cotton bud dipped in D-PBS, and the outer membrane was stained with 0.25% crystal violet for 10 minutes. The inserts were then washed with D-PBS and allowed to air dry. Images were recorded using an Olympus CKX41 inverted microscope (Olympus, Germany) with attached camera and cells were counted using Image J software (ImageJ 1.48v).

2.13 Invasion Assays

All invasion assays were carried out using the xCELLigence System as described in section 2.12.1 with the exception that the upper chambers were coated with matrigel^{TM} (BD Biosciences, Belgium) at 1 mg/mL diluted in SFM. Matrigel was added to each upper chamber at 50 µl, 30 µl of which was immediately removed to ensure an even coating of matrigel in the wells. The upper chamber was then placed at 37°C for 4 hours to allow for polymerisation of the matrigel. Invasion assays were incubated for 48 hours.

2.14 Proliferation Assays

2.14.1 Monoculture Proliferation Assay

Changes in cell proliferation between untreated MSCs and MSCs treated for 10, 20 and 30 days in PC3 cell CM were tested using the alamar blue assay. Cells were harvested as described in section 2.3. The cells were seeded at a concentration of 1 x 10^3 cells per well of a 96-well cell+ plate (Sarstedt, Nümbrecht, Germany) with one plate allocated per time-point. After 24 hours media was aspirated from each well of a 96-well plate. Fresh complete medium was added to each well at volume of 200 µl followed by the addition of 560 µM resazurin/alamar Blue (Sigma, MO, USA). The plate was left to incubate for 6 hours at 37°C after which they the fluorescence was read at 560 nm using the Wallac Victor 3 1420 Multilabel counter (PerkinElmer, OH, USA). The first reading is referred to as 'day 0' and the assay is then repeated every 48 hours until day 8.

2.14.2 Proliferation of PC3 Cells in Untreated and PC3 Educated MSC derived Conditioned Media

Conditioned media was collected from untreated MSCs and PC3 educated MSCs that had been treated for 30 days in PC3 cell CM. The conditions were consistent prior to sample collection. Cells were seeded onto a petri dish containing 10 ml complete medium at a concentration of 8.6 x 10^4 cells per cm^2. Supernatant was collected after 24 hours and centrifuged for 10 minutes at 300 x g to remove any remaining cells. The supernatant was then frozen at -80°C until use.

PC3 cells were harvested as described in section 2.3 and seeded at a concentration of 7 x 10^3 cells per well of a 24-well cell+ plate (Sarstedt, Nümbrecht, Germany) with one plate allocated per time-point. The wells were then filled with 200 µl of untreated MSC CM or PC3 educated MSC CM at a 1:1 ratio with complete medium. After 24 hours the alamar Blue assay was performed as described in the previous section. The first reading is referred to as 'day 0' and the assay is then repeated every 48 hours until day 6.

2.14.3 Co-culture Proliferation Assays

Untreated MSCs and MSCs that had been treated for 30 days in PC3 CM were harvested as described in section 2.3 and seeded into inserts with a 0.4 µm pore size (24-well format; BD Biosciences, Belgium) in complete medium at a concentration of 2 x 10^3 cells/cm^2. The inserts were placed in 24-well plates with each well containing 400 µl complete medium and the cells were left to grow for 2 - 3 days.

PC3 cells were harvested as described in section 2.3 and seeded at a concentration of 7 x 10^3 cells per well of a 24-well cell+ plate in complete medum (Sarstedt, Nümbrecht, Germany), with one plate allocated per time-point. After 24 hours the alamar Blue assay was performed as described in the section 2.14.1. After the first reading (day 0), the MSC containing inserts were placed in each well with the exception of the control wells with PC3 cells alone. The alamar blue assay was repeated every 24 hours until day 3.

2.15 Cell Morphology and Size

Images were taken of untreated MSCs and MSCs treated for 30 days in PC3 CM using an Olympus CKX41 inverted microscope (Olympus, Germany). The cells were harvested as described in section 2.3 and an aliquot of cells was mixed at a 1:1 ratio with trypan blue (Sigma, MO, USA). Images were taken using an Olympus CKX41 inverted microscope (Olympus, Germany) and the diameter of the cells was measured using cellSens Entry version 1.5 (Olympus, Germany).

2.16 Adipogenesis

2.16.1 Adipogenic Differentiation

Untreated MSCs and MSCs treated with PC3 CM for 30 days were tested for their adipogenic differentiation capacity. Cells were harvested as described in section 2.3 and seeded at a density of 2.0 x 10^4 cells/cm^2 in each well of a 24-well cell+ plate (Sarstedt, Nümbrecht, Germany). The cells were incubated at 37°C with 5% CO_2 until they formed a monolayer, approximately 2 – 3 days. Once confluent, 1 ml of adipogenic induction medium was added to each test well and complete medium was added to control wells. See table 2.5 for adipogenic induction medium components and concentrations. The plate was incubated at 37°C with 5% CO_2 for 3 days after which medium was removed from all wells and 1 ml adipogenic maintenance medium was added to each test well for 1 day. See table 2.5 for adipogenic maintenance medium components and concentrations. These two steps were repeated until 3 cycles in adipogenic induction medium and maintenance medium were completed and maintenance medium was finally left on the cells for a further 5-7 days.

2.16.2 Analysis and Measurement of Adipogenesis

Following completion of the differentiation induction period the cells were analysed for adipogenesis. This was achieved using the Oil Red O stain (Sigma, MO, USA) to visualise cellular lipid droplets and real-time PCR to analyse the expression of PPARγ (see section 2.10). Primer sequences are described in table 2.4.

A working solution of Oil Red O was made up by diluting 6 parts of Oil Red O stock solution with 4 parts distilled water which was left to stand for 10 minutes. The solution was filtered using Whatman no.1 filter paper (Whatman, Maidstone, UK). Medium was removed from the wells followed by 2 washes with D-PBS. The cells were then fixed with 10% Neutral Buffered Formalin (ThermoFisher, MA, USA) for 10 minutes to an hour at room temperature, after which the plate was washed with distilled water. The wells were then covered with the working solution of Oil Red O and left for 5 minutes at room temperature. The stain was removed and excess stain was cleared using 2 ml per well 60% isopropanol. The plate was then washed using

distilled water until the water was clear. A working solution of Haematoxylin (Sigma, MO, USA) was made using a 1 in 10 dilution with distilled water and added to each well for 1 min. Excess stain was removed with warm tap water and images were obtained using an Olympus CKX41 inverted microscope (Olympus, Germany).

Once the images were taken the water was removed and the Oil Red O was extracted using 350 µl 99% isopropanol which was then placed in separate 1.5 ml tubes (Eppendorf, Hamburg, Germany). The tubes were centrifuged at 500 x g for 2 minutes to remove any debris. The extracted stain was added to a 96-well plate (Sarstedt, Nümbrecht, Germany) in triplicate at 100 µl per well and the absorbance was read using the dual-beam Cytofluor 4000 fluorimeter at 520 nm.

Reagent	**Final Concentration**
DMEM (Dulbecco's Modified Eagle Medium), high-glucose (HG)	
Dexamethasone 1mM	1µM
Insulin 1mg/ml	10µg/ml
Indomethacin 100mM	200µM
500mM MIX	500µM
Penecillin/Streptomycin	100U/mL penicillin 100µg/mL streptomycin
FBS	10%

Table 2.5. Adipogenic induction medium components and concentrations.

Reagent	Final Concentration
DMEM (HG)	
Insulin 1mg/ml	10μg/ml
Penecillin/Streptomycin	100U/mL penicillin 100μg/mL streptomycin
FBS	10%

Table 2.6. Adipogenic maintenance medium components and concentrations.

2.17 Osteogenesis

2.17.1 Osteogenic Differentiation

Untreated MSCs and MSCs treated with PC3 CM for 30 days were tested for their osteogenic differentiation capacity. Cells were harvested as described in section 2.3 and seeded at a density of 2.0 x 10^4 cells/cm^2 in each well of a 24-well cell+ plate (Sarstedt, Nümbrecht, Germany). The cells were incubated at 37°C with 5% CO_2 until they formed a monolayer, approximately 2 – 3 days. Once confluent, 1 ml of osteogenic induction medium was added to each test well and complete medium was added to control wells. See table 2.7 for osteogenic induction medium components and concentrations. The plate was incubated at 37°C with 5% CO_2 and the medium was changed twice a week for 15 – 17 days.

Following completion of the differentiation induction period the cells were analysed for osteogenesis. The level of osteogenic differentiation is assessed by measuring calcium using the StanBio Calcium Liquicolor Test (Stanbio, TX, USA) and staining deposited calcium with Alizarin Red (Sigma, MO, USA). Real-time PCR was performed to analyse the expression of RUNX2 (see section 2.10). Primer sequences are described in table 2.4.

2.17.2 Alizarin Red

Cells were washed twice in D-PBS and fixed in 90% Methanol (Sigma, MO, USA) for 10 minutes. The cells were washed and 2% Alizarin Red Solution (diluted using distilled water and brought to a pH of 4.1-4.3) for 5 minutes. The wells were then

washed in distilled H_2O and left to dry until microscopy upon which water was added. Images were obtained using an Olympus CKX41 inverted microscope (Olympus, Germany).

2.17.3 Calcium Assay

The medium was removed and wells were washed twice with D-PBS, followed by the addition of 200 µl of 0.5 M HCl. The cells were scraped out of each well and placed into individual 1.5 ml tubes (Eppendor, Hamburg, Germany). The tubes were left to shake overnight at 4°C. The samples were then centrifuged at 500 x g for 2 minutes to remove any cell debris and the Stanbio Kit (Stanbio, TX, USA) was used to measure the calcium in each sample following the manufacturer's guidelines.

The standard was made up in triplicate to a 96-well cell+ plate (Sarstedt, Nümbrecht, Germany) in volumes presented in table 2.8, with 10 µl of 0.5 M HCl. The sample was then added in triplicate in 10 µl volumes. A 1:1 solution of binding reagent and working dye (StanBio Calcium Liquicolor Test) was prepared and 200 µl was added to each of the wells. The absorbance was read using the dual-beam Cytofluor 4000 fluorimeter at 595 nm.

Reagent	**Final Concentration**
DMEM (LG)	
Dexamethasone 1mM	100nM
Ascorbic acid 2-P 10mM	100µM
β glycerophosphate 1M	10mM
FBS**	10%
Penecillin/Streptomycin	100U/mL penicillin 100µg/mL streptomycin

Table 2.7. Osteogenic induction medium components and concentrations.

Concentraion (µg/well)	Volume per well
0	0
0.05	0.5µl
0.1	1 µl
0.2	2 µl
0.4	4 µl
0.6	6 µl
0.8	8 µl
1	10µl

Table 2.8. Stanbio Kit Calcium Standard Dilutions.

2.18 Cytoxicity Assays

2.18.1 Cytoxicity Assays in Monoculture

Cells were harvested as described in section 2.3. The cells were resuspended in fresh complete medium at 3 x 10^4 cells/ml (MSCs) or 5 x 10^4 cells/ml (PC3 cells) and 100 µl of cell suspension was seeded into each well of a cell+ 96-well plate and cultured overnight in 5% CO_2 at 37°C. A range of concentrations of docetaxel (Sigma, MO, USA) originally diluted in DMSO and further diluted in complete medium, was prepared. The MSCs were treated with a range of 0 – 800 µM of docetaxel and PC3 cells were treated with a range of 0 – 10 µM of docetaxel and 0 – 100 µM of Paclitaxel. The medium in the wells was replaced with the drug dilutions and controls of DMSO only, and incubated at 37 °C in 5% CO_2 for a further 72 hours. Following this, the media was replaced with 200 µL fresh complete medium with an added 40 µL of 560 µM resazurin. The cells were incubated for 6 hours at 37°C. Plates were read using the dual-beam Cytofluor 4000 fluorimeter (Applied Biosystems, ThermoFisher, MA, USA) at excitation 530/25 and emission 620/40. A percentage (%) survival curve was calculated based on the generated values and the IC50 was determined using the

untreated cultures as reference comparison for uninhibited (100%) growth. The IC50 value was used for further experiments on MSC and PC3 cell cytoxicity.

2.18.2 Cytoxicity Assays in Co-culture

Untreated MSCs and MSCs treated for 30 days in PC3 CM were harvested as described in section 2.3. The MSCs were resuspended in fresh complete medium and seeded into the 0.4 µm microporous upper chamber wells of a HTS Transwell 96-well Permeable Plate (Corning) at a concentration of 2 x 10^4 cells/cm^2. The cells were allowed to form a monolayer. In the meantime, in a separate plate, PC3 cells were harvested and resuspended at 5 x 10^4 cells/ml and 100 µl was added to wells of the bottom chamber. The PC3 cells were left for 24 hours to allow the cells to attach. Following this, the concentration determined to be the IC50 in previous experiments using docetaxel and paclitaxel was made up in complete medium and 100 µl was added to the appropriate wells of the bottom chamber. The upper chamber containing the MSC monolayers placed over the wells containing the PC3 cells and the plate was incubated for 72 hours at 37°C with 5% CO_2. The alamar blue assay was carried out as described in the previous section.

2.19 Statistical Analysis

Statistical analyses were performed with GraphPad Prism software 6.0 (GraphPad Software, La Jolla, CA, USA). Error bars represent the standard deviation (SD) on most graphs and were calculated using GraphPad Prism. In graphs representing real-time PCR, the error bars represent upper and lower limits. Specific statistical tests used were paired and unpaired student's *t* tests or two-way ANOVAs, and all p values < 0.05 were considered statistically significant.

Chapter 3

Molecular Characterisation of Prostate Cancer Educated MSCs

3.1 Introduction

The tumour microenvironment is a chronic site of inflammation (Dvorak, 1986). Tumour cells release pro-inflammatory cytokines and chemokines that attract innate immune cells to the tumour which in turn release factors that activate the immune system. This cytokine rich milieu stimulates growth of the tumour and its invasive capacity (Hanahan and Coussens, 2012). MSCs have been found to migrate towards inflammatory sites and in normal tissue have a reparative function (Ortiz et al., 2003, Sato et al., 2005, Wu et al., 2003). Recent studies have shown a role for MSCs in tumour promotion and although the mechanisms are not yet clear, they have been found to release and respond to cytokines at the tumour site (Li et al., 2015, Dwyer et al., 2007, Menon et al., 2007). Additionally, tumour growth relies on new blood capillary formation and MSCs have been suggested to contribute to neovascularisation through the secretion of growth factors including VEGF (Suzuki et al., 2011, Kinnaird et al., 2004).

The first part of this study aims to investigate the secretory profile of MSCs that have been exposed to prostate cancer cell CM for up to 30 days and to assess whether changes in the secretion profile occur and if they are sustained after the exposure period. Particular focus was given to the secretion of cytokines, chemokines and growth factors. MSCs were initially grown for a 48 hour period in prostate cancer cell CM, however it was thought that given the plasticity of MSCs, a longer conditioning period may evoke cell differentiation or a permanently altered state of activation. The cells were thus grown for 20 and 30 day periods in 22Rv1, DU145 and PC3 CM to allow time for cell differentiation to occur. MSCs grown in each different prostate cancer cell CM varied in their cytokine and chemokine secretory profile in comparison to the untreated MSCs, particularly DU145 and PC3 conditioned MSCs which showed the greatest similarities. MSCs exposed to PC3 cell CM had the most diverse secretory profile and these cells were chosen for further validation studies.

It cannot be concluded from the data that the cells are differentiating however, they did show a sustained response in cytokine and growth factor production after the conditioning period and were therefore termed ‘educated’ for the purpose of the

study. With this in mind, we considered it important to molecularly and functionally characterise the educated MSCs before addressing their effect on tumour cell function.

The second part of the study focuses on whether the educated MSCs display alterations in the molecular characteristics classically associated with MSCs, and thus were analysed for the presence of MSC cell surface markers CD105, CD90 and CD73. Also, MSCs are considered as a possible origin of cancer associated fibroblasts (CAFs) and in previous research it has been found that long-term conditioning of MSCs in breast and ovarian cancer cell CM resulted in the formation of CAFs (Mishra et al., 2008, Spaeth et al., 2009). It was therefore relevant to this study to determine whether PC3 educated MSCs could be characterised as CAFs and so they were analysed for the presence of the CAF markers - αSMA, FSP1, FAP and vimentin.

The MSCs used for this study were derived from the bone marrow of healthy male donors at at ages 38 (donor 1), 25 (donor 2), 20 (donor 3) and 26 (donor 4) as described in section 2.1. The age of the MSC donors does not represent the age cohort of prostate cancer patients; however MSCs derived from younger healthy donors are useful for preliminary proof-of-concept studies. The MSCS were isolated at passage 0 or 1 and used experimentally up to passage 7. PC3 and DU145 cells are human male cells originally derived from the bone and brain metastatic site, respectively. The human prostate cancer cell line, 22Rv1, was originally derived from a castrate resistant mouse xenograft model of parental CWR22 (section 2.2). The subsequent cell line 22Rv1 is androgen independent through a mutation in the androgen receptor and is non-metastatic. MSCs and cancer cells were grown in the same MSC complete growth medium throughout the duration of the study.

3.2 Results

3.2.1 Short-term Conditioning of MSCs with Prostate Cancer Conditioned Medium Increases Growth Factor Secretion

MSCs have been shown to secrete pro-angiogenic growth factors that could enhance neovascularisation at the tumour site (Suzuki et al., 2011, Kinnaird et al., 2004). We

therefore considered an increase in the secretion of growth factors in MSCs in response to factors released by prostate cancer cells. The impact of conditioning MSCs for 48 hours was initially investigated. Following the 48 hour treatment, the MSCs were grown for a further 48 hours in fresh complete medium in order to detect factors secreted by the treated MSCs alone (described in section 2.4). The samples were analysed for the secretion of VEGF, placental growth factor (PlGF), soluble fms-like tyrosine kinase-1 (sFlt-1) and FGF2 using the MesoScale Discovery system as described in section 2.6.2. The experiment was repeated using two human male MSC donors. The lower limit of detection of each analyte is described in table 2.1.

MSCs derived from donor 1 and 4 showed an increase in the secretion of VEGF following 48 hours of treatment in PC3 and DU145 CM, while MSCs derived from donor 4 but not donor 1 showed an increase in VEGF secretion following 48 hours of treatment in 22Rv1 CM (figure 3.1 A+B). Overall, pooling data from both donors, the difference was statistically significant in MSCs treated with PC3 CM (paired student's t-test; two-tailed; $p<0.01$; n=2 biological replicates) and DU145 CM (paired student's t-test; two-tailed; $p<0.05$; n=2 biological replicates) but not 22Rv1 CM (paired student's t-test; two-tailed; n=2 biological replicates).

MSCs derived from donor 1 and 4 showed an increase in the secretion of PlGF following 48 hours of treatment in PC3, DU145 and 22Rv1 CM (figure 3.1 C+D). Overall, pooling data from both donors, the difference was statistically significant in MSCs treated with PC3 CM (paired student's t-test; two-tailed; $p<0.01$; n=2 biological replicates) and DU145 CM (paired student's t-test; two-tailed; $p<0.001$; n=2 biological replicates) but not 22Rv1 CM (paired student's t-test; two-tailed; n=2 biological replicates).

In a similar trend to the VEGF secretion (figure 3.1 A+B), MSCs derived from donor 1 and 4 showed an increase in the secretion of sFlt-1 following 48 hours of treatment in PC3 and DU145 CM, while MSCs derived from donor 4 but not donor 1 showed an increase in sFlt-1 secretion following 48 hours of treatment in 22Rv1 CM (figure 3.1 E+F). However, the overall difference was not statistically significant in MSCs treated

with PC3, DU145 or 22Rv1 CM (paired student's t-test; two-tailed; n=2 biological replicates).

The cells were tested for the secretion of FGF2 however, the levels were below the limits of detection and the data is therefore not shown.

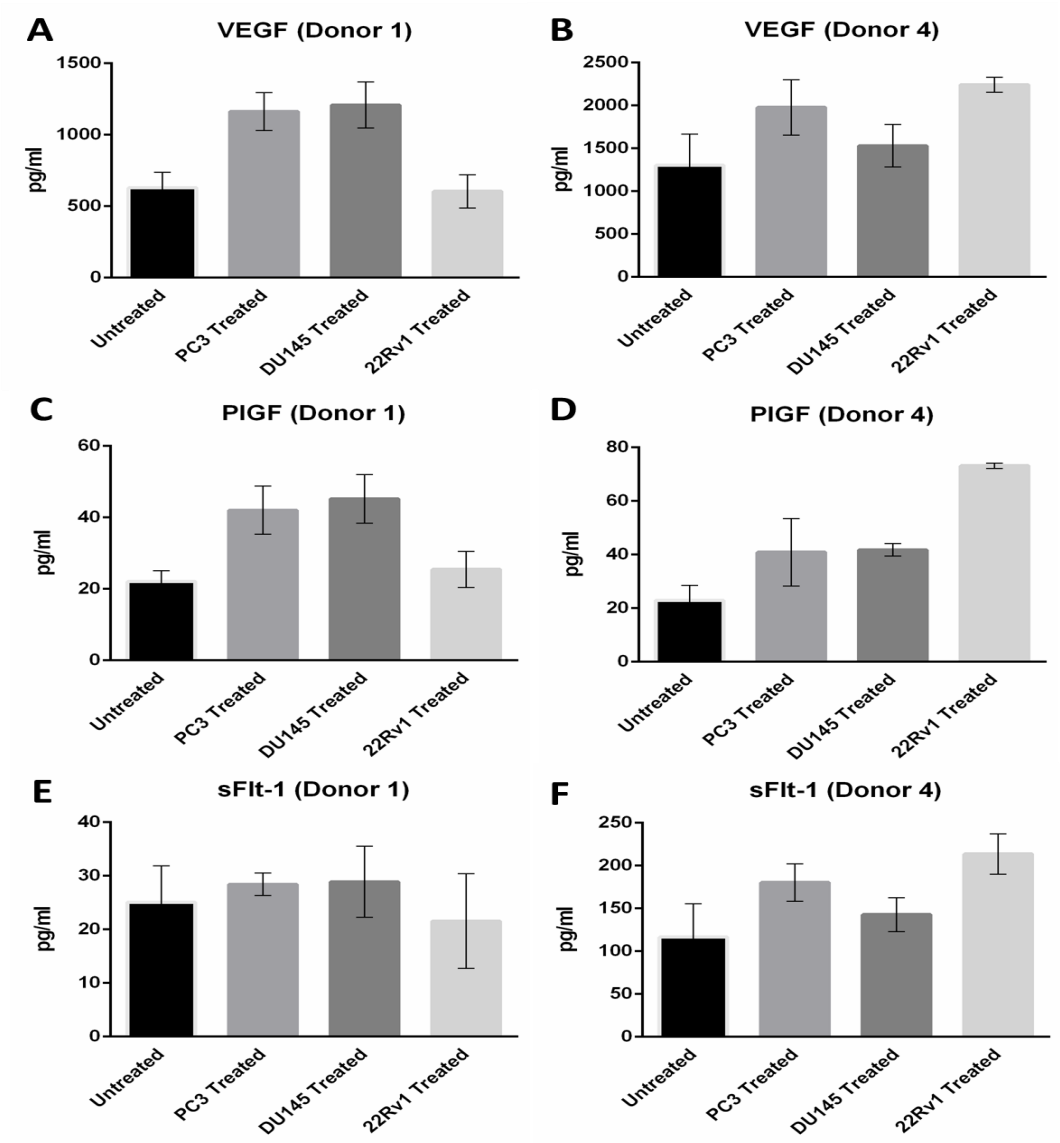

Figure 3.1. Secretion of Growth Factors from MSCs exposed for 48 hours to Prostate Cancer Cell CM. The MesoScale Discovery system was used to quantitatively detect growth factor secretion in MSCs treated for 48 hours with PC3, DU145 and 22Rv1 CM. MSCs derived from donor 1 and 4 showed an increase in VEGF (A+B) and sFlt-1 (E+F) secretion following treatment in PC3 and DU145 CM, while MSCs from donor 4 but not donor 1 showed an increase in VEGF (A+B) and sFlt-1 (E+F) secretion following treatment in 22Rv1 CM. MSCs derived from donor 1 and 4 showed an increase in PlGF secretion (C+D) following treatment with PC3, DU145 and 22Rv1 CM. Overall, pooling data from both donors, the difference in VEGF secretion was statistically significant in MSCs treated with PC3 CM (paired student's t-test; two-tailed; $p<0.01$; n=2 biological replicates) and DU145 CM (paired student's t-test; two-tailed; $p<0.05$; n=2 biological replicates) but not 22Rv1 CM (paired student's t-test; two-tailed; n=2 biological replicates). The difference in PlGF secretion was statistically significant in MSCs treated with PC3 CM (paired student's t-test; two-tailed; $p<0.01$; n=2 biological replicates) and DU145 CM (paired student's t-test; two-tailed; $p<0.001$; n=2 biological replicates) but not 22Rv1 CM (paired student's t-test; two-tailed; n=2 biological replicates). The difference in sFlt-1 secretion was not statistically significant in MSCs treated with PC3, DU145 or 22Rv1 CM (paired student's t-test; two-tailed; n=2 biological replicates). Data represents the mean of technical replicates ± SD.

3.2.2 Secretory Profile of Long-term Conditioned MSCs

This study aims to investigate the impact on MSCs following long-term exposure to the secretome derived from prostate cancer cells. To this end we examined the molecular changes that occur in MSCs that were educated in PC3, DU145 and 22Rv1 CM for 20 days. The cells were then harvested, re-seeded and grown for a further 24 hours in fresh complete medium to ensure assessment of the MSC secretion profile alone. The cytokine and chemokine screen was performed using proteome profilers as described in section 2.7.

Untreated MSCs and 22Rv1 educated MSCs share a similar secretory profile however, densitometry analysis shows 22Rv1 educated MSCs have decreased production of plasminogen activator inhibitor-1 (PAI-1) in comparison to DU145 educated, PC3 educated and untreated MSCs (figure 3.2 A+B). DU145 and PC3 educated MSCs were found to be more active in pro-inflammatory cytokine production (figure 3.2 A). DU145 and PC3 educated MSCs showed similar levels of OPN, YKL-40 (also known as chitinase-3-like protein 1), FGF-19 and IL-17A secretion (figure 3.2 A+B). Nonetheless, PC3 educated MSCs had the greatest response to the 20 day treatment in relation to cytokine production and secreted elevated IL-6, IL-8, endoglin (CD105), MCP-1, IL-11 and macrophage migration inhibitory factor (MIF) in comparison to 22Rv1 educated, DU145 educated and untreated MSCs (figure 3.2 A+B).

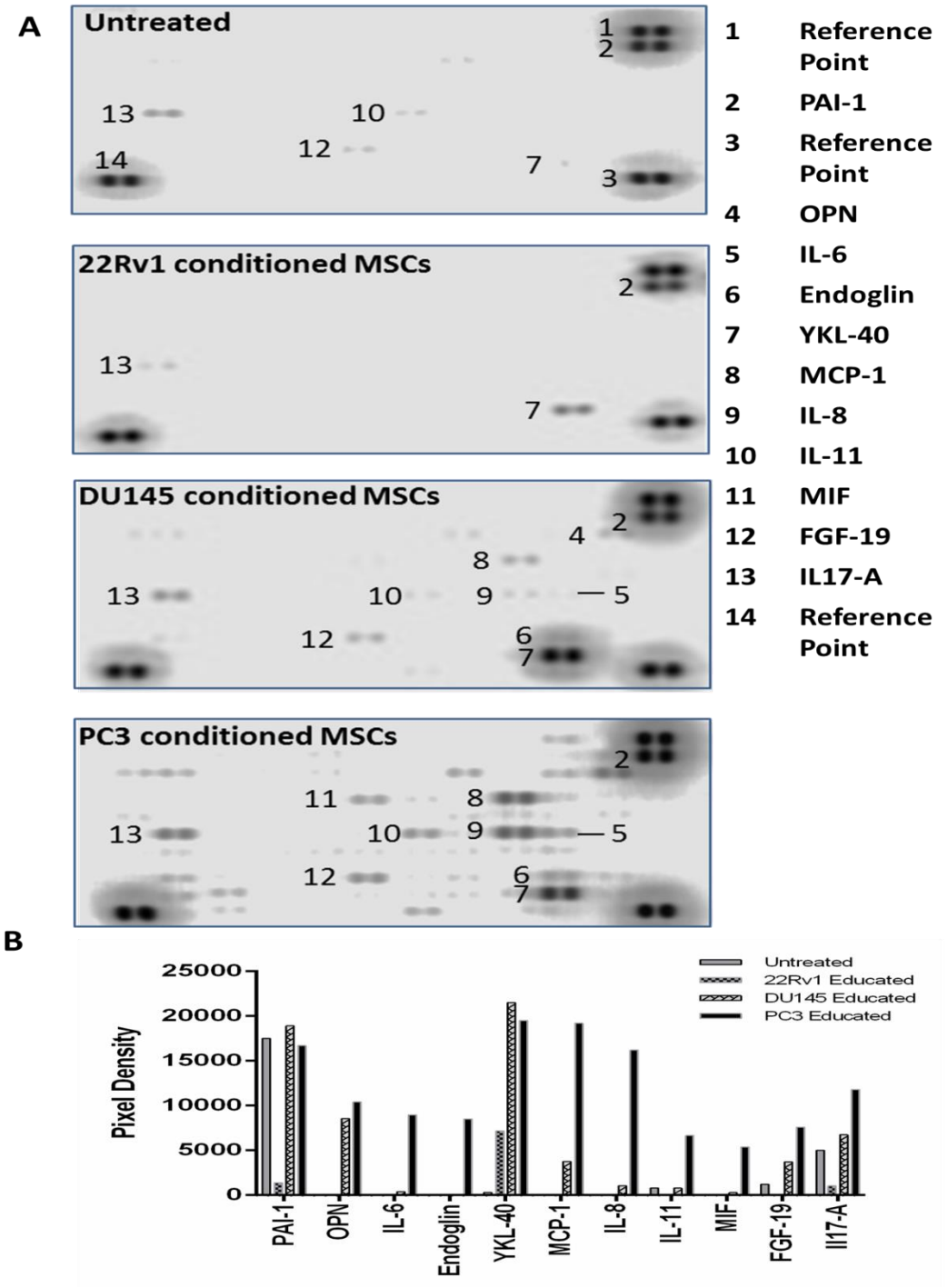

Figure 3.2. Cytokine and Chemokine Secretory Profile of 22Rv1, DU145 and PC3 Educated MSCs. Proteome profilers were used to screen untreated MSCs and educated MSCs for cytokine and chemokine secretion. Untreated MSCs and 22Rv1 educated MSCs showed a similar secretory profile following 20 days of treatment, while DU145 and PC3 educated MSCs showed the most activity in cytokine and chemokine production (A). Densitometry analysis revealed that 22Rv1 educated MSCs secreted decreased PAI-1 in comparison to DU145 educated, PC3 educated and untreated MSCs (B). Both DU145 and PC3 educated MSCs showed an increase in the production of OPN, YKL-40 (also known as chitinase-3-like protein 1), FGF-19 and IL-17A in comparison to untreated MSCs (A+B). PC3 educated MSCs secreted elevated IL-6, IL-8, endoglin (CD105), MCP-1, IL-11 and MIF following 20 days of treatment in comparison to untreated MSCs (A+B).

3.2.2.1 *Secretory Profile of PC3 educated MSCs following 30 days of Conditioning*

MSCs were found to be the most responsive, in terms of cytokine and chemokine production, to PC3 CM in comparison to 22Rv1 CM and DU145 CM following 20 days of conditioning (section 3.2.2). We then treated the PC3 educated MSCs for a further 10 days with PC3 CM to evaluate whether a longer treatment period could induce a more enhanced response. MSCs were treated for 30 days with PC3 CM, the cells were then harvested, re-seeded and grown for a further 24 hours in fresh complete medium to ensure assessment of the MSC secretion profile alone. The cytokine and chemokine screen was performed using proteome profilers as described in section 2.7. Similar to the 20 day treatment, MSCs treated for 30 days in PC3 CM showed an increase in the secretion of OPN, IL-6, IL-8, endoglin (CD105), MCP-1 and MIF with additional detection of insulin-like growth factor binding protein-2 (IGFBP-2), Dickkopf WNT signalling pathway inhibitor 1 (DKK-1), VEGF and extracellular matrix metalloproteinase inducer (EMMPRIN) in comparison to untreated MSCs (figure 3.3 A+B).

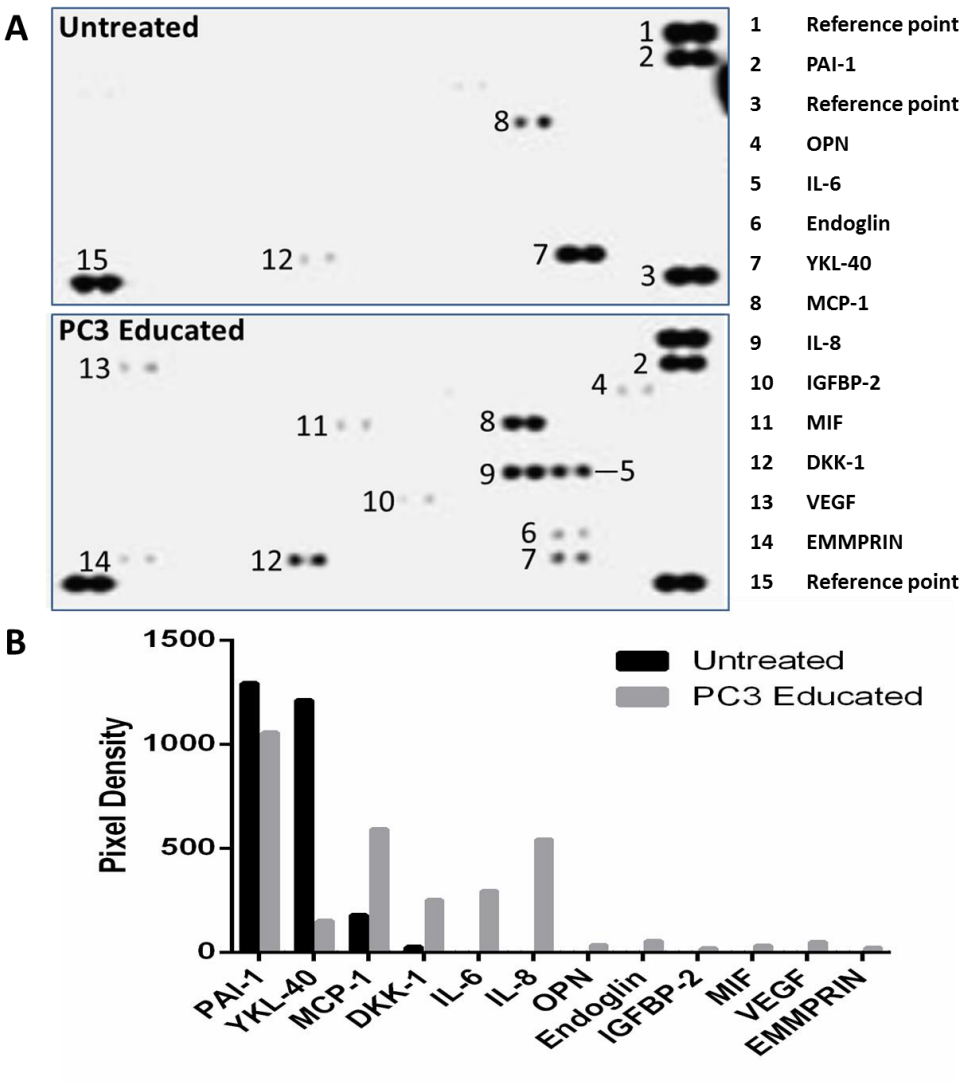

Figure 3.3. Cytokine and Chemokine Secretory Profile of PC3 Educated MSCs Following 30 days of conditioning. As with the MSCs that were treated for 20 days in PC3 CM, MSCs treated for 30 days in PC3 CM showed an increase in the secretion of OPN, IL-6, IL-8, endoglin (CD105), MCP-1 and MIF with additional detection of IGFBP-2, DKK-1, VEGF and EMMPRIN following 30 days of treatment (A+B).

3.2.3 Cytokine and Chemokine Screen of Prostate Cancer Cell Conditioned Medium

The CM isolated from 22Rv1, DU145 and PC3 cells (as described in section 2.4) was screened for the presence of cytokines and chemokines using proteome profilers (as described in section 2.7). Insight into the secretion profile of the cell lines used in this study will aid in deciphering what active factors released by the cancer cells contribute to molecular and functional changes in the educated MSCs. PC3 CM contains the highest level of secretion factors including PAI-1, Gro-α, ENA-78 (also known as CXCL5), Lipocalin-2, IL-8, Angiogenin, MIF, FGF-9, Thrombospondin-1 (TSP-

1), DKK-1, growth differentiation factor-15 (GDF-15), IL-17A, granulocyte macrophage colony stimulating factor (GM-CSF) and EMMPRIN (figure 3.4). DU145 cells share a similar secretion profile with PC3 cells in the production of Gro-α, ENA-78, IL-8, Angiogenin, DKK-1, IL-17A, GM-CSF and EMMPRIN. However, DU145 CM was the only supernatant to contain detectable levels of urokinase receptor (uPAR) and VEGF (figure 3.4). Although 22Rv1 cells were found to secrete the highest level of angiogenin they showed the lowest level of cytokine and chemokine production with the only other detectable protein being MIF (figure 3.4).

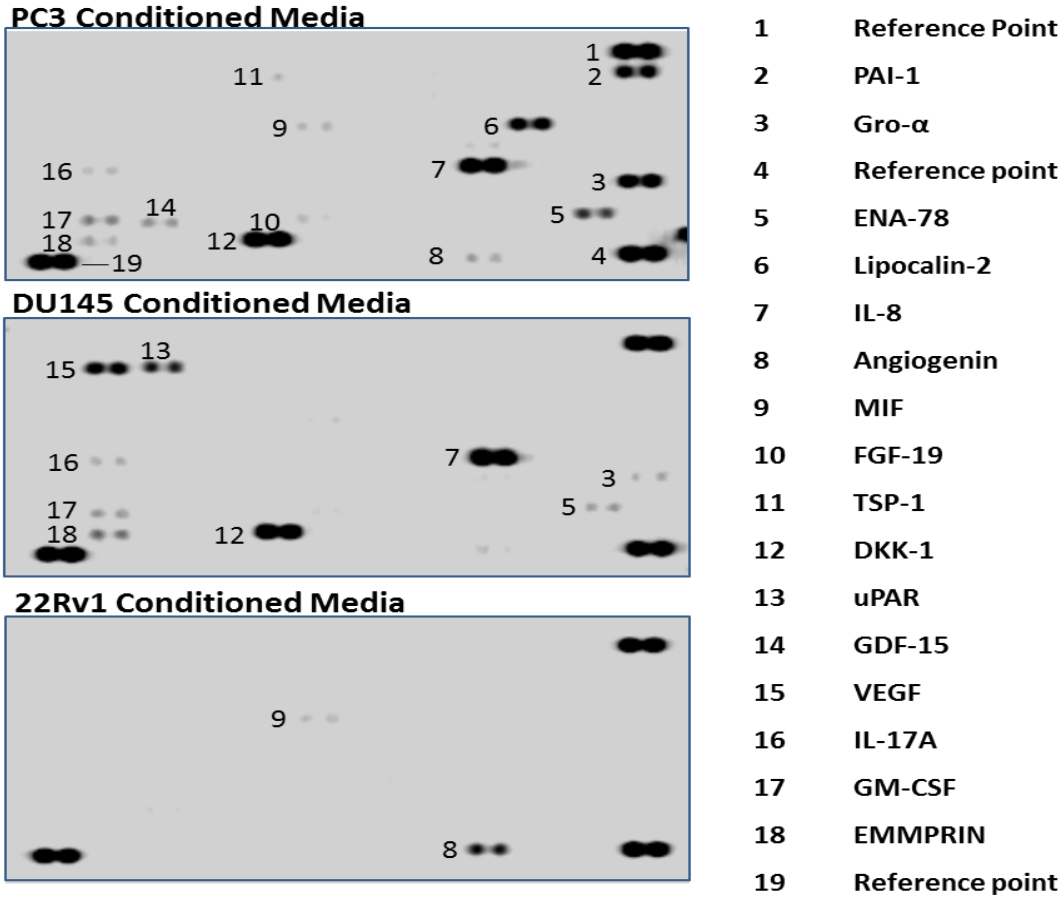

Figure 3.4. Cytokine and Chemokine Profile of Prostate Cancer Cell CM. The secretion profile of the prostate cancer cell CM used in this study was assessed using proteome profilers. PC3 cells showed the highest level of cytokine and chemokine production with the release of PAI-1, Gro-α, ENA-78, Lipocalin-2, IL-8, Angiogenin, MIF, FGF-9, Thrombospondin-1 (TSP-1), DKK-1, GDF-15, Il17-A, GM-CSF and EMMPRIN. DU145 CM shares a similar profile in the production of Gro-α, ENA-78, IL-8, Angiogenin, DKK-1, IL-17A, GM-CSF and EMMPRIN with the addition of uPAR and VEGF. 22Rv1 cells were found to secrete the lowest level cytokine and chemokines yet produced MIF and the highest level of Angiogenin.

3.2.4 Quantitative Validation of Cytokine Secretion from PC3 Educated MSCs

Selected cytokines shown to be secreted by PC3 educated MSCs in section 3.2.2 were quantitatively analysed using the MesoScale Discovery system for protein quantification (described in section 2.6.1) and real-time PCR for mRNA quantification (as described in section 2.10). Due to the reduced quality in mRNA from one of three donor MSCs at the time of analysis, mRNA from only two MSC donors was used during this study. The cells were harvested at 10, 20 and 30 day time-points as described in section 2.3 and placed in fresh complete medium for 24 hours in order to assess the secretion of the indicated proteins by the PC3 educated MSCs without the presence of PC3 CM. Additionally, MSCs treated for 30 days in PC3 CM were then grown for an extended period (12 - 16 days) in normal complete medium to assess whether any change in cytokine secretion was sustained. Gene expression was analysed at the 30 day time-point only. OPN, MCP-1, IL-6 and IL-8 were chosen to be quantitatively validated. The lower limit of detection of each analyte is described in table 2.1. The secretion of SDF-1α was evaluated using the enzyme-linked immunosorbant assay method however, the protein was below the limits of detection in the supernatants collected from untreated MSCs and PC3 educated MSCs at each time-point (data not shown).

3.2.4.1 PC3 Educated MSCs Secrete Increased Osteopontin

MSCs derived from all donors showed an increase in OPN secretion following 10 days of treatment in PC3 CM. While the untreated MSCs secreted a mean of 38.7 pg/ml of OPN, the PC3 educated MSCs secreted a 4.5 fold increase at 175.5 pg/ml with donor 3 cells showing the highest increase (figure 3.5 A) and overall, the difference was statistically significant (paired student's t-test; two-tailed; $p<0.01$; n=3 biological replicates). PC3 educated MSCs from donors 1 and 3 show the same trend following 20 days of treatment secreting 423 and 459 pg/ml respectively. MSCs derived from donor 2 did not respond to the 20 day conditioning period with OPN secretion at a similar level to the untreated MSCs (figure 3.5 B). However, overall, combining data from all donor MSCs, the difference was statistically significant (paired student's t-test; two-tailed; $p<0.05$; n=3 biological replicates). All donor MSCs responded to the 30 day exposure to PC3 CM with an increase in OPN (figure 3.5 C). Untreated MSCs

secreted a mean of 72.7 pg/ml while the PC3 educated MSCs secreted a 5.6 fold increase at 411.6 pg/ml and the difference between untreated MSCs and PC3 educated MSCs was statistically significant (paired student's t-test; two-tailed; $p<0.0001$; n=3 biological replicates) (figure 3.5 C). The PC3 educated MSCs continued to secrete higher levels of OPN following extended growth in complete medium post-conditioning, particularly in MSCs from donors 1 and 2, however to a lesser degree. A mean of 47.5 pg/ml was detected in the untreated MSCs while a 4.3 fold increase at 206.5 pg/ml was detected in the PC3 educated MSCs post-conditioning, and the difference was statistically significant (paired student's t-test; two-tailed; $p<0.01$; n=3 biological replicates) (figure 3.5 D).

Furthermore, gene expression analysis showed a 39.5 and 33.0 fold increase in the expression of SPP1 (OPN) mRNA in 30 day treated PC3 educated MSCs from donor 1 and 3, respectively, compared to the untreated MSCs. Overall, combining data from both donor MSCs, the result was statistically significant (unpaired student's t-test, two-tailed, $p<0.01$; n=2 biological replicates). Taken together, MSCs exposed to PC3 CM for 30 days results in an increase in OPN production.

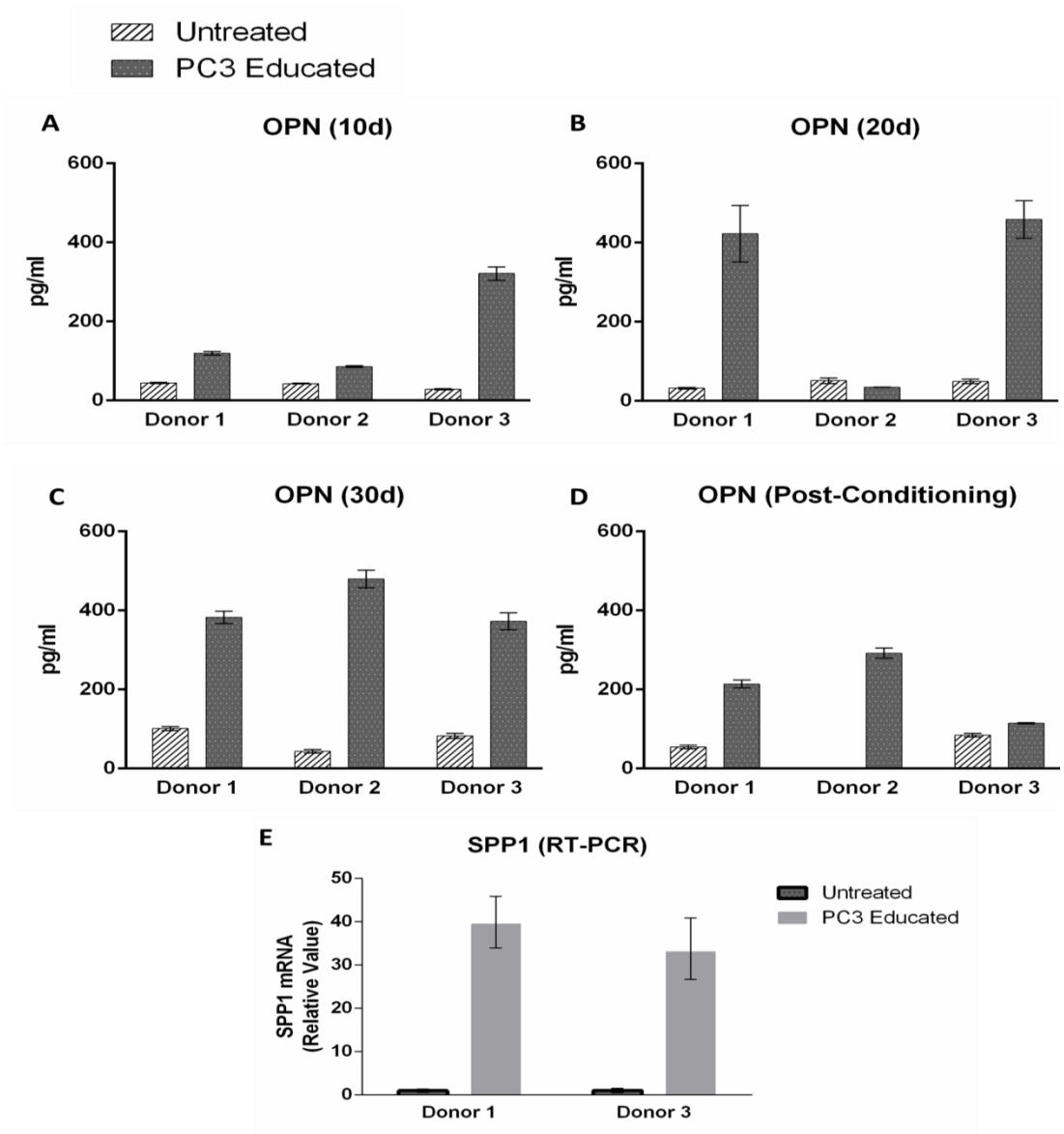

Figure 3.5. Quantitative Analysis of OPN Secretion from PC3 Educated MSCs. OPN secretion was quantitatively measured using the MesoScale Discovery system. A statistically significant increase in OPN was detected in all donor MSCs following 10 days of treatment with PC3 CM (paired student's t-test; two-tailed; $p<0.01$; n=3 biological replicates) (A). Following 20 days exposure to PC3 CM, MSCs derived from donors 1 and 3 responded with an increase in OPN, while MSCs derived from donor 2 had a similar secretion level to the untreated MSCs (B). MSCs from all donors responded to the 30 day treatment with an increase in the secretion of OPN, which overall was statistically significant (paired student's t-test; two-tailed; $p<0.0001$; n=3 biological replicates) (C). The 30 day conditioned MSCs grown for an extended period in complete medium sustained an increase in OPN secretion, particularly in MSCs derived from donors 1 and 2. Although the secretion was at a lower level to the 30 day time-point, it was found to be statistically significant (paired student's t-test; two-tailed; $p<0.01$; n=3 biological replicates) (D). Data represents the mean of technical replicates ± SD. Gene expression analysis using showed an overall statistically significant upregulation in SPP1 (OPN) expression (unpaired student's t-test, two-tailed, $p<0.01$; n=2 biological replicates). Values for gene expression analysis were normalised to the untreated controls (E). Data represents the mean of technical replicates with upper and lower limits.

3.2.4.2 PC3 Educated MSCs Secrete Increased MCP-1

MSCs derived from all donors showed an increase in the secretion of MCP-1 following 10 days exposure to PC3 CM and the difference was statistically significant (paired student's t-test; two-tailed; $p<0.01$; n=3 biological replicates). The untreated MSCs secreted a mean of 1257.83 pg/ml of MCP-1 while the PC3 educated MSCs secreted a 1.5 fold increase at 1881.5 pg/ml (figure 3.6 A). MSCs derived from donors 1 and 3 maintained an increase following 20 days exposure to PC3 CM while MSCs from donor 2 showed a decrease. The overall difference after 20 days of conditioning however, was not statistically significant (paired student's t-test; two-tailed; n=3 biological replicates) (figure 3.6 B). PC3 educated MSCs from each donor showed a consistent increase in the secretion of MCP-1 following 30 days of conditioning, which was considerably increased in donors 1 and 2 in comparison to previous time-points. A mean of 831.5 pg/ml was detected in untreated MSC supernatants while the PC3 educated MSCs secreted a 3.6 fold increase in MCP-1 at 3017.1 pg/ml and overall, combining data from all donors, the difference was statistically significant (paired student's t-test; two-tailed; $p<0.0001$; n=3 biological replicates) (figure 3.6 C).

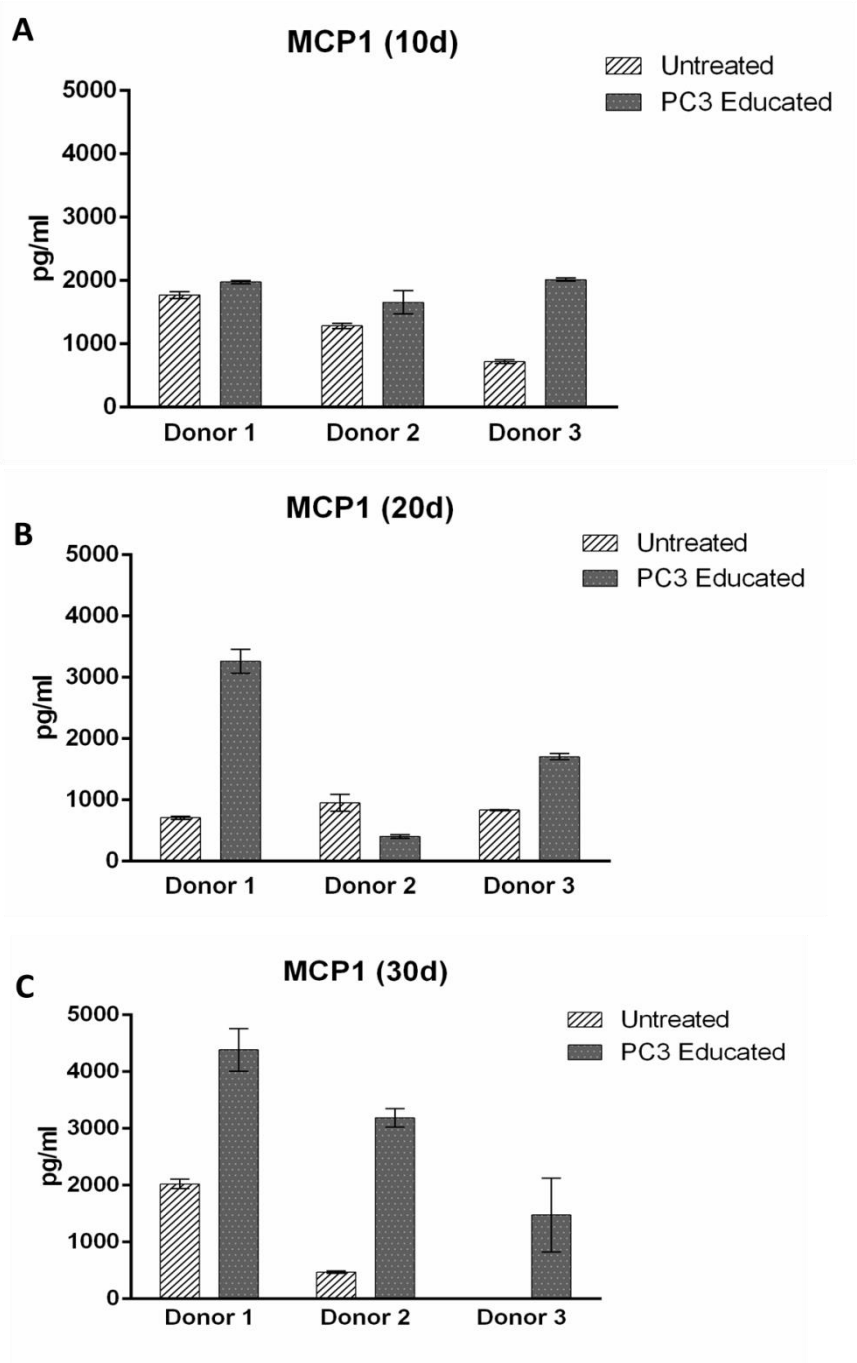

Figure 3.6. Quantitative Analysis of MCP-1 Secretion from PC3 Educated MSCs. MCP-1 secretion was measured quantitatively using the MesoScale Discovery system. There was an increase in MCP-1 production in all donor MSCs that had been treated for 10 days in PC3 CM, which taken together was statistically significant (paired student's t-test; two-tailed; $p<0.01$; n=3 biological replicates). An increase was found in MSCs derived from donors 1 and 3 following 20 days of treatment but not donor 2, however, overall the difference was not statistically significant (paired student's t-test; two-tailed; n=3 biological replicates). All donor MSCs showed an increase in MCP-1 secretion following 30 days of treatment in PC3 CM. A noticeable increase was found in PC3 educated MSCs from donors 1 and 2 in comparison to previous time-points and taken together the difference was statistically significant (paired student's t-test; two-tailed; $p<0.0001$; n=3 biological replicates). Data represents the mean of technical replicates ± SD.

3.2.4.3 PC3 Educated MSCs and IL-6 Secretion

An increase in IL-6 secretion was found in all donor MSCs that had been treated for 10 days in PC3 CM and overall the difference was statistically significant (paired student's t-test; two-tailed; $p<0.001$; n=3 biological replicates). The untreated MSCs secreted a mean of 13375.9 pg/ml, whereas the PC3 educated MSCs secreted 22479.5 pg/ml (figure 3.7 A). Similar to MCP-1 secretion at the 20 day time-point (figure 3.7 B), an increase in the secretion of IL-6 was found in MSCs derived from donors 1 and 3 exposed to PC3 CM for 20 days but not in MSCs derived from donor 2 and the difference was statistically significant (paired student's t-test; two-tailed; $p<0.05$; n=3 biological replicates) (figure 3.7 B). The increase in IL-6 secretion found in MSCs derived from donor 1 was maintained at the 30 day time-point but not in MSCs derived from donor 3 (figure 3.7 C). The increase in IL-6 secretion from donor 1 MSCs that were treated for 30 days in PC3 CM was not maintained following growth post-conditioning (figure 3.7 D). Furthermore, using gene expression analysis, MSCs derived from two separate donors (note - limited mRNA was available from donors and so not all donors were included in RT-PCR experiments) and treated for 30 days in PC3 CM did not show upregulation in IL-6 expression in comparison to the untreated MSCs and overall, combining data from both donor MSCs, the difference was not statistically significant (unpaired student's t-test, two-tailed; n=2 biological replicates) (figure 3.7 E). Taken together, PC3 CM exposure does not induce an increase in IL-6 production following 20 and 30 days of conditioning.

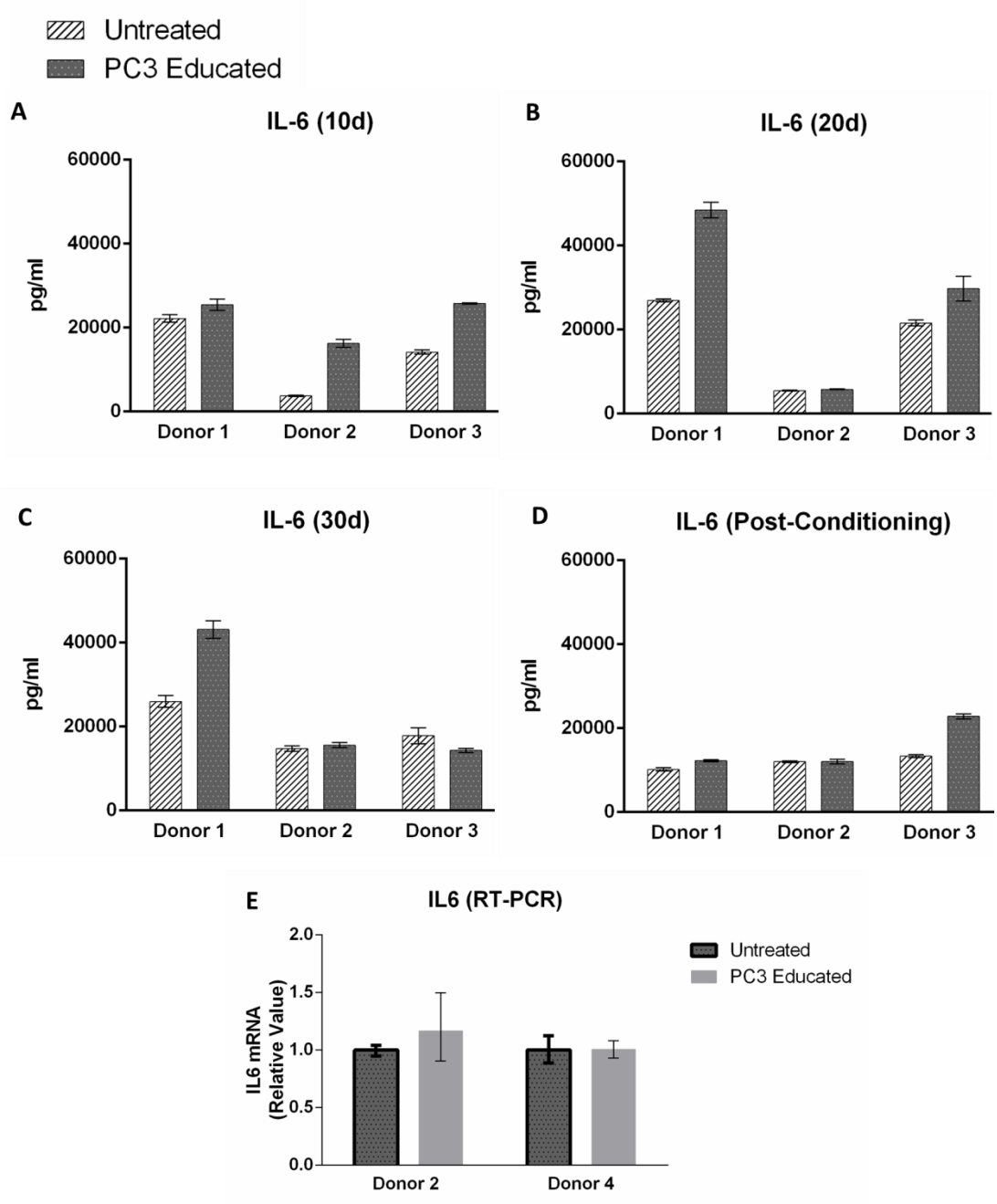

Figure 3.7. Quantitative Analysis of IL-6 Secretion from PC3 Educated MSCs. IL-6 secretion was measured using the MesoScale Discovery system. An increase was found in all donor MSCs exposed to PC3 CM for 10 days and overall, the difference was statistically significant (paired student's t-test; two-tailed; $p<0.001$; n=3 biological replicates) (A). MSCs derived from donors 1 and 3 secreted an increase in IL-6 following 20 days exposure to PC3 CM and overall, combining data from all donors, the difference was significant (paired student's t-test; two-tailed; $p<0.05$; n=3 biological replicates) (B). Following 30 days of conditioning, the increase in IL-6 secretion was maintained in PC3 educated MSCs from donor 1 only (C), this however was not maintained following long-term culture in complete medium post-conditioning (D). Data represents the mean of technical replicates ± SD. Gene expression analysis showed no upregulation of IL-6 in MSCs that had been treated for 30 days in PC3 CM. Values for gene expression analysis were normalised to the untreated controls (E). Data represents the mean of technical replicates with upper and lower limits.

3.2.4.4 PC3 Educated MSCs Secrete Increased IL-8

A consistent increase in IL-8 secretion was found in all donor MSCs exposed to PC3 CM for 10 days. Untreated MSCs were found to secrete IL-8 at a mean of 23495.5 pg/ml, whereas the PC3 educated MSCs secreted a 6.8 fold increase at 158654.1 pg/ml and the overall difference was statistically significant (paired student's t-test; two-tailed; $p<0.0001$; n=3 biological replicates) (figure 3.8 A). Following 20 days of exposure, MSCs derived from donor 1 were the most responsive to PC3 CM (up to 646442 pg/ml IL-8). Overall, combining data from all donors, the difference between the untreated MSCs and PC3 educated MSCs at day 20 was statistically significant (paired student's t-test; two-tailed; $p<0.05$; n=3 biological replicates) (figure 3.8 B). Furthermore, an increase was found in IL-8 secretion in all donor MSCs exposed to PC3 CM for 30 days. The mean IL-8 secretion in the untreated MSCs was 32703.9 pg/ml while the PC3 educated MSCs secreted a 6.5 fold increase at 212227.2 pg/ml (figure 3.8 C). The increase, like at the previous time-point, was most pronounced in donor 1 MSCs and overall, combining data from all donors, the difference between untreated MSCs and PC3 educated MSCs was statistically significant (paired student's t-test; two-tailed; $p<0.05$; n=3 biological replicates).

A considerable drop was noted in IL-8 secretion from donor 1 and 3 PC3 educated MSCs, following long-term culture in complete medium (figure 3.8 D). Nonetheless, a statistically significant increase in the secretion of IL-8 was found between all untreated MSCs and PC3 educated MSCs post-conditioning (paired student's t-test; two-tailed; $p<0.01$; n=3 biological replicates). Taken together, MSCs secreted increased IL-8 following 10, 20 and 30 days exposure to PC3 CM, and an increase was sustained following long-term culture in complete medium. The results were further validated using gene expression analysis. Furthermore, MSCs derived from two separate donors and treated for 30 days with PC3 CM showed an upregulation in the gene expression of IL-8 in comparison to the untreated MSCs however overall, given the variation in expression between donors, the difference was not statistically significant (unpaired student's t-test, two-tailed; n=2 biological replicates) (figure 3.8 E).

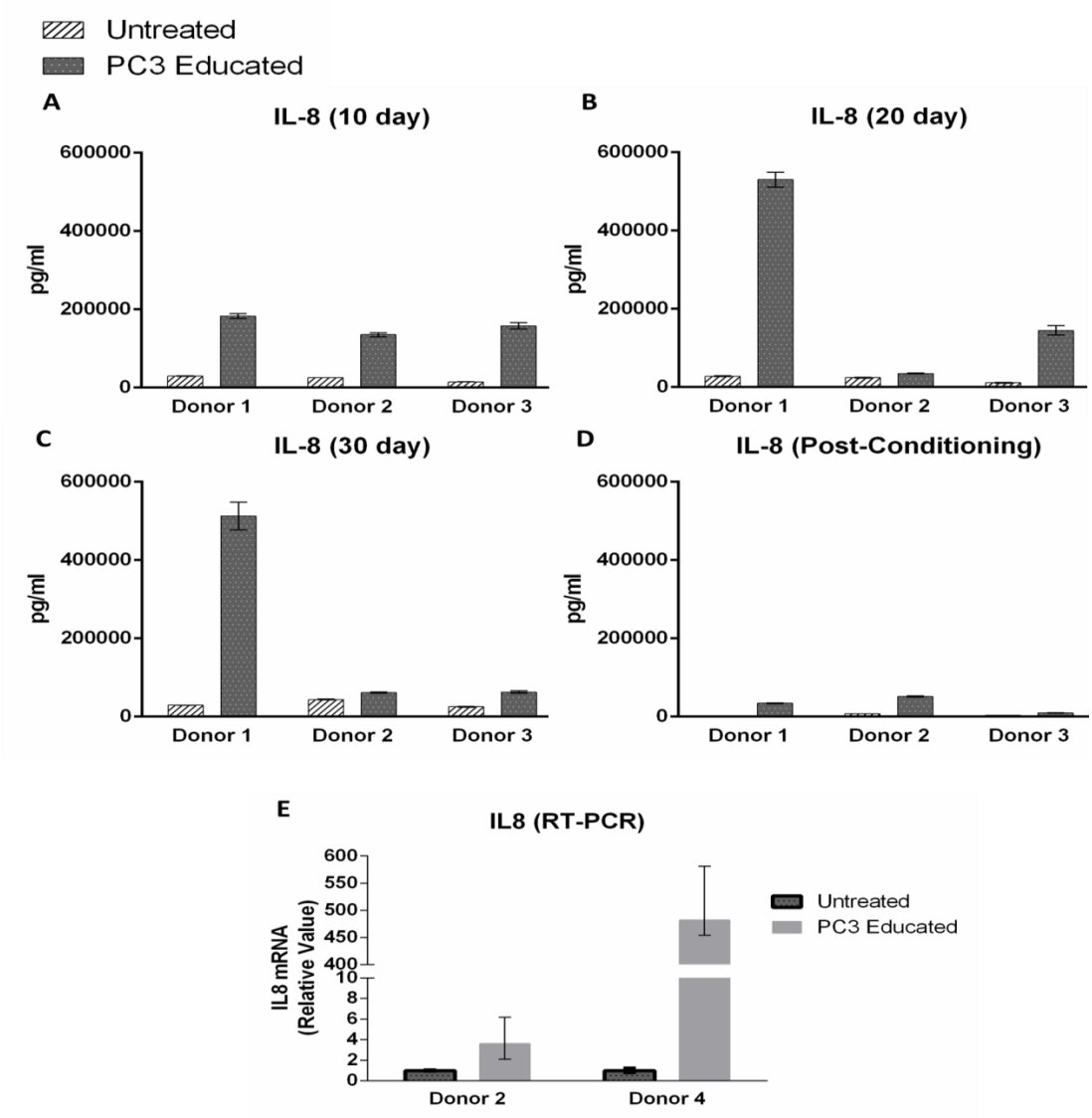

Figure 3.8. Quantitative Analysis of IL-8 Secretion from PC3 Educated MSCs. Quantitative measurement of IL-8 secretion was assessed using the MesoScale Discovery Platform. All PC3 educated donor MSCs showed an increase in IL-8 secretion in comparison to the untreated MSCs at all time-points and this was maintained in 30 day treated MSCs that were cultured for long-term in complete medium (A-D). The level of increase was consistent at the 10 day time-point (A), with an overall statistically significant difference (paired student's t-test; two-tailed; $p<0.0001$; n=3 biological replicates). Donor 1 PC3 educated MSCs had the highest production at the 20 and 30 day time-points (B+C), which decreased considerably following long-term culture in complete medium (D). While, PC3 educated MSCs derived from donors 2 and 3 were more fluctuant in their secretion patterns (A, B+C), PC3 educated MSCs from both donors sustained an increase post-conditioning. The overall difference between untreated MSC and PC3 educated MSC secretion was statistically significant at the 20 (paired student's t-test; two-tailed; $p<0.05$; n=3 biological replicates) and 30 day (paired student's t-test; two-tailed; $p<0.05$; n=3 biological replicates) time-points and post-conditioning (paired student's t-test; two-tailed; $p<0.01$; n=3 biological replicates). Data represents the mean of technical replicates ± SD. Gene expression analysis shows a similar trend where PC3 educated MSCs conditioned for 30 days showed upregulated IL-8 expression. Values for gene expression analysis were normalised to the untreated controls (E). Data represents the mean of technical replicates with upper and lower limits.

3.2.5 Quantitative Validation of Growth Factor Secretion from PC3 Educated MSCs

Selected growth factors were quantitatively analysed using the MesoScale Discovery system (described in section 2.6.2). The cells were harvested at 10, 20 and 30 day time-points as described in section 2.3 and placed in fresh complete medium for 24 hours in order to assess PC3 educated MSC secretion without the presence of PC3 CM. MSCs treated for 30 days in PC3 CM were then grown an extended period (12 - 16 days) in complete medium to assess whether any change in cytokine secretion was sustained. VEGF, PlGF, sFlt-1 and FGF-2 were chosen to be quantitatively measured. The lower limit of detection of each analyte is described in table 2.1.

3.2.5.1 PC3 Educated MSCs do not Display Altered VEGF Secretion

In contrast to the results obtained in the short-term experiments (section 3.2.1), there was no clear trend in the increase or decrease of VEGF secretion at any time-point (figure 3.9 A-D). The mean secretion levels in the untreated MSCs was 1906 pg/ml and 1850 pg/ml in PC3 educated MSCs and overall the difference was not found to be statistically significant at any time-point (paired student's t-test; two-tailed; n=3 biological replicates).

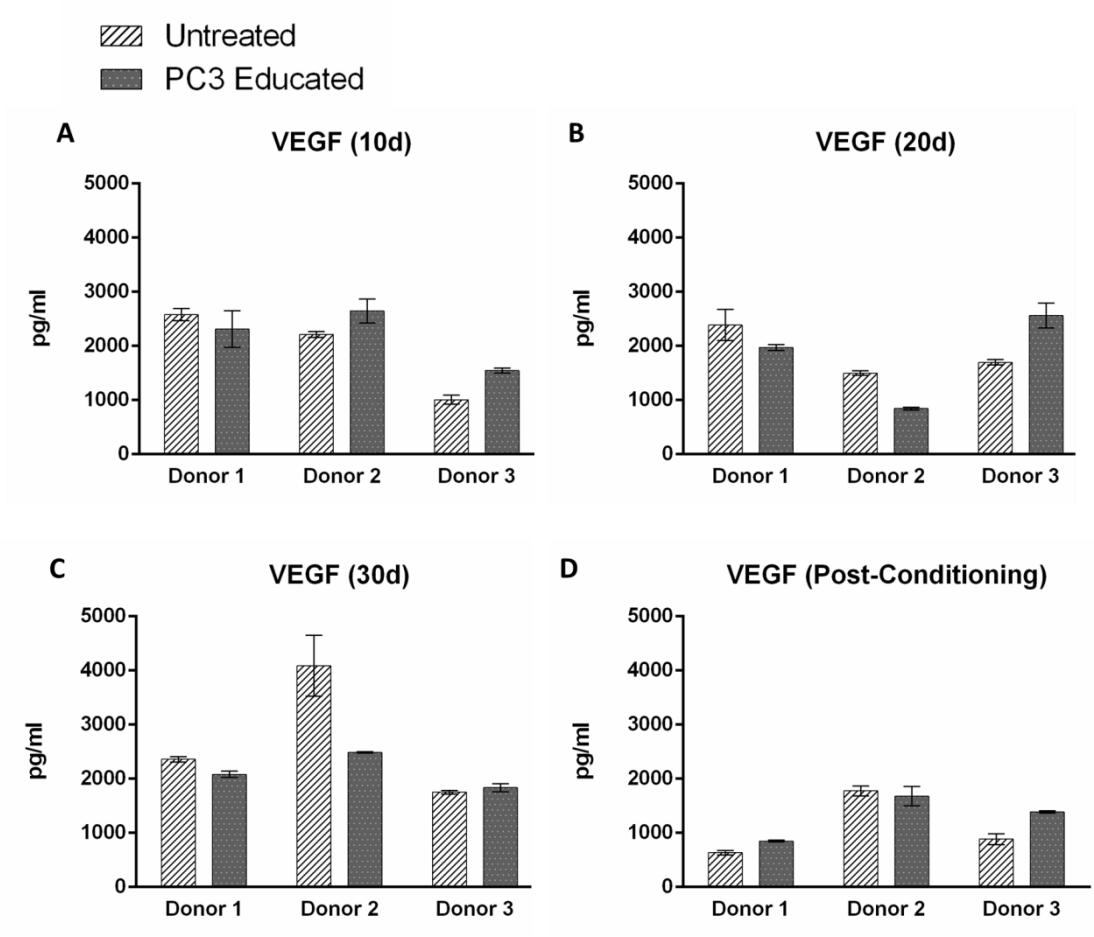

Figure 3.9. Quantitative Measurement of VEGF Secretion in PC3 Educated MSCs. VEGF was quantitatively measured in untreated MSCs and PC3 educated MSCs at 10, 20 and 30 day time-points (A-C) and in 30 day educated MSCs grown for an extended period in complete medium (D). No trend was observed in the increase or decrease of VEGF at any time-point (A-D) and no statistically significant difference between untreated MSCs and PC3 educated MSCs was found (paired student's t-test; two-tailed; n=3 biological replicates). Data represents the mean of technical replicates ± SD.

3.2.5.2 PC3 Educated MSCs do not Display Altered PlGF Secretion

Similar to the results obtained for VEGF, we observed a contrast to the results obtained in the short-term experiments (section 3.2.1) as there was no clear trend in the increase or decrease of PlGF secretion at any time-point (figure 3.1- A-D). The secretion levels in the untreated MSCs ranged between 1.6 and 68 pg/ml and between 2.2 and 77.6 pg/ml in PC3 educated MSCs and overall the difference was not statistically significant at any time-point (paired student's t-test; two-tailed; n=3 biological replicates).

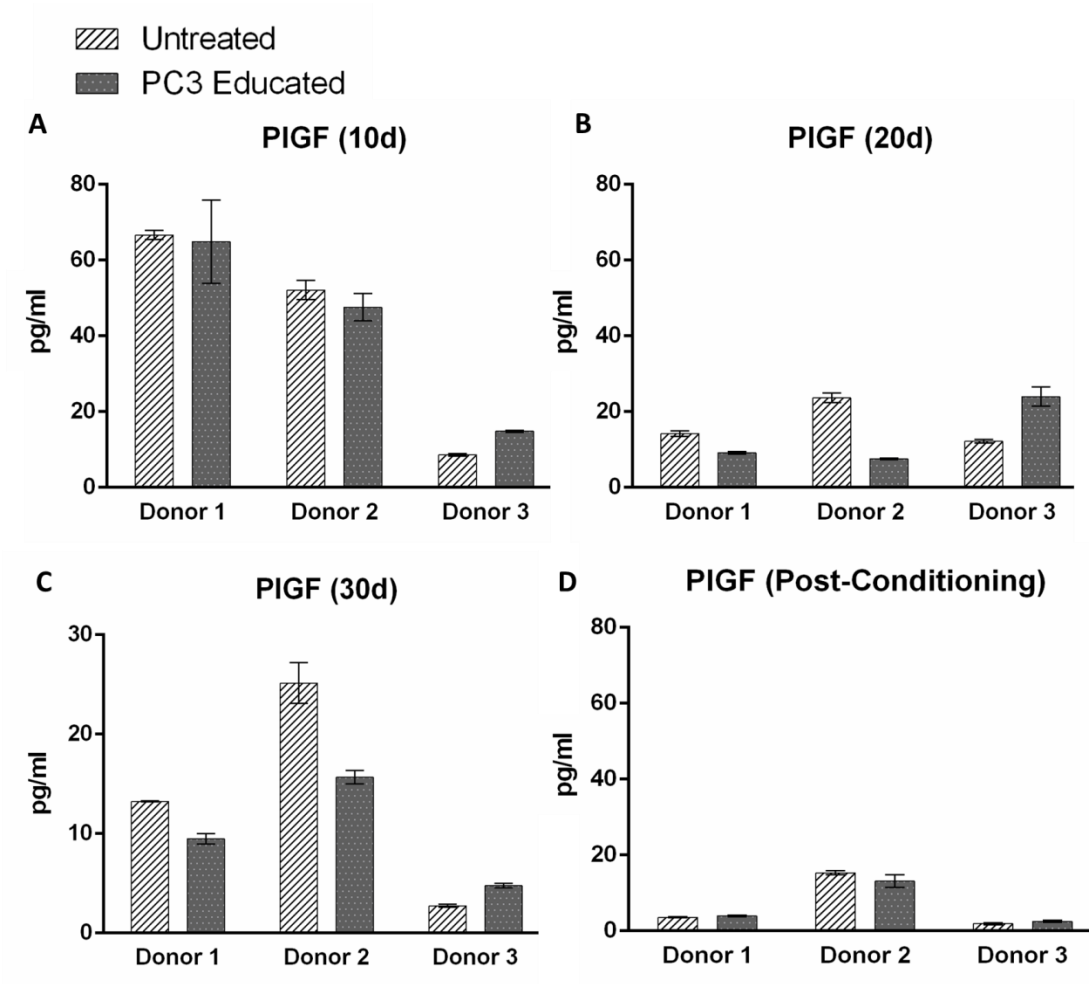

Figure 3.10. Quantitative Measurement of PlGF Secretion in PC3 Educated MSCs. PlGF was quantitatively measured using the MesoScale Discovery system in untreated MSCs and PC3 educated MSCs at 10, 20 and 30 day time-points (A-C) and in 30 day educated MSCs grown for an extended period in complete medium (D). No trend was observed in the increase or decrease of PlGF at any time-point (A-D) and no statistically significant difference between untreated MSCs and PC3 educated MSCs was found (paired student's t-test; two-tailed; n=3 biological replicates). Data represents the mean of technical replicates ± SD.

3.2.5.3 PC3 Educated MSCs Secrete Decreased sFlt-1

A decrease in sFlt-1 secretion was observed from PC3 educated MSCs from all donors at the 10, 20 and 30 day time-points (figure 3.11 A-C). Donor 1 MSCs were the most responsive to PC3 CM exposure and the decrease was sustained in PC3 educated MSCs following long-term culture in complete medium, while donor 3 PC3 educated MSCs were the only cells not to sustain the effect (figure 3.11 A-D). Following 30 days of conditioning, untreated MSCs secreted a mean of 20.1 pg/ml of sFlt-1 while PC3 educated MSCs secreted 8.4 pg/ml. Overall, combining data from all donors, the

difference between untreated MSCs and PC3 educated MSC secretion was statistically significant (paired student's t-test; two-tailed; n=3 biological replicates) at the 10 day ($p<0.05$), 20 day ($p<0.05$), 30 day ($p<0.05$) time-points but not in the 30 day educated MSCs post-conditioning.

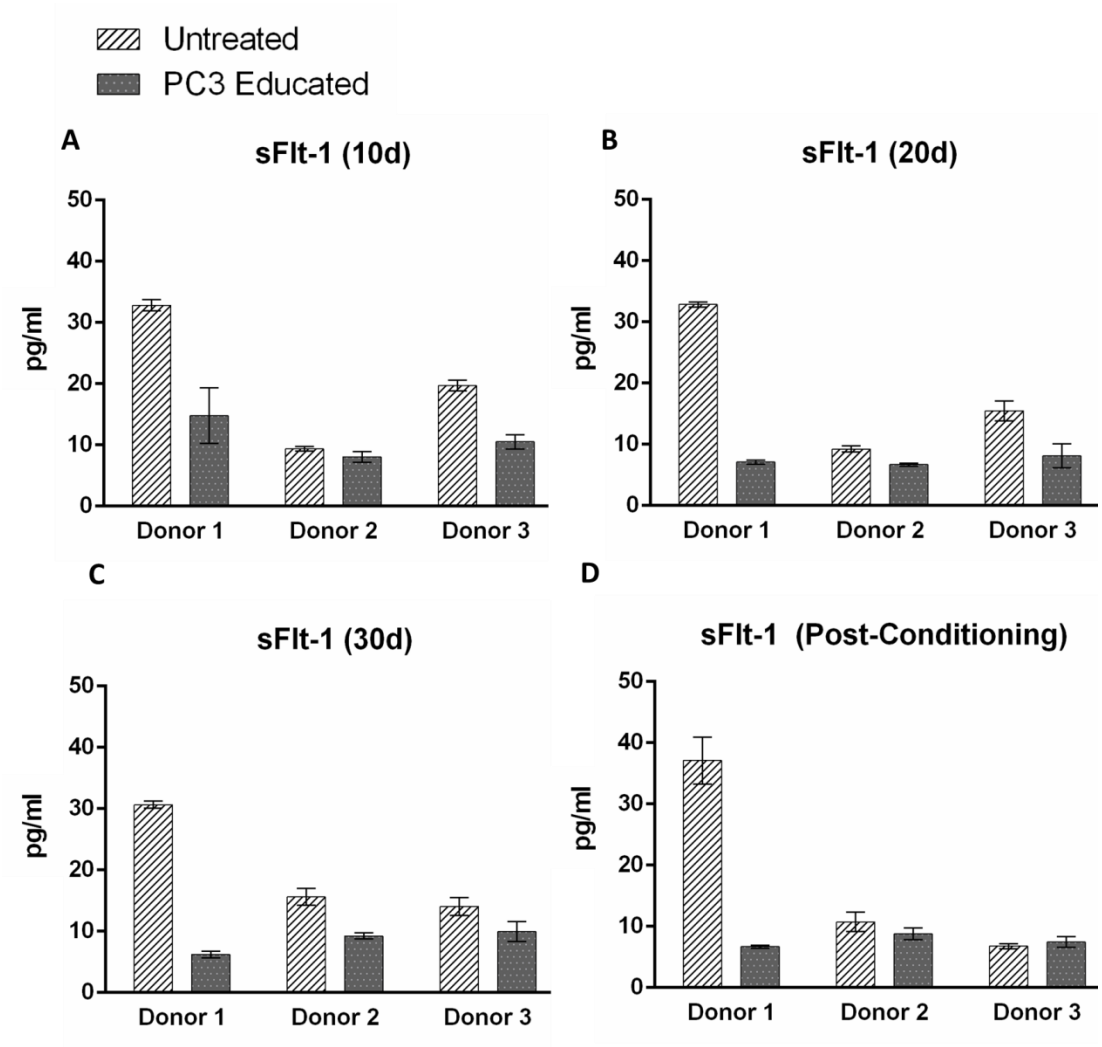

Figure 3.11. Quantitative Analysis of sFlt1 Secretion from PC3 Educated MSCs. sFlt-1 was quantitatively measured in untreated MSCs and PC3 educated MSCs at 10, 20 and 30 day time-points (A-C) and in PC3 educated MSCs grown for an extended period in complete medium (D) using the MesoScale Discovery system. All donor MSCs showed a decrease in the secretion of sFlt-1 at the 10 day (A), 20 day (B) and 30 day (C) time-points. The effect was sustained in donor 1 and donor 2 MSCs post-conditioning (D). Overall, the difference between untreated MSC and PC3 educated MSC secretion was statistically significant (paired student's t-test, two-tailed n=3 biological replicates) at the 10 day ($p<0.05$), 20 day ($p<0.05$), 30 day ($p<0.05$) time-points but not in the 30 day educated MSCs post-conditioning. Data represents the mean of technical replicates ± SD.

3.2.5.4 PC3 Educated MSCs Secrete Increased FGF2

While the MSCs growth medium was supplemented with 1ng/ml FGF2, it was not added to the media used during any assay. All donor MSCs conditioned with PC3 CM for 10 and 20 days showed an increase in FGF2 secretion in comparison to the untreated MSCs (figure 3.12 A+B). Untreated MSCs secreted a mean of 40.9 and 21.0 pg/ml at the 10 and 20 day time-points while PC3 educated MSCs secreted 147.8 and 189.5 pg/ml, respectively. The increase continued in donor 1 and 2 MSCs following 30 days of conditioning, and the mean of all untreated MSCs and PC3 educated MSCs was 47.2 and 111.9 pg/ml respectively (figure 3.12 C). PC3 educated MSCs from all donors secreted increased FGF2 post-conditioning; however, it was lower on average in comparison to previous time-points. Untreated MSCs secreted a mean of 22.06 pg/ml, whereas PC3 educated MSCs secreted a 2.8 fold increase at 61.4 pg/ml. Overall, combining data from all donors, the difference between untreated MSC and PC3 educated MSC secretion was statistically significant (paired student's t-test; two-tailed; n=3 biological replicates) at the 10 day ($p<0.01$), 20 day ($p<0.01$), 30 day ($p<0.01$) time-and in the 30 day educated MSCs post-conditioning ($p<0.0001$).

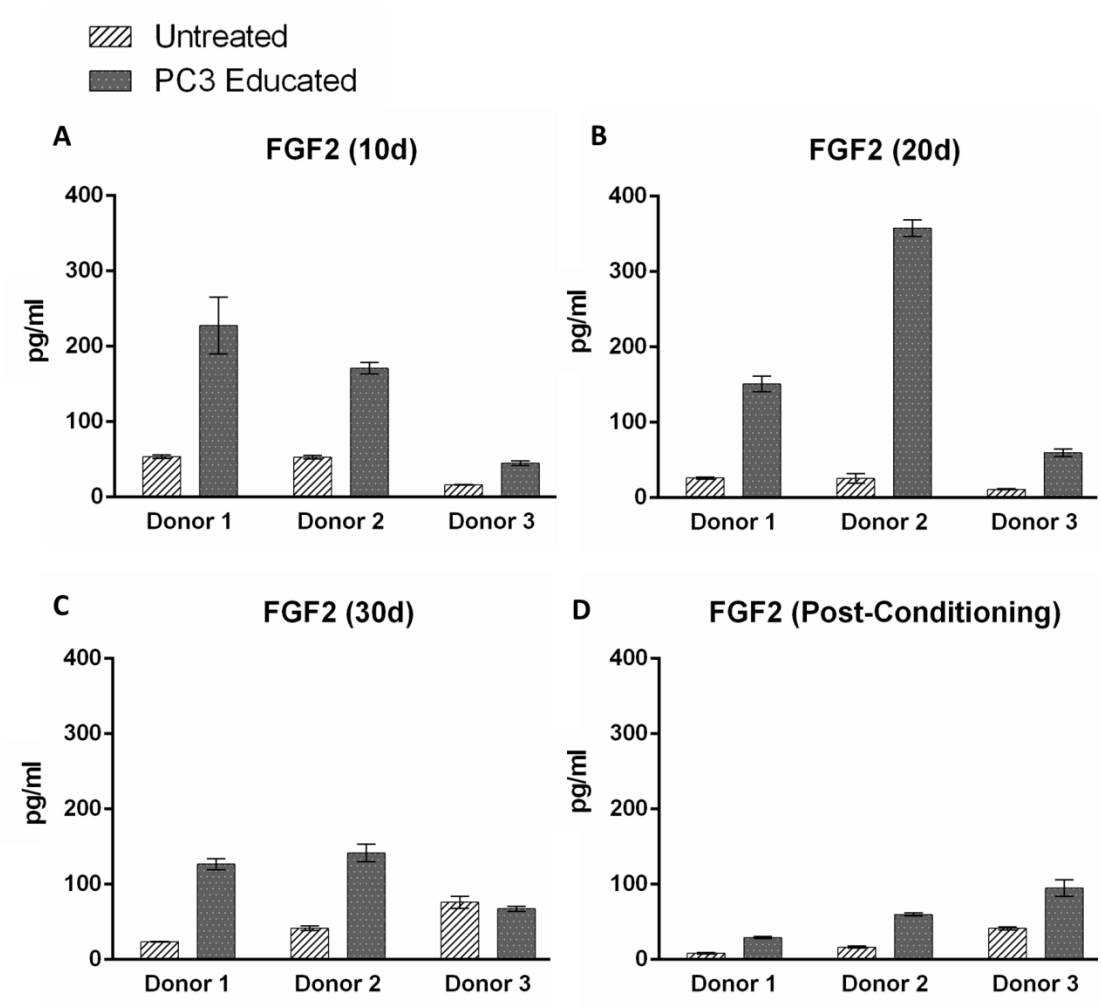

Figure 3.12. Quantitative Analysis of FGF2 Secretion from PC3 Educated MSCs. FGF2 was quantitatively measured in untreated MSCs and PC3 educated MSCs at 10, 20 and 30 day time-points (A-C) and in 30 day educated MSCs grown for an extended period in complete medium post-conditioning (D) using the MesoScale Discovery system. PC3 educated MSCs from all donors showed an increase in FGF2 secretion at the 10 and 20 day time-points (A+B). The effect was sustained in donor 1 and 2 cells at the 30 day time-point (C) and 30 day treated PC3 educated donor MSCs from all donors showed an increase in FGF2 secretion post-conditioning (D). Overall, the difference between untreated MSC and PC3 educated MSC secretion was statistically significant (paired student's t-test; two-tailed; n=3 biological replicates) at the 10 day ($p<0.01$), 20 day ($p<0.01$), 30 day ($p<0.01$) time-points and in 30 day educated MSCs post-conditioning ($p<0.0001$). Data represents the mean of technical replicates ± SD.

3.2.6 PC3 Educated MSCs do Show an Increase in the Expression of CAF Markers

MSCs are postulated to be CAF precursors and it has previously shown that long-term conditioning in breast cancer and ovarian cancer tumour cell line CM induces expression of CAF markers (Mishra et al., 2008, Spaeth et al., 2009). In this study a key question was whether PC3 CM could induce a CAF-like phenotype through

upregulation of CAF-associated markers. Immunofluorescence, western blotting and real-time PCR (see sections 2.8, 2.9 and 2.10) were employed to establish whether PC3 educated MSCs produce an increase in CAF-associated markers αSMA, vimentin, FAP and FSP1 as well as CAF-associated factors TNC, COL1A1 and COL5A1. The MSCs used in the experiments were cultured for 30 days in PC3 CM.

3.2.6.1 Protein Analysis: PC3 Educated MSCs do not express an Increase in CAF Markers

PC3 educated MSCs were tested for the protein expression of CAF markers αSMA, FSP1, FAP and vimentin using immunofluorescence staining (figure 3.13 A) and western blotting (figure 3.13 B). Fibroblasts were treated for 5 days with TGFβ to induce a myofibroblast-like phenotype and were used as a positive control for αSMA, FSP1 and FAP expression, which are indicative of fibroblast activation. Furthermore, TGFβ activated fibroblasts express αSMA that form stress fibres typical of CAF and myofibroblast morphology (figure 3.13 A). Images from the immunofluorescence staining are representative images taken from three independent experiments using MSCs from three donors.

Using immunofluoresence staining, MSCs were found to express αSMA in the treated and untreated MSCs however, the vast majority of cells did not form stress fibres (figure 3.13 A). Moreover, densitometry analysis of the western blot image showed that PC3 educated MSCs produced decreased αSMA in all donor cells in comparison to the untreated MSCs (figure 3.13 B+C). FSP1 expression was barely detectable using immunofluorescence staining and could not be detected using western blot imaging in PC3 educated MSCs and untreated MSCs (figure 3.13 A+B). FAP was found to be expressed in both untreated MSCs and PC3 educated MSCs and PC3 educated MSCs showed an increase in bright spots around the nuclei as seen in the TGFβ treated fibroblasts (figure 3.13 A). Finally, vimentin expression was shown to be decreased in the PC3 educated MSCs using immunofluorescence staining and in all donors analysed using western blotting (figure 3.13 A-C). Overall, PC3 educated MSCs do not express increased αSMA, FSP1 and vimentin.

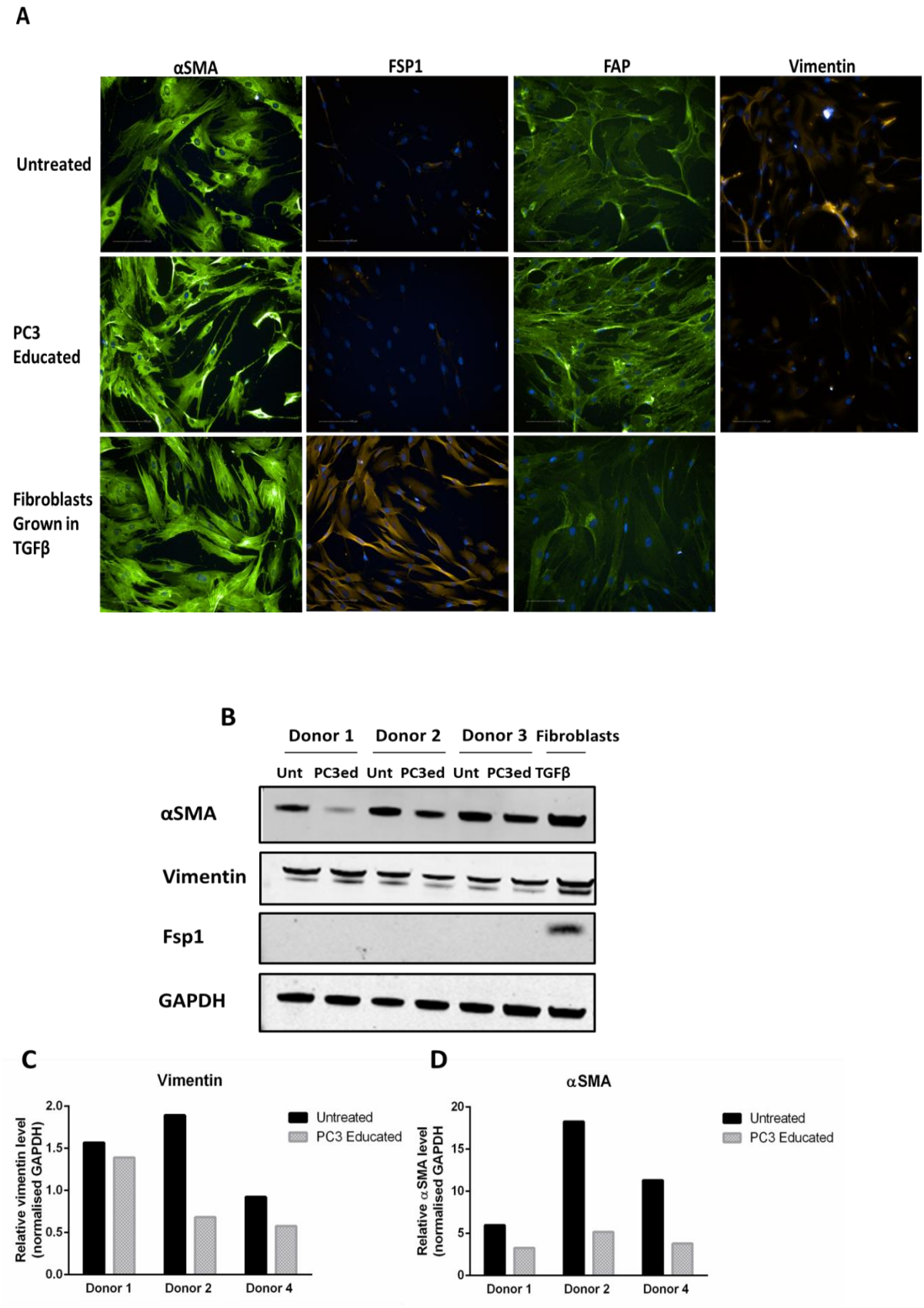

Figure 3.13. (Overleaf)

Figure 3.13. Protein Analysis to Detect the Expression of CAF Marker in PC3 Educated MSCs. The protein expression of CAF markers αSMA, FSP1, FAP and vimentin was assessed using immunofluorescence staining (A) and western blotting (B). Expression of αSMA was found to be decreased in PC3 educated MSCs from all donors as shown following densitometry analysis of the western blot image (B+C). The expressed αSMA did not form stress fibres in the PC3 educated MSCs or untreated MSCs in comparison to the TGFβ treated fibroblasts (A). FSP1 expression was barely detected in the PC3 educated MSCs and untreated MSCs using immunofluorescence staining and was not at all detected using western blot imaging (A+B). FAP was expressed in the untreated MSCs and PC3 educated MSCs using immunofluorescence staining and a higher level of bright spots around the nuclei could be detected in the PC3 educated MSCs in comparison to the untreated MSCs, using TGFβ treated fibroblasts as a reference (A). Vimentin was found to be decreased in the PC3 educated MSCs as shown from immunofluorescence staining and in all donors analysed using densitometry of the western blot image (A, B+D). Images from the immunofluorescence staining are representative images taken from three independent experiments using three separate donors.

3.2.6.2 Gene Expression Analysis: PC3 Educated MSCs do not Upregulate CAF Associated Factors

Real-time PCR was used to analyse gene expression of vimentin, FAP, TNC, COL1A1 and COL5A1 in untreated MSCs and PC3 educated MSCs. As expected based on the protein analysis shown in the previous section, vimentin was downregulated in the PC3 educated MSCs from donors 2 and 4 in comparison to the untreated MSCs (figure 3.14 A). Similar results were found with FAP expression (figure 3.14 B). Overall, combining data from all donors, the difference between untreated MSCs and PC3 educated MSCs was statistically significant in the gene expression of vimentin (unpaired student's t-test; two-tailed; $p<0.05$; n=2 biological replicates) and FAP (unpaired student's t-test, two-tailed, $p<0.001$; n=2 biological replicates). However, TNC, COL1A1 and COL5A1 showed varying gene expression between donors (figure 3.14 C-E) and overall, combining data from all donors, the difference between untreated MSCs and PC3 educated MSCs was not statistically significant for either factor (unpaired student's t-test, two-tailed; n=2 biological replicates).

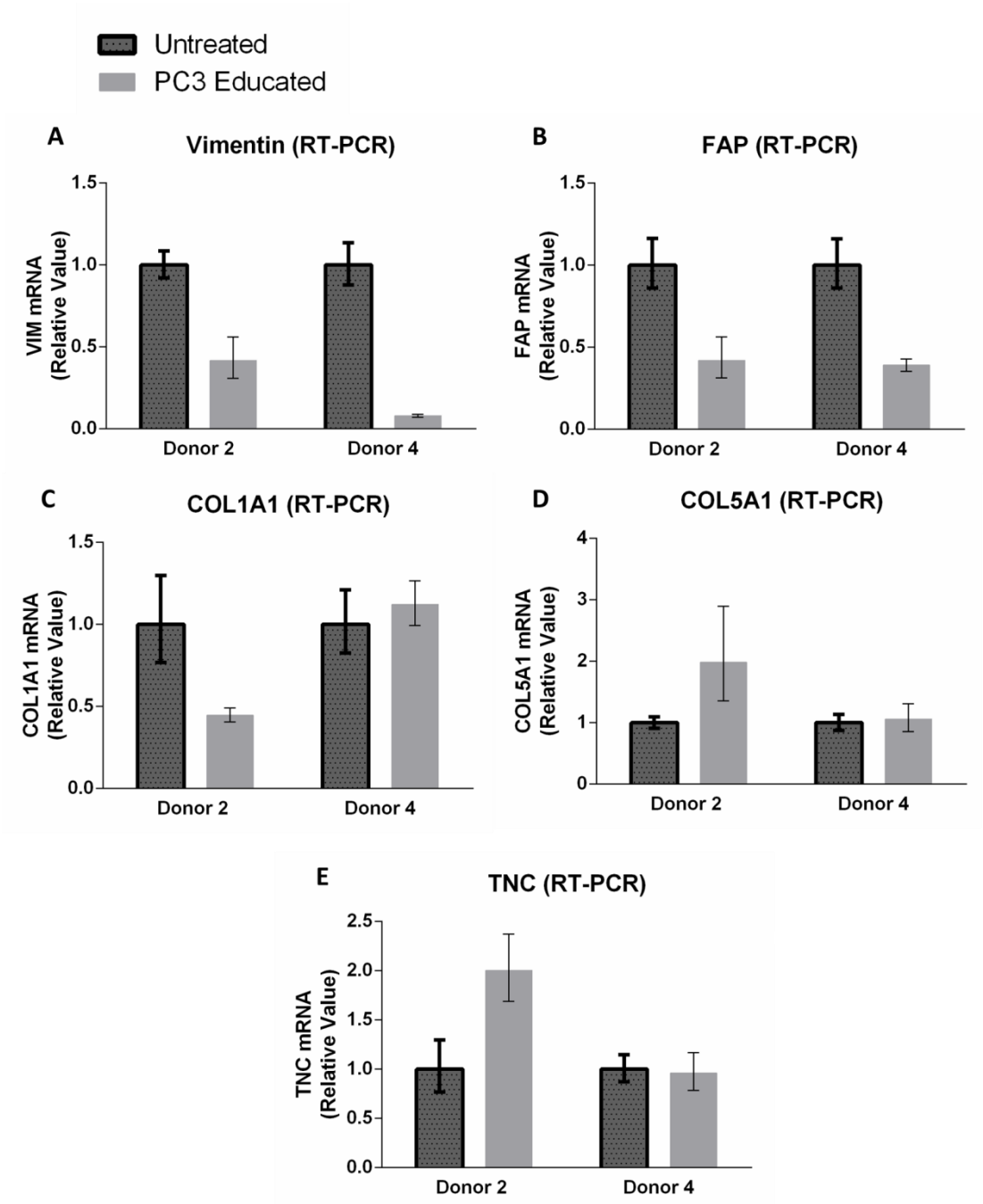

Figure 3.14. Genetic Analysis of CAF Associated Factors. The gene expression of CAF-associated factors in PC3 educated MSCs was assessed using real-time PCR. Vimentin and FAP were found to be downregulated in the PC3 educated MSCs from donor 2 and 4 (A+B). Varying expression of TNC, COL1A1 and COL5A1 was found between untreated MSCs and PC3 educated MSCs (D-E). Overall, combining data from all donors, the difference between untreated MSCs and PC3 educated MSCs was statistically significant in the gene expression of vimentin (unpaired student's t-test, two-tailed, $p<0.05$; n=2 biological replicates) and FAP (unpaired student's t-test, two-tailed, $p<0.001$; n=2 biological replicates). However, TNC, COL1A1 and COL5A1 showed varying gene expression between donors (C-E) and overall, combining data from all donors, the difference between untreated MSCs and PC3 educated MSCs was not statistically significant for either factor (unpaired student's t-test, two-tailed; n=2 biological replicates). Values were normalised to untreated controls and data represents the mean of technical replicates with upper and lower limits.

3.2.7 MSC Cell Surface Marker Expression

MSCs are characterised based on their differentiation potential and on the presence of cell surface markers CD90, CD105 and CD73 (Dominici et al., 2006). In this study, flow cytometry was used to test whether PC3 educated MSCs maintained cell surface expression of these markers as described in section 2.11. Varying results were found between donor MSCs, with MSCs from donor 1 and 2 showing the most similarities (figure 3.15 A-F). CD73 expression was similar between untreated MSCs and PC3 educated MSCs from all donor cells analysed (figure 3.15 C+F+I). Fewer PC3 educated MSCs from donors 1 and 2 were found to be positive for CD105 while no change was observed in PC3 educated MSCs from donor 4 (figure 3.15 B+E+H). The expression of CD105 was found to be at 98.1% and 99.0% in untreated MSCs from donor 1 and 2, respectively, whereas the expression was at 59.6% in PC3 educated MSCs from donor 1 and 88.9% in PC3 educated MSCs from donor 2 (figure 3.15 J). Interestingly, two populations were found in PC3 educated MSCs from donor 4 when fluorescently stained for CD90, which was not observed in the other donor MSCs (figure 3.15 A+D+G). The expression of CD90 was found to be at 97.1% in untreated MSCs from donor 4, whereas the expression was at 72.2% in PC3 educated MSCs from donor 4 (figure 3.15 J).

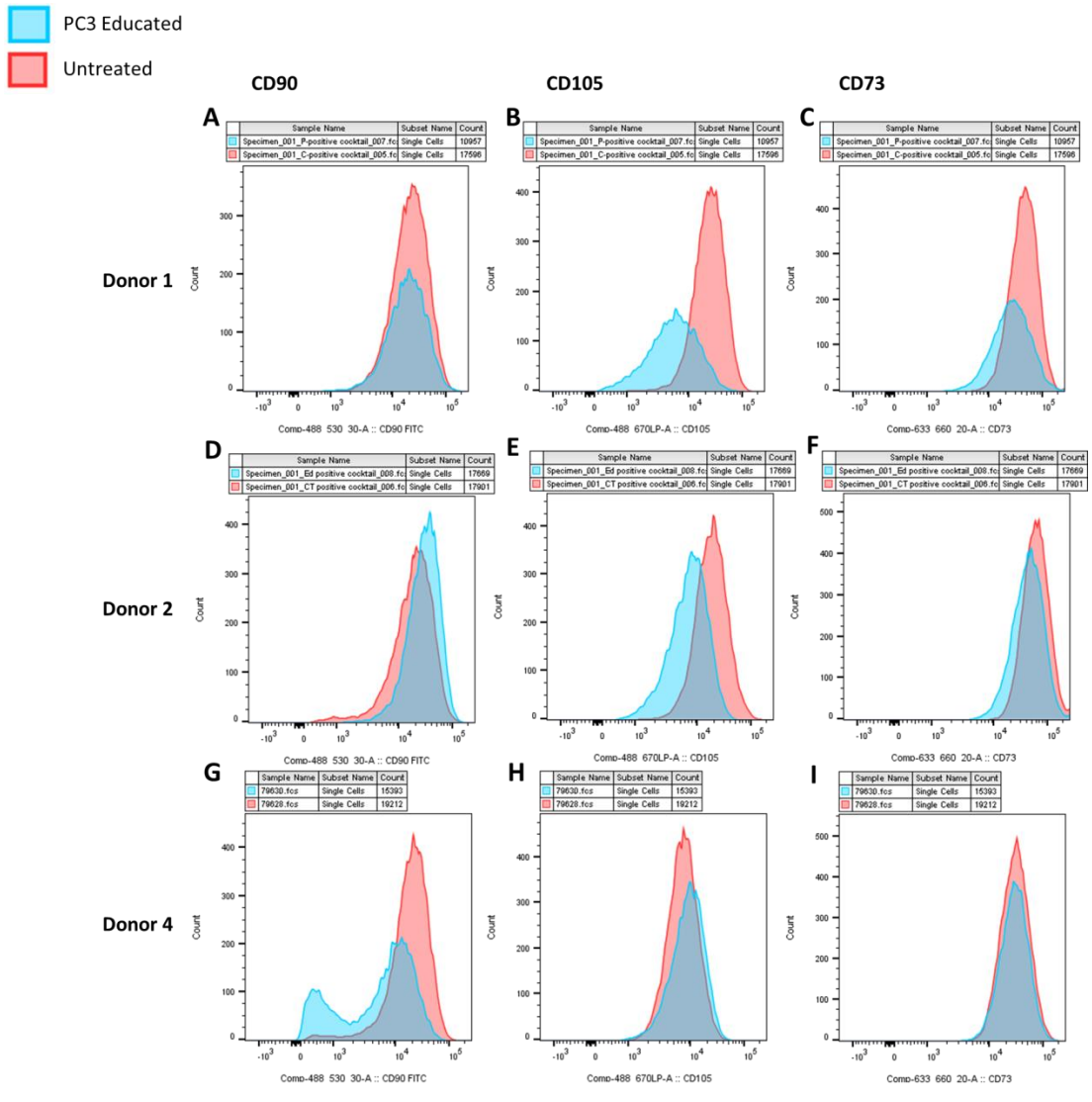

J

	CD90 (%)	CD105 (%)	CD73 (%)
Untreated (Donor 1)	99.6	98.1	99.6
PC3 Educated (Donor 1)	98.8	59.6	91.3
Untreated (Donor 2)	95.8	99.0	98.6
PC3 Educated (Donor 2)	99.1	88.9	97.6
Untreated (Donor 4)	97.1	84.3	96.1
PC3 Educated (Donor 4)	72.2	83.7	93.1

Figure 3.15. MSC Cell Surface Marker Expression. Untreated MSCs and PC3 educated MSCs were tested for the cell surface expression of CD90, CD105 and CD73. Two populations of cells were found in the PC3 educated MSCs from donor 4 when fluorescently stained for CD90 (G), whereas this was not observed in cells from donor 1 and 2 (A+G). Fewer PC3 educated MSCs from donor 1 and 2 (B+E) expressed CD105 while no obvious change was observed in cells from donor 4 (H). No clear difference was observed in the expression of CD73 between untreated MSCs and PC3 educated MSCs from any of the three donors (C+F+I). The percentage of expression of each surface marker within each population of cells is represented in a table (J).

3.3 Discussion

It is now established that MSCs can form part of the tumour microenvironment (Ame-Thomas et al., 2007, Kansy et al., 2014, Hossain et al., 2015, Karnoub et al., 2007, Prantl et al., 2010). The key question is how they interact there. It is still unclear as to whether MSCs have a tumour promoting or tumour suppressive role or whether the function is dependent on the conditions (Klopp et al., 2011). MSCs may interact with tumour cells and cells of the tumour stoma through paracrine signalling. On the other hand, MSCs have the capacity to differentiate to several different cell types such as osteocytes, chondrocytes, myocytes and neurons, and it is possible that MSCs differentiate at the tumour site (Pittenger et al., 1999, Wakitani et al., 1995, Kopen et al., 1999). It has been suggested that MSCs may contribute to angiogenesis at the tumour through differentiation to endothelial cells or pericytes (Rajantie et al., 2004, Al-Khaldi et al., 2003). Particular attention has been paid to the proposal that MSCs are a source of CAFs and studies have found that long-term exposure of MSCs to breast and ovarian cell CM induces a CAF-like phenotype (Mishra et al., 2008, Spaeth et al., 2009). Another possibility, we can consider, is that the MSCs become 'tumour associated' or 'activated' in response to tumour related stimuli which would lead to a cell with similar characteristics to the original MSC but with a tumour promoting or tumour suppressive function.

The aim of this study was to develop an *in vitro* experimental approach to examining MSC and prostate cancer cell interactions. The MSCs were cultured for up to 20 days in 22Rv1, DU145 and PC3 CM to examine any potential paracrine effects of prostate cancer secretomes on MSCs. The cytokine and chemokine secretory profile of the cells was assessed using a proteome profiler array. The PC3 educated MSCs showed the strongest response to the conditioning and so were chosen for further detailed characterisation. It should be noted that MSCs are a heterogenous population of cells and MSCs derived from different donors can also have a heterogenous response. MSCs derived from donor 2, for example, showed a different trend in response to the PC3 conditioned media, particularly in OPN, MCP1, IL-6 and IL-8 secretion following 20 days of conditioning. For this reason it is important to assess the overall trend in cytokine and growth factor secretion.

Early experiments focused on short-term treatment of MSCs with prostate cancer cell CM. MSCs were treated for 48 hours with 22Rv1, DU145 and PC3 CM followed by 48 hours in fresh complete medium. The resulting supernatant was tested for VEGF, PlGF, FGF2 and sFlt-1 secretion. VEGF and PlGF are key factors in angiogenesis and vasculogenesis and both are secreted at a baseline level in MSCs (Kinnaird et al., 2004). Moreover, MSCs have been shown to be active in promoting angiogenesis in wound healing and ischaemic heart diseases (Wu et al., 2007, Tang et al., 2004, Sadat et al., 2007). The 48 hour treatment resulted in an increase in VEGF secretion in all treatments and a near two-fold statistically significant increase in PlGF secretion (see section 3.2.1). However, no consistent increase was observed in the long-term treatments at the 10, 20 or 30 day time-points (see section 3.2.5.1 and 3.2.5.2). This could be due to a less robust experimental procedure in the early experiment where only two donor cells were tested and the cells were counted and plated 6 days previously, whereas in the long-term experiments MSCs derived from three different donors were used and the cells were plated 24 hours in advance. On the other hand the MSCs may have an early response to prostate cancer cell CM that differs following continuous exposure.

Interestingly, sFlt-1 was consistently decreased in the PC3 educated MSCs in comparison to the untreated MSCs, at the 10, 20 and 30 day time-points and from all donor cells (3.2.5.3). sFlt-1 is a negative regulator of angiogenesis and functions by trapping VEGF and PlGF (Shibuya, 2011). Several studies have found that sFlt-1 can inhibit tumour growth and angiogenesis and bone marrow MSCs genetically engineered to produce sFlt-1 as a delivery vehicle to the tumour were shown to have therapeutic potential (Mori et al., 2000, Lin et al., 1998, Goldman et al., 1998, Hu et al., 2008). Therefore, while PC3 educated MSCs maintain a comparable level of VEGF and PlGF secretion to untreated MSCs, their effect would be more potent given the decrease in sFlt-1 secretion.

FGF2 was increased in PC3 educated MSCs from almost all donors analysed at each time-point (section 3.2.5.4). Although, the increase in FGF2 secretion was sustained in PC3 educated MSCs post-conditioning, the level of secretion was lower to what was observed during the exposure period, which could be due to a loss of paracrine

signalling following removal of the PC3 CM (section 3.2.5.4). FGF2 is a known promoter of angiogenesis and it has been found to be expressed in PC3 and DU145 cells (Connolly and Rose, 1998, Cronauer et al., 1997). Higher levels of FGF2 have been found in the primary prostate tumour in comparison to the non-cancerous surrounding tissue and studies have shown the increase to be localised at the tumour stroma (Giri et al., 1999, Berger et al., 2003). Moreover, TGFβ1 stimulation was shown to induce FGF2 expression in prostate cancer stromal cells which led to increased tumour growth and metastasis (Yang et al., 2008). We found a statistically significant increase in FGF2 secretion from all PC3 educated donor MSCs at the 10, 20 and 30 day conditioning time-points (see section 3.2.5.4). Similarly, in a study by Nishimori *et al.*, it was found that co-culture of pre-osteoblastic MC3T3-E1 cells with the prostate cancer cell line LnCaP and BMP-4 stimulated FGF2 production in the MC3T3-E1 cells which in turn stimulated LnCaP proliferation (Nishimori et al., 2012). FGF2 is expressed by osteoblasts and is known to play a role in bone development and homeostasis (Fallon et al., 1994, Coffin et al., 1995, Montero et al., 2000). It was found that FGF2 regulated the transcription of bone sialoprotein (BSP) in MCF7 breast cancer cells (Li et al., 2010) and furthermore, FGF2 was found to maintain MSC osteogenic differentiation potential during proliferation (Tsutsumi et al., 2001, Quarto and Longaker, 2006).

Following the chemokine and cytokine screen of the prostate cancer cell educated MSCs it was revealed that DU145 and PC3 educated MSCs shared a similar secretory profile while MSCs conditioned with the non-metastatic cell line 22Rv1 had a comparable profile to untreated MSCs. MSCs were highly responsive to the PC3 CM and after 20 days of conditioning were shown to secrete OPN, IL-6, CD105, MIF, MCP-1, IL-8, IL-11 and FGF-19 with the addition of DKK-1, EMMPRIN and IGFBP-2 after 30 days of conditioning. These factors are each known to play a role in tumour progression.

It has been shown that FGF19 is expressed in PC3 and DU145 cell lines and in the prostate tumour stoma and interaction with its receptor, FGFR-4, stimulates prostate cancer growth progression (Feng et al., 2013, Dakhova et al., 2009). MIF is likewise expressed by prostate cancer cells, which we also detected in the secretory profile of

PC3 and 22Rv1 cells (see section 3.2.3), and has been found to promote tumour growth and metastasis (Meyer-Siegler et al., 2005, Meyer-Siegler et al., 2006, Hussain et al., 2013, Meyer-Siegler and Hudson, 1996). IGFBP-2 was found at a higher level in prostate cancer patients than control patients and EMMPRIN was shown to be highly expressed in malignant prostate tumour tissue in comparison to non-cancerous tissue (Han et al., 2009, Cohen et al., 1993, Kanety et al., 1993). EMMPRIN is an activator of MMP-1, MMP-2 and MMP-3 and thus may be active inducer of metastatic progression (Gabison et al., 2005). It has additionally been found to co-localise with MMPs in prostate cancer and can indicate poor prognosis in patients (Han et al., 2009, Madigan et al., 2008). Furthermore, knockdown of EMMPRIN in PC3 cells resulted in a decreased capacity for the cells to form filipodia and an increase in the expression of adhesion and gap-junction proteins, indicating a role for EMMPRIN in the metastatic function of PC3 cells (Zhu et al., 2012).

The detection of IL-11 in PC3 educated MSC supernatants is interesting as IL-11 is a known inducer of bone resorption through the promotion of osteoclastogenesis and inhibition of osteoblast activity (Girasole et al., 1994). A study by Zhang and colleagues found that growth of bone marrow derived endothelial cells in human melanoma cell (A375M) CM induced production of IL-11 and the CM from the stimulated endothelial cells was shown to promote bone resorption of neonatal mouse calvaria (Zhang et al., 1998). Both A375M cells and PC3 cells form osteolytic bone metastatic cancer and perhaps this is due to the stimulation of bone resorption promoting factors from cells at the metastatic site (Zhang et al., 1998, Nemeth et al., 2002). Additionally, DKK-1 is a Wnt antagonist and has been found to inhibit bone formation in osteoblastic prostate cancer bone metastasis (Thudi et al., 2011). PC3 cells transfected with DKK1 shRNA induced increased osteogenic differentiation of the bone marrow stromal cell line ST-2 in comparison to normal PC3 cells thereby suggesting a role for Wnt signalling in the stimulation of osteogenesis (Hall et al., 2005). PC3 cells were isolated from a bone metastatic patient and their interaction within the bone marrow microenvironment, in this case with respect to the resident MSCs, could drive the creation of a favourable niche for tumour cell growth while consequently disrupting normal MSC function and bone homeostasis.

MSCs educated for 30 days in PC3 CM were chosen for further molecular characterisation and the secretion of OPN, MCP-1, IL-6 and IL-8 were selected for quantitative validation. Prostate cancer cells have been shown to secrete IL-6, including PC3 cells, although it was not detected in our proteome profiling experiments (see section 3.2.3) (Chung et al., 1999). IL-6 has been found to interact prostate cancer cells in an autocrine and paracrine manner however, the results are conflicted as to whether this stimulates tumour cell growth or suppression (Chung et al., 1999, Okamoto et al., 1997, Giri et al., 2001, Lou et al., 2000, Mori et al., 1999, Hobisch et al., 1998). An increase in secretion of IL-6 was detected in the cytokine screen in section 3.2.2 in MSCs conditioned in PC3 CM for 20 and 30 days. However, no consistent increase could be quantitatively detected in the three MSC donors analysed at the 20 and 30 day time-points (section 3.2.4.3). The increase in all donors that was observed following 10 days of conditioning and in PC3 educated MSCs derived from donor 1 at each timepoint would suggest a role for tumour stromal MSCs in the paracrine signalling of IL-6 between factors released in the PC3 CM and the MSCs as no obvious increase in IL-6 secretion was detected post-conditioning (section 3.2.4.3).

IL-8 was consistently increased in PC3 educated MSCs from all donors analysed at each time-point (section 3.2.4.4). While, the increase in IL-8 secretion was sustained in PC3 educated MSCs post-conditioning suggesting MSC reprogramming, the level of secretion was lower to what was observed during the exposure period (section 3.2.4.4). This drop in secretion level could be explained by a loss of paracrine signalling following removal of the PC3 CM.

Interestingly, MSCs isolated from gastric cancer tumours were found to produce increased IL-8 in comparison to MSCs derived from adjacent non-cancerous tissue or the bone marrow. The tumour derived MSCs were found to stimulate tumour cell proliferation and angiogenic activity in an IL-8 dependent manner (Li et al., 2015). We also detected IL-8 secretion from DU145 and PC3 cells but not 22Rv1 cells using a protein array (see section 3.2.3). IL-8 interacts with chemokine receptors CXCR1 and CXCR2 which are present on prostate cancer cells, endothelial cells, neutrophils, monocytes and MSCs (Murphy et al., 2005, Kim et al., 2001, Schraufstatter et al.,

2001, Gordon et al., 2005, Bi et al., 2014). An increased presence of IL-8 at the tumour could thus have a multi-layered effect. In a study of isolated clonal populations of PC3 cells secreting low to high levels of IL-8, upon injection into the prostate of nude mice, the PC3 cells secreting high levels of IL-8 were found to produce faster growing, more highly vascularised tumours with an increased incidence of metastasis in comparison to the clones producing low levels of IL-8 (Kim et al., 2001). Similarly, neutralisation of IL-8 using antisera was found to inhibit PC3 mediated tumour growth and angiogenic activity in a mouse model (Moore et al., 1999).

An elevation in serum IL-8 levels was correlated with prostate cancer and particularly bone metastasis in male patients (Lehrer et al., 2004). Moreover, IL-8 was found to directly stimulate osteoclastogenesis in peripheral blood mononuclear cells (PBMCs) and indirectly through the induction of RANKL expression in osteoblasts (Bendre et al., 2003). Further research showed that breast cancer cell lines with higher osteolytic potential *in vivo* were found to express higher levels of IL-8 and neutralisation of IL-8 in CM collected from these cells reduced PBMC differentiation to osteoclasts (Bendre et al., 2005).

MCP-1 secretion was slightly increased in the PC3 educated MSCs derived from all donors following 10 days of conditioning in comparison to the control and in two of three donors following 20 days of conditioning (section 3.2.4.2). However, this difference was increased by over two-fold in PC3 educated MSCs from all donors following 30 days of conditioning (section 3.2.4.2). This suggests that the change in secretion is dependent on a long-term conditioning period and indicates that cell reprogramming could be occurring. MCP-1 was found by numerous studies to promote prostate cancer growth and progression (Lu et al., 2006, Loberg et al., 2006, Loberg et al., 2007a, Salcedo et al., 2000, Zhang et al., 2010, Goede et al., 1999). Like IL-8, MCP-1 has also been shown to exert a tumour promoting effect through stimulation of angiogenesis whereby MCP-1 interacts with its receptor, CCR2 on endothelial cells (Salcedo et al., 2000, Hong et al., 2005). In this study MSCs from three different donors treated for 30 days with PC3 CM showed increased MCP-1 secretion in comparison to the untreated MSCs. Interestingly, PC3 cells transfected with IL-8 targeted shRNA showed decreased proliferation in response to MCP-1 in

comparison to naïve PC3 cells suggesting an IL-8 mediated sensitivity or responsiveness to MCP-1 (Maxwell et al., 2014). Furthermore, IL-8 and MCP-1 in PC3 CM were found to stimulate osteoclast differentiation of human bone marrow mononuclear cells (Lu et al., 2007a, Mizutani et al., 2009). Several studies have attributed a role in bone resorption to MCP-1 with endothelial cells and osteoblasts being a potential source (Cai et al., 2009, Li et al., 2009, Lu et al., 2009, Lu et al., 2007b, Loberg et al., 2006, Kim et al., 2005). MSCs educated by bone metastatic tumour cells to secrete increased MCP-1 might be another source for MCP-1 and IL-8, both of which contribute to osteoclast formation.

Finally, OPN secretion levels were quantitatively validated and the strongest response to PC3 conditioning was found in all donor MSCs after 30 days of treatment (section 3.2.4.1). Increased OPN levels were found to be correlated with prostate cancer progression and an indicator of the presence of distant metastases (Khodavirdi et al., 2006, Castellano et al., 2008, Forootan et al., 2006, Ramankulov et al., 2007). OPN deficient mice when injected with B16 melanoma cells developed decreased bone metastasis in comparison to wild-type mice (Nemoto et al., 2001). OPN has several functions which serve to promote metastasis at different stages of progression. Tumour cell invasiveness can be modulated by OPN as it was shown that OPN can induce MMP-2 and MMP-9 expression in PC3 cells (Liu et al., 2010, Desai et al., 2007, Gupta et al., 2013) and uPA expression has been found to be mediated by OPN in breast and hepatocarcinoma cells (Das et al., 2004, Mi et al., 2006, Chen et al., 2011). Secretion of uPA and MMPs increase the tumour cells capacity to remodel the ECM and invade out of the tumour. OPN is a chemoattractant with adhesive properties and can facilitate invasion through the binding of integrins, mainly $\alpha_v\beta_1$, $\alpha_v\beta_3$, $\alpha_v\beta_5$, $\alpha_v\beta_6$, $\alpha_8\beta_1$ and $\alpha_5\beta_1$, on many cell types (Hu et al., 1995, Liaw et al., 1995, Denda et al., 1998, Yokosaki et al., 1999). The integrin $\alpha_v\beta_3$ is expressed on PC3 cells and the binding of OPN to $\alpha_v\beta_3$ has been found to activate the PI3-kinase signalling pathway and mediate PC3 cell migration (Zheng et al., 2000).

OPN is expressed by several bone marrow resident cells such as osteoblasts, osteoclast progenitors and plays a role in bone remodelling (Yamate et al., 1997, Ishijima et al., 2001, Klein-Nulend et al., 1997). We found a consistent increase in OPN

secretion in PC3 educated MSCs from each donor following 30 days of conditioning. Interestingly, a study found multiple myeloma derived MSCs secreted an increased level of OPN in comparison to healthy bone marrow cells. (Zdzisinska et al., 2008). OPN facilitates osteoclastogenesis by mediating osteoclast motility and anchorage to the bone mineral matrix (Ishijima et al., 2001, Chellaiah et al., 2003, Reinholt et al., 1990, Ross et al., 1993, Yamate et al., 1997). Changes in OPN production within the bone marrow could therefore disrupt bone homeostasis as expression of OPN in breast cancer has been found to be associated with osteolytic bone metastasis (Ibrahim et al., 2000, Adwan et al., 2004). Another more recent function attributed to OPN is the stimulation of CAF formation from MSCs in breast cancer (Weber et al., 2015, Sharon et al., 2015, Mi et al., 2011). MSCs isolated from lung and liver metastases in a mouse xenograft breast cancer model expressed CAF markers αSMA, FSP-1, TN-C, SDF-1α and MMP-2 and 9 in a OPN dependent manner (Mi et al., 2011). CAF transition was found to be due to release of TGFβ upon the binding of OPN to MSC integrin receptors (Weber et al., 2015).

The aim of the second part of this study was to evaluate whether the PC3 educated MSCs retain the classical characteristics associated with MSCs or whether they transitioned into a CAF-like phenotype. It has previously been found that long-term conditioning of MSCs in breast cancer and ovarian cancer resulted in the transition of MSCs to CAFs (Mishra et al., 2008, Spaeth et al., 2009). It was therefore a relevant question to ask whether PC3 educated MSCs could be characterised as CAFs. To test this we looked at protein expression of CAF markers αSMA, FSP1, FAP and vimentin and gene expression of CAF-associated factors TNC, COL1A1 and COL5A1 (section 3.2.6.1 and 3.2.6.2). We found that rather than an increase in the expression of CAF markers the PC3 educated MSCs expressed decreased vimentin and αSMA protein and FAP mRNA. Low expression of FSP1 was detected in the untreated MSCs and PC3 educated MSCs using immunofluorescence staining, while no expression was detected using western blot analysis. Moreover, the visualisation of αSMA expression using immunofluorescence staining revealed that the protein did not form stress fibres and the cells did not have the myofibroblast-like morphological features associated with CAFs (section 3.2.6.1). From this we can conclude that MSCs treated

for 30 days with PC3 CM do not transition into CAFs. What is interesting however, is the decrease in expression of αSMA and particularly vimentin. Both αSMA and vimentin are structural proteins and vimentin is a mesenchymal cell marker (Hinz et al., 2001, Ivaska et al., 2007). Change in the expression of these factors would suggest a possible change in cell type or cellular function which will be discussed in further detail in subsequent chapters.

Analysis of MSC cell surface markers CD105, CD90 and CD73 also suggest that the PC3 educated MSCs are altering their molecular phenotype though the results are not as consistent (section 3.2.7). While CD73 cell surface expression did not change in response to PC3 CM, there was a shift in CD105 expression in donor 1 and 2 derived MSCs with fewer PC3 educated MSCs expressing the surface marker than the untreated MSCs which may correlate with the increased secretion level detected in the proteome profiler in section 3.2.2. However, this result was not found using cells from donor 4. On the other hand, assessment of CD90 cell surface expression revealed two populations of cells in PC3 educated MSCs from donor 4 but not from donor 1 or 2. This suggests a donor dependent response to PC3 CM and perhaps even a divide in responsiveness within the donor population due to the heterogeneity of MSCs.

In conclusion, PC3 educated MSCs secrete increased tumour promoting factors in comparison to naïve MSCs. Many of the factors detected in PC3 educated MSC supernatants are also known promoters of bone resorption such as IL-11, IL-8, MCP-1 and OPN. Given that PC3 cells form osteolytic bone metastases *in vivo* (Nemeth et al., 2002), their interaction with cells within the bone marrow microenvironment could create a supportive niche for growth which results in a disruption of bone homeostasis which in this case leads to increased osteolysis. We also discovered a donor dependent shift in the expression of MSC cell surface markers in PC3 educated MSCs which suggests a change in cell phenotype within the population. Transition to a CAF-like phenotype was ruled out as the cells did not increase in the expression of αSMA, FSP1, FAP or vimentin. Instead, there was a decrease in their αSMA and vimentin expression which could mean a change in cell structure or function.

Chapter 4

Functional Characterisation of Prostate Cancer Educated MSCs

4.1 Introduction

MSCs have multiple functions within the body. Several studies have reported the migration of MSCs to the heart following myocardial infarction (Orlic et al., 2001, Barbash et al., 2003, Wu et al., 2003), as well as the lungs (Ortiz et al., 2003), liver (Sato et al., 2005) and brain (Mahmood et al., 2003) during injury. This migratory function allows MSCs to home to injured tissue and contribute to repair. Although the mechanisms are not fully understood, there is evidence to suggest that MSCs are stimulated to migrate to these tissues through the release of cytokines and chemokines present in the inflammatory sites that bind to their corresponding receptors on the MSCs (Chamberlain et al., 2007, Rustad and Gurtner, 2012, Wang et al., 2002, Ji et al., 2004). The tumour microenvironment is a known site of inflammation and the factors released by the tumour stimulate the homing of MSCs to the primary site whereby they form part of the stroma (Karnoub et al., 2007, Prantl et al., 2010, Wu et al., 2008, Kidd et al., 2009). The mechanisms by which the MSCs interact with the surrounding cells however, are still largely unknown.

The aim of this study was to determine the functional characteristics of the PC3 educated MSCs and assess whether they differed to naïve MSCs. The question then was whether any observed functional change was sustained following growth without the presence of CM. Firstly we examined the migration capacity of 22Rv1, DU145 and PC3 educated MSCs following 5, 10 and 20 days of conditioning. The PC3 educated MSCs were found to have the greatest response to the conditioning and so were more robustly examined for their migration capacity at 10, 20 and 30 day conditioning time-points. As movement from the bone marrow to the blood vessel requires the MSC to breakdown the ECM and invade, the PC3 educated MSCs were also examined for their capacity to invade. MSCs under normal conditions can self-renew and growth with the addition of FGF2 (see section 2.3) allows prolonged culture *in vitro* while maintaining a multipotent state (Tsutsumi et al., 2001). The PC3 educated MSCs were thus tested for their proliferation rate to assess whether the conditioning period at 10, 20 and 30 day time-points would impact this function.

MSCs are functionally characterised by their capacity to differentiate to osteocytes, adipocytes and chondrocytes (Pittenger et al., 1999, Dominici et al., 2006). Bone marrow resident MSCs have an integral function in bone remodelling and play a supportive role for HSCs (Bruder et al., 1998, Majumdar et al., 1998). Therefore, disruption of their function within the bone marrow could have major consequences on bone homeostasis. We therefore sought to determine whether PC3 educated MSCs retained a similar differentiation potential to the untreated MSCs. The cells were tested for their capacity to differentiate to adipocytes and osteocytes following 30 days of conditioning in PC3 cell CM.

The MSCs used for this study were derived from the bone marrow of healthy male donors at ages 38 (donor 1), 25 (donor 2), 20 (donor 3) and 26 (donor 4) as described in section 2.1. The age of the MSC donors does not represent the age cohort of prostate cancer patients; however MSCs derived from younger healthy donors are useful for preliminary proof-of-concept studies. The MSCS were isolated at passage 0 or 1 and used experimentally up to passage 7. PC3 and DU145 cells are human male cells originally derived from the bone and brain metastatic site, respectively. The human prostate cancer cell line, 22Rv1, was originally derived from a castrate resistant mouse xenograft model of parental CWR22 (section 2.2). The subsequent cell line 22Rv1 is androgen independent through a mutation in the androgen receptor and is non-metastatic. MSCs and cancer cells were grown in the same MSC complete growth medium throughout the duration of the study.

4.2 Results

4.2.1 Long-term Conditioning of MSCs in 22Rv1, DU145 and PC3 CM Reduces their Migration Capacity

Initial studies were carried out to evaluate the migration capacity of 22Rv1, DU145 and PC3 educated MSCs following 5, 10 and 20 day conditioning periods using MSCs derived from donor 3. Cell migration potential was tested in real-time using the xCelligence system as described in section 2.12.1 with the cells in serum free medium migrating towards medium containing 10% serum. Migration is measured by electrical impedance as the cells migrate through pores in the upper chamber of the

CIM-plate and the value is given as 'cell index'. All selected MSCs had a similar migration capacity following 5 days of conditioning with the untreated MSCs showing the greatest rate of migration (figure 4.1 A) and the difference was statistically significant between untreated MSCs and MSCs after 5 days of treatment with 22Rv1 CM (two-way ANOVA, $p<0.0001$), DU145 CM (two-way ANOVA, $p<0.0001$) and PC3 CM (two-way ANOVA, $p<0.0001$). After 10 and 20 days of conditioning, the 22Rv1, DU145 and PC3 educated MSCs show an obvious decreased rate of migration in comparison to the untreated MSCs with the DU145 and PC3 educated MSCs consistently showing the lowest rate of migration (figure 4.1 A+B). The difference was statistically significant between untreated MSCs and MSCs after both 10 and 20 days of treatment with 22Rv1 CM (two-way ANOVA, $p<0.0001$), DU145 CM (two-way ANOVA, $p<0.0001$) and PC3 CM (two-way ANOVA, $p<0.0001$).

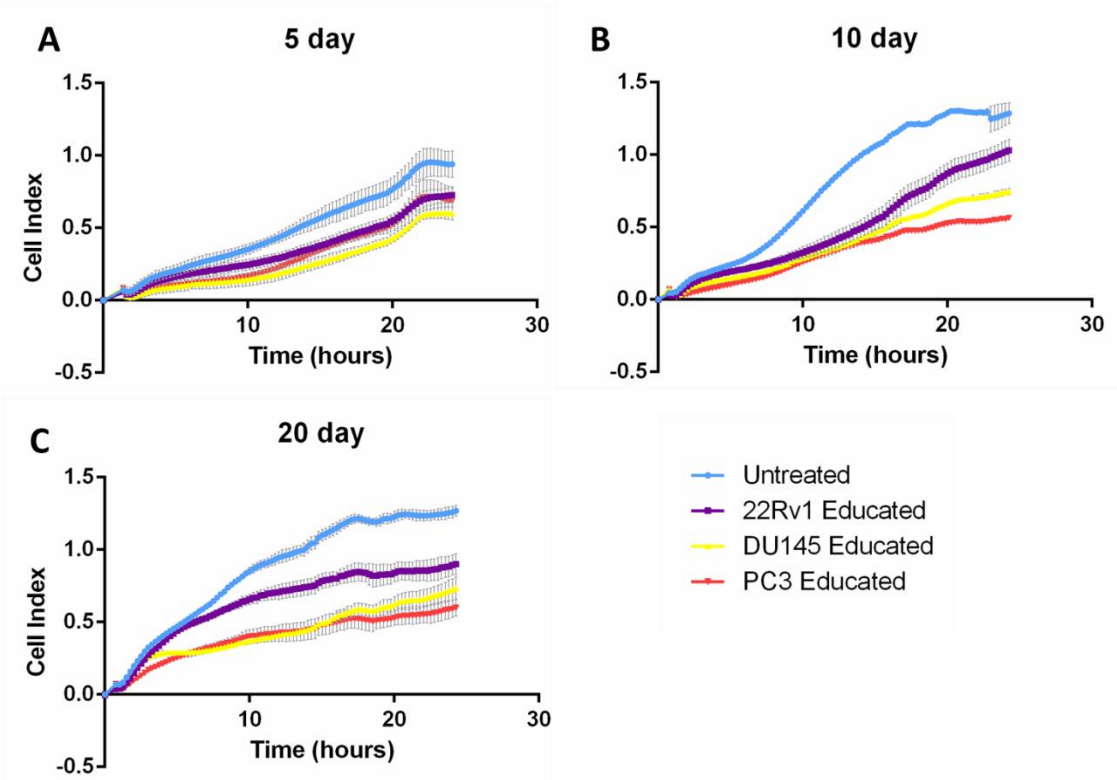

Figure 4.1 Migration Capacity of 22Rv1, DU145 and PC3 Educated MSCs. The migration capacity of 22Rv1, DU145 and PC3 educated MSCs was tested using the xCelligence system. The cells were conditioned for 5 (A), 10 (B) and 20 (C) days using MSCs from donor 3. While all cell types showed a similar rate of migration at the 5 day time-point (A), the untreated MSCs consistently showed the greatest rate of migration at each time-point (A-C) and the difference was statistically significant between untreated MSCs and MSCs after 5 days of treatment with 22Rv1 CM (two-way ANOVA, $p<0.0001$), DU145 CM (two-way ANOVA, $p<0.0001$) and PC3 CM (two-way ANOVA, $p<0.0001$). Nonetheless, an obvious decrease in the migration capacity of the 22Rv1, DU145 and PC3 educated MSCs was visible at the 10 and 20 day time-points with the DU145 and PC3 educated MSCs showing the lowest rate of migration (B+C). The difference was statistically significant between untreated MSCs and MSCs after both 10 and 20 days of treatment with 22Rv1 CM (two-way ANOVA, $p<0.0001$), DU145 CM (two-way ANOVA, $p<0.0001$) and PC3 CM (two-way ANOVA, $p<0.0001$). Data represents the mean of technical replicates ± SD.

4.2.2 Migration Capacity of PC3 Educated MSCs

The cell migration capacity of PC3 educated MSCs was validated using MSCs derived from three separate donors in real-time using the xCelligence system as described in section 2.12.1 with the MSCs in serum free medium migrating towards medium containing 10% serum. MSCs were treated for 10, 20 and 30 days in PC3 CM prior to experimental use. Migration was measured by electrical impedance as the cells migrate through pores in the upper chamber of the CIM-plate and the value was given

as 'cell index'. The 30 day treated cells were subsequently grown for an extended period (12 - 16 days) in complete medium to test whether any change in migration potential was sustained.

4.2.2.1 PC3 Educated MSCs Showed an Increased Migration Capacity Following 10 Days of Conditioning

MSCs from three donors were conditioned for 10 days in PC3 CM. The cells were tested for their capacity to migrate towards medium containing 10% serum. The PC3 educated MSCs from each donor were found to migrate at a greater rate compared to the untreated MSCs (figure 4.2 A-C). The difference in the migration rate between untreated MSCs and PC3 educated MSCs was statistically significant in MSCs derived from donor 1 (two-way ANOVA, $p<0.0001$), donor 2 (two-way ANOVA, $p<0.0001$) and donor 3 (two-way ANOVA, $p<0.0001$). Overall, combining data from all donor MSCs, the difference was also found to be statistically significant (two-way ANOVA, $p<0.0001$) (figure 4.2 D).

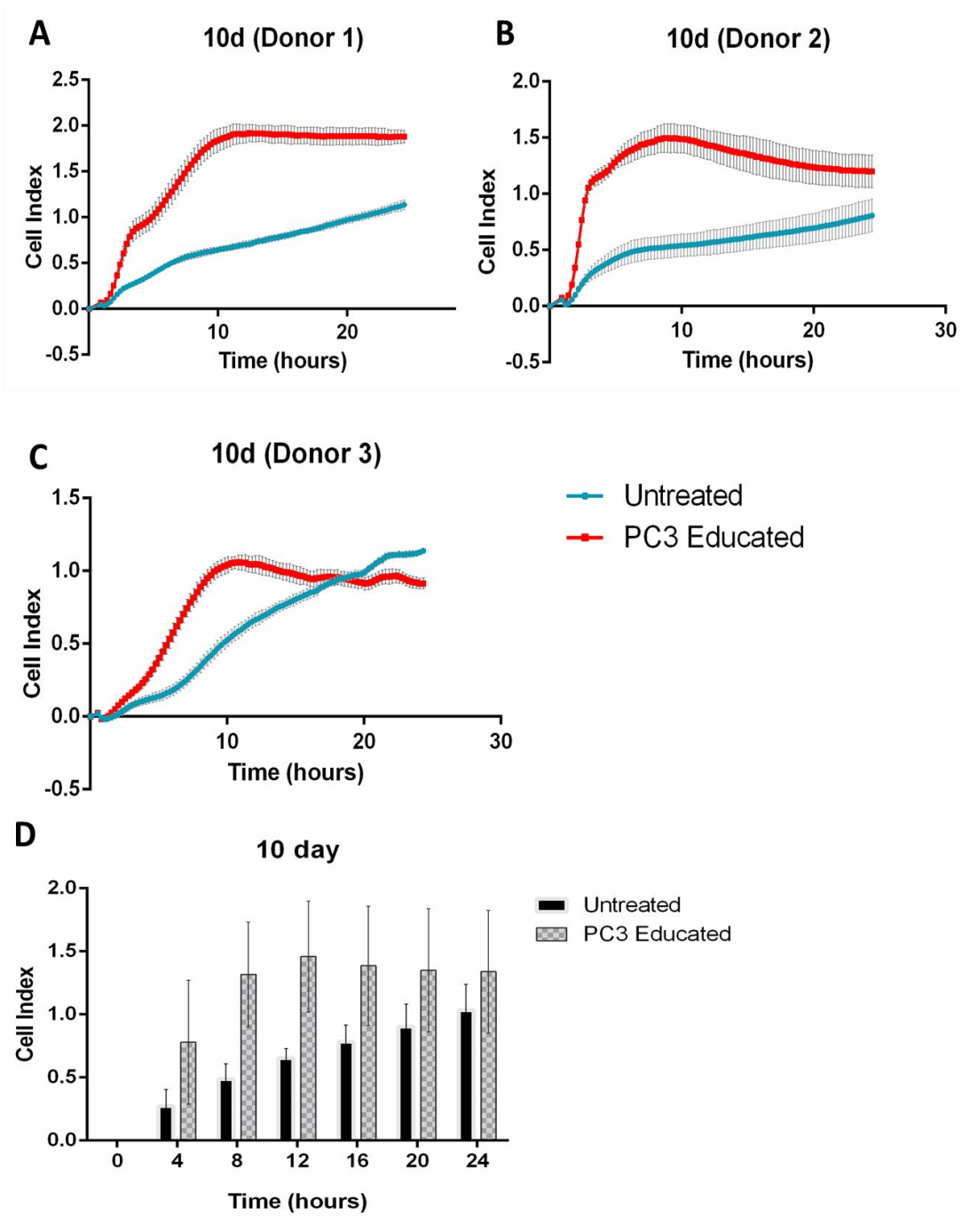

Figure 4.2. Migration Capacity of PC3 Educated MSCs Following 10 days of Conditioning. MSCs treated for 10 days with PC3 CM were tested for their capacity to migrate using the xCelligence system. The PC3 educated MSCs from each donor were found to migrate at a greater rate to the untreated MSCs (A-C). The difference in the migration rate between untreated MSCs and PC3 educated MSCs was statistically significant in MSCs derived from donor 1 (two-way ANOVA, $p<0.0001$), donor 2 (two-way ANOVA, $p<0.0001$) and donor 3 (two-way ANOVA, $p<0.0001$). Overall (D), the difference was statistically significant (two-way ANOVA, $p<0.0001$). Data represents the mean of technical replicates ± SD.

4.2.2.2 PC3 Educated MSCs Showed a Decreased Migration Capacity Following 20 Days of Conditioning

MSCs from three donors were conditioned for 20 days in PC3 CM. The cells were tested for their capacity to migrate towards medium containing 10% serum. The PC3 educated MSCs from each donor, particularly 2 and 3, were found to migrate at a decreased rate in comparison to the untreated MSCs (figure 4.3 A-C). The difference in the migration rate between untreated MSCs and PC3 educated MSCs was statistically significant in MSCs derived from donor 1 (two-way ANOVA, $p<0.0001$), donor 2 (two-way ANOVA, $p<0.0001$) and donor 3 (two-way ANOVA, $p<0.0001$). However, overall, combining data from all donor MSCs, the difference was not statistically significant (two-way ANOVA) (figure 4.3 D). This could be due to the limitations of combining data from all donor MSCs as naïve MSCs from different donors will have varying baseline migration rates.

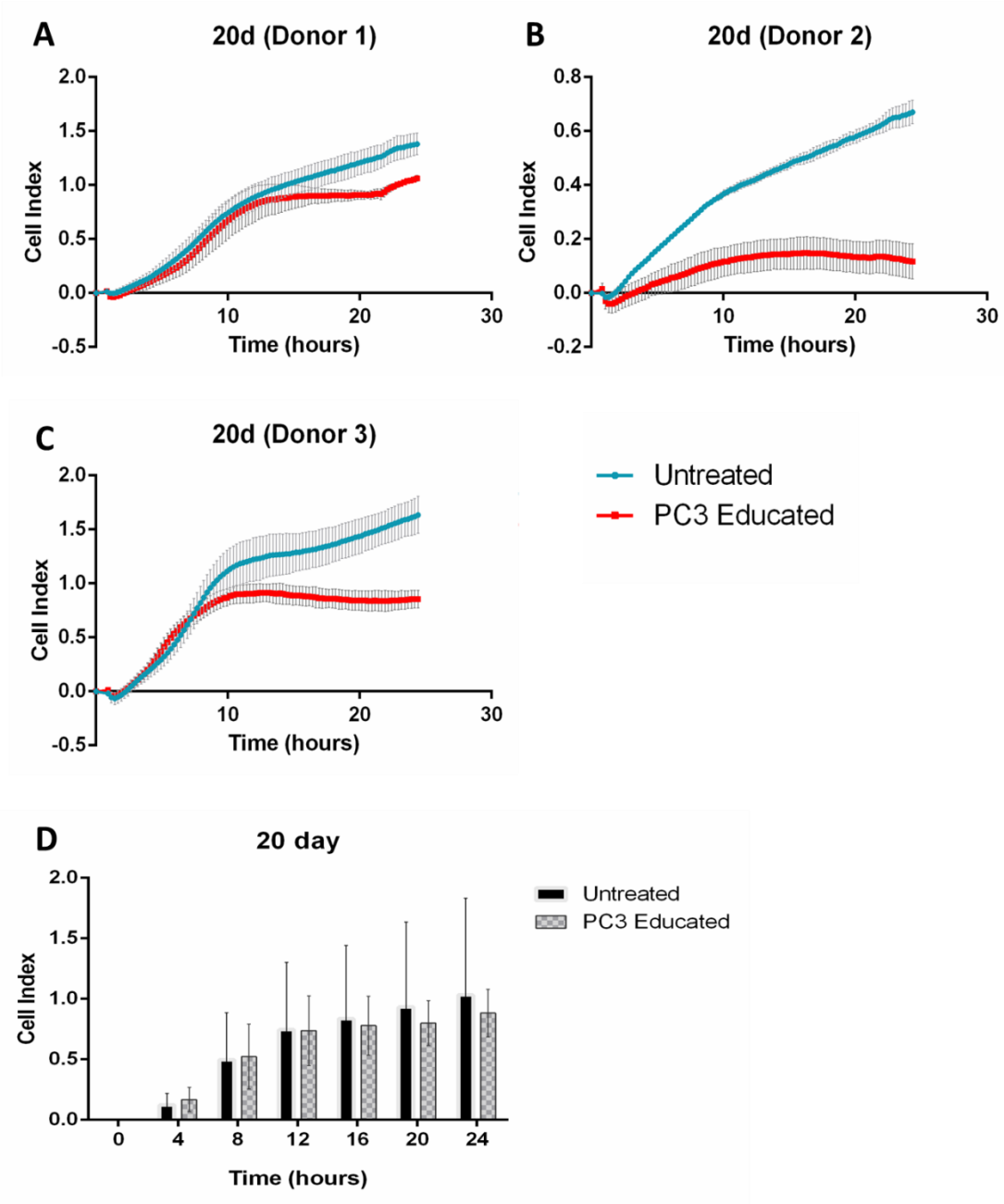

Figure 4.3. Migration Capacity of PC3 Educated MSCs Following 20 days of Conditioning. MSCs treated for 20 days with PC3 CM were tested for their capacity to migrate using the xCelligence system. The PC3 educated MSCs from each donor were found to migrate at a decreased rate in comparison to the untreated MSCs (A-C), though the most obvious difference was found in the treated MSCs from donors 2 and 3 (B+C). The difference in the migration rate between untreated MSCs and PC3 educated MSCs was statistically significant in MSCs derived from donor 1 (two-way ANOVA, $p<0.0001$), donor 2 (two-way ANOVA, $p<0.0001$) and donor 3 (two-way ANOVA, $p<0.0001$). However, overall (D) the difference was not statistically significant (two-way ANOVA). Data represents the mean of technical replicates ± SD.

4.2.2.3 PC3 Educated MSCs Showed an Decreased Migration Capacity Following 30 Days of Conditioning

MSCs from three donors were conditioned for 30 days in PC3 CM. The cells were tested for their capacity to migrate towards medium containing 10% serum. The PC3 educated MSCs from each donor were found to migrate at a decreased rate compared to the untreated MSCs (figure 4.4 A-C). The difference in the migration rate between untreated MSCs and PC3 educated MSCs was statistically significant in MSCs derived from donor 1 (two-way ANOVA, $p<0.0001$), donor 2 (two-way ANOVA, $p<0.0001$) and donor 3 (two-way ANOVA, $p<0.0001$). Overall, combining data from all donor derived MSCs the difference was statistically significant (two-way ANOVA, $p<0.05$) (figure 4.4 D).

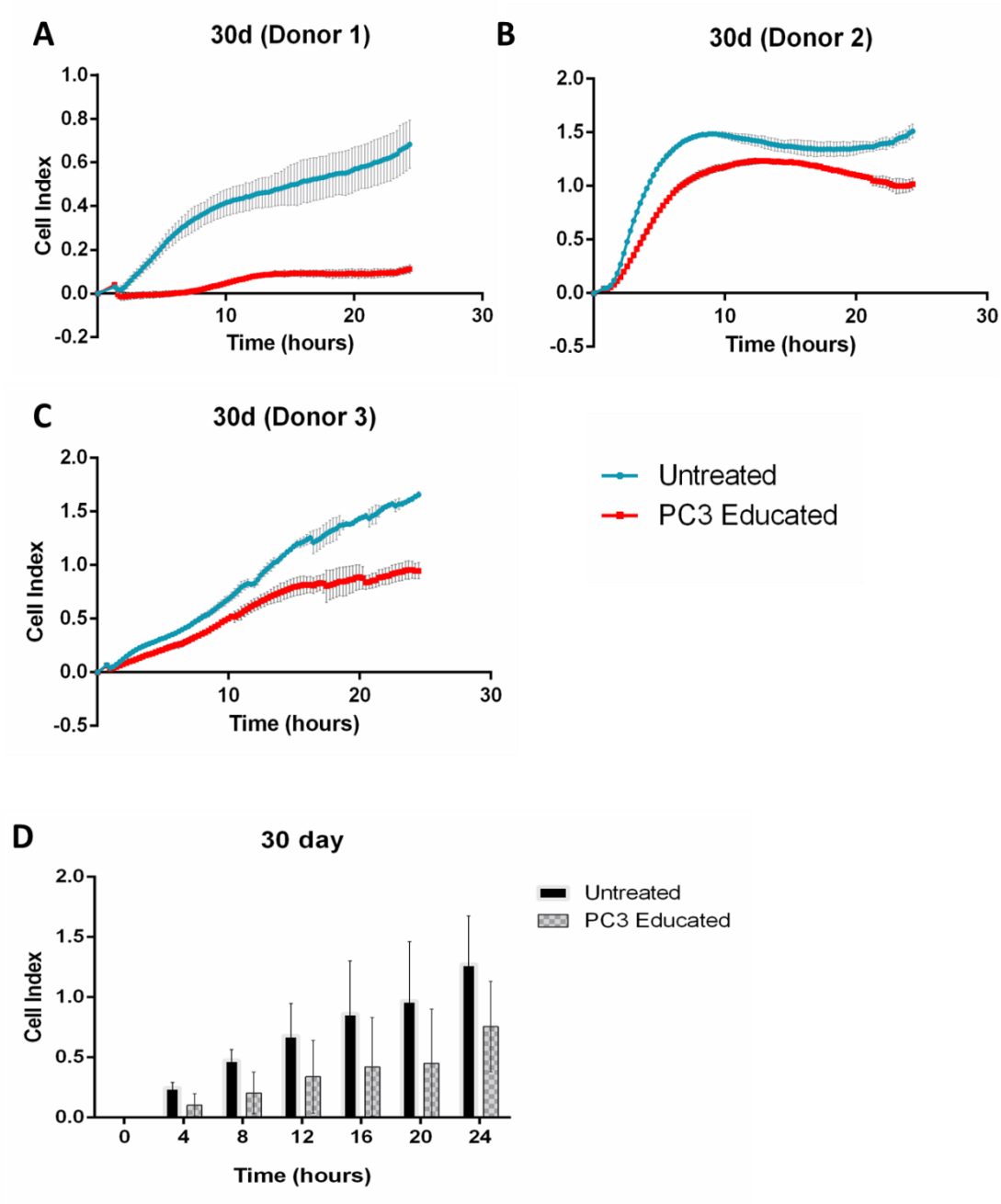

Figure 4.4. Migration Capacity of PC3 Educated MSCs Following 30 days of Conditioning. MSCs treated for 30 days with PC3 CM were tested for their capacity to migrate using the xCelligence system. The PC3 educated MSCs from each donor were found to migrate at a decreased rate in comparison to the untreated MSCs (A-C). The difference in the migration rate between untreated MSCs and PC3 educated MSCs was statistically significant in MSCs derived from donor 1 (two-way ANOVA, $p<0.0001$), donor 2 (two-way ANOVA, $p<0.0001$) and donor 3 (two-way ANOVA, $p<0.0001$). Overall (D) the difference was statistically (two-way ANOVA, $p<0.05$). Data represents the mean of technical replicates ± SD.

4.2.2.4 PC3 Educated MSCs Show an Increased Migration Capacity Post-Conditioning

MSCs conditioned for 30 days in PC3 CM were subsequently grown in complete medium for an extended period to decipher whether the decrease in migration capacity seen in the previous figure was sustained. Migration towards medium containing 10% serum was tested using the xCelligence system. In contrast to the previous finding whereby 30 day conditioned MSCs were found to migrate at a decreased rate in comparison to the untreated MSCs, the PC3 educated MSCs showed an increase in their capacity to migrate following growth without PC3 CM in comparison to the untreated MSCs. The increase was found to be statistically significant in the PC3 educated MSCs from donors 2 (two-way ANOVA, $p<0.0001$) and 3 (two-way ANOVA, $p<0.0001$) but not from donor 1 (two-way ANOVA) in comparison to the untreated MSCs (figure 4.5 A-C). Overall, combining data from all donor MSCs, the difference was not statistically significant (two-way ANOVA).

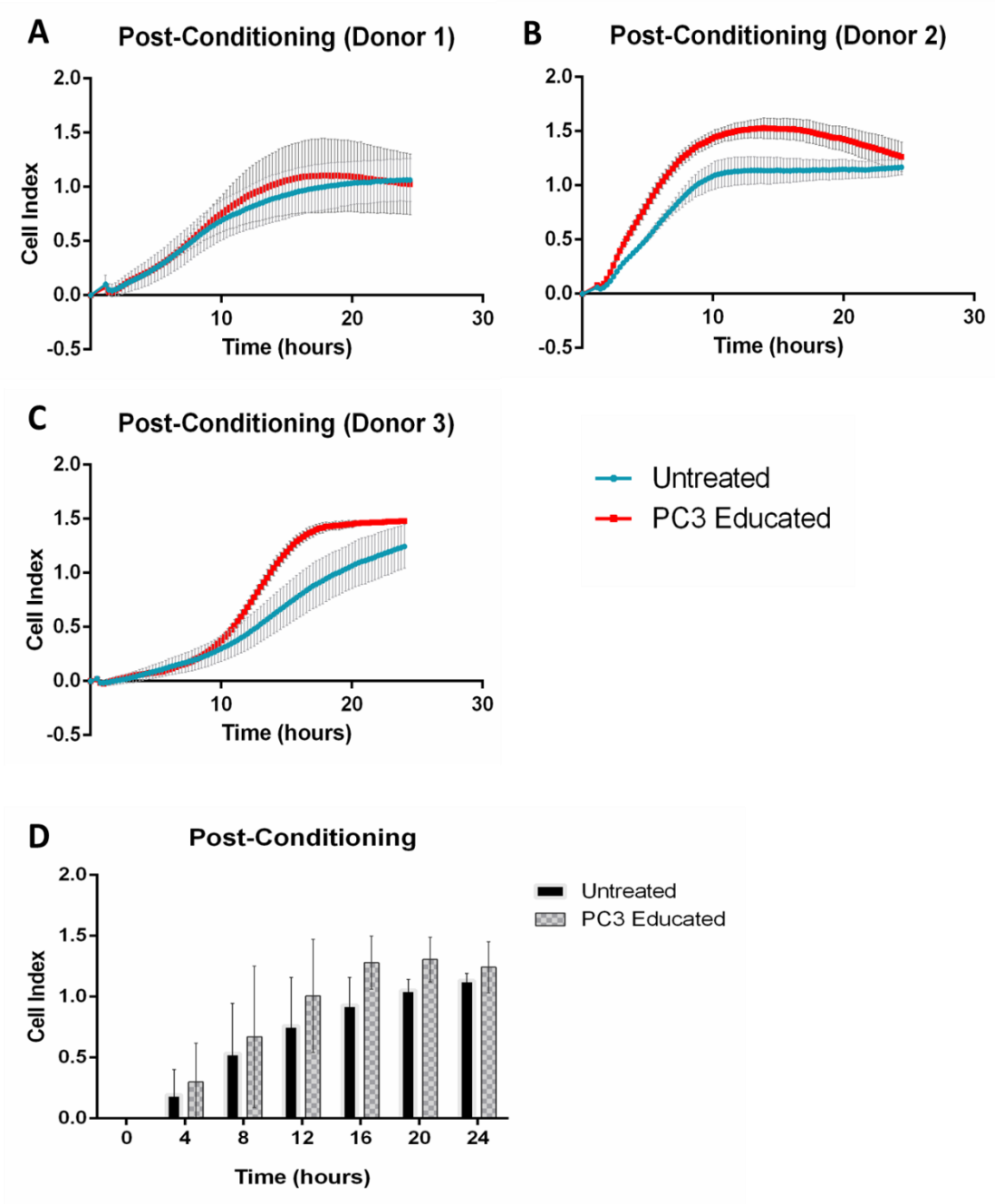

Figure 4.5. Migration Capacity of PC3 Educated MSCs Post-Conditioning. MSCs treated for 30 days with PC3 CM were grown for an extended period in complete medium and the cells were subsequently tested for their capacity to migrate using the xCelligence system. The PC3 educated MSCs from donors 2 and 3 (B+C) were found to migrate at an increased rate to the untreated MSCs (A-C). The difference was found to be statistically significant in MSCs from donors 2 (two-way ANOVA, $p<0.0001$) and 3 (two-way ANOVA, $p<0.0001$), but not from donor 1 (two-way ANOVA). However, the overall (D) difference however was not statistically significant (two-way ANOVA). Data represents the mean of technical replicates ± SD.

4.2.3 Long-term Conditioning in DU145 and PC3 CM Reduces the Invasion Capacity of MSCs

Initial studies were carried out to evaluate the invasion capacity of 22Rv1, DU145 and PC3 educated MSCs following 5, 10 and 20 day conditioning periods using MSCs derived from donor 3. The invasion potential of the cells was tested in real-time using the xCelligence system as described in section 2.12.1 and the MSCs invaded through a layer of 1 mg/ml Matrigel towards medium containing 10% serum. Invasion was measured by electrical impedance after the cells invade through the Matrigel and pores in the upper chamber of the CIM-plate and the value was given as 'cell index'. Following 5, 10 and 20 days of conditioning in DU145 and PC3 CM, the MSCs decrease in their invasion potential in comparison to the untreated MSCs (figure 4.1). The difference was statistically significant between untreated MSCs and MSCs after 5, 10 and 20 days of treatment with DU145 CM (two-way ANOVA, $p<0.0001$) and PC3 CM (two-way ANOVA, $p<0.0001$). The 22Rv1 educated MSCs show a similar invasive capacity to the untreated MSCs and do not show a statistically significant change in their rate of invasion following 10 days of treatment (two-way ANOVA). However, the MSCs showed a statistically significant decrease in their rate of invasion following 5 (two-way ANOVA, $p<0.0001$) and 20 days (two-way ANOVA, $p<0.0001$) of treatment with 22Rv1 CM (figure 4.6).

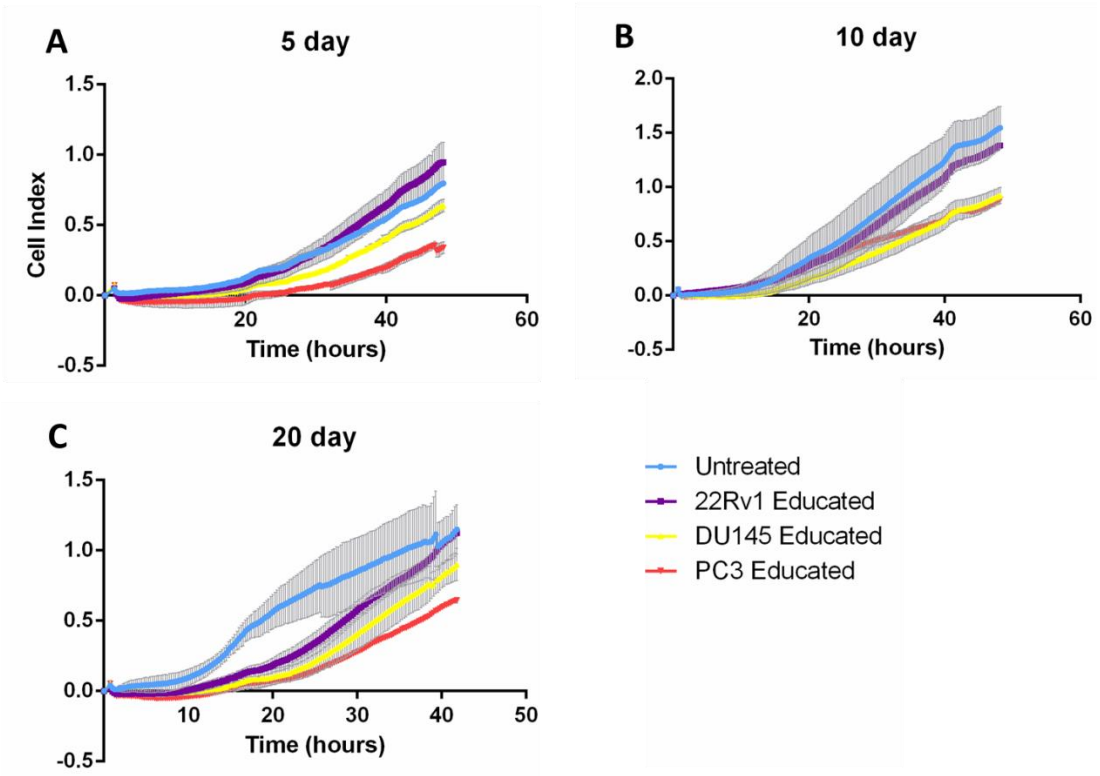

Figure 4.6 Invasion Capacity of 22Rv1, DU145 and PC3 Educated MSCs. The invasion capacity of 22Rv1, DU145 and PC3 educated MSCs were tested using the xCelligence system. The cells were conditioned for 5 (A), 10 (B) and 20 (C) days using MSCs from donor 3. While the 22Rv1 educated MSCs showed a similar rate of invasion at the 5 (A) and 10 day (B) time-points to the control, the DU145 and PC3 educated MSCs showed a consistent decrease in their capacity to invade at each time-point (A-C). The difference was statistically significant between untreated MSCs and MSCs after 5, 10 and 20 days of treatment with DU145 CM (two-way ANOVA, $p<0.0001$) and PC3 CM (two-way ANOVA, $p<0.0001$). The 22Rv1 educated MSCs did not show a statistically significant change following 10 days of treatment (two-way ANOVA). However, the MSCs showed a statistically significant decrease in their rate of invasion following 5 (two-way ANOVA, $p<0.0001$) and 20 (two-way ANOVA, $p<0.0001$) days of treatment with 22Rv1 CM. Data represents the mean of technical replicates ± SD.

4.2.4 PC3 Educated MSCs Showed a Decreased Invasion Capacity Following 30 Days of Conditioning

MSCs from three donors were conditioned for 30 days in PC3 CM. The cells were tested for their capacity to invade through a layer of 1 mg/ml Matrigel towards medium containing 10% serum (see section 2.13). The PC3 educated MSCs from donors 1 and 3 were found to invade at a decreased rate compared to the untreated MSCs (figure 4.7 A+C). The difference in the invasion rate between untreated MSCs

and PC3 educated MSCs was statistically significant in MSCs derived from donor 1 (two-way ANOVA, $p<0.0001$), donor 2 (two-way ANOVA, $p<0.001$) and donor 3 (two-way ANOVA, $p<0.0001$). The overall difference, combining data from all donor MSCs, was not found to be statistically significant (two-way ANOVA) (figure 4.7 D). We also analysed the gene expression levels of MMP9, a factor involved in ECM degradation, in untreated MSCs and PC3 educated MSCs that were conditioned for 30 days. We found that PC3 educated MSCs from donors 2 and 4 expressed decreased MMP9 in comparison to untreated MSCs (figure 4.7 E) which overall, combining data from both donor MSCs, was found to be statistically significant (unpaired student's t-test, two-tailed, $p<0.05$; n=2 biological replicates).

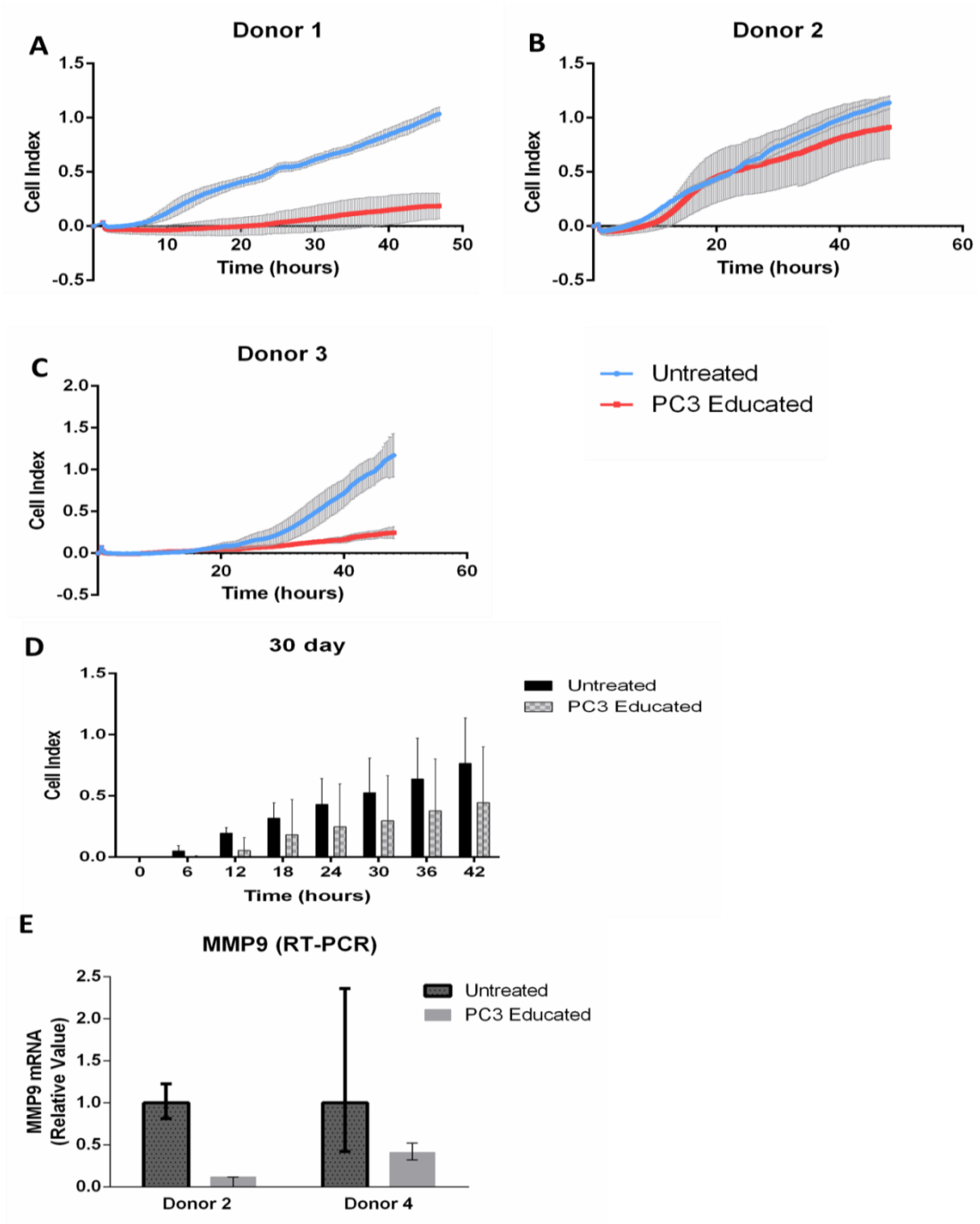

Figure 4.7. Invasion Capacity of PC3 Educated MSCs Following 30 days of Conditioning. MSCs treated for 30 days with PC3 CM were tested for their capacity to invade through Matrigel using the xCelligence system. The PC3 educated MSCs from each donor were found to decrease in their capacity to invade in comparison to the untreated MSCs (A-C), with PC3 educated MSCs from donors 1 and 3 showing the greatest change (A+C). Overall (D) the difference was not statistically significant (two-way ANOVA). Data represents the mean of technical replicates ± SD. The gene expression levels of MMP9 were analysed in untreated MSCs and PC3 educated MSCs that were conditioned for 30 days from donors 2 and 4 and found to show a decrease in expression of MMP9 (E) Overall, combining data from both donor MSCs, the difference was statistically significant (unpaired student's t-test, two-tailed, $p<0.05$; n=2 biological replicates). Data represents the mean of technical replicates with upper and lower limits.

4.2.5 Proliferation Capacity of PC3 Educated MSCs

PC3 educated MSCs were tested for their proliferation capacity using the alamar blue assay as described in section 2.14.1. The MSCs were treated for 10, 20 and 30 days in PC3 CM prior to experimental use. PC3 educated MSCs after 30 days of conditioning were grown for an extended period (12 – 16 days) in complete medium to decipher whether the cells would retain any change in their proliferation capacity.

4.2.5.1 Proliferation Capacity of PC3 Educated MSCs Following 10 Days of Conditioning

The proliferation capacity of MSCs treated for 10 days in PC3 CM was tested using the alamar blue assay (see section 2.14.1). The proliferation rate of the PC3 educated MSCs was found to be decreased in comparison to untreated MSCs from all donors (figure 4.8). The proliferation rates begin to separate by day 8 and the difference between untreated MSCs and PC3 educated MSCs was statistically significant in MSCs derived from donor 1 (paired student's t-test; two-tailed; $p<0.001$; n=3 technical replicates), donor 2 (paired student's t-test; two-tailed; $p<0.001$; n=3 technical replicates) and donor 3 (paired student's t-test; two-tailed; $p<0.05$; n=3 technical replicates). Overall, combining data from all donor MSCs, the difference in proliferation rate, taken from values at day 8, was statistically significant (paired student's t-test; two-tailed; $p<0.001$; n=3 biological replicates).

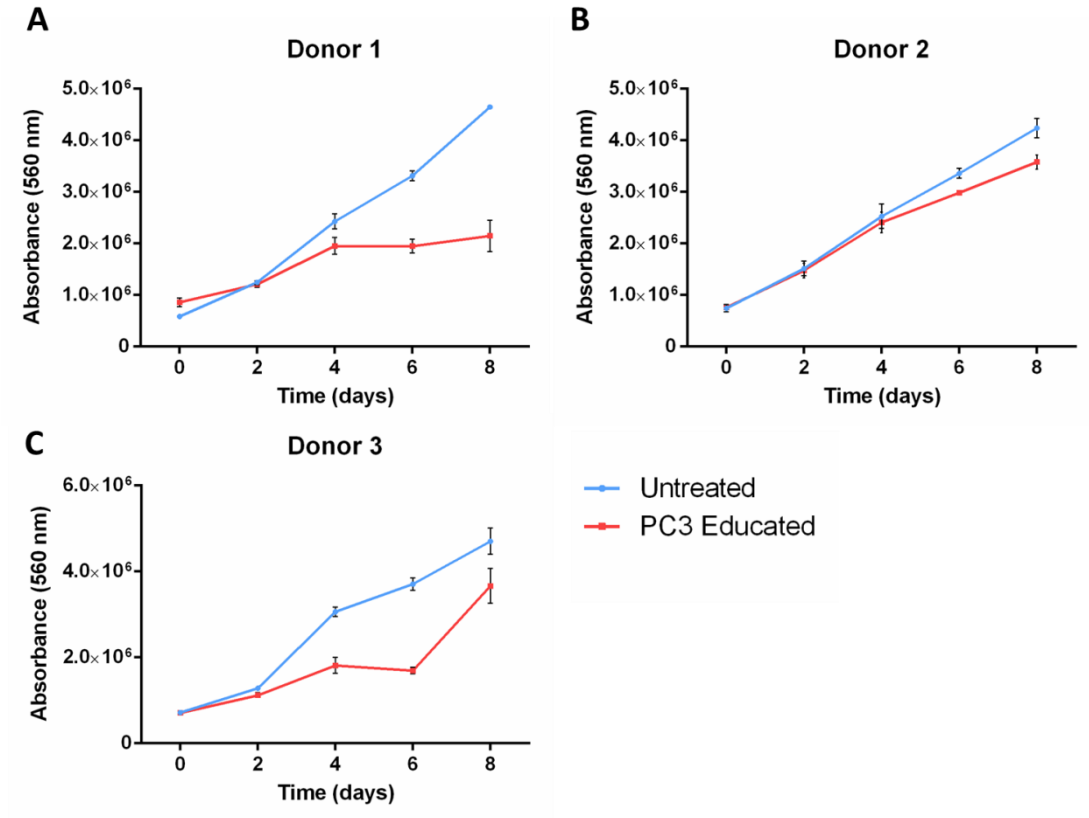

Figure 4.8. Proliferation Capacity of PC3 Educated MSCs Following 10 days of Conditioning. MSCs treated for 10 days in PC3 CM were tested for their proliferation capacity using the alamar blue assay. Readings were taken every 2 days. The PC3 educated MSCs were found to have a decreased rate of proliferation in comparison to the untreated MSCs from all donors (A-C). The difference between untreated MSCs and PC3 educated MSCs at day 8 was statistically significant in MSCs derived from donor 1 (paired student's t-test; two-tailed; $p<0.001$; n=3 technical replicates), donor 2 (paired student's t-test; two-tailed; $p<0.001$; n=3 technical replicates) and donor 3 (paired student's t-test; two-tailed; $p<0.05$; n=3 technical replicates). Overall, combining data from all donor MSCs the difference was statistically significant (paired student's t-test; two-tailed; $p<0.001$; n=3 biological replicates). Data represents mean of technical replicates ± SD.

4.2.5.2 PC3 Educated MSCs Decrease in their Proliferation Capacity Following 20 days of Conditioning

The proliferation capacity of MSCs treated for 20 days in PC3 CM was tested using the alamar blue assay (see section 2.14.1). The proliferation rate of the PC3 educated MSCs was found to be consistently decreased in comparison to untreated MSCs from donor (figure 4.9). The proliferation rates were distinctly separated by day 8 and the difference between untreated MSCs and PC3 educated MSCs was statistically significant in MSCs derived from donor 1 (paired student's t-test; two-tailed; $p<0.01$;

n=3 technical replicates), donor 2 (paired student's t-test; two-tailed; p<0.01; n=3 technical replicates) and donor 3 (paired student's t-test; two-tailed; p<0.05; n=3 technical replicates). Overall, combining data from all donor MSCs the difference in proliferation rate, taken from values at day 8, was statistically significant (paired student's t-test; two-tailed; p<0.0001; n=3 biological replicates).

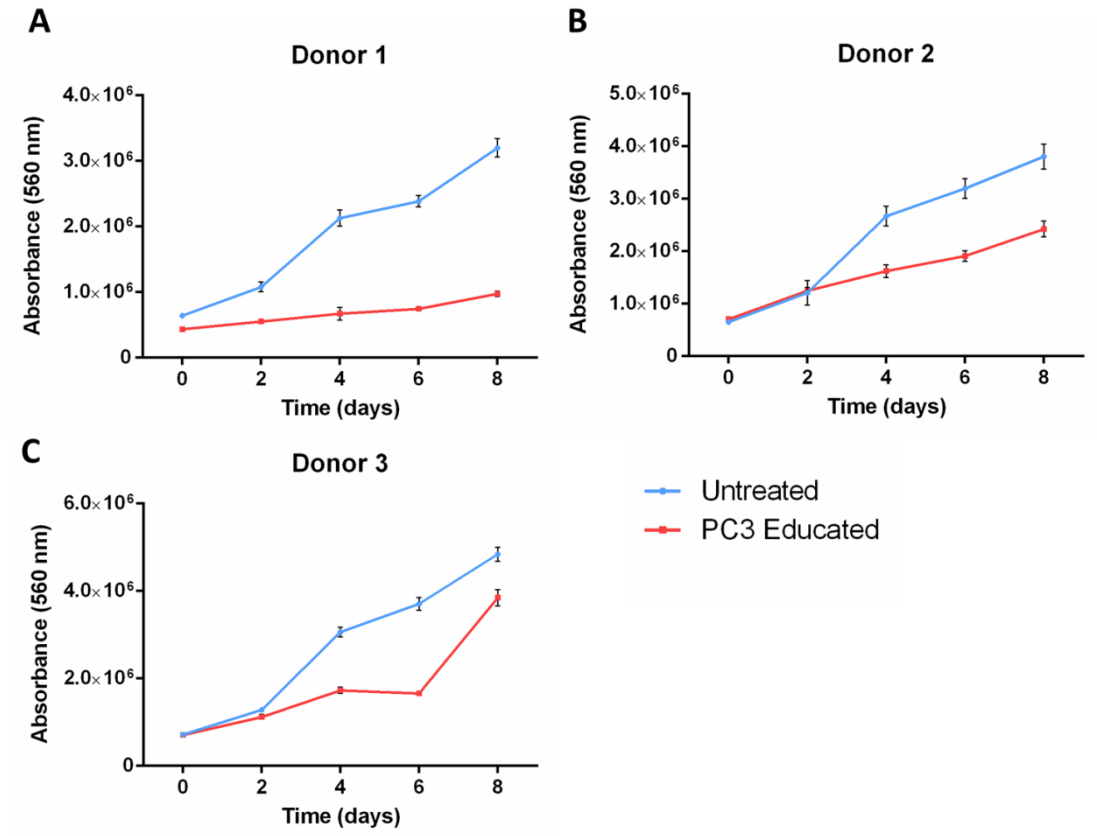

Figure 4.9. Proliferation Capacity of PC3 Educated MSCs Following 20 days of Conditioning. MSCs treated for 20 days in PC3 CM were tested for their proliferation capacity using the alamar blue assay. Readings were taken every 2 days. The PC3 educated MSCs showed a consistent decrease in their rate of proliferation from each donor in comparison to the untreated MSCs (A-C). The difference between untreated MSCs and PC3 educated MSCs at day 8 was statistically significant in MSCs derived from donor 1 (paired student's t-test; two-tailed; p<0.01; n=3 technical replicates), donor 2 (paired student's t-test; two-tailed; p<0.01; n=3 technical replicates) and donor 3 (paired student's t-test; two-tailed; p<0.05; n=3 technical replicates). Overall, combining data from all donor MSCs the difference was statistically significant (paired student's t-test; two-tailed; p<0.0001; n=3 biological replicates). Data represents mean of technical replicates ± SD.

4.2.5.3 PC3 Educated MSCs Decrease in their Proliferation Capacity Following 30 days of Conditioning

The proliferation capacity of MSCs treated for 30 days in PC3 CM was tested using the alamar blue assay (see section 2.14.1). The most evident decrease in proliferation rate was shown in the MSCs conditioned for 30 days, with cells from each donor showing a consistent decrease in comparison to untreated MSCs (figure 4.10). The proliferation rates were distinctly separated by day 8 and the difference between untreated MSCs and PC3 educated MSCs was statistically significant in MSCs derived from donor 1 (paired student's t-test; two-tailed; $p<0.01$; n=3 technical replicates), donor 2 (paired student's t-test; two-tailed; $p<0.0001$; n=3 technical replicates) and donor 3 (paired student's t-test; two-tailed; $p<0.001$; n=3 technical replicates). Overall, combining data from all donors, the difference in proliferation rate, taken from values at day 8, was statistically significant (paired student's t-test; two-tailed; $p<0.0001$; n=3 biological replicates).

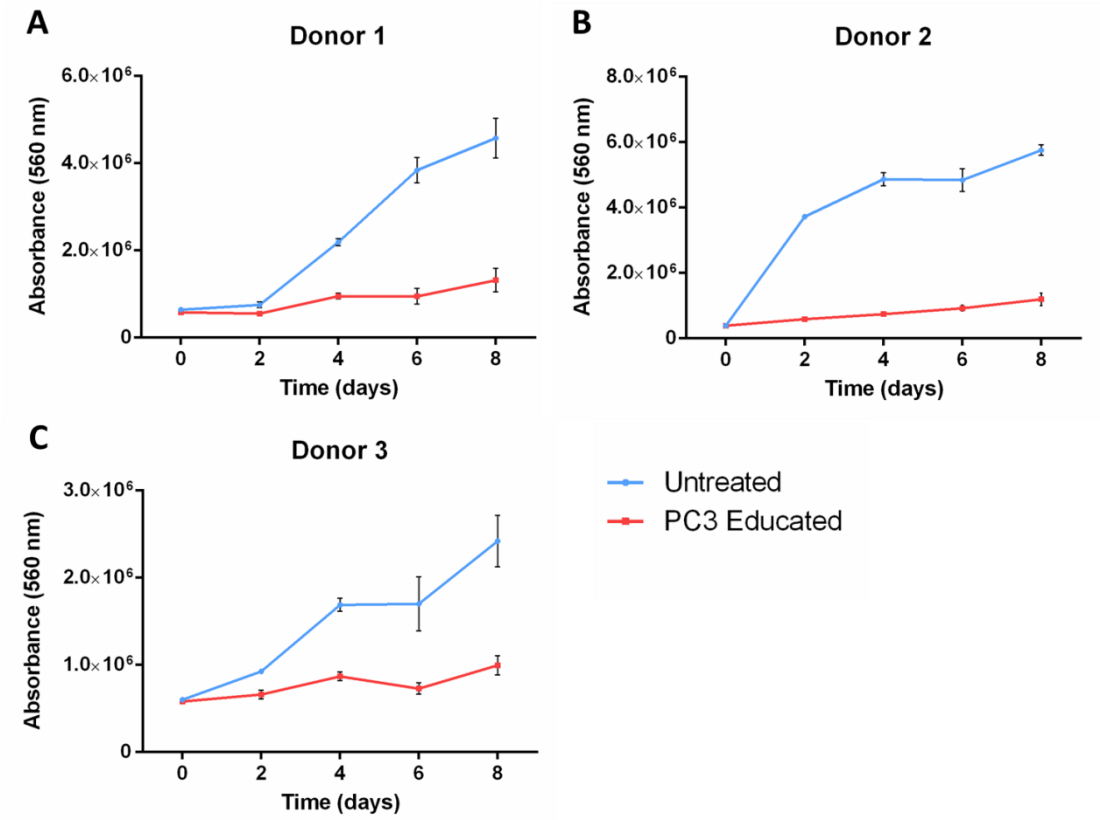

Figure 4.10. Proliferation Capacity of PC3 Educated MSCs Following 30 days of Conditioning. MSCs treated for 30 days in PC3 CM were tested for their proliferation capacity using the alamar blue assay. Readings were taken every 2 days. The PC3 educated MSCs from each donor showed a consistent decrease in their proliferation capacity in comparison to the untreated MSCs (A-C). The difference between untreated MSCs and PC3 educated MSCs was statistically significant in MSCs derived from donor 1 (paired student's t-test; two-tailed; $p<0.01$; n=3 technical replicates), donor 2 (paired student's t-test; two-tailed; $p<0.0001$; n=3 technical replicates) and donor 3 (paired student's t-test; two-tailed; $p<0.001$; n=3 technical replicates). Overall, combining data from all donor MSCs the difference was statistically significant (paired student's t-test; two-tailed; $p<0.0001$; n=3 biological replicates). Data represents mean of technical replicates ± SD.

4.2.5.4 Proliferation Capacity of PC3 Educated MSCs Post-Conditioning

MSCs were treated for 30 days in PC3 CM followed by extended growth in complete medium. The cells were then harvested and their proliferation capacity was tested using the alamar blue assay (see section 2.14.1). PC3 educated MSCs from donor 2 appeared to retain their decreased rate of proliferation (figure 4.11 B) however, PC3 educated MSCs from donors 1 and 3 regained their proliferative function and showed a similar rate to the untreated MSCs. The difference between untreated MSCs and

PC3 educated MSCs was statistically significant at day 8 of the proliferation assay in MSCs derived from donor 1 (paired student's t-test; two-tailed; $p<0.05$; n=3 technical replicates), donor 2 (paired student's t-test; two-tailed; $p<0.0001$; n=3 technical replicates) but not donor 3 (paired student's t-test; two-tailed; n=3 technical replicates). Overall, combining data from all donor MSCs the difference in proliferation rate, taken from values at day 8, was not statistically significant (paired student's t-test; two-tailed; n=3 biological replicates).

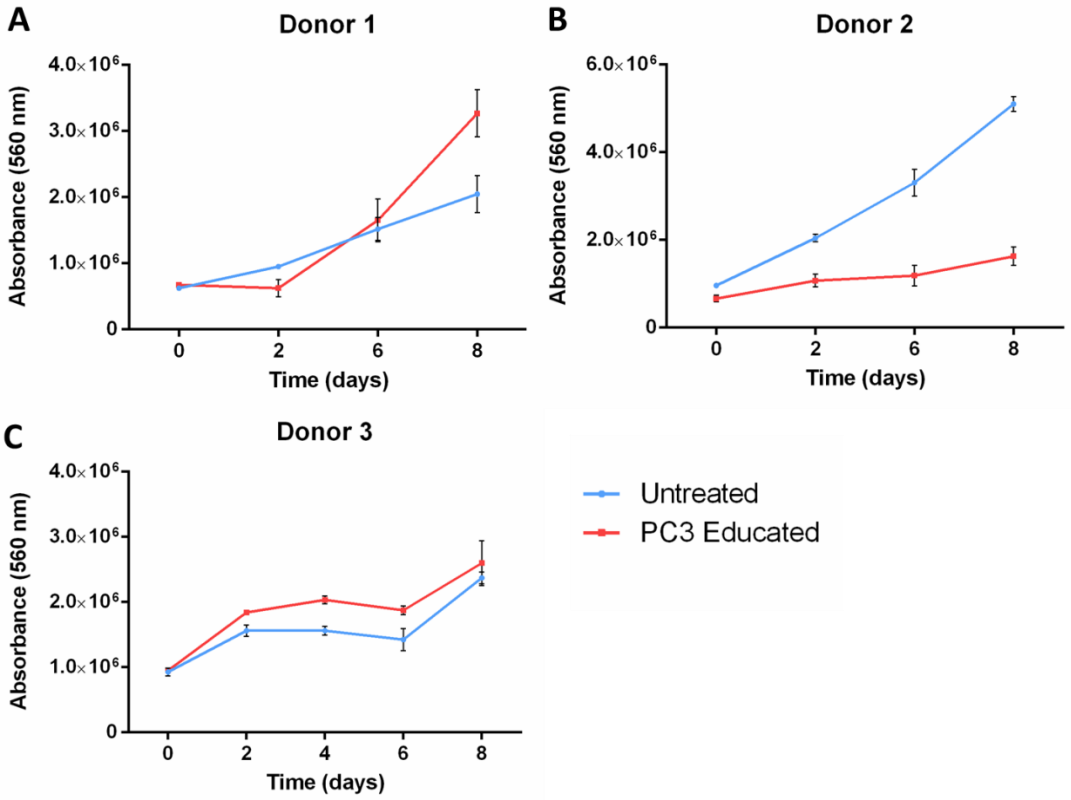

Figure 4.11. Proliferation Capacity of PC3 Educated MSCs Post-Conditioning. MSCs were treated for 30 days in PC3 CM followed by extended growth in complete medium. Proliferation capacity of the cells was tested using the alamar blue assay. Readings were taken every 2 days. The PC3 educated MSCs from donor 2 retained a decreased proliferation rate however, PC3 educated MSCs from donors 1 and 3 regained their proliferation capacity and showed a similar proliferation rate to the untreated MSCs (A-C). The difference between untreated MSCs and PC3 educated MSCs was statistically significant at day 8 of the proliferation assay in MSCs derived from donor 1 (paired student's t-test; two-tailed; $p<0.05$; n=3 technical replicates), donor 2 (paired student's t-test; two-tailed; $p<0.0001$; n=3 technical replicates) but not donor 3 (paired student's t-test; two-tailed; n=3 technical replicates). Overall, combining data values at day 8, the difference was not statistically significant (paired student's t-test; two-tailed; n=3 biological replicates). Data represents mean of technical replicates ± SD.

4.2.6 PC3 Educated MSCs are Larger in Size but do not Change in Morphology

PC3 educated MSCs were evaluated for changes in cell morphology and size. The MSCs were treated for 30 days with PC3 CM and the diameter of the cells was measured using the cellSens Entry (version 1.5) imaging system when in suspension using trypan blue to recognise viable cells. The PC3 educated MSCs were morphologically similar to the untreated MSCs and retain a fibroblastic shape (figure 4.12 A). However, there was a noticeable change in cell size, which was more visible when the cells were in suspension (figure 4.12 B). The diameter of 100 PC3 educated MSCs and untreated MSCs from each of 3 donors were measured and the PC3 educated MSCs were found to be larger in size than the untreated MSCs (figure 4.12 C-E). Overall, the untreated MSCs had a mean diameter of 26.32 µm, whereas the PC3 educated MSCs had a mean diameter of 32.76 µm and the difference was statistically significant (paired student's t-test; two-tailed; $p<0.0001$; n=3 biological donors).

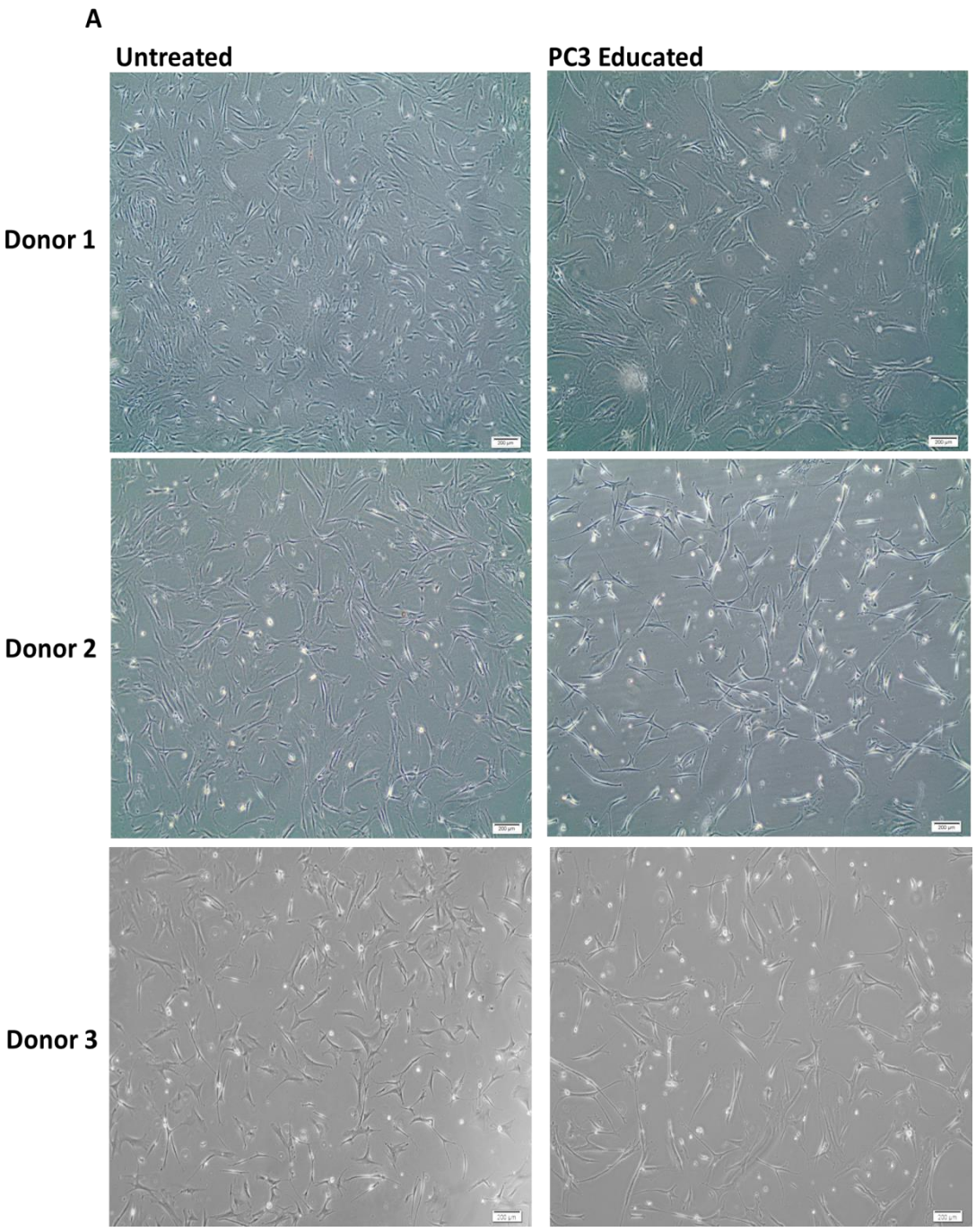
A
Untreated
PC3 Educated
Donor 1
Donor 2
Donor 3

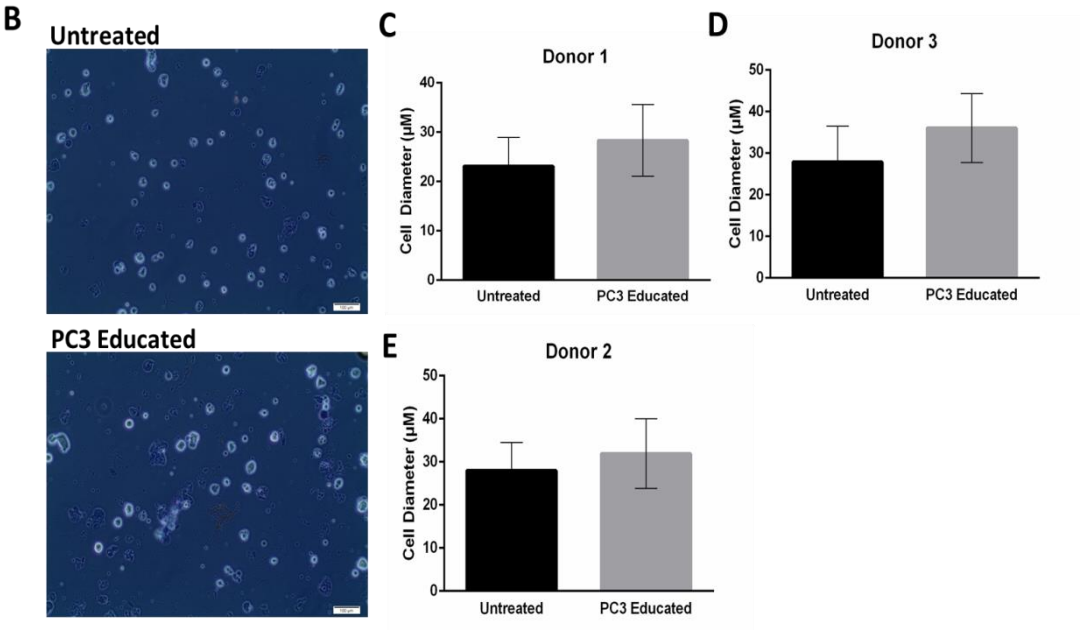

Figure 4.12. Cell Morphology and Size. MSCs were treated for 30 days in PC3 CM and evaluated for changes in cell size and morphology. The diameter of the cells was measured when in suspension and trypan blue was used to recognise viable cells (B). The PC3 educated MSCs retained the fibroblastic morphology and were similar in shape to the untreated MSCs (A). The PC3 educated MSCs were visibly larger in cell size (A), which was particularly apparent when in suspension (B). One hundred cells were measured from each of 3 donor MSCs (C-E). The PC3 educated MSCs were found to be larger in size than the untreated MSCs and the difference was statistically significant (paired student's t-test; two-tailed; $p<0.0001$; n=3 biological donors). Data represents the mean of technical replicates ± SD.

4.2.7 The Adipogenic Differentiation Potential of PC3 Educated MSCs

MSCs are partly characterised by their capacity to differentiate to adipocytes, osteocytes and chondrocytes (Dominici et al., 2006). To decipher whether PC3 educated MSCs, conditioned for 30 days, could retain some of the functional characteristics of naïve MSCs the cells were tested for adipogenic differentiation potential. The adipogenesis assay was performed and analysed as described in section 2.15. The Oil Red O assay allows you to visualise lipid droplets within the cell which indicates that adipogenesis has occurred. Both untreated MSCs and PC3 educated MSCs from each donor analysed were found to have the capacity to differentiate to adipocytes (figure 4.13). Visually, it appears that PC3 educated MSCs from donor 1 and 2 have a decreased capacity to differentiate to adipocytes (figure 4.13 A). In order to quantitatively analyse the differentiation of the MSCs, the Oil Red

O stain was removed from each well and the absorbance was quantified at 520nm. Consistent with the reduction in the level of PC3 educated MSC derived adipocytes seen in the images (figure 4.13 A), a lower amount of Oil Red O was present in wells containing the PC3 educated MSCs compared to the untreated MSCs derived from donor 1 and donor 2 but not from donor 4 (figure 4.14 B). Overall, combining data from all donor MSCs, the result was found to be statistically significant (paired student's t-test; two-tailed; $p<0.05$; n=3 biological replicates).

Given that we found the PC3 educated MSCs to be larger in size than the untreated MSCs (see section 4.2.6), the cell number within the well could differ between the treated and untreated MSCs. The gene expression of PPARγ, an adipocyte marker, was therefore analysed using real-time PCR (as described in section 2.10). PPARγ expression was found to be downregulated in PC3 educated MSCs from donors 1 and 4 and upregulated in cells from donor 2 in comparison to untreated MSCs. When data from all donors was combined, no statistically significant difference was found in PPARγ expression between the PC3 educated MSCs and untreated MSCs (figure 4.14 C) and taken together we could not conclude that the conditioning affects MSC adipogenic potential.

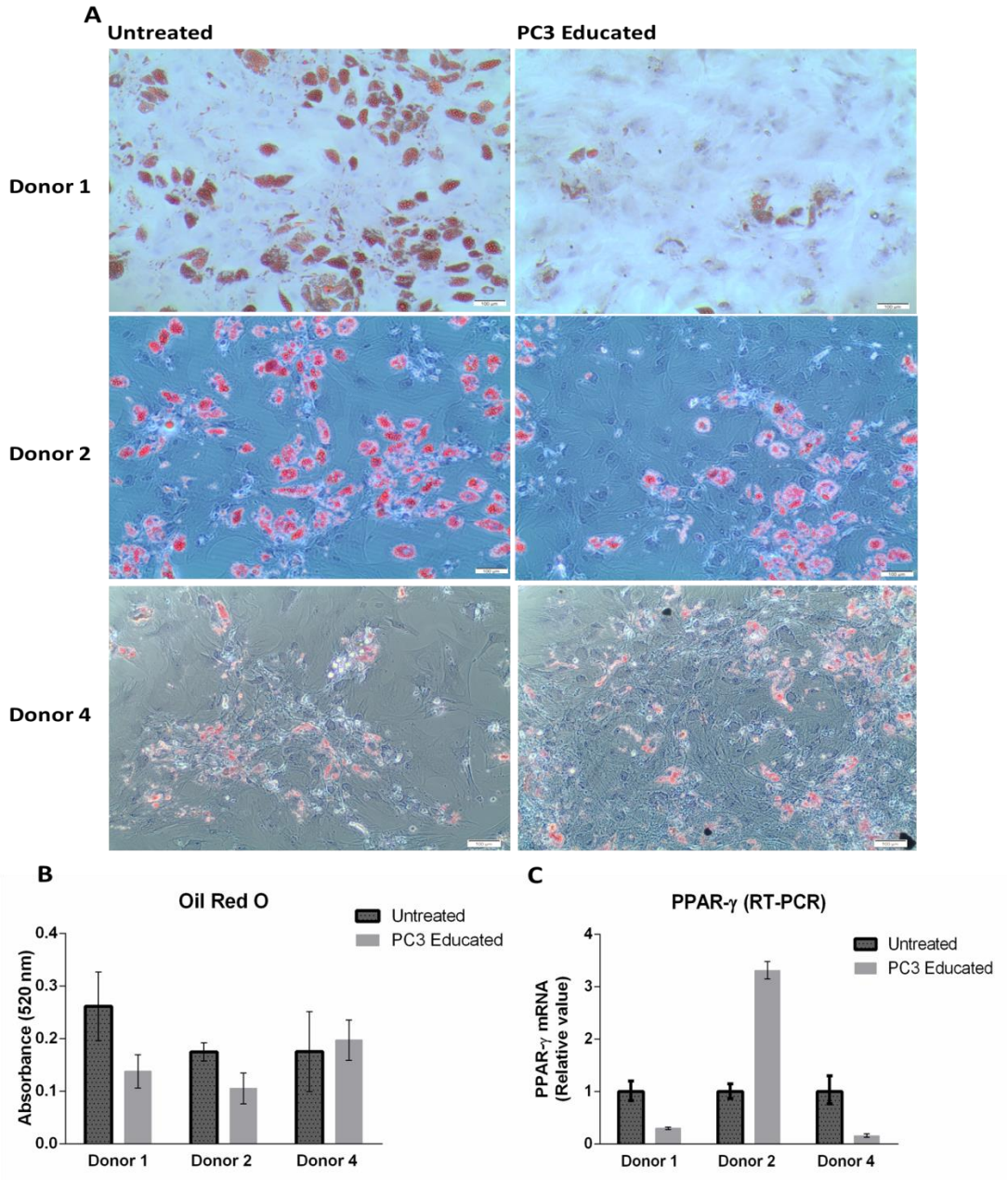

Figure 4.13. Adipogenesis. PC3 educated MSCs were tested for their adipogenic differentiation capacity. The cells were grown in adipogenic differentiation medium and analysed for lipid production using the Oil Red O assay. Visually, the PC3 educated MSCs from donors 1 and 2 were shown to have a reduced capacity for adipogenesis (A). The Oil Red O was removed from each well and the absorbance was quantified (B). A reduced amount of Oil Red O was present in wells containing the PC3 educated MSCs compared to the untreated MSCs derived from donor 1 and donor 2 but not from donor 4 (figure 4.14 B). Overall, combining data from all donor MSCs, the result was found to be statistically significant (paired student's t-test; two-tailed; $p<0.05$; n=3 biological replicates) (B). Data represents mean of technical replicates ± SD. The gene expression of the adipocyte marker PPAR-γ was tested using real-time PCR. PPAR-γ was found to be downregulated in PC3 educated MSCs from donor 1 and 4 however, overall no statistically significant difference was detected (paired student's t-test; two-tailed; $p<0.05$; n=3 technical replicates). Values were normalised to the untreated controls (C). Data represents the mean of technical replicates with upper and lower limits.

4.2.8 PC3 Educated MSCs do not Change in their Osteogenic Differentiation Potential

PC3 educated MSCs, conditioned for 30 days, were analysed for their osteogenic differentiation potential to evaluate whether the cells retain the functional characteristic of naïve MSCs. The osteogenesis assay was performed and analysed as described in section 2.16. Following 15 days of growth in osteogenic differentiation medium the cells were stained with Alizarin Red to identify calcium deposition. No clear difference in calcium deposition could be visualised between the PC3 educated MSCs and untreated MSCs (figure 4.14 A). The calcium production was quantitatively validated per well containing a cellular monolayer using the Stanbio Calcium Liquicolor test as described in section 2.16.3. The PC3 educated MSCs (20.6 µg per well) from donor 2 were found to produce less calcium than the untreated MSCs (24.5 µg per well) (figure 4.14 B). The untreated MSCs from donor 4 produced 15.8 µg per well while the PC3 educated MSCs from donor 4 produced 15.9 µg per well. Gene expression of RUNX2, a transcription factor associated with osteoblast differentiation, was assessed using real-time PCR (as described in section 2.10). No statistically significant change in the gene expression of RUNX2 was found in PC3 educated MSCs in comparison to untreated MSCs using data taken from three donor MSCs (unpaired student's t-test; two-tailed; n=3 biological replicates) (figure 4.14 C).

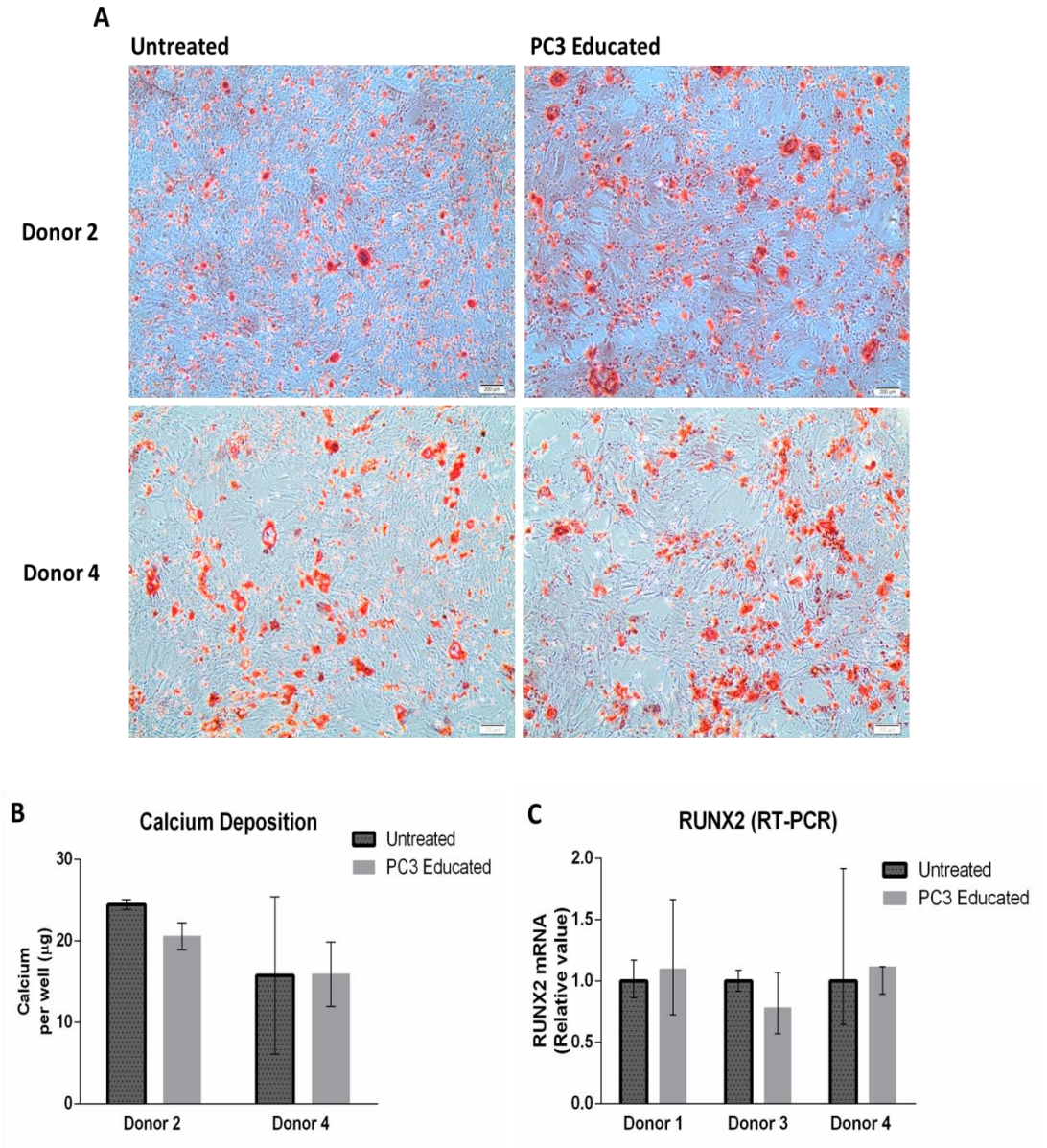

Figure 4.14. Osteogenesis. PC3 educated MSCs were tested for their osteogenic differentiation capacity. The cells were grown in osteogenic differentiation medium for 15 days and subsequently analysed for calcium production visually using the Alizarin Red stain (A) and quantitatively using the Stanbio Calcium Liquicolor test (B). No obvious difference in calcium deposition could be visually identified between the PC3 educated MSCs and untreated MSCs (A). Following quantitative analysis of calcium production, PC3 educated MSCs (20.6 µg per well) from donor 2 were found to produce less calcium than the untreated MSCs (24.5 µg per well), whereas no change was found between untreated MSCs (15.8 µg per well) and PC3 educated MSCs (15.9 µg per well) from donor 4 (B). Data represents mean of technical replicates ± SD. Gene expression of RUNX2 was analysed using real-time PCR and no statistically significant difference was found between the untreated MSCs and PC3 educated MSCs in data collected from all donors student's t-test; two-tailed; n=3 biological replicates). Values were normalised to the untreated controls (C). Data represents the mean of technical replicates with upper and lower limits.

4.3 Discussion

The aim of this study was to test the functional characteristics of the PC3 educated MSCs. MSCs are migratory cells and are known to home to inflammatory sites *in vivo* such as the heart (Orlic et al., 2001), lung (Ortiz et al., 2003), liver (Sato et al., 2005) and brain (Mahmood et al., 2003) during injury. Although the mechanisms by which the MSCs home to the various tissues is unclear, they do express different chemokine receptors and it is thought that migration is due in part to a response to cytokines and chemokines released by the tissue (Sordi et al., 2005, Von Luttichau et al., 2005, Wynn et al., 2004, Honczarenko et al., 2006).

We initially tested the migration (figure 4.1) and invasion (figure 4.6) capacity of 22Rv1, DU145 and PC3 educated MSCs that were treated with prostate cancer cell CM for 5, 10 and 20 days. All cell types showed a comparable rate of migration after 5 days of conditioning. There was however a visible decrease in the migration rate of the prostate cancer cell conditioned MSCs in comparison to the untreated MSCs after 10 and 20 days of conditioning. The MSCs treated with CM from the metastatic cell lines, DU145 and PC3, showed a similar rate of migration, which was lower than the 22Rv1 educated MSCs and untreated MSCs (figure 4.1). Interestingly, while DU145 and PC3 educated MSCs were found to have a decreased rate of migration and invasion, the 22Rv1 educated MSCs were found to have a decreased rate of migration (figure 4.1) but not invasion (figure 4.6) which suggests a tumour cell specific conditioning of MSCs.

We then carried out more robust testing on the migration capacity of PC3 educated MSCs following 10, 20 and 30 days of conditioning. Interestingly and in contrast to the previous experiment, the PC3 educated MSCs showed an increase in migration in comparison to the untreated MSCs following 10 days of conditioning. This increase was detected in cells from all three donors tested (figure 4.2). After 20 and 30 days of conditioning the PC3 educated MSCs showed a consistent decrease in their rate of migration in cells from all donors used in comparison to untreated MSCs (figure 4.3 and 4.4). Nonetheless, the PC3 educated MSCs recover their migration capacity and the cells from donors 2 and 3 show an increase in migration in comparison to the

untreated MSCs (figure 4.5). A decreased invasion capacity in the PC3 educated MSCs that were conditioned for 30 days was also observed in comparison to untreated MSCs, which may be related to the decrease in the gene expression of MMP-9 in PC3 educated MSCs (figure 4.7). It can therefore be concluded that long-term conditioning in PC3 CM results in at least a temporary inhibition of migration and invasion.

Similar results were observed after testing the proliferation rate of the PC3 educated MSCs but with a consistent decrease in PC3 educated MSC proliferation following 10, 20 and 30 days of conditioning in comparison to the untreated MSCs. The PC3 educated MSCs then regained a similar proliferation rate to the untreated MSCs in cells from 2 of 3 donors following extended growth in complete medium. Interestingly, MSCs derived from prostate cancer tumours were found to have an increased rate of proliferation when compared with bone marrow derived MSCs (Ding et al., 2012). However, in a study by Reagan and colleagues it was found that bone marrow derived MSCs grown in co-culture with multiple myeloma cells in 3D silk scaffolds showed a decreased migration and proliferation capacity in comparison to when grown without the cancer cells (Reagan et al., 2014). Although some reports are conflicting (Corre et al., 2007, Noll et al., 2014), several studies have found multiple myeloma derived MSCs to have a decreased proliferation rate in comparison to MSCs derived from healthy bone marrow (Garderet et al., 2007, Andre et al., 2013, Jurczyszyn et al., 2015). A downregulation of genes associated with proliferation were also observed in healthy and multiple myeloma derived MSCs when in co-culture with multiple myeloma cells (MM1S) (Garcia-Gomez et al., 2014).

A decrease in the expression of growth factors – nerve growth factor receptor (NGFR), platelet-derived growth factor β receptor (PDGFβR), basic fibroblast growth factor receptor (bFGFR), insulin-like growth factor-1 receptor (IGF-1R), and epidermal growth factor receptor (EGFR) – was also found in multiple myeloma derived MSCs in comparison to healthy bone marrow MSCs, which may explain the reduced rate in proliferation (Garderet et al., 2007). We did not explore the growth factor expression of the PC3 educated MSCs though this might be of interest in future studies. A decrease in chemokine and growth factor receptor expression might also explain the

low migration rate. It has been shown that a 1 day pre-treatment of MSCs with TNF-α increases CCR2, CCR3, and CCR4 expression resulting in increased migration and invasion (Ponte et al., 2007, Waterman et al., 2010). Yet, an interesting finding is that short-term stimulation by lipopolysaccharide (LPS), a TLR4 ligand, or poly(I:C), a TLR3 ligand, increased bone marrow derived MSC migration following 1 hour of incubation but inhibited migration following 24 hours of migration (Waterman et al., 2010). The complexity of the effect of secretory factors on cell migration based on exposure time may explain the increase in migration we found in MSCs conditioned for 10 days in PC3 CM versus the decrease following 20 and 30 days of conditioning.

In the next part of the study we examined the morphology of the PC3 educated MSCs and measured their cell size following 30 days of conditioning. The PC3 educated MSCs, upon visual examination, retained a similar fibroblastic and spindle shaped morphology to the untreated MSCs (figure 4.12 A). The diameter was then measured when the cells were in suspension and we found the PC3 educated MSCs to be larger in size than the untreated MSCs (figure 4.12 B). There could be many explanations, one of which could be that the cells are in the process of differentiation, resulting in a change in cell size. Another explanation could be that the PC3 educated MSCs are arrested in their cell cycle as an increase in cell size is associated with an arrest in G1 (Goranov et al., 2009). Withdrawal from cell cycle is also associated with the differentiation of many cell types and so coupling of these two mechanisms must also be considered (Scott et al., 1982, Ntambi and Young-Cheul, 2000, Peunova and Enikolopov, 1995, Bories et al., 1989, Zarrilli et al., 1999). Due to difficulties in harvesting large quantities of MSCs at the end of each conditioning period, only a selection of experiments could be performed and thus investigation into cell cycle arrest as a cause for the observed increase in size should be considered for future studies. Interestingly, it was found that stimulation of cytokines, particularly GM-CSF, G-CSF, IL-6 and IL-2 in neutrophils resulted in an enlargement of cell size in neutrophils (Yuan et al., 1993) and production of IL-2 in PBMCs was found to correlate with increased cell size (Bjork et al., 1996). Therefore, the increase in cytokine production found in the PC3 educated MSCs could be correlated with the increase found in their cell size. The induction of senescence was also considered as an

explanation for the increase in cell size observed in the PC3 educated MSCs. MSCs, like somatic cells have a limited lifespan *in vitro*, however it has been found that senescent fibroblasts within the tumour microenvironment can be metabolically active with an increase in the secretion of pro-inflammatory cytokines that results in a senescence associated secretory phenotype (SASP). It is therefore theoretically possible that the PC3 educated MSCs have acquired the SASP. However, as the PC3 educated MSCs maintained a fibroblastic, spindle-like morphology and did not develop a flattened, irregular morphology – typical of a senescent MSC – it was not further investigated (Wagner et al., 2008). Nonetheless, future studies that confirm whether or not PC3 educated MSCs are senescent should be considered.

MSCs are molecularly characterised by cell surface markers – CD105, CD73 and CD90 – and functionally characterised by the capacity to differentiate to osteocytes, chondrocytes and adipocytes (Dominici et al., 2006). MSCs isolated from gastric (Cao et al., 2009), lung (Berger et al., 2015) and breast (Zhang et al., 2013a) cancer show similar adipogenic and osteogenic differentiation potentials in comparison to bone marrow derived MSCs. However, several studies show a reduction in the osteogenic potential of multiple myeloma derived MSCs in comparison to MSCs derived from healthy bone marrow (Corre et al., 2007, Garderet et al., 2007, Li et al., 2007).

In this study, we investigated the adipogenic and osteogenic differentiation capacity of PC3 educated MSCs following 30 days of conditioning. Following growth in adipogenic and osteogenic differentiation medium, untreated MSCs and PC3 educated MSCs were visually and quantitatively assessed for lipid formation or calcium production (figure 4.13 A+B and figure 4.14 A+B). We also quantitatively analysed the gene expression of the adipogenic and osteogenic differentiation markers PPAR-γ and RUNX2, respectively (figure 13 C and figure 4.14 C). We did not however find sufficient evidence to suggest that the PC3 educated MSCs differed in their adipogenic or osteogenic differentiation potential.

In contrast to our research, it was found in two separate studies that PC3 CM can induce increased osteogenic differentiation potential, however the experiments involved growing naïve MSCs in osteogenic differentiation medium and PC3 CM

simultaneously (Borghese et al., 2013, Fritz et al., 2011). These results, in light of what we have found could signify impairment of MSC osteogenic or adipogenic differentiation capacity that is dependent on paracrine signalling from PC3 cells. Moreover, gene analysis of PC3 holoclones showed suppression of genes associated with osteogenic differentiation (Gallagher et al., 2015). Borghese and colleagues also found that simultaneous growth of bone marrow derived MSCs in adipogenic differentiation medium and PC3 CM resulted in decreased adipogenic differentiation potential (Borghese et al., 2013). Similarly, bone marrow derived MSCs grown with adipogenic differentiation medium and DU145 cell derived exosomes also resulted in decreased adipogenesis (Chowdhury et al., 2015). Therefore, future studies involving continuous exposure to PC3 CM could alter the osteogenic and adipogenic differentiation potential of the MSCs.

In conclusion, we found that long-term culture in PC3 CM inhibits the migration and proliferation of MSCs and that both functions can be recovered following growth in complete medium. PC3 educated MSCs following 30 days of conditioning were found to have a similar fibroblastic, spindle-like morphology to untreated MSCs, although they were found to be larger in size. The PC3 educated MSCs, when removed from CM retain their capacity for osteogenesis and adipogenesis.

Chapter 5

Impact of PC3 Educated MSCs on Tumour Cell Progression

5.1 Introduction

It is now understood that MSCs home to the tumour site and interact with the surrounding cells (Ame-Thomas et al., 2007, Kansy et al., 2014, Hossain et al., 2015, Karnoub et al., 2007, Prantl et al., 2010). Moreover, metastasis to the bone involves the migration of prostate cancer cells to where MSCs are resident. Research is conflicted however as to whether MSCs have a tumour promoting or suppressive function (Klopp et al., 2011). MSC and tumour cell interactions could be dependent on MSC ratio within the tumour, MSC origin as well as tumour cell type and grade (Klopp et al., 2011). Nonetheless, the majority of studies find that MSCs have a tumour promoting function in the stimulation of tumour growth, invasion and metastasis (Karnoub et al., 2007, Prantl et al., 2010, Ye et al., 2012, Mi et al., 2011). It has also been shown that co-culture with MSCs results in increased chemoresistance in leukemia cells, an outcome found to be dependent on SDF-1α/CXCR4 interaction (Ito et al., 2015, Xia et al., 2015, Zeng et al., 2009).

In this study, we investigated whether PC3 educated MSC interactions evoked functional, tumour promoting or suppressive reactions in various prostate cancer cells. The PC3 educated MSCs were conditioned for 30 days prior to each experiment. The cytotoxic response of PC3 educated MSCs was initially assessed using the chemotherapeutic drug, docetaxel to determine whether there was any change in their cytotoxic sensitivity. The taxane, docetaxel, is an inhibitor of mircrotubule depolymerisation and docetaxel-based treatment has shown survival benefit in patients with metastatic castration-resistant prostate cancer in two randomized phase III clinical trials (Verweij et al., 1994, Petrylak et al., 2004, Tannock et al., 2004). PC3 cells were then grown in an indirect co-culture system with untreated MSCs and PC3 educated MSCs, and treated with either docetaxel or paclitaxel to examine whether PC3 educated MSCs had a chemoprotective effect on PC3 cells. The proliferation rate of PC3 cells in response to untreated MSCs and PC3 educated MSCs was assessed using a similar approach. PC3 cells were examined for their proliferation rate using an indirect co-culture system with untreated MSCs and PC3 educated MSCs over a 72 hour period.

Finally, PC3 educated MSCs were found to release an increase in known chemoattractant factors - MCP-1, IL8 and OPN - in previous experiments shown in chapter 3. It was therefore considered that PC3 educated MSCs may stimulate increased chemotaxis of prostate cancer cells. The migration of 22Rv1, DU145 and PC3 cells towards a monolayer of untreated MSCs and PC3 educated MSCs was thus evaluated.

The MSCs used for this study were derived from the bone marrow of healthy male donors at ages 38 (donor 1), 25 (donor 2), 20 (donor 3) and 26 (donor 4) as described in section 2.1. The age of the MSC donors does not represent the age cohort of prostate cancer patients; however MSCs derived from younger healthy donors are useful for preliminary proof-of-concept studies. The MSCS were isolated at passage 0 or 1 and used experimentally up to passage 7. PC3 and DU145 cells are human male cells originally derived from the bone and brain metastatic site, respectively. The human prostate cancer cell line, 22Rv1, was originally derived from a castrate resistant mouse xenograft model of parental CWR22 (section 2.2). The subsequent cell line 22Rv1 is androgen independent through a mutation in the androgen receptor and is non-metastatic. MSCs and cancer cells were grown in the same MSC complete growth medium throughout the duration of the study.

5.2 Results

5.2.1 PC3 Educated MSCs do not Change in their Cytotoxic Response to Docetaxel

PC3 educated MSCs that were conditioned for 30 days were tested for their cytotoxic resistance to docetaxel in comparison to untreated MSCs. Initially, untreated MSCs were treated with a range of docetaxel concentrations for 72 hours followed by an alamar blue viability assay as described in section 2.17. A dose-response curve was generated and the IC_{50} was determined at 800 µM, which was used to test PC3 educated MSC cytotoxic resistance (figure 5.1 A). However, no change in cytotoxic resistance was detected in PC3 educated MSCs compared to the untreated MSCs (figure 5.1 B). Survival for untreated MSCs was found at 56.7% and at 59.5% for the PC3 educated MSCs. The difference was not found to be statistically significant (paired student's t-test; two-tailed; n=3 biological replicates). Values were

normalised to the untreated controls and the data was collected from 3 separate donors and represents the mean ± SD.

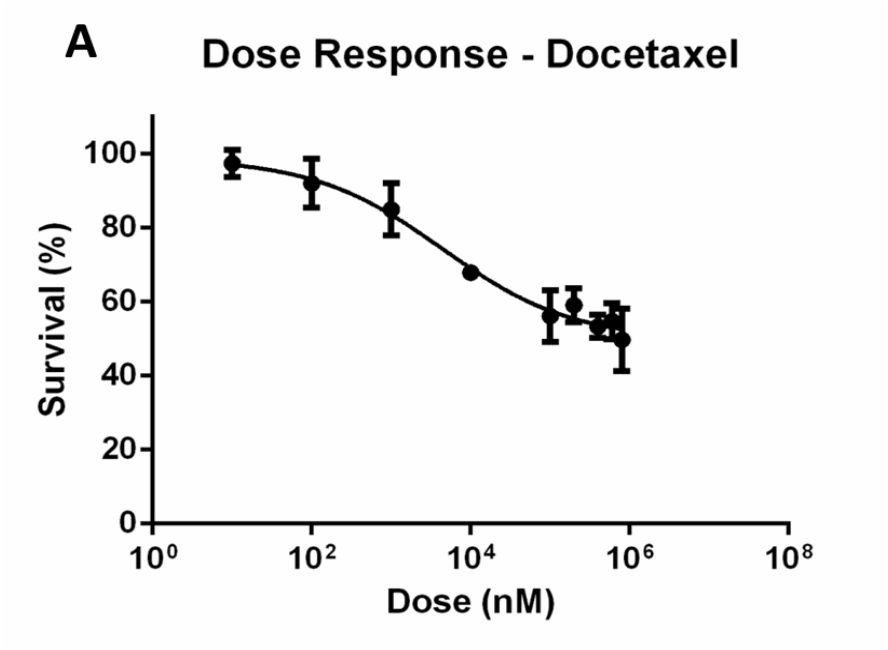

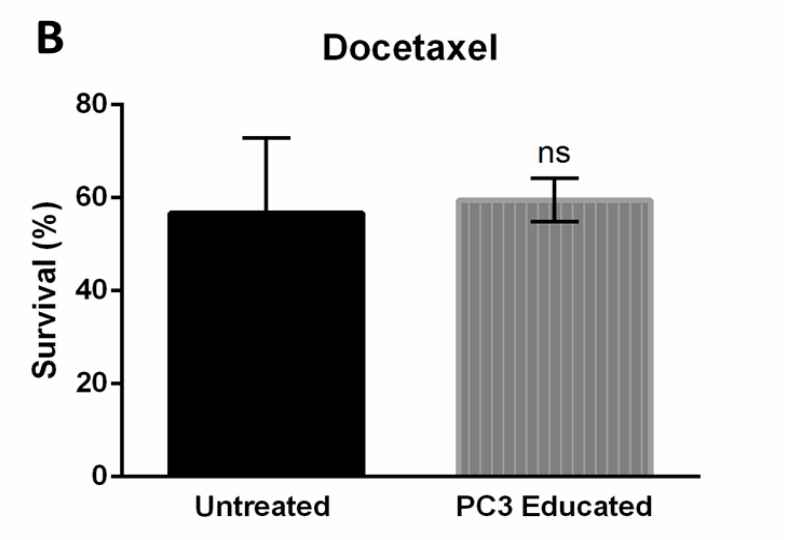

Figure 5.1. Cytotoxic Resistance of PC3 Educated MSCs. PC3 educated MSCs that were conditioned for 30 days were tested for cytotoxic resistance to docetaxel. Untreated MSCs were treated with a range of concentrations to generate a dose-response curve (A). The untreated MSCs and PC3 educated MSCs were then treated with the IC_{50} (800 µM docetaxel). The PC3 educated MSCs were not found to change in their resistance to docetaxel and the difference was not found to be statistically significant (paired student's t-test; two-tailed; n=3 biological replicates). Values were normalised to the untreated controls and the data was collected from 3 independent experiments using 3 separate donors (B) and represents the mean ± SD.

5.2.2 PC3 cells do not Change in their Cytotoxic Response when Grown in Co-culture with PC3 Educated MSCs

Cytotoxic resistance was tested in PC3 cells following indirect co-culture with untreated MSCs or PC3 educated MSCs. The PC3 cells in monoculture were initially treated with a range of docetaxel and paclitaxel concentrations for 72 hours followed by an alamar blue viability assay as described in section 2.17. A dose-response curve was generated for each drug tested (figure 5.2 A+B) and used to determine the IC_{50}. PC3 cells were then grown in an indirect co-culture system with either untreated MSCs or PC3 educated MSCs as described in section 2.17.2. The MSCs were grown in the upper chamber wells, on a 0.4 µm porous membrane, of a 96-well permeable plate and the PC3 cells were grown in the bottom wells.

The PC3 cells were treated for 72 hours with the IC_{50} determined for docetaxel (743 nM) and Paclitaxel (470 nM) and viability was assessed using the alamar blue assay. No change in cytotoxic resistance was found between PC3 cells grown in co-culture with either untreated MSCs or PC3 educated MSCs following treatment with either docetaxel or paclitaxel (figure 5.2 C+D). Survival for PC3 cells in co-culture with untreated MSCs and PC3 educated MSCs following treatment with docetaxel was found at 63.67% and 62.52%, respectively and survival for PC3 cells in co-culture with untreated MSCs and PC3 educated MSCs following treatment with paclitaxel was 53.07% and 50.75%, respectively. The difference in percentage survival was not found to be statistically significant between the PC3 cells grown in co-culture with untreated MSCs or PC3 educated MSCs using either docetaxel or paclitaxel (paired student's t-test; two-tailed; n=3 biological replicates). Values were normalised to the untreated controls and the data is collected from 3 independent experiments using 3 separate donors and represents the mean ± SD.

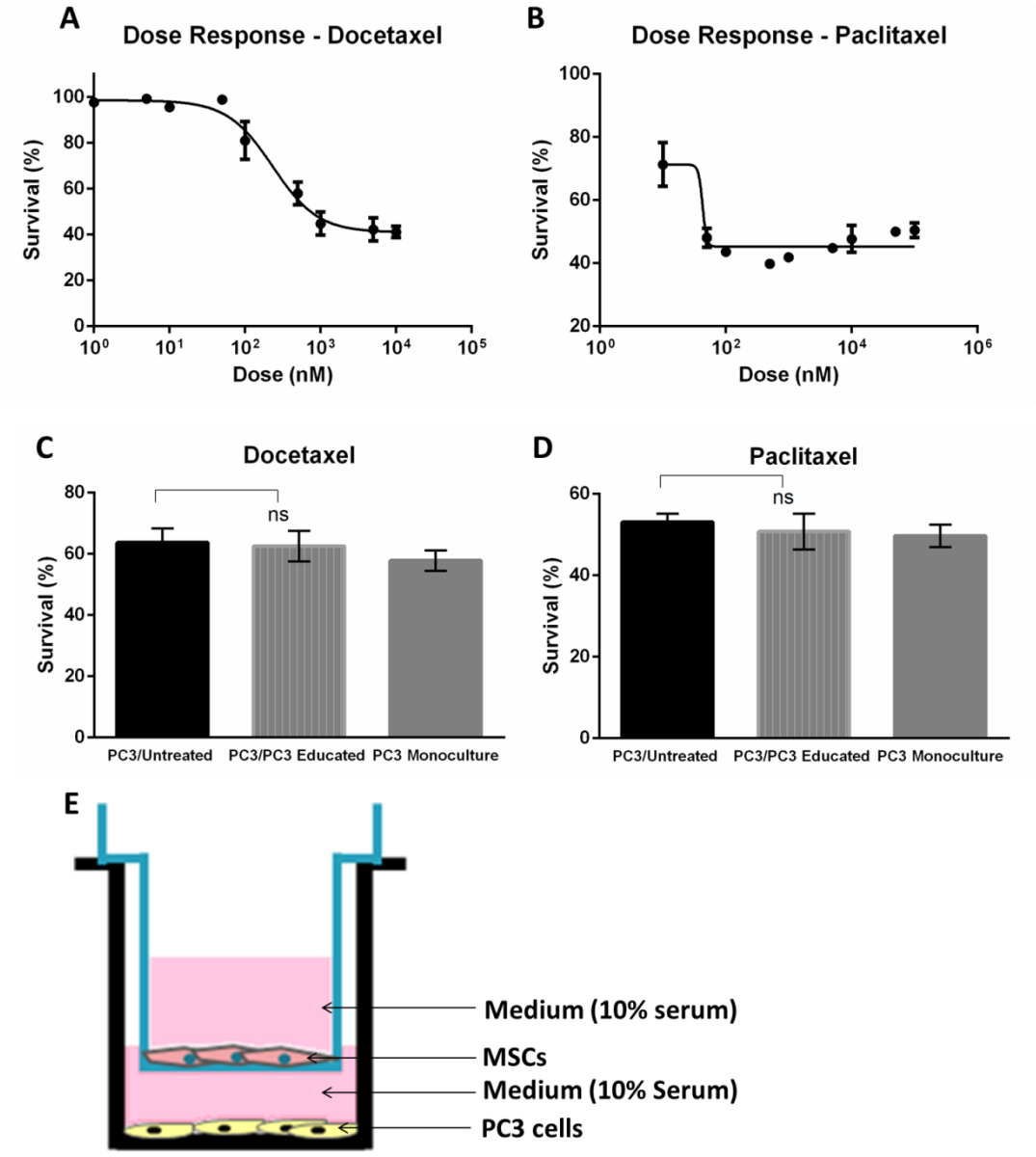

Figure 5.2. Cytotoxicity of PC3 Cells in Co-culture with PC3 Educated MSCs. PC3 cells were tested for their cytotoxic resistance to docetaxel and paclitaxel in monoculture or following indirect co-culture with untreated MSCs or PC3 educated MSCs. The PC3 cells were initially treated with a range of docetaxel and paclitaxel concentrations to generate a dose-response curve and determine the IC_{50} of each drug (A+B). The PC3 cells in co-culture with untreated MSCs or PC3 educated MSCs were then tested for cytotoxic resistance using the IC_{50} determined for docetaxel (743 nM) and paclitaxel (470 nM). No change or statistically significant difference was found in the cytotoxic resistance to docetaxel (C) or paclitaxel (D) between PC3 cells grown in co-culture with either untreated MSCs or PC3 educated MSCs (paired student's t-test; two-tailed; n=3 biological replicates). E. Illustration depicting the indirect co-culture system. Values were normalised to the untreated controls and the data was collected from 3 independent experiments using 3 separate donors (C+D) and represents the mean ± SD.

5.2.3 Proliferation of PC3 Cells in Response to Conditioned Medium Derived from PC3 Educated MSCs

PC3 cells were grown in CM derived from PC3 educated MSCs and examined for their rate of proliferation over a 6 day period. Briefly, the MSCs were grown for 30 days in PC3 cell CM, harvested, re-seeded and grown for a further 24 hours in complete medium prior to the collection of CM. The PC3 cells were then grown in 50% CM (untreated MSCs or PC3 educated MSCs) and 50% complete medium or 100% complete medium for the duration of the assay. The viability was assessed every 2 days for 6 days using the alamar blue assay as described in section 2.14.

The PC3 cells showed similar rates of proliferation following growth in untreated MSC CM, PC3 educated MSC CM or complete medium. The trend was the same between the two separate donors whereby the growth was slowest in PC3 educated MSC CM and highest in complete medium (figure 5.3). The proliferation rates begin to separate slightly by day 6. The difference between PC3 cells grown in untreated MSC CM and PC3 educated MSC CM was not statistically significant at day 6 in MSCs derived from either donor 1 or donor 2 (paired student's t-test; two-tailed; n=3 technical replicates). However, overall, combining data from both donors, the difference was statistically significant (paired student's t-test; two-tailed; $p<0.05$; n=2 biological replicates). The difference between PC3 cells grown alone and in untreated MSC CM was statistically significant at day 6 using CM from donor 1 (paired student's t-test; two-tailed; $p<0.05$; n=3 technical replicates) and donor 2 (paired student's t-test; two-tailed; $p<0.01$; n=3 technical replicates) and when combining data from both donors (paired student's t-test; two-tailed; $p<0.001$; n=2 biological replicates). The difference between PC3 cells grown alone and in PC3 educated MSC CM was also statistically significant at day 6 using CM from donor 1 (paired student's t-test; two-tailed; $p<0.01$; n=3 technical replicates) and donor 2 (paired student's t-test; two-tailed; $p<0.01$; n=3 technical replicates) and when combining data from both donors (paired student's t-test; two-tailed; $p<0.0001$; n=2 biological replicates).

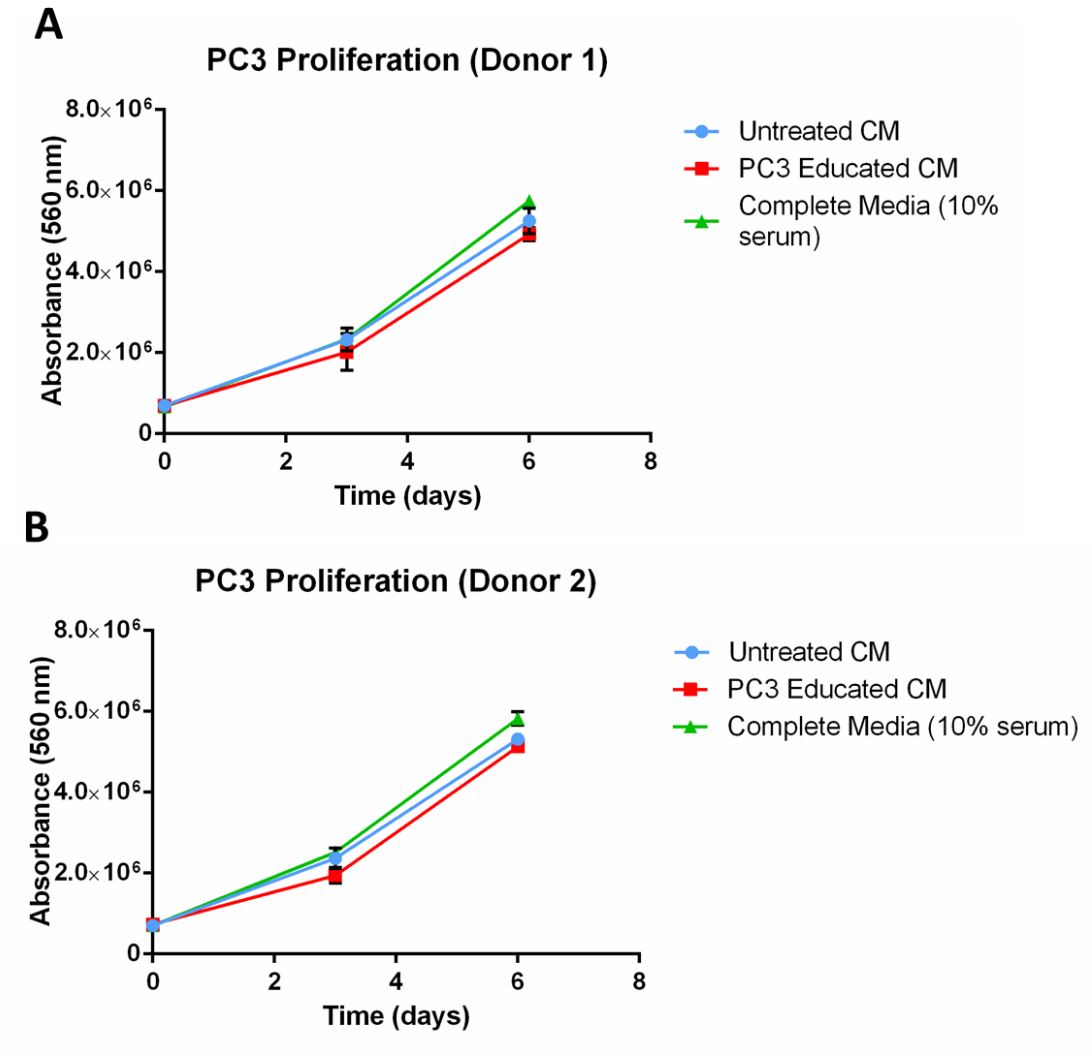

Figure 5.3. Proliferation of PC3 Cells in Response to Conditioned Medium Derived from PC3 Educated MSCs. PC3 cells were tested for their rate of proliferation using the alamar blue method. The cells were grown in either 50% untreated MSC CM and 50% complete medium, 50% PC3 educated MSC CM and 50% complete medium or 100% complete medium for the duration of the assay. The MSCs used were derived from donors 1 (A) and 2 (B). Viability was assessed every 2 days for 6 days. PC3 cells were found to proliferate at a similar rate in each condition although the trend shows PC3 cells grown in PC3 educated MSC CM grow at the slowest rate and PC3 cells grown in complete medium grow at the fastest rate (A+B). When combining data from both donors at day 6 of the assay, the difference was statistically significant between PC3 cells grown in untreated MSC CM and PC3 educated MSC CM (paired student's t-test; two-tailed; $p<0.05$; n=2 biological replicates), when grown alone vs. in untreated MSC CM paired student's t-test; two-tailed; $p<0.001$; n=2 biological replicates) and when grown alone vs. in PC3 educated MSC CM (paired student's t-test; two-tailed; $p<0.0001$; n=2 biological replicates). Values were normalised to viability at 'day 0' and data represents the mean of technical replicates ± SD.

5.2.4 Proliferation Rate of PC3 Cells when Grown in Co-culture with PC3 Educated MSCs

To assess whether cellular cross-talk could change the proliferation rate of PC3 cells, they were grown in indirect co-culture with untreated MSCs and PC3 educated MSCs as described in section 2.14.2. Briefly, the PC3 cells were grown in complete medium in 24-well plates and left until the following day, which was determined as 'day 0'. The untreated MSCs and PC3 educated MSCs were seeded onto 0.4 µm porous inserts, left for 1 day in complete medium and then placed into wells containing PC3 cells at day 0. The PC3 cells were tested every 24 hours for 72 hours using the alamar blue viability assay. The PC3 cells were found to grow at a similar rate in monoculture and in co-culture with untreated MSCs and PC3 educated MSCs from 3 separate donors (figure 5.4).

The proliferation rates begin to separate slightly by 72 hours. The difference between PC3 cells grown in co-culture with untreated MSCs and PC3 educated MSCs was statistically significant at the 72 hour time-point in MSCs derived from donor 1 (paired student's t-test; two-tailed; $p<0.05$; n=3 technical replicates) but not from donor 2 or 4 (paired student's t-test; two-tailed; n=3 technical replicates). However, overall, combining data from all donors, the difference was statistically significant (paired student's t-test; two-tailed; $p<0.01$; n=3 biological replicates). The difference between PC3 cells grown alone and in co-culture with untreated MSCs was statistically significant at the 72 hour time-point from donor 1 (paired student's t-test; two-tailed; $p<0.05$; n=3 technical replicates) but not from donor 2 or 4 (paired student's t-test; two-tailed; n=3 technical replicates) and when combining data from all donors the difference was statistically significant (paired student's t-test; two-tailed; $p<0.001$; n=3 biological replicates). The difference between PC3 cells grown alone and in co-culture with PC3 educated MSCs was also statistically significant at the 72 hour time-point using cells from donor 1 (paired student's t-test; two-tailed; $p<0.01$; n=3 technical replicates) and donor 4 (paired student's t-test; $p<0.01$ two-tailed; n=3 technical replicates) but not from donor 2 (paired student's t-test; two-tailed; n=3 technical replicates) and when combining data from all donors (paired student's t-test; two-tailed; $p<0.0001$; n=3 biological replicates).

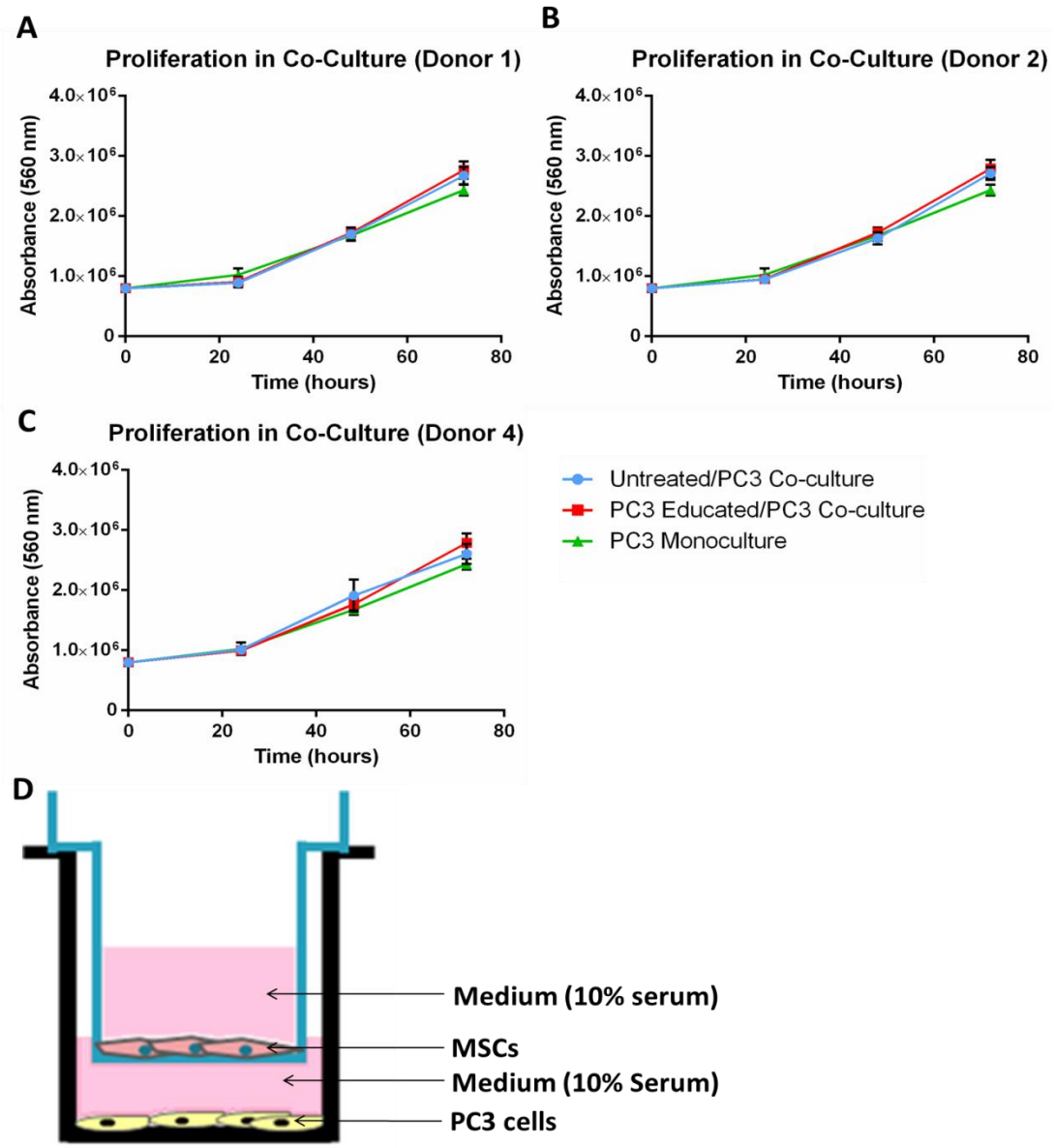

Figure 5.4. PC3 Cell Proliferation in Co-culture with PC3 Educated MSCs. PC3 cells were tested for their proliferation rate when grown in monoculture and indirect co-culture with untreated MSCS and PC3 educated MSCs. 'Day 0' was determined as the first day the cells were placed in co-culture. The growth rate was assessed every 24 hours for 72 hours using the alamar blue viability assay. The PC3 cells were found to grow at a similar rate in monoculture and in co-culture with untreated MSCs and PC3 educated MSCs from 3 different donors although, there was a slight increase in the proliferation of PC3 cells in co-culture with untreated MSCs and PC3 educated MSCs in comparison to when grown alone (A-C). D. Illustration depicting the indirect co-culture system. When combining data from all donors at the 72 hour time-point in the assay, the difference was statistically significant between PC3 cells grown in co-culture with untreated MSCs and PC3 educated MSCs (paired student's t-test; two-tailed; $p<0.01$; n=3 biological replicates) and when grown alone vs. in co-culture with untreated MSCs (paired student's t-test; two-tailed; $p<0.001$; n=3 biological replicates) and when grown alone vs. in co-culture with PC3 educated MSCs (paired student's t-test; two-tailed; $p<0.0001$; n=3 biological replicates). Values were normalised to viability at 'day 0' and data represents the mean of technical replicates ± SD.

5.2.5 Prostate Cancer Cell Chemoattraction toward PC3 Educated MSCs

Given that long-term treatment with PC3 CM was found to inhibit MSC migration yet induce increased secretion of chemoattractant factors such as MCP-1, OPN and IL-8, we considered that migration of prostate cancer cells would be more enhanced towards a monolayer of PC3 educated MSCs than untreated MSCs. Briefly, either untreated MSCs or PC3 educated MSCs were seeded in 24-well plates in complete medium at 5 x 10^4 cells per well and left to form a monolayer. 22Rv1, DU145 and PC3 cells were added in serum free medium to 8.0 µm porous inserts at 1 x 10^5 cells per insert and placed over MSC monolayers in serum free medium. 22Rv1 cells were left to migrate for 48 hours, DU145 cells for 24 hours and PC3 cells for 30 hours. The migrated cells were detected and visualised using the crystal violet stain as described in section 2.12.2.

5.2.5.1 Migration of 22Rv1 Cells towards PC3 Educated MSCs

The migration of the non-metastatic 22Rv1 cell line toward a monolayer of untreated MSCs or PC3 educated MSCs was examined. 22Rv1 cells that had migrated through the insert were stained with crystal violet. The 22Rv1 cells did not show sufficient migration toward either monolayer (figure 5.5) but did migrate toward medium containing 10% serum and thus were not quantified.

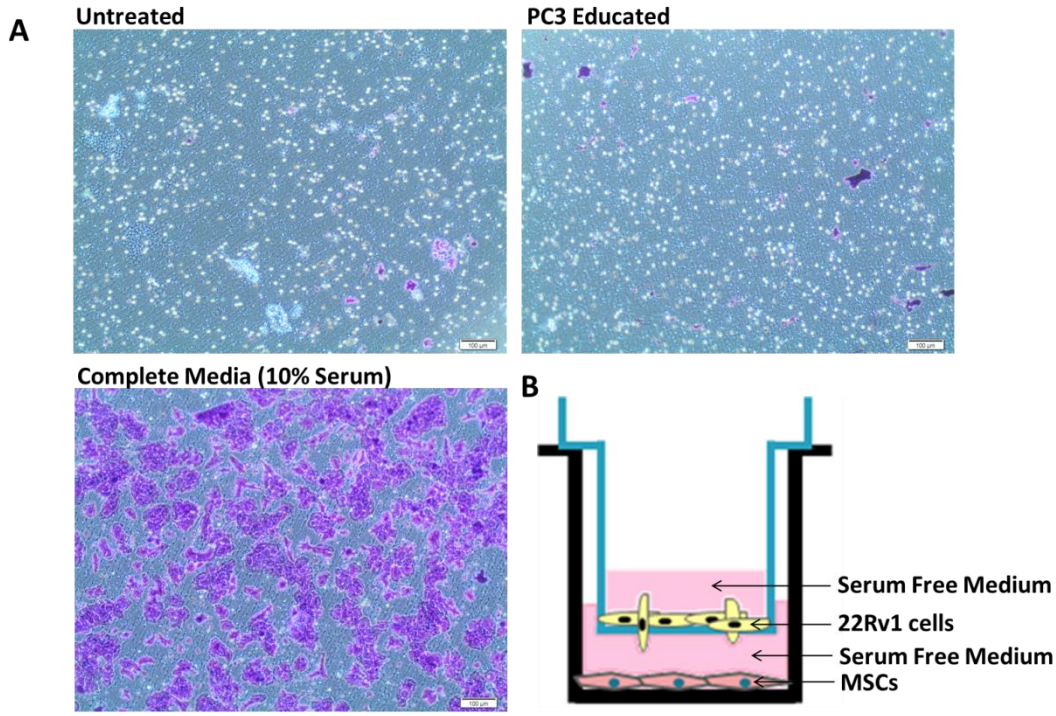

Figure 5.5. Migration of 22Rv1 Cells towards a Monolayer of PC3 Educated MSCs. 22Rv1 cells were examined for their chemoattraction towards a monolayer of untreated MSCs or PC3 educated MSCs. Cells that had migrated through the insert were stained with crystal violet. While the 22Rv1 cells did migrate toward medium containing 10% serum the migration of 22Rv1 toward either monolayer was not sufficient to be quantified. B. Illustration depicting the indirect co-culture system. The images are representative of 2 independent experiments using MSCs from 2 different donors.

5.2.5.2 Migration of DU145 cells towards PC3 Educated MSCs

DU145 cells were examined for their chemoattraction to a monolayer of untreated MSCs or PC3 educated MSCs. The DU145 cells that had migrated through the insert were stained with crystal violet and quantified using ImageJ software. However, the DU145 cells did not differ in their migration towards the untreated MSC or PC3 educated MSC monolayer (figure 5.6) and the data was not found to be statistically significant (paired student's t-test; two-tailed; n=3 biological replicates).

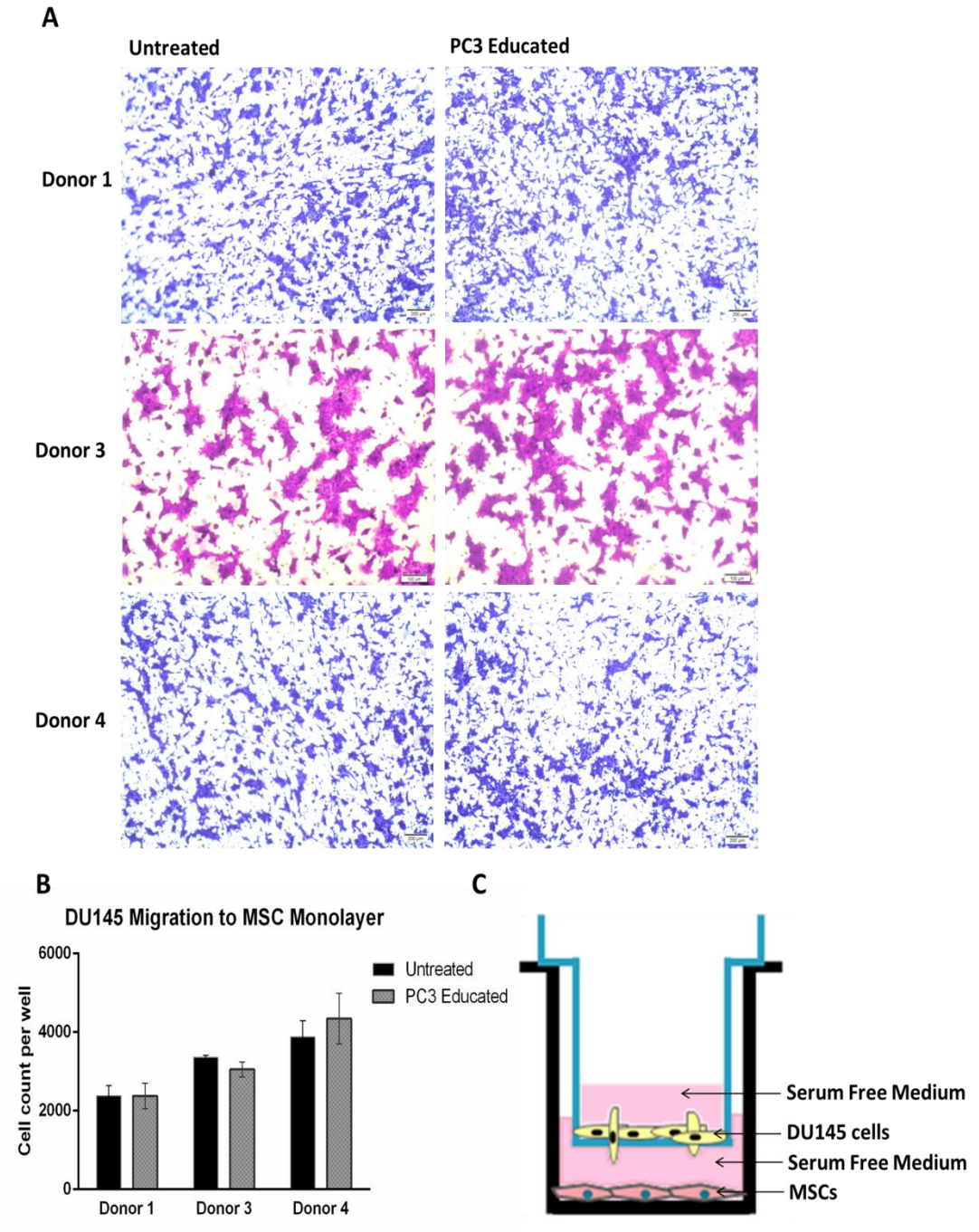

Figure 5.6. Migration of DU145 Cells towards a Monolayer of PC3 Educated MSCs. DU145 cells were examined for their chemoattraction towards a monolayer of untreated MSCs or PC3 educated MSCs. DU145 cells that had migrated through the insert were stained with crystal violet (A) and quantified (B). The DU145 cells did not differ in their migration toward the untreated MSCs or PC3 educated MSCs and the data was not statistically significant (paired student's t-test; two-tailed; n=3 biological replicates) (B). C. Illustration depicting the indirect co-culture system. Data represents mean of technical replicates ± SD.

5.2.5.3 PC3 Cells show Increased Chemoattraction toward PC3 Educated MSC Monolayers

PC3 cells were examined for their chemoattraction to a monolayer of untreated MSCs or PC3 educated MSCs. The PC3 cells that had migrated through the insert were stained with crystal violet and quantified using ImageJ software. The PC3 cells showed an increase in migration towards PC3 educated MSC monolayers from each donor in comparison to the untreated MSC monolayer and overall, combining data from all donor MSCs, the PC3 cells showed a 1.9 fold increase in migration towards the PC3 educated MSC monolayer in comparison to the untreated MSC monolayer (figure 5.7). The difference was found to be statistically significant (paired student's t-test; two-tailed; $p<0.05$; n=3 biological replicates).

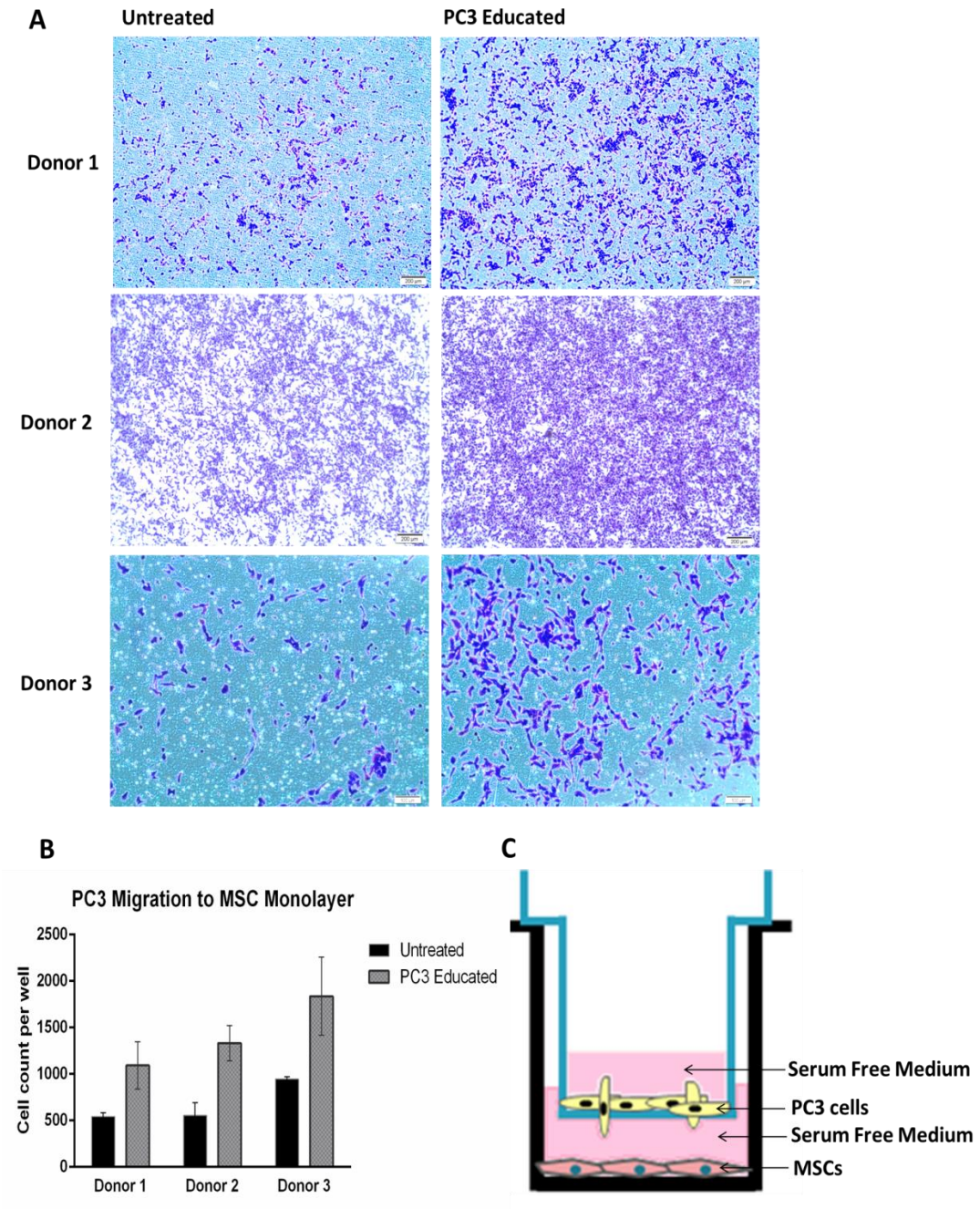

Figure 5.7. Migration of PC3 Cells towards a Monolayer of PC3 Educated MSCs. PC3 cells were examined for their chemoattraction towards a monolayer of untreated MSCs or PC3 educated MSCs. PC3 cells that had migrated through the insert were stained with crystal violet (A) and quantified (B). The PC3 cells showed an increase in migration towards PC3 educated MSC monolayers from each donor in comparison to the untreated MSC monolayer. Overall, PC3 cells showed a 1.9 fold increase towards the PC3 educated MSC monolayer in comparison to the untreated MSCs and the result was statistically significant (paired student's t-test; two-tailed; $p<0.05$; n=3 biological replicates) (B). C. Illustration depicting the indirect co-culture system. Data represents mean of technical replicates ± SD.

5.3 Discussion

We initially aimed to molecularly and functionally characterise PC3 educated MSCs and gain insight into whether PC3 CM temporarily or permanently alters the MSC phenotype. The focus of this study however, is to assess whether the interaction of PC3 educated MSCs with prostate cancer cells could promote tumour cell progression. Cancer therapies classically target tumour cells yet, what remains is an activated stroma that provides an encouraging microenvironment for any surviving tumour cells. Evidence to support this comes from studies in breast cancer in which stromal-related gene expression or gene signatures was predictive of clinical outcome (Farmer et al., 2009, Finak et al., 2008). Moreover, pre-treatment of MSCs to concentrations of cisplatin which were toxic to breast cancer cell but not MSCs *in vitro* was found induce changes in kinase phosphorylation and increased cytokine production in the MSCs and co-culture with breast cancer cells lead to chemoresistance in the tumour cells (Skolekova et al., 2016). To this end we investigated the chemoresistance of PC3 educated MSCs following treatment with docetaxel. Docetaxel is an inhibitor of microtubule depolymerisation and docetaxel-based treatment has shown survival benefit in patients with metastatic castration-resistant prostate cancer in two randomized phase III clinical trials (Verweij et al., 1994, Tannock et al., 2004, Petrylak et al., 2004).

It is thought that patient MSCs can survive radiation doses lethal to the haematopoietic system as it has been shown that following bone marrow transplantation, used as treatment after total body irradiation, the haematopoietic cells were of donor origin while the MSCs were of host origin (Dickhut et al., 2005). Interestingly, we found that docetaxel is not as effective on MSCs as it is on PC3 cells and requires a greater dose to reach the IC_{50} which indicates that treatment with docetaxel does not target the tumour stroma. Nonetheless, untreated MSCs and PC3 educated MSCs did not differ in their resistance to docetaxel (figure 5.1).

There is also evidence to suggest that tumour-stromal cell interaction can mediate tumour cell resistance to chemotherapeutics. Fibroblasts were found to induce etoposide resistance in pancreatic cancer through the secretion of NO which through

paracrine signalling leads to tumour cell release of IL-1β (Muerkoster et al., 2004). Stromal fibroblasts were found to induce lung cancer chemoresistance to EGFR-selective tyrosine kinase inhibitors through the production of HGF (Wang et al., 2009) and bone marrow derived MSCs were found to induce increased chemoresistance through the release of platinum-induced fatty acids (Roodhart et al., 2011). Moreover, inhibition of tumour stroma derived PDGF receptor enhances chemotherapeutic efficacy by increasing of trans-capillary transport of the drug (Pietras et al., 2002, Pietras et al., 2001).

We considered the possibility that PC3 educated MSCs could induce a protective effect on PC3 cells following treatment with chemotherapeutic agents, docetaxel and paclitaxel. The PC3 cells were placed in an indirect co-culture system with untreated MSCs or PC3 educated MSCs and treated for 72 hours with docetaxel or paclitaxel (section 5.2.2). We did not however, find any difference in the response of PC3 cells to docetaxel or paclitaxel treatment when in indirect co-culture with PC3 educated MSCs in comparison to co-culture with untreated MSCs (figure 5.2).

Due to difficulties in obtaining large cell numbers at the end of each conditioning period, experiments requiring low cell numbers were selected for this study. The in-direct co-culture system was therefore chosen; however future studies should consider a direct co-culture system followed by fluorescence-activated cell sorting analysis. MSCs were found to consist of approximately 0.01 – 1.1% of the prostate cancer primary tumour (Brennen et al., 2013), and so the indirect co-culture of prostate cancer cell with a monolayer of MSCs is not representative of ratios *in vivo*. However, given the length of time necessary for completion of each co-culture assay and the difference in proliferation rate between untreated MSCs and PC3 educated MSCs, it was decided the formation of a monolayer would allow a more accurate comparison.

Bone marrow derived MSCs were found to induce increased chemoresistance in leukemia cells. Direct co-culture with MSCs and leukemic cells resulted in decreased apoptosis and an increase in the expression of c-Myc. Interestingly, the finding could not be reproduced using an indirect co-culture system suggesting cell-to-cell contact

as key to the protective mechanism (Ito et al., 2015, Xia et al., 2015). Similarly, it was found that TGF-β released by bone marrow derived MSCs enhances chemoresistance in leukemia cells, an effect which is more prominent when the cells were in direct contact (Xu et al., 2008). Ovarian carcinoma-associated MSCs were also found to induce ovarian cancer cell chemoresistance when treated with paclitaxel in a direct co-culture system which was not reproducible in a transwell system (Rafii et al., 2008). This may explain why we could not detect a significant difference in PC3 cell chemoresistance when in indirect co-culture with untreated MSCs and PC3 educated MSCs in comparison to when cultured alone (figure 5.2).

In contrast to our findings Borghese *et al.* found that MSC CM increased the chemoresistance of PC3 cells to docetaxel and the outcome was more pronounced when the MSCs were pre-treated with PC3 CM (Borghese et al., 2013). There are some experimental differences between the two studies. Their study used a dose of docetaxel of 5nM, which based on our dose-response curve would have resulted in 99.2% PC3 cell survival, whereas we used 743 nM. Furthermore, they treated the PC3 cells for 24 hours with docetaxel, allowed 3 days growth and subsequently tested cell proliferation through incorporation of the thymidine synthetic, BrdU (Borghese et al., 2013). Their approach was arguably more sensitive which might explain the difference in findings.

Next, we examined PC3 cell proliferation in response to untreated MSCs and PC3 educated MSCs in a similar approach to the cytotoxicity experiment. An indirect co-culture system was employed where the untreated MSCs and PC3 educated MSCs formed a monolayer on 0.4 μm porous inserts and were subsequently placed in wells containing PC3 cells. PC3 cell growth was monitored every 24 hours for 72 hours using the alamar blue viability assay (section 5.2.4). We detected a slight increase in PC3 cell proliferation when grown in co-culture with untreated MSCs as well as PC3 educated MSCs (figure 5.4). However, a more sensitive approach, possibly using BrdU incorporation might be more indicative.

Research is conflicted as to whether MSCs promote or repress tumour growth or tumour cell proliferation. MSCs have been found to promote tumour growth in

melanoma (Djouad et al., 2003), osteosarcoma (Xu et al., 2009), prostate (Prantl et al., 2010), breast (Muehlberg et al., 2009) and colon cancer (Zhu et al., 2006) *in vivo*. Karnoub and colleagues found that of four breast cancer cell lines examined (MDA-MB-231, HMLR, MDA-MB-435 and MCF7), co-injection of bone marrow derived MSCs with MCF7 cells only, lead to increased tumour growth (Karnoub et al., 2007). On the other hand several studies have found that MSCs suppress tumour growth (Sun et al., 2009, Khakoo et al., 2006, Otsu et al., 2009, Qiao et al., 2008, Ohta et al., 2015). MSCs, co-injected at a 1:1 or 1:3 ratio, were found to have a cytotoxic effect on the tumour in melanoma mouse models though the release of reactive oxygen species. The cytotoxic effect was reduced by lowering the tumour cell to MSC ratio (Otsu et al., 2009).

Studies examining the effect of MSCs or tumour derived MSCs on tumour cell proliferation *in vitro* also show conflicting results. Borghese *et al.* showed that bone marrow derived MSCs enhanced clonogenic growth of PC3 cells, which was more pronounced using MSCs that were pre-treated for 10 days with PC3 CM (Borghese et al., 2013). Umbilical cord derived MSCs however, were found to inhibit PC3 cell growth and induce apoptosis when co-cultured using a transwell system. The anti-proliferative and anti-apoptotic effect was dependent on PC3 to MSC ratio where the effect decreased by reducing the number of MSCs (Han et al., 2014). Moreover, gastric cancer (Kim et al., 2013), lymphoma (Ren et al., 2014) and glioma (Hossain et al., 2015) derived MSCs were found to increase tumour cell proliferation yet, ovarian carcinoma-associated MSCs do not alter tumour cell proliferation rate (Pasquet et al., 2010). Taken together, the MSC/tumour cell interactions are complex and depend on *in vitro* and *in vivo* conditions such as MSC to tumour cell ratio, tumour cell type and possibly MSC origin.

In previous experiments, described in chapter three, we investigated the PC3 educated MSC secretome. We found PC3 educated MSCs that had been conditioned for 30 days in PC3 CM, secreted increased MCP-1 and IL-8 compared to untreated MSCs. These are known chemoattractant factors and have each been shown to stimulate PC3 cell migration (Loberg et al., 2006, Reiland et al., 1999). We therefore considered that prostate cancer cells would show increased migration towards PC3

educated MSCs than untreated MSCs. To investigate this we used a transwell system whereby 22Rv1, DU145 and PC3 cells were placed in an 8.0 µm porous insert and allowed migrate towards a monolayer of untreated MSCs or PC3 educated MSCs (section 5.2.5). We found that the non-metastatic cell line, 22Rv1, was not stimulated to migrate towards either untreated MSCs or PC3 educated MSCs (figure 5.5). The brain metastatic cell line, DU145, did migrate towards the untreated MSCs and PC3 educated monolayers, though quantitative analysis revealed that there was no difference in migration towards either untreated MSCs or PC3 educated MSCs (figure 5.6). We did however find a 1.9 fold increase in PC3 cell migration towards the PC3 educated MSCs compared to the untreated MSCs (figure 5.7).

It has been hypothesised that circulating factors released by the primary tumour can interact with cells of bone marrow microenvironment to create a 'pre-metastatic' niche that stimulates metastatic tumour cells to home to a hospitable setting (Kaplan et al., 2005, Steeg, 2005). PC3 cells were originally derived from a bone metastasis and their cross-talk with bone marrow derived MSCs could upregulate the secretion of chemotactic factors of which PC3 cells are responsive to. It was found that MSCs secrete increased CCL5 in response to breast cancer and osteosarcoma cells which in turn binds to the receptor CCR4 on the tumour cells thus increasing their motility and metastatic potential (Karnoub et al., 2007, Mi et al., 2011, Xu et al., 2009). Several other studies show that tumour cell chemoattraction to the bone is mediated by MSC secretion of SDF-1α (Cooper et al., 2003, Zhang et al., 2013b, Corcoran et al., 2008). However, we did not discover detectable levels of SDF-1α in untreated MSCs or PC3 educated MSC supernatants making it an unlikely component in the chemoattraction of PC3 cells shown in our study (data not shown).

In conclusion, we found that PC3 educated MSCs do not differ in their chemoresistance to docetaxel, nor do they have a protective effect on PC3 cells in response to cytotoxic treatment. Furthermore, PC3 cells do not change in their rate of proliferation when in indirect co-culture with untreated MSCs or PC3 educated MSCs. However, we did find that PC3 cells increased in their rate of migration towards PC3 educated MSCs in comparison to untreated MSCs and of the three cells lines examined (22Rv1, DU145 and PC3), the effect was specific only to PC3 cells.

Chapter 6

General Discussion

6.1 PC3 Educated MSCs Differ to Untreated MSCs in their Secretory Profile

The tumour microenvironment is a chronic site of inflammation and has been described as a wound that never heals (Dvorak, 1986). Tumour cells secrete cytokines, chemokines and growth factors that recruit immune cells as well as MSCs to the tumour site, as well as acting as autocrine factors supporting cell growth (Hanahan and Coussens, 2012). This forms a dynamic microenvironment in which tumour cells interact with non-malignant cells of the tumour stroma to further promote tumour growth and progression (Hanahan and Coussens, 2012, Pietras and Ostman, 2010). To examine the interaction between bone marrow derived MSCs and prostate cancer cells we set up an *in vitro* system which involved the long-term conditioning of MSCs derived from healthy male donors in prostate cancer cell CM. Our prostate cancer cell lines included the non-metastatic androgen receptor positive cell line 22Rv1, which represents localised prostate cancer and the metastatic androgen receptor negative cell lines – PC3 and DU145 – which represent prostate cancer that has metastasised to the bone and brain, respectively. This allows us to make preliminary interpretations on the impact of prostate cancer at different stages of progression on MSCs. We initially screened the supernatants of MSCs that were treated for 20 days in 22Rv1, DU145 and PC3 CM for the secretion of cytokines and chemokines (section 3.2.2). We found MSCs exposed to CM from the bone metastatic cell line, PC3, had the greatest response. A selection of cytokines and growth factors were then validated in supernatant derived from MSCs that had been treated for 10, 20 and 30 days in PC3 CM.

We found that PC3 educated MSCs had a secretion profile that would indicate a tumour promoting phenotype. Following quantitative validation, we confirmed that PC3 educated MSCs secreted increased OPN, MCP-1, IL-8, and FGF-2 and decreased sFlt-1 in comparison to untreated MSCs. Increased levels of FGF2 in the prostate cancer tumour have been found to be localised within tumour stroma (Giri et al., 1999, Berger et al., 2015). FGF2 is a pro-angiogenic factor and has been implicated in the promotion of tumour angiogenesis and growth (Mattern et al., 1997, Nissen et al., 2007, Bremnes et al., 2006, Bos et al., 2005, Cronauer et al., 1997). sFlt-1 is known to negatively regulate angiogenesis and functions by trapping VEGF and PlGF and

delivery to the tumour has been found to inhibit angiogenesis and growth (Shibuya, 2011, Goldman et al., 1998, Hu et al., 2008). Therefore, the stimulation of FGF2 production and sFlt-1 inhibition indicates a pro-angiogenic phenotype in PC3 educated MSCs. However, the evidence is preliminary and further studies involving functional *in vitro* assays and *in vivo* models would be required to draw any conclusion.

PC3 cells are human prostate cancer cells that are derived from bone metastases and their activity within the bone marrow microenvironment disrupts bone homeostasis, favouring bone resorption. MSCs are supportive of the HSC niche within the bone marrow microenvironment and play an integral role in maintaining bone homeostasis through the differentiation to osteoblasts (Almeida-Porada et al., 2000, Maitra et al., 2004, Raggatt and Partridge, 2010). Therefore, cross-talk between PC3 cells and MSCs that alter MSC function could have consequences in bone remodelling. MCP-1 (Lu et al., 2006, Loberg et al., 2006), IL-8 (Kim et al., 2001) and OPN (Khodavirdi et al., 2006) have all been found to promote prostate cancer progression. IL-8 was found to be elevated in the serum of men with prostate cancer and bone metastasis (Lehrer et al., 2004). MCP-1 has been found to stimulate PC3 cell proliferation and migration through a dose-dependent activation of the PI3-kinase/Akt signaling pathway (Lu et al., 2006, Loberg et al., 2006). PC3 cells secreting high levels of IL-8 were found to promote increased tumour growth, metastasis and vascularisation following injection into the prostate of nude mice in comparison to PC3 cells secreting low levels of IL-8 (Kim et al., 2001). OPN was found to be correlated with prostate cancer grade and has also been found to enhance PC3 cell migration through the binding of the integrin $\alpha_v\beta_3$, expressed on PC3 cells and activation of the PI3-kinase signalling pathway (Zheng et al., 2000).

These factors have also been shown to play a role in bone resorption. IL-8 and MCP-1 have been found to stimulate the osteoclast differentiation of osteoclast progenitors within PBMC and human bone marrow mononuclear cell populations (Bendre et al., 2003, Lu et al., 2007a, Mizutani et al., 2009). While, OPN expression has been associated with osteolytic bone metastasis in breast cancer (Ibrahim et al., 2000, Adwan et al., 2004) and has been found to mediate osteoclast motility and

anchorage to the bone mineral matrix (Ishijima et al., 2001, Reinholt et al., 1990, Ross et al., 1993). Bone remodelling relies on a balance between bone formation and bone resorption, therefore changes in the production of factors that influence either mechanism can cause a dysregulation in bone homeostasis. Prostate cancer bone metastasis more commonly involves excessive bone formation although both bone formation and bone resorption are increased in patients with prostate cancer bone metastasis in comparison to healthy patients (Garnero et al., 2000). PC3 cells form predominantly osteoclastic bone metastasis *in vivo* (Nemeth et al., 2002), although the mechanisms by which are not understood, their activity within the bone marrow could induce an increase in the secretion of factors that promote bone resorption such as IL-8, MCP-1 and OPN from bone marrow resident cells.

6.2 PC3 Cell Conditioning Temporarily Inhibits MSC Migration and Proliferation Capacity

To establish whether PC3 CM could induce functional changes in MSCs, we examined the migration, invasion and proliferation capacity of PC3 educated MSCs. MSCs are stimulated to home to injured tissue *in vivo* such as heart (Orlic et al., 2001), lung (Ortiz et al., 2003), liver (Sato et al., 2005) and brain (Mahmood et al., 2003) as well as the tumour (Kansy et al., 2014, Prantl et al., 2010). Bone marrow derived MSCs were found to express chemokine receptors CCR1, CCR4, CCR7, CCR10, and CXCR5, CXCR4 (Von Luttichau et al., 2005, Wynn et al., 2004), which may explain their migration in response to cytokines and chemokines released from inflammatory sites.

We investigated the migration and proliferation capacity of PC3 educated MSCs following 10, 20 and 30 days of conditioning and the invasion potential following 30 days of conditioning. PC3 educated MSCs showed a reduced rate of proliferation at each time-point and were less invasive following 30 days of conditioning in comparison to untreated MSCs. Strangely, we found an increase in migration of PC3 educated MSCs following 10 days of conditioning, yet following 20 and 30 days of conditioning the migration rate was consistently decreased in comparison to untreated MSCs. A possible explanation for this is that the MSCs are being reprogrammed and consequently reduce their functional activity. PC3 cells and PC3

educated MSCs were both found to secrete PA1, IL-8, MIF, DKK-1 and EMMPRIN as detected by proteome profiling (section 3.2.2.1 and 3.2.3). Therefore, another possible explanation for this is that MSCs have an initial response to PC3 CM and long-term conditioning leads to oversaturation of chemokine or growth factor receptors inhibiting their chemotactic response. Thus, growth in complete medium, when the PC3 educated MSCs are no longer exposed to PC3 CM, could result in relief of some of the receptors and a subsequent increase in migration and proliferation. For example PAI-1 is a uPA inhibitor and its presence at a high level during the conditioning period could result in inhibition of the migration and invasion capacity of PC3 educated MSCs (Vassalli et al., 1991, Chandrasekar et al., 2003). Moreover, IL-8 can stimulate chemotaxis, and oversaturation of its complimentary chemokine receptors could inhibit the migration of PC3 educated MSCs towards medium containing 10% serum (Reiland et al., 1999).

Interestingly, we found a decrease in the expression of vimentin in PC3 educated MSCs following 30 days of conditioning in comparison to untreated MSCs. Vimentin is a type III intermediate filament protein that is expressed in mesenchymal cells (Ivaska et al., 2007). Several studies have found vimentin to have a role in cell adhesion and migration in many cell types (Ivaska et al., 2007, Gilles et al., 1999, Wu et al., 2009, Eckes et al., 1998, McInroy and Maatta, 2007, Nieminen et al., 2006). The decrease in vimentin expression might therefore explain the decrease in migration capacity found in PC3 educated MSCs. Furthermore, αSMA expression in fibroblasts has been shown to correlate with increased migration and so the decrease in αSMA expression found in PC3 educated MSCs may also be causative in their decreased migration capacity (Kawamoto et al., 1997, Murray and Spector, 2001).

6.3 PC3 Educated MSCs as a Unique Cell Type

It has previously been shown that macrophages, recruited to the tumour site, change in their molecular phenotype to either promote or suppress tumour growth (Mantovani et al., 2002, Sica et al., 2006, Allavena et al., 2008, Solinas et al., 2009). It has now been established that MSCs home to the tumour site and form part of the tumour stroma (Ame-Thomas et al., 2007, Kansy et al., 2014, Hossain et al., 2015,

Karnoub et al., 2007, Prantl et al., 2010). The question is whether they retain their molecular and functional phenotype, differentiate into another cell type or become activated to promote tumour progression.

To examine whether the molecular and functional response to PC3 CM was dependent on continuous exposure, we cultured PC3 educated MSCs for 12 - 16 days in normal growth medium. We investigated the secretion of IL-8, OPN, FGF2, and sFlt-1 from PC3 educated MSCs post-conditioning as well as their migration and proliferation capacity. The level of OPN and IL-8 secretion remained increased in comparison to untreated MSCs, although not to the same extent as it did following continuous exposure to PC3 CM. However, we also found that PC3 educated MSCs regained a similar rate of proliferation and a slight increase in migration compared to the untreated MSCs in cells from two of three donors.

We also examined the morphology and measured the size of PC3 educated MSCs following 30 days of conditioning. We found that PC3 educated MSCs maintain a similar fibroblastic, spindle-shaped morphology to untreated MSCs however, upon measurement of cell diameter, they were found to be larger in size in comparison to untreated MSCs. Interestingly, while the PC3 educated MSCs were found have an increased cell size they were also found to express decreased αSMA and vimentin. αSMA is a myofibroblast marker that plays a role in fibroblast contractility and vimentin is a mesenchymal marker that functions in cell adhesion and migration (Hinz et al., 2001, Ivaska et al., 2007). Therefore, reduction in the expression of these proteins signifies a change in cellular function and possibly a phenotypic change.

Interestingly, PC3, DU145 and 22Rv1 educated MSCs were found to have different migration and invasion capacities as well as secretory profiles. This suggests the response of MSCs to tumour cell CM is dependent on the tumour cell type and possibly grade. This may explain MSCs derived from multiple myeloma, lymphoma, glioma, gastric, ovarian and breast cancers differ in their phenotype. MSCs derived from gliomas (Hossain et al., 2015), lymphomas (Ren et al., 2014), breast cancer (Zhang et al., 2013a) and gastric cancer (Li et al., 2015) were found to promote tumour cells growth, whereas ovarian carcinoma-associated MSCs had no effect on

tumour cell growth (Pasquet et al., 2010). Moreover, gastric (Cao et al., 2009) and prostate cancer derived MSCs (Ding et al., 2012) were found to proliferate at increased rates in comparison to bone marrow derived MSCs, whereas multiple myeloma derived MSCs were found to have a slower rate of proliferation (Jurczyszyn et al., 2015).

Multiple myeloma derived MSCs make a good model for the purpose of this study as they are the most extensively studied tumour derived MSC and multiple myeloma tumour cells are located within the bone marrow which eventually cause osteolytic bone destruction (Nash Smyth et al., 2016). Human multiple myeloma derived MSCs have also been found to produce increased DKK-1 and OPN in comparison to healthy MSCs (Garderet et al., 2007, Zdzisinska et al., 2008), which correlates with our finding in section 3.2.2 where an increase in DKK-1 and OPN secretion was detected in PC3 educated MSCs following 30 days of conditioning in comparison to untreated MSCs. Although reports are conflicting (Corre et al., 2007, Noll et al., 2014) the majority of studies have found that human multiple myeloma derived MSCs to have a decreased proliferation rate in comparison to healthy bone marrow derived MSCs (Garderet et al., 2007, Andre et al., 2013, Jurczyszyn et al., 2015). Furthermore, Reagan and colleagues found that bone marrow derived MSCs grown in co-culture with multiple myeloma cells in 3D silk scaffolds showed a decreased migration and proliferation capacity in comparison to when grown alone (Reagan et al., 2014). Expression of growth factors – NGFR, PDGFβR, bFGFR, IGF-1R, and EGFR – were found to be decreased in multiple myeloma derived MSCs (Garderet et al., 2007) and it would be interesting to investigate the expression of these factors in PC3 educated MSCs in future studies and determine whether there is a correlation with the decrease in migration. However, several studies show a reduction in the osteogenic potential of human multiple myeloma derived MSCs in comparison to MSCs derived from healthy bone marrow (Corre et al., 2007, Garderet et al., 2007, Li et al., 2007), whereas we did not find a change in the osteoblastic differentiation of PC3 educated MSCs in comparison to untreated MSCs.

PC3 educated MSCs have a unique, secretory profile compared to 22Rv1 educated, DU145 educated and untreated MSCs which suggests a conditioning response

specific to tumour cell type. Furthermore, in comparison to untreated MSCs, PC3 educated MSCs have a cytokine-rich secretory profile with factors found to have a pro-tumorigenic function indicating a tumour 'activated' phenotype. Although it was not investigated in our study, this 'activated' phenotype could also have an impact on other non-malignant cell types that are present in the tumour stroma such as macrophages, fibroblasts and endothelial cells. Nonetheless, it is difficult to assess whether the cells are being reprogrammed or differentiating to a different cell type. Within the limitations of this study, we could not associate the change in molecular and functional characteristics to another known cell type. PC3 educated MSCs, conditioned for 30 days, retained the capacity to differentiate to adipocytes and osteocytes, two of the classical characteristics used to define MSCs, however investigation into the expression of MSC surface markers – CD73, CD105 and CD90 – showed that while PC3 educated MSCs showed similar expression of CD73 to untreated MSCs there was a shift in the expression of CD105 within the population of cells from 2 of 3 donors and a shift in CD90 expression in the population of cells from the remaining donor. This suggests a donor dependent response to PC3 CM and possibly a polarisation within the population of cells.

6.4 PC3 Educated MSCs do not Exhibit CAF Characteristics

CAFs are a tumour-promoting, heterogenous population of cells that are phenotypically similar to myofibroblasts (Kellermann et al., 2008). The cause for the heterogeneity found in CAFs is that they have been shown to originate from different cell types such as fibroblasts, MSCs and through transdifferentiation of endothelial and epithelial cells (Spaeth et al., 2009, Evans et al., 2003, Zeisberg et al., 2007). It has previously been shown that MSCs develop a CAF-like phenotype following long-term conditioning in breast cancer cell and ovarian cancer cell CM (Mishra et al., 2008, Spaeth et al., 2009). We therefore considered the possibility that long-term treatment of MSCs with PC3 CM could induce a CAF-like phenotype.

However, while PC3 educated MSCs did express the CAF markers, rather than an increase in expression of αSMA, vimentin and FAP, we found a decrease in comparison to untreated MSCs. Moreover, using gene expression analysis we did not

find a significant increase in CAF-associated factors – TNC, MMP-9, COL1A1 and COL5A1. We can therefore conclude that using our experimental design, it is unlikely that PC3 educated MSCs differentiate into CAFs.

6.5 PC3 Cells do not Change in their Cytotoxic Response when in Co-culture with Untreated MSCs or PC3 Educated MSCs

Bone marrow derived MSCs were found to induce increased chemoresistance in leukemia cells (Ito et al., 2015, Xia et al., 2015, Xu et al., 2008). Ovarian carcinoma-associated MSCs were also found to induce ovarian cancer cell chemoresistance when treated with paclitaxel (Rafii et al., 2008). Each of these studies required direct cell-to-cell contact to induce the chemoprotective effect, however, in a similar study to ours, where bone marrow derived MSCs were treated for 10 days in PC3 CM, they found that exposure of PC3 cells to CM derived from the conditioned MSCs resulted in the chemoresistance of PC3 cells to docetaxel (Borghese et al., 2013). We used an indirect co-culture system to assess whether cross-talk between PC3 educated MSCs and untreated MSCs would have a chemoprotective effect on PC3 cells following treatment with docetaxel and paclitaxel. However, we did not find any change in the chemoresistance of PC3 cells while in co-culture with untreated MSCs or PC3 educated MSCs (section 5.2.2).

6.6 The Rate of Proliferation of PC3 cells when in Co-culture with Untreated MSCs or PC3 Educated MSCs

We used an indirect co-culture system to examine PC3 cell proliferation in the presence of untreated MSCs or PC3 educated MSCs. We found a slight yet statistically significant increase in the proliferation rate of PC3 cells in co-culture with PC3 educated MSCs in comparison to untreated MSCs (section 5.2.4). Research is conflicted as to whether MSCs promote or suppress tumour growth (Klopp et al., 2011). Gastric cancer (Kim et al., 2013), lymphoma (Ren et al., 2014) and glioma (Hossain et al., 2015) derived MSCs were found to increase tumour cell proliferation yet, ovarian carcinoma-associated MSCs did not affect tumour cell proliferation rate (Pasquet et al., 2010). Interestingly, umbilical cord derived MSCs were found to inhibit PC3 cell growth when co-cultured using a transwell system though the effect

was dependent on PC3 to MSC ratio where the effect decreased by reducing the number of MSCs (Han et al., 2014) and Borghese *et al.* showed that bone marrow derived MSCs enhanced clonogenic growth of PC3 cells (Borghese et al., 2013) Therefore, PC3 cell proliferation in response to MSCs could be dependent on the cell ratio between the two cell types. A more sensitive approach, possibly using BrdU incorporation or the clonogenic growth assay could further clarify the increase in proliferation rate we found during this study.

6.7 PC3 Cells Show Increased Migration towards PC3 Educated MSCs

We investigated the migration of 22Rv1, DU145 and PC3 cells towards a monolayer of untreated MSCs or PC3 educated MSCs (section 5.2.5). We found that 22Rv1 cells were not stimulated to migrate towards either untreated MSCs or PC3 educated MSCs (figure 5.5). The brain metastatic cell line, DU145, migrated towards both untreated MSCs and PC3 educated monolayers, though there was no quantitative difference in their migration towards either untreated MSCs or PC3 educated MSCs (figure 5.6). We did however find a 1.9 fold increase in PC3 cell migration towards the PC3 educated MSCs in comparison to untreated MSCs (figure 5.7).

PC3 educated MSCs were found to secrete increased MCP-1, IL-8 and OPN in comparison to untreated MSCs. IL-8, MCP-1 and OPN have previously been found to stimulate PC3 cell migration (Loberg et al., 2006, Reiland et al., 1999) and PC3 cells overexpressing OPN were found to have an increased migration rate (Desai et al., 2007, Tilli et al., 2012). Interestingly, PC3 cells but not LNCaP cells, the lymph node metastatic prostate cancer cell line, were found to migrate at an increased rate on OPN through its binding to integrin $\alpha_v\beta_3$, expressed on PC3 cells and activation of the PI3-kinase signalling pathway (Zheng et al., 2000). MCP-1 has previously been shown to stimulate monocyte migration through the binding of receptor CCR2 (Sozzani et al., 1993) and has also been found to induce tumour cell migration in multiple myeloma (Vanderkerken et al., 2002), breast (Youngs et al., 1997) and prostate (Loberg et al., 2006) cancer. Interestingly, it was found that while IL-8 and MCP-1 administered together could stimulate PC3 cell migration, the cells migrated at a more enhanced rate following exposure to MCP-1 alone (Maxwell et al., 2014).

The ‘seed’ and ‘soil’ hypothesis was initially described by Paget in 1889 which proposes the idea that the tumour cell migrates to specific tissues based on favourable interactions with the given secondary site (Paget, 1989). The theory has since been developed to suggest that circulating factors released by the primary tumour interact with cells of the secondary site, in this case the bone marrow, to create a ‘pre-metastatic’ niche that stimulates chemotaxis of the metastatic tumour cells to a favourable microenvironment (Kaplan et al., 2005, Steeg, 2005). Based on our research it could be proposed that factors released by circulating metastatic prostate cancer cells educate bone marrow resident MSCs to secrete chemoattractant factors that enhance migration towards the bone while desensitising MSCs to cytokines and chemokines released by the tumour cells in order to prevent their migration away from the bone.

6.8 Limitations and Future Directions

The aim of this study was to investigate the response of MSCs to long-term treatment in prostate cancer cell CM. We initially sought to characterise the PC3 educated MSCs based on their molecular and functional phenotype and followed by investigation into whether these conditioned cells could promote or suppress tumour cell progression. We developed an *in vitro* model system to examine tumour cell/MSC interactions and so the findings are preliminary. Future studies should consider:

- Investigation into what instigating factors in the conditioning medium that are causing the change in phenotype such as exosomes, miRNAs and selected proteins.
- Further molecular characterisation of the PC3 educated MSCs post-conditioning to determine whether the MSCs are being reprogrammed in response to PC3 CM.
- The isolation and characterisation of MSCs derived from the bone metastatic site of prostate cancer patients.
- The conditioning and characterisation of MSCs using a wider range of tumour cell types in order to evaluate whether the response is correlated with tumour cell type or grade. This would include investigation into whether tumour

educated MSCs specifically stimulate the migration of the tumour cells used during the conditioning process.

- The impact of a wider range of chemotherapeutic drugs as well as radiation on PC3 cell resistance when in co-culture with PC3 educated MSCs, given that we only investigated one family of chemotherapeutic agents with similar mechanisms of action.
- Development of a 3D co-culture modelling system.
- Investigation into whether the osteogenic and adipogenic differentiation capacity of PC3 educated MSCs would be altered if the PC3 educated MSCs were continuously exposed to PC3 CM during the differentiation process.
- The examination of PC3 educated MSCs for the expression of senescence markers.
- Investigation into whether PC3 educated MSCs change in the expression of markers associated with endoderm, ectoderm and mesoderm differentiation as well as pluripotency markers such as Oct4, Nanog and SSEA-4.

6.9 Final Conclusions

In this study we found that MSCs treated for 30 days with PC3 CM secreted an increase in pro-tumourigenic factors - MCP-1, IL-8, OPN and FGF2 - in comparison to untreated MSCs, which was sustained following extended culture in normal growth medium. The migration and proliferation capacity of MSC was temporarily inhibited following 20 and 30 days of conditioning. PC3 educated MSCs were found to maintain the capacity for osteogenesis and adipogenesis and did not express an increase in CAF-associated markers. PC3 cells, but not DU145 or 22Rv1 cells showed increased migration towards PC3 educated MSCs in comparison to untreated MSCs. Therefore, PC3 CM induces an ‘activated’ phenotype in MSCs that is specific to PC3 cell conditioning.

Bibliography

ADWAN, H., BAUERLE, T. J. & BERGER, M. R. 2004. Downregulation of osteopontin and bone sialoprotein II is related to reduced colony formation and metastasis formation of MDA-MB-231 human breast cancer cells. *Cancer Gene Ther,* 11, 109-20.

AL-KHALDI, A., ELIOPOULOS, N., MARTINEAU, D., LEJEUNE, L., LACHAPELLE, K. & GALIPEAU, J. 2003. Postnatal bone marrow stromal cells elicit a potent VEGF-dependent neoangiogenic response in vivo. *Gene Ther,* 10, 621-9.

ALBARENQUE, S. M., ZWACKA, R. M. & MOHR, A. 2011. Both human and mouse mesenchymal stem cells promote breast cancer metastasis. *Stem Cell Res,* 7, 163-71.

ALLAVENA, P., SICA, A., GARLANDA, C. & MANTOVANI, A. 2008. The Yin-Yang of tumor-associated macrophages in neoplastic progression and immune surveillance. *Immunol Rev,* 222, 155-61.

ALMEIDA-PORADA, G., PORADA, C. D., TRAN, N. & ZANJANI, E. D. 2000. Cotransplantation of human stromal cell progenitors into preimmune fetal sheep results in early appearance of human donor cells in circulation and boosts cell levels in bone marrow at later time points after transplantation. *Blood,* 95, 3620-3627.

AME-THOMAS, P., MABY-EL HAJJAMI, H., MONVOISIN, C., JEAN, R., MONNIER, D., CAULET-MAUGENDRE, S., GUILLAUDEUX, T., LAMY, T., FEST, T. & TARTE, K. 2007. Human mesenchymal stem cells isolated from bone marrow and lymphoid organs support tumor B-cell growth: role of stromal cells in follicular lymphoma pathogenesis. *Blood,* 109, 693-702.

ANDERBERG, C., LI, H., FREDRIKSSON, L., ANDRAE, J., BETSHOLTZ, C., LI, X., ERIKSSON, U. & PIETRAS, K. 2009. Paracrine signaling by platelet-derived growth factor-CC promotes tumor growth by recruitment of cancer-associated fibroblasts. *Cancer Res,* 69, 369-78.

ANDRE, T., MEULEMAN, N., STAMATOPOULOS, B., DE BRUYN, C., PIETERS, K., BRON, D. & LAGNEAUX, L. 2013. Evidences of early senescence in multiple myeloma bone marrow mesenchymal stromal cells. *PLoS One,* 8, e59756.

ANGELUCCI, A., FESTUCCIA, C., D'ANDREA, G., TETI, A. & BOLOGNA, M. 2002. Osteopontin modulates prostate carcinoma invasive capacity through RGD-dependent upregulation of plasminogen activators. *Biol Chem,* 383, 229-34.

ARA, T., SONG, L., SHIMADA, H., KESHELAVA, N., RUSSELL, H. V., METELITSA, L. S., GROSHEN, S. G., SEEGER, R. C. & DECLERCK, Y. A. 2009. Interleukin-6 in the bone marrow microenvironment promotes the growth and survival of neuroblastoma cells. *Cancer Res,* 69, 329-37.

ATTARD, G., PARKER, C., EELES, R. A., SCHRODER, F., TOMLINS, S. A., TANNOCK, I., DRAKE, C. G. & DE BONO, J. S. 2015. Prostate cancer. *Lancet*.

BAGULEY, B. C. 2010. Multiple drug resistance mechanisms in cancer. *Mol Biotechnol,* 46, 308-16.

BARBASH, I. M., CHOURAQUI, P., BARON, J., FEINBERG, M. S., ETZION, S., TESSONE, A., MILLER, L., GUETTA, E., ZIPORI, D., KEDES, L. H., KLONER, R. A. & LEOR, J. 2003. Systemic delivery of bone marrow-derived mesenchymal stem cells to the infarcted myocardium: feasibility, cell migration, and body distribution. *Circulation,* 108, 863-8.

BEHRENS, J., FRIXEN, U., SCHIPPER, J., WEIDNER, M. & BIRCHMEIER, W. 1992. Cell adhesion in invasion and metastasis. *Semin Cell Biol,* 3, 169-78.

BEHRENS, J., MAREEL, M. M., VAN ROY, F. M. & BIRCHMEIER, W. 1989. Dissecting tumor cell invasion: epithelial cells acquire invasive properties after the loss of uvomorulin-mediated cell-cell adhesion. *J Cell Biol,* 108, 2435-47.

BENDRE, M. S., MARGULIES, A. G., WALSER, B., AKEL, N. S., BHATTACHARRYA, S., SKINNER, R. A., SWAIN, F., RAMANI, V., MOHAMMAD, K. S., WESSNER, L. L., MARTINEZ, A.,

GUISE, T. A., CHIRGWIN, J. M., GADDY, D. & SUVA, L. J. 2005. Tumor-derived interleukin-8 stimulates osteolysis independent of the receptor activator of nuclear factor-kappaB ligand pathway. *Cancer Res,* 65, 11001-9.

BENDRE, M. S., MONTAGUE, D. C., PEERY, T., AKEL, N. S., GADDY, D. & SUVA, L. J. 2003. Interleukin-8 stimulation of osteoclastogenesis and bone resorption is a mechanism for the increased osteolysis of metastatic bone disease. *Bone,* 33, 28-37.

BERGER, A. P., KOFLER, K., BEKTIC, J., ROGATSCH, H., STEINER, H., BARTSCH, G. & KLOCKER, H. 2003. Increased growth factor production in a human prostatic stromal cell culture model caused by hypoxia. *Prostate,* 57, 57-65.

BERGER, L., SHAMAI, Y., SKORECKI, K. & TZUKERMAN, M. 2015. Tumor Specific Recruitment and Reprogramming of Mesenchymal Stem Cells in Tumorigenesis. *Stem Cells*.

BI, L. K., ZHOU, N., LIU, C., LU, F. D., LIN, T. X., XUAN, X. J., JIANG, C., HAN, J. L., HUANG, H., ZHANG, C. X., DONG, W., LIU, H., HUANG, J. & XU, K. W. 2014. Kidney cancer cells secrete IL-8 to activate Akt and promote migration of mesenchymal stem cells. *Urol Oncol,* 32, 607-12.

BIRCHMEIER, W. & BEHRENS, J. 1994. Cadherin expression in carcinomas: role in the formation of cell junctions and the prevention of invasiveness. *Biochim Biophys Acta,* 1198, 11-26.

BJORK, L., FEHNIGER, T. E., ANDERSSON, U. & ANDERSSON, J. 1996. Computerized assessment of production of multiple human cytokines at the single-cell level using image analysis. *J Leukoc Biol,* 59, 287-95.

BOCELLI-TYNDALL, C., BRACCI, L., SPAGNOLI, G., BRACCINI, A., BOUCHENAKI, M., CEREDIG, R., PISTOIA, V., MARTIN, I. & TYNDALL, A. 2007. Bone marrow mesenchymal stromal cells (BM-MSCs) from healthy donors and auto-immune disease patients reduce the proliferation of autologous- and allogeneic-stimulated lymphocytes in vitro. *Rheumatology (Oxford),* 46, 403-8.

BORGHESE, C., CATTARUZZA, L., PIVETTA, E., NORMANNO, N., DE LUCA, A., MAZZUCATO, M., CELEGATO, M., COLOMBATTI, A. & ALDINUCCI, D. 2013. Gefitinib inhibits the cross-talk between mesenchymal stem cells and prostate cancer cells leading to tumor cell proliferation and inhibition of docetaxel activity. *J Cell Biochem,* 114, 1135-44.

BORIES, D., RAYNAL, M. C., SOLOMON, D. H., DARZYNKIEWICZ, Z. & CAYRE, Y. E. 1989. Down-regulation of a serine protease, myeloblastin, causes growth arrest and differentiation of promyelocytic leukemia cells. *Cell,* 59, 959-68.

BOS, R., VAN DIEST, P. J., DE JONG, J. S., VAN DER GROEP, P., VAN DER VALK, P. & VAN DER WALL, E. 2005. Hypoxia-inducible factor-1alpha is associated with angiogenesis, and expression of bFGF, PDGF-BB, and EGFR in invasive breast cancer. *Histopathology,* 46, 31-6.

BREHMER, B., BIESTERFELD, S. & JAKSE, G. 2003. Expression of matrix metalloproteinases (MMP-2 and -9) and their inhibitors (TIMP-1 and -2) in prostate cancer tissue. *Prostate Cancer Prostatic Dis,* 6, 217-22.

BREMNES, R. M., CAMPS, C. & SIRERA, R. 2006. Angiogenesis in non-small cell lung cancer: the prognostic impact of neoangiogenesis and the cytokines VEGF and bFGF in tumours and blood. *Lung Cancer,* 51, 143-58.

BRENNEN, W. N., CHEN, S., DENMEADE, S. R. & ISAACS, J. T. 2013. Quantification of Mesenchymal Stem Cells (MSCs) at sites of human prostate cancer. *Oncotarget,* 4, 106-17.

BROCKE-HEIDRICH, K., KRETZSCHMAR, A. K., PFEIFER, G., HENZE, C., LOFFLER, D., KOCZAN, D., THIESEN, H. J., BURGER, R., GRAMATZKI, M. & HORN, F. 2004. Interleukin-6-dependent gene expression profiles in multiple myeloma INA-6 cells reveal a Bcl-2

family-independent survival pathway closely associated with Stat3 activation. *Blood,* 103, 242-51.

BRUDER, S. P., KURTH, A. A., SHEA, M., HAYES, W. C., JAISWAL, N. & KADIYALA, S. 1998. Bone regeneration by implantation of purified, culture-expanded human mesenchymal stem cells. *J Orthop Res,* 16, 155-62.

BRYDEN, A. A., FREEMONT, A. J., CLARKE, N. W. & GEORGE, N. J. 1999. Paradoxical expression of E-cadherin in prostatic bone metastases. *BJU Int,* 84, 1032-4.

BUBENDORF, L., SCHOPFER, A., WAGNER, U., SAUTER, G., MOCH, H., WILLI, N., GASSER, T. C. & MIHATSCH, M. J. 2000. Metastatic patterns of prostate cancer: an autopsy study of 1,589 patients. *Hum Pathol,* 31, 578-83.

BUGANIM, Y., MADAR, S., RAIS, Y., POMERANIEC, L., HAREL, E., SOLOMON, H., KALO, E., GOLDSTEIN, I., BROSH, R., HAIMOV, O., AVIVI, C., POLAK-CHARCON, S., GOLDFINGER, N., BARSHACK, I. & ROTTER, V. 2011. Transcriptional activity of ATF3 in the stromal compartment of tumors promotes cancer progression. *Carcinogenesis,* 32, 1749-57.

BUSSEMAKERS, M. J., VAN MOORSELAAR, R. J., GIROLDI, L. A., ICHIKAWA, T., ISAACS, J. T., TAKEICHI, M., DEBRUYNE, F. M. & SCHALKEN, J. A. 1992. Decreased expression of E-cadherin in the progression of rat prostatic cancer. *Cancer Res,* 52, 2916-22.

CAI, J., TANG, H., XU, L., WANG, X., YANG, C., RUAN, S., GUO, J., HU, S. & WANG, Z. 2012. Fibroblasts in omentum activated by tumor cells promote ovarian cancer growth, adhesion and invasiveness. *Carcinogenesis,* 33, 20-9.

CAI, Z., CHEN, Q., CHEN, J., LU, Y., XIAO, G., WU, Z., ZHOU, Q. & ZHANG, J. 2009. Monocyte chemotactic protein 1 promotes lung cancer-induced bone resorptive lesions in vivo. *Neoplasia,* 11, 228-36.

CALON, A., TAURIELLO, D. V. & BATLLE, E. 2014. TGF-beta in CAF-mediated tumor growth and metastasis. *Semin Cancer Biol,* 25, 15-22.

CAO, H., XU, W., QIAN, H., ZHU, W., YAN, Y., ZHOU, H., ZHANG, X., XU, X., LI, J., CHEN, Z. & XU, X. 2009. Mesenchymal stem cell-like cells derived from human gastric cancer tissues. *Cancer Lett,* 274, 61-71.

CASTELLANO, G., MALAPONTE, G., MAZZARINO, M. C., FIGINI, M., MARCHESE, F., GANGEMI, P., TRAVALI, S., STIVALA, F., CANEVARI, S. & LIBRA, M. 2008. Activation of the osteopontin/matrix metalloproteinase-9 pathway correlates with prostate cancer progression. *Clin Cancer Res,* 14, 7470-80.

CHAMBERLAIN, G., FOX, J., ASHTON, B. & MIDDLETON, J. 2007. Concise review: mesenchymal stem cells: their phenotype, differentiation capacity, immunological features, and potential for homing. *Stem Cells,* 25, 2739-49.

CHANDRASEKAR, N., MOHANAM, S., GUJRATI, M., OLIVERO, W. C., DINH, D. H. & RAO, J. S. 2003. Downregulation of uPA inhibits migration and PI3k/Akt signaling in glioblastoma cells. *Oncogene,* 22, 392-400.

CHATURVEDI, P., GILKES, D. M., WONG, C. C., KSHITIZ, LUO, W., ZHANG, H., WEI, H., TAKANO, N., SCHITO, L., LEVCHENKO, A. & SEMENZA, G. L. 2013. Hypoxia-inducible factor-dependent breast cancer-mesenchymal stem cell bidirectional signaling promotes metastasis. *J Clin Invest,* 123, 189-205.

CHELLAIAH, M. A., KIZER, N., BISWAS, R., ALVAREZ, U., STRAUSS-SCHOENBERGER, J., RIFAS, L., RITTLING, S. R., DENHARDT, D. T. & HRUSKA, K. A. 2003. Osteopontin deficiency produces osteoclast dysfunction due to reduced CD44 surface expression. *Mol Biol Cell,* 14, 173-89.

CHEN, R. X., XIA, Y. H., XUE, T. C., ZHANG, H. & YE, S. L. 2011. Down-regulation of osteopontin inhibits metastasis of hepatocellular carcinoma cells via a mechanism involving MMP-2 and uPA. *Oncol Rep,* 25, 803-8.

CHITTETI, B. R., CHENG, Y. H., POTEAT, B., RODRIGUEZ-RODRIGUEZ, S., GOEBEL, W. S., CARLESSO, N., KACENA, M. A. & SROUR, E. F. 2010. Impact of interactions of cellular

components of the bone marrow microenvironment on hematopoietic stem and progenitor cell function. *Blood,* 115, 3239-48.

CHOWDHURY, R., WEBBER, J. P., GURNEY, M., MASON, M. D., TABI, Z. & CLAYTON, A. 2015. Cancer exosomes trigger mesenchymal stem cell differentiation into pro-angiogenic and pro-invasive myofibroblasts. *Oncotarget,* 6, 715-31.

CHUNG, T. D., YU, J. J., SPIOTTO, M. T., BARTKOWSKI, M. & SIMONS, J. W. 1999. Characterization of the role of IL-6 in the progression of prostate cancer. *Prostate,* 38, 199-207.

CLARKE, N. W., HART, C. A. & BROWN, M. D. 2009. Molecular mechanisms of metastasis in prostate cancer. *Asian J Androl,* 11, 57-67.

COFFIN, J. D., FLORKIEWICZ, R. Z., NEUMANN, J., MORT-HOPKINS, T., DORN, G. W., 2ND, LIGHTFOOT, P., GERMAN, R., HOWLES, P. N., KIER, A., O'TOOLE, B. A. & ET AL. 1995. Abnormal bone growth and selective translational regulation in basic fibroblast growth factor (FGF-2) transgenic mice. *Mol Biol Cell,* 6, 1861-73.

COHEN, P., PEEHL, D. M., STAMEY, T. A., WILSON, K. F., CLEMMONS, D. R. & ROSENFELD, R. G. 1993. Elevated levels of insulin-like growth factor-binding protein-2 in the serum of prostate cancer patients. *J Clin Endocrinol Metab,* 76, 1031-5.

COLEMAN, R. E. 1997. Skeletal complications of malignancy. *Cancer,* 80, 1588-94.

CONNOLLY, J. M. & ROSE, D. P. 1998. Angiogenesis in two human prostate cancer cell lines with differing metastatic potential when growing as solid tumors in nude mice. *J Urol,* 160, 932-6.

COOK, P. J., DOLL, R. & FELLINGHAM, S. A. 1969. A mathematical model for the age distribution of cancer in man. *Int J Cancer,* 4, 93-112.

COOPER, C. R., CHAY, C. H., GENDERNALIK, J. D., LEE, H. L., BHATIA, J., TAICHMAN, R. S., MCCAULEY, L. K., KELLER, E. T. & PIENTA, K. J. 2003. Stromal factors involved in prostate carcinoma metastasis to bone. *Cancer,* 97, 739-47.

CORCIONE, A., BENVENUTO, F., FERRETTI, E., GIUNTI, D., CAPPIELLO, V., CAZZANTI, F., RISSO, M., GUALANDI, F., MANCARDI, G. L., PISTOIA, V. & UCCELLI, A. 2006. Human mesenchymal stem cells modulate B-cell functions. *Blood,* 107, 367-72.

CORCORAN, K. E., TRZASKA, K. A., FERNANDES, H., BRYAN, M., TABORGA, M., SRINIVAS, V., PACKMAN, K., PATEL, P. S. & RAMESHWAR, P. 2008. Mesenchymal stem cells in early entry of breast cancer into bone marrow. *PLoS One,* 3, e2563.

CORRE, J., MAHTOUK, K., ATTAL, M., GADELORGE, M., HUYNH, A., FLEURY-CAPPELLESSO, S., DANHO, C., LAHARRAGUE, P., KLEIN, B., REME, T. & BOURIN, P. 2007. Bone marrow mesenchymal stem cells are abnormal in multiple myeloma. *Leukemia,* 21, 1079-88.

CRONAUER, M. V., HITTMAIR, A., EDER, I. E., HOBISCH, A., CULIG, Z., RAMONER, R., ZHANG, J., BARTSCH, G., REISSIGL, A., RADMAYR, C., THURNHER, M. & KLOCKER, H. 1997. Basic fibroblast growth factor levels in cancer cells and in sera of patients suffering from proliferative disorders of the prostate. *Prostate,* 31, 223-33.

DAKHOVA, O., OZEN, M., CREIGHTON, C. J., LI, R., AYALA, G., ROWLEY, D. & ITTMANN, M. 2009. Global gene expression analysis of reactive stroma in prostate cancer. *Clin Cancer Res,* 15, 3979-89.

DAS, R., MAHABELESHWAR, G. H. & KUNDU, G. C. 2004. Osteopontin induces AP-1-mediated secretion of urokinase-type plasminogen activator through c-Src-dependent epidermal growth factor receptor transactivation in breast cancer cells. *J Biol Chem,* 279, 11051-64.

DENDA, S., REICHARDT, L. F. & MULLER, U. 1998. Identification of osteopontin as a novel ligand for the integrin alpha8 beta1 and potential roles for this integrin-ligand interaction in kidney morphogenesis. *Mol Biol Cell,* 9, 1425-35.

DESAI, B., ROGERS, M. J. & CHELLAIAH, M. A. 2007. Mechanisms of osteopontin and CD44 as metastatic principles in prostate cancer cells. *Mol Cancer,* 6, 18.

DESHMANE, S. L., KREMLEV, S., AMINI, S. & SAWAYA, B. E. 2009. Monocyte chemoattractant protein-1 (MCP-1): an overview. ***J Interferon Cytokine Res,*** **29, 313-26.**

DI NICOLA, M., CARLO-STELLA, C., MAGNI, M., MILANESI, M., LONGONI, P. D., MATTEUCCI, P., GRISANTI, S. & GIANNI, A. M. 2002. Human bone marrow stromal cells suppress T-lymphocyte proliferation induced by cellular or nonspecific mitogenic stimuli. ***Blood,*** **99, 3838-43.**

DICKHUT, A., SCHWERDTFEGER, R., KUKLICK, L., RITTER, M., THIEDE, C., NEUBAUER, A. & BRENDEL, C. 2005. Mesenchymal stem cells obtained after bone marrow transplantation or peripheral blood stem cell transplantation originate from host tissue. ***Ann Hematol,*** **84, 722-7.**

DIEL, I. J., SOLOMAYER, E. F., COSTA, S. D., GOLLAN, C., GOERNER, R., WALLWIENER, D., KAUFMANN, M. & BASTERT, G. 1998. Reduction in new metastases in breast cancer with adjuvant clodronate treatment. ***N Engl J Med,*** **339, 357-63.**

DING, G., SHAO, J., DING, Q., FANG, Z., WU, Z., XU, J. & GAO, P. 2012. Comparison of the characteristics of mesenchymal stem cells obtained from prostate tumors and from bone marrow cultured in conditioned medium. ***Exp Ther Med,*** **4, 711-715.**

DIREKZE, N. C., HODIVALA-DILKE, K., JEFFERY, R., HUNT, T., POULSOM, R., OUKRIF, D., ALISON, M. R. & WRIGHT, N. A. 2004. Bone marrow contribution to tumor-associated myofibroblasts and fibroblasts. ***Cancer Res,*** **64, 8492-5.**

DIREKZE, N. C., JEFFERY, R., HODIVALA-DILKE, K., HUNT, T., PLAYFORD, R. J., ELIA, G., POULSOM, R., WRIGHT, N. A. & ALISON, M. R. 2006. Bone marrow-derived stromal cells express lineage-related messenger RNA species. ***Cancer Res,*** **66, 1265-9.**

DJOUAD, F., PLENCE, P., BONY, C., TROPEL, P., APPARAILLY, F., SANY, J., NOEL, D. & JORGENSEN, C. 2003. Immunosuppressive effect of mesenchymal stem cells favors tumor growth in allogeneic animals. ***Blood,*** **102, 3837-3844.**

DOITSIDOU, M., REICHMAN-FRIED, M., STEBLER, J., KOPRUNNER, M., DORRIES, J., MEYER, D., ESGUERRA, C. V., LEUNG, T. & RAZ, E. 2002. Guidance of primordial germ cell migration by the chemokine SDF-1. ***Cell,*** **111, 647-59.**

DOMINICI, M., LE BLANC, K., MUELLER, I., SLAPER-CORTENBACH, I., MARINI, F., KRAUSE, D., DEANS, R., KEATING, A., PROCKOP, D. & HORWITZ, E. 2006. Minimal criteria for defining multipotent mesenchymal stromal cells. The International Society for Cellular Therapy position statement. ***Cytotherapy,*** **8, 315-7.**

DONG, Z., SALIGANAN, A. D., MENG, H., NABHA, S. M., SABBOTA, A. L., SHENG, S., BONFIL, R. D. & CHER, M. L. 2008. Prostate cancer cell-derived urokinase-type plasminogen activator contributes to intraosseous tumor growth and bone turnover. ***Neoplasia,*** **10, 439-49.**

DUDA, D. G., DUYVERMAN, A. M., KOHNO, M., SNUDERL, M., STELLER, E. J., FUKUMURA, D. & JAIN, R. K. 2010. Malignant cells facilitate lung metastasis by bringing their own soil. ***Proc Natl Acad Sci U S A,*** **107, 21677-82.**

DVORAK, H. F. 1986. Tumors: wounds that do not heal. Similarities between tumor stroma generation and wound healing. ***N Engl J Med,*** **315, 1650-9.**

DVORAK, H. F. 2015. Tumors: wounds that do not heal-redux. ***Cancer Immunol Res,*** **3, 1-11.**

DWYER, R. M., POTTER-BEIRNE, S. M., HARRINGTON, K. A., LOWERY, A. J., HENNESSY, E., MURPHY, J. M., BARRY, F. P., O'BRIEN, T. & KERIN, M. J. 2007. Monocyte chemotactic protein-1 secreted by primary breast tumors stimulates migration of mesenchymal stem cells. ***Clin Cancer Res,*** **13, 5020-7.**

ECK, S. M., COTE, A. L., WINKELMAN, W. D. & BRINCKERHOFF, C. E. 2009. CXCR4 and matrix metalloproteinase-1 are elevated in breast carcinoma-associated fibroblasts and in normal mammary fibroblasts exposed to factors secreted by breast cancer cells. ***Mol Cancer Res,*** **7, 1033-44.**

ECKES, B., DOGIC, D., COLUCCI-GUYON, E., WANG, N., MANIOTIS, A., INGBER, D., MERCKLING, A., LANGA, F., AUMAILLEY, M., DELOUVEE, A., KOTELIANSKY, V., BABINET, C. & KRIEG, T. 1998. Impaired mechanical stability, migration and contractile capacity in vimentin-deficient fibroblasts. *J Cell Sci,* 111 (Pt 13), 1897-907.

ELZAOUK, L., MOELLING, K. & PAVLOVIC, J. 2006. Anti-tumor activity of mesenchymal stem cells producing IL-12 in a mouse melanoma model. *Exp Dermatol,* 15, 865-74.

EREZ, N., TRUITT, M., OLSON, P., ARRON, S. T. & HANAHAN, D. 2010. Cancer-Associated Fibroblasts Are Activated in Incipient Neoplasia to Orchestrate Tumor-Promoting Inflammation in an NF-kappaB-Dependent Manner. *Cancer Cell,* 17, 135-47.

EVANS, R. A., TIAN, Y. C., STEADMAN, R. & PHILLIPS, A. O. 2003. TGF-beta1-mediated fibroblast-myofibroblast terminal differentiation-the role of Smad proteins. *Exp Cell Res,* 282, 90-100.

FALLON, J. F., LOPEZ, A., ROS, M. A., SAVAGE, M. P., OLWIN, B. B. & SIMANDL, B. K. 1994. FGF-2: apical ectodermal ridge growth signal for chick limb development. *Science,* 264, 104-7.

FARMER, P., BONNEFOI, H., ANDERLE, P., CAMERON, D., WIRAPATI, P., BECETTE, V., ANDRE, S., PICCART, M., CAMPONE, M., BRAIN, E., MACGROGAN, G., PETIT, T., JASSEM, J., BIBEAU, F., BLOT, E., BOGAERTS, J., AGUET, M., BERGH, J., IGGO, R. & DELORENZI, M. 2009. A stroma-related gene signature predicts resistance to neoadjuvant chemotherapy in breast cancer. *Nat Med,* 15, 68-74.

FEIG, C., JONES, J. O., KRAMAN, M., WELLS, R. J., DEONARINE, A., CHAN, D. S., CONNELL, C. M., ROBERTS, E. W., ZHAO, Q., CABALLERO, O. L., TEICHMANN, S. A., JANOWITZ, T., JODRELL, D. I., TUVESON, D. A. & FEARON, D. T. 2013. Targeting CXCL12 from FAP-expressing carcinoma-associated fibroblasts synergizes with anti-PD-L1 immunotherapy in pancreatic cancer. *Proc Natl Acad Sci U S A,* 110, 20212-7.

FENG, S., DAKHOVA, O., CREIGHTON, C. J. & ITTMANN, M. 2013. Endocrine fibroblast growth factor FGF19 promotes prostate cancer progression. *Cancer Res,* 73, 2551-62.

FESTUCCIA, C., DOLO, V., GUERRA, F., VIOLINI, S., MUZI, P., PAVAN, A. & BOLOGNA, M. 1998. Plasminogen activator system modulates invasive capacity and proliferation in prostatic tumor cells. *Clin Exp Metastasis,* 16, 513-28.

FINAK, G., BERTOS, N., PEPIN, F., SADEKOVA, S., SOULEIMANOVA, M., ZHAO, H., CHEN, H., OMEROGLU, G., METERISSIAN, S., OMEROGLU, A., HALLETT, M. & PARK, M. 2008. Stromal gene expression predicts clinical outcome in breast cancer. *Nat Med,* 14, 518-27.

FOROOTAN, S. S., FOSTER, C. S., AACHI, V. R., ADAMSON, J., SMITH, P. H., LIN, K. & KE, Y. 2006. Prognostic significance of osteopontin expression in human prostate cancer. *Int J Cancer,* 118, 2255-61.

FOUILLARD, L., BENSIDHOUM, M., BORIES, D., BONTE, H., LOPEZ, M., MOSELEY, A. M., SMITH, A., LESAGE, S., BEAUJEAN, F., THIERRY, D., GOURMELON, P., NAJMAN, A. & GORIN, N. C. 2003. Engraftment of allogeneic mesenchymal stem cells in the bone marrow of a patient with severe idiopathic aplastic anemia improves stroma. *Leukemia,* 17, 474-6.

FRIEDENSTEIN, A. J., CHAILAKHJAN, R. K. & LALYKINA, K. S. 1970. The development of fibroblast colonies in monolayer cultures of guinea-pig bone marrow and spleen cells. *Cell Tissue Kinet,* 3, 393-403.

FRITZ, V., BRONDELLO, J. M., GORDELADZE, J. O., RESELAND, J. E., BONY, C., YSSEL, H., NOEL, D. & JORGENSEN, C. 2011. Bone-metastatic prostate carcinoma favors mesenchymal stem cell differentiation toward osteoblasts and reduces their osteoclastogenic potential. *J Cell Biochem,* 112, 3234-45.

GABISON, E. E., HOANG-XUAN, T., MAUVIEL, A. & MENASHI, S. 2005. EMMPRIN/CD147, an MMP modulator in cancer, development and tissue repair. ***Biochimie,*** **87, 361-8.**

GALLAGHER, M. F., SALLEY, Y., SPILLANE, C. D., FFRENCH, B., EL BARUNI, S., BLACKSHEILDS, G., SMYTH, P., MARTIN, C., SHEILS, O., WATSON, W. & O'LEARY, J. J. 2015. Enhanced regulation of cell cycle and suppression of osteoblast differentiation molecular signatures by prostate cancer stem-like holoclones. ***J Clin Pathol,*** **68, 692-702.**

GARCIA-GOMEZ, A., DE LAS RIVAS, J., OCIO, E. M., DIAZ-RODRIGUEZ, E., MONTERO, J. C., MARTIN, M., BLANCO, J. F., SANCHEZ-GUIJO, F. M., PANDIELLA, A., SAN MIGUEL, J. F. & GARAYOA, M. 2014. Transcriptomic profile induced in bone marrow mesenchymal stromal cells after interaction with multiple myeloma cells: implications in myeloma progression and myeloma bone disease. ***Oncotarget,*** **5, 8284-305.**

GARDERET, L., MAZURIER, C., CHAPEL, A., ERNOU, I., BOUTIN, L., HOLY, X., GORIN, N. C., LOPEZ, M., DOUCET, C. & LATAILLADE, J. J. 2007. Mesenchymal stem cell abnormalities in patients with multiple myeloma. ***Leuk Lymphoma,*** **48, 2032-41.**

GARNERO, P., BUCHS, N., ZEKRI, J., RIZZOLI, R., COLEMAN, R. E. & DELMAS, P. D. 2000. Markers of bone turnover for the management of patients with bone metastases from prostate cancer. ***Br J Cancer,*** **82, 858-64.**

GILLES, C., POLETTE, M., ZAHM, J. M., TOURNIER, J. M., VOLDERS, L., FOIDART, J. M. & BIREMBAUT, P. 1999. Vimentin contributes to human mammary epithelial cell migration. ***J Cell Sci,*** **112 (Pt 24), 4615-25.**

GIRASOLE, G., PASSERI, G., JILKA, R. L. & MANOLAGAS, S. C. 1994. Interleukin-11: a new cytokine critical for osteoclast development. ***J Clin Invest,*** **93, 1516-24.**

GIRI, D., OZEN, M. & ITTMANN, M. 2001. Interleukin-6 is an autocrine growth factor in human prostate cancer. ***Am J Pathol,*** **159, 2159-65.**

GIRI, D., ROPIQUET, F. & ITTMANN, M. 1999. Alterations in expression of basic fibroblast growth factor (FGF) 2 and its receptor FGFR-1 in human prostate cancer. ***Clin Cancer Res,*** **5, 1063-71.**

GOEDE, V., BROGELLI, L., ZICHE, M. & AUGUSTIN, H. G. 1999. Induction of inflammatory angiogenesis by monocyte chemoattractant protein-1. ***Int J Cancer,*** **82, 765-70.**

GOLDMAN, C. K., KENDALL, R. L., CABRERA, G., SOROCEANU, L., HEIKE, Y., GILLESPIE, G. Y., SIEGAL, G. P., MAO, X., BETT, A. J., HUCKLE, W. R., THOMAS, K. A. & CURIEL, D. T. 1998. Paracrine expression of a native soluble vascular endothelial growth factor receptor inhibits tumor growth, metastasis, and mortality rate. ***Proc Natl Acad Sci U S A,*** **95, 8795-800.**

GORANOV, A. I., COOK, M., RICICOVA, M., BEN-ARI, G., GONZALEZ, C., HANSEN, C., TYERS, M. & AMON, A. 2009. The rate of cell growth is governed by cell cycle stage. ***Genes Dev,*** **23, 1408-22.**

GORDON, J. R., LI, F., ZHANG, X., WANG, W., ZHAO, X. & NAYYAR, A. 2005. The combined CXCR1/CXCR2 antagonist CXCL8(3-74)K11R/G31P blocks neutrophil infiltration, pyrexia, and pulmonary vascular pathology in endotoxemic animals. ***J Leukoc Biol,*** **78, 1265-72.**

GRONTHOS, S., MANKANI, M., BRAHIM, J., ROBEY, P. G. & SHI, S. 2000. Postnatal human dental pulp stem cells (DPSCs) in vitro and in vivo. ***Proc Natl Acad Sci U S A,*** **97, 13625-30.**

GUISE, T. A., YIN, J. J. & MOHAMMAD, K. S. 2003. Role of endothelin-1 in osteoblastic bone metastases. ***Cancer,*** **97, 779-84.**

GUO, X., OSHIMA, H., KITMURA, T., TAKETO, M. M. & OSHIMA, M. 2008. Stromal fibroblasts activated by tumor cells promote angiogenesis in mouse gastric cancer. ***J Biol Chem,*** **283, 19864-71.**

GUPTA, A., ZHOU, C. Q. & CHELLAIAH, M. A. 2013. Osteopontin and MMP9: Associations with VEGF Expression/Secretion and Angiogenesis in PC3 Prostate Cancer Cells. *Cancers (Basel),* 5, 617-38.

HALL, B., ANDREEFF, M. & MARINI, F. 2007. The participation of mesenchymal stem cells in tumor stroma formation and their application as targeted-gene delivery vehicles. *Handb Exp Pharmacol*, 263-83.

HALL, C. L., BAFICO, A., DAI, J., AARONSON, S. A. & KELLER, E. T. 2005. Prostate cancer cells promote osteoblastic bone metastases through Wnts. *Cancer Res,* 65, 7554-60.

HAN, I., YUN, M., KIM, E. O., KIM, B., JUNG, M. H. & KIM, S. H. 2014. Umbilical cord tissue-derived mesenchymal stem cells induce apoptosis in PC-3 prostate cancer cells through activation of JNK and downregulation of PI3K/AKT signaling. *Stem Cell Res Ther,* 5, 54.

HAN, Z. D., BI, X. C., QIN, W. J., HE, H. C., DAI, Q. S., ZOU, J., YE, Y. K., LIANG, Y. X., ZENG, G. H., CHEN, Z. N. & ZHONG, W. D. 2009. CD147 expression indicates unfavourable prognosis in prostate cancer. *Pathol Oncol Res,* 15, 369-74.

HANAHAN, D. & COUSSENS, L. M. 2012. Accessories to the crime: functions of cells recruited to the tumor microenvironment. *Cancer Cell,* 21, 309-22.

HART, C. A., SCOTT, L. J., BAGLEY, S., BRYDEN, A. A., CLARKE, N. W. & LANG, S. H. 2002. Role of proteolytic enzymes in human prostate bone metastasis formation: in vivo and in vitro studies. *Br J Cancer,* 86, 1136-42.

HINZ, B., CELETTA, G., TOMASEK, J. J., GABBIANI, G. & CHAPONNIER, C. 2001. Alpha-smooth muscle actin expression upregulates fibroblast contractile activity. *Mol Biol Cell,* 12, 2730-41.

HOBISCH, A., EDER, I. E., PUTZ, T., HORNINGER, W., BARTSCH, G., KLOCKER, H. & CULIG, Z. 1998. Interleukin-6 regulates prostate-specific protein expression in prostate carcinoma cells by activation of the androgen receptor. *Cancer Res,* 58, 4640-5.

HONCZARENKO, M., LE, Y., SWIERKOWSKI, M., GHIRAN, I., GLODEK, A. M. & SILBERSTEIN, L. E. 2006. Human bone marrow stromal cells express a distinct set of biologically functional chemokine receptors. *Stem Cells,* 24, 1030-41.

HONG, K. H., RYU, J. & HAN, K. H. 2005. Monocyte chemoattractant protein-1-induced angiogenesis is mediated by vascular endothelial growth factor-A. *Blood,* 105, 1405-7.

HONN, K. V. & TANG, D. G. 1992. Adhesion molecules and tumor cell interaction with endothelium and subendothelial matrix. *Cancer Metastasis Rev,* 11, 353-75.

HORWITZ, E. M., GORDON, P. L., KOO, W. K., MARX, J. C., NEEL, M. D., MCNALL, R. Y., MUUL, L. & HOFMANN, T. 2002. Isolated allogeneic bone marrow-derived mesenchymal cells engraft and stimulate growth in children with osteogenesis imperfecta: Implications for cell therapy of bone. *Proc Natl Acad Sci U S A,* 99, 8932-7.

HORWITZ, E. M., LE BLANC, K., DOMINICI, M., MUELLER, I., SLAPER-CORTENBACH, I., MARINI, F. C., DEANS, R. J., KRAUSE, D. S., KEATING, A. & INTERNATIONAL SOCIETY FOR CELLULAR, T. 2005. Clarification of the nomenclature for MSC: The International Society for Cellular Therapy position statement. *Cytotherapy,* 7, 393-5.

HOSSAIN, A., GUMIN, J., GAO, F., FIGUEROA, J., SHINOJIMA, N., TAKEZAKI, T., PRIEBE, W., VILLARREAL, D., KANG, S. G., JOYCE, C., SULMAN, E., WANG, Q., MARINI, F. C., ANDREEFF, M., COLMAN, H. & LANG, F. F. 2015. Mesenchymal Stem Cells Isolated From Human Gliomas Increase Proliferation and Maintain Stemness of Glioma Stem Cells Through the IL-6/gp130/STAT3 Pathway. *Stem Cells,* 33, 2400-15.

HU, D. D., LIN, E. C., KOVACH, N. L., HOYER, J. R. & SMITH, J. W. 1995. A biochemical characterization of the binding of osteopontin to integrins alpha v beta 1 and alpha v beta 5. *J Biol Chem,* 270, 26232-8.

HU, M., YANG, J. L., TENG, H., JIA, Y. Q., WANG, R., ZHANG, X. W., WU, Y., LUO, Y., CHEN, X. C., ZHANG, R., TIAN, L., ZHAO, X. & WEI, Y. Q. 2008. Anti-angiogenesis therapy based on the bone marrow-derived stromal cells genetically engineered to express sFlt-1 in mouse tumor model. *BMC Cancer,* 8, 306.

HUANG, G. T., GRONTHOS, S. & SHI, S. 2009. Mesenchymal stem cells derived from dental tissues vs. those from other sources: their biology and role in regenerative medicine. *J Dent Res,* 88, 792-806.

HUANG, J. I., BEANES, S. R., ZHU, M., LORENZ, H. P., HEDRICK, M. H. & BENHAIM, P. 2002. Rat extramedullary adipose tissue as a source of osteochondrogenic progenitor cells. *Plast Reconstr Surg,* 109, 1033-41; discussion 1042-3.

HUANG, Y., YU, P., LI, W., REN, G., ROBERTS, A. I., CAO, W., ZHANG, X., SU, J., CHEN, X., CHEN, Q., SHOU, P., XU, C., DU, L., LIN, L., XIE, N., ZHANG, L., WANG, Y. & SHI, Y. 2014. p53 regulates mesenchymal stem cell-mediated tumor suppression in a tumor microenvironment through immune modulation. *Oncogene,* 33, 3830-8.

HUSSAIN, F., FREISSMUTH, M., VOLKEL, D., THIELE, M., DOUILLARD, P., ANTOINE, G., THURNER, P., EHRLICH, H., SCHWARZ, H. P., SCHEIFLINGER, F. & KERSCHBAUMER, R. J. 2013. Human anti-macrophage migration inhibitory factor antibodies inhibit growth of human prostate cancer cells in vitro and in vivo. *Mol Cancer Ther,* 12, 1223-34.

IARC 2012. GLOBOCAB 2012: Estimated Incidence, Mortality and Prevalence Worldwide in 2012. *International Agency for Research on Cancer*.

IBRAHIM, T., LEONG, I., SANCHEZ-SWEATMAN, O., KHOKHA, R., SODEK, J., TENENBAUM, H. C., GANSS, B. & CHEIFETZ, S. 2000. Expression of bone sialoprotein and osteopontin in breast cancer bone metastases. *Clin Exp Metastasis,* 18, 253-60.

ISHII, G., SANGAI, T., ODA, T., AOYAGI, Y., HASEBE, T., KANOMATA, N., ENDOH, Y., OKUMURA, C., OKUHARA, Y., MAGAE, J., EMURA, M., OCHIYA, T. & OCHIAI, A. 2003. Bone-marrow-derived myofibroblasts contribute to the cancer-induced stromal reaction. *Biochem Biophys Res Commun,* 309, 232-40.

ISHIJIMA, M., RITTLING, S. R., YAMASHITA, T., TSUJI, K., KUROSAWA, H., NIFUJI, A., DENHARDT, D. T. & NODA, M. 2001. Enhancement of osteoclastic bone resorption and suppression of osteoblastic bone formation in response to reduced mechanical stress do not occur in the absence of osteopontin. *J Exp Med,* 193, 399-404.

ITO, S., BARRETT, A. J., DUTRA, A., PAK, E., MINER, S., KEYVANFAR, K., HENSEL, N. F., REZVANI, K., MURANSKI, P., LIU, P., MELENHORST, J. J. & LAROCHELLE, A. 2015. Long term maintenance of myeloid leukemic stem cells cultured with unrelated human mesenchymal stromal cells. *Stem Cell Res,* 14, 95-104.

IVASKA, J., PALLARI, H. M., NEVO, J. & ERIKSSON, J. E. 2007. Novel functions of vimentin in cell adhesion, migration, and signaling. *Exp Cell Res,* 313, 2050-62.

JACOB, K., WEBBER, M., BENAYAHU, D. & KLEINMAN, H. K. 1999. Osteonectin promotes prostate cancer cell migration and invasion: a possible mechanism for metastasis to bone. *Cancer Res,* 59, 4453-7.

JEDESZKO, C., VICTOR, B. C., PODGORSKI, I. & SLOANE, B. F. 2009. Fibroblast hepatocyte growth factor promotes invasion of human mammary ductal carcinoma in situ. *Cancer Res,* 69, 9148-55.

JI, J. F., HE, B. P., DHEEN, S. T. & TAY, S. S. 2004. Interactions of chemokines and chemokine receptors mediate the migration of mesenchymal stem cells to the impaired site in the brain after hypoglossal nerve injury. *Stem Cells,* 22, 415-27.

JIA, C. C., WANG, T. T., LIU, W., FU, B. S., HUA, X., WANG, G. Y., LI, T. J., LI, X., WU, X. Y., TAI, Y., ZHOU, J., CHEN, G. H. & ZHANG, Q. 2013. Cancer-associated fibroblasts from hepatocellular carcinoma promote malignant cell proliferation by HGF secretion. *PLoS One,* 8, e63243.

JING, Y., HAN, Z., LIU, Y., SUN, K., ZHANG, S., JIANG, G., LI, R., GAO, L., ZHAO, X., WU, D., CAI, X., WU, M. & WEI, L. 2012. Mesenchymal stem cells in inflammation microenvironment accelerates hepatocellular carcinoma metastasis by inducing epithelial-mesenchymal transition. ***PLoS One,*** **7, e43272.**

JONES, M. L., SIDDIQUI, J., PIENTA, K. J. & GETZENBERG, R. H. 2013. Circulating fibroblast-like cells in men with metastatic prostate cancer. ***Prostate,*** **73, 176-81.**

JOSEPH, J., SHIOZAWA, Y., JUNG, Y., KIM, J. K., PEDERSEN, E., MISHRA, A., ZALUCHA, J. L., WANG, J., KELLER, E. T., PIENTA, K. J. & TAICHMAN, R. S. 2012. Disseminated prostate cancer cells can instruct hematopoietic stem and progenitor cells to regulate bone phenotype. ***Mol Cancer Res,*** **10, 282-92.**

JURCZYSZYN, A., CZEPIEL, J., GDULA-ARGASINSKA, J., PERUCKI, W., SKOTNICKI, A. B. & MAJKA, M. 2015. The Analysis of the Relationship between Multiple Myeloma Cells and Their Microenvironment. ***J Cancer,*** **6, 160-8.**

KALLURI, R. & ZEISBERG, M. 2006. Fibroblasts in cancer. ***Nat Rev Cancer,*** **6, 392-401.**

KANETY, H., MADJAR, Y., DAGAN, Y., LEVI, J., PAPA, M. Z., PARIENTE, C., GOLDWASSER, B. & KARASIK, A. 1993. Serum insulin-like growth factor-binding protein-2 (IGFBP-2) is increased and IGFBP-3 is decreased in patients with prostate cancer: correlation with serum prostate-specific antigen. ***J Clin Endocrinol Metab,*** **77, 229-33.**

KANSY, B. A., DISSMANN, P. A., HEMEDA, H., BRUDEREK, K., WESTERKAMP, A. M., JAGALSKI, V., SCHULER, P., KANSY, K., LANG, S., DUMITRU, C. A. & BRANDAU, S. 2014. The bidirectional tumor--mesenchymal stromal cell interaction promotes the progression of head and neck cancer. ***Stem Cell Res Ther,*** **5, 95.**

KAPLAN, R. N., RIBA, R. D., ZACHAROULIS, S., BRAMLEY, A. H., VINCENT, L., COSTA, C., MACDONALD, D. D., JIN, D. K., SHIDO, K., KERNS, S. A., ZHU, Z., HICKLIN, D., WU, Y., PORT, J. L., ALTORKI, N., PORT, E. R., RUGGERO, D., SHMELKOV, S. V., JENSEN, K. K., RAFII, S. & LYDEN, D. 2005. VEGFR1-positive haematopoietic bone marrow progenitors initiate the pre-metastatic niche. ***Nature,*** **438, 820-7.**

KARNOUB, A. E., DASH, A. B., VO, A. P., SULLIVAN, A., BROOKS, M. W., BELL, G. W., RICHARDSON, A. L., POLYAK, K., TUBO, R. & WEINBERG, R. A. 2007. Mesenchymal stem cells within tumour stroma promote breast cancer metastasis. ***Nature,*** **449, 557-63.**

KAWAMOTO, M., MATSUNAMI, T., ERTL, R. F., FUKUDA, Y., OGAWA, M., SPURZEM, J. R., YAMANAKA, N. & RENNARD, S. I. 1997. Selective migration of alpha-smooth muscle actin-positive myofibroblasts toward fibronectin in the Boyden's blindwell chamber. ***Clin Sci (Lond),*** **93, 355-62.**

KELLERMANN, M. G., SOBRAL, L. M., DA SILVA, S. D., ZECCHIN, K. G., GRANER, E., LOPES, M. A., KOWALSKI, L. P. & COLETTA, R. D. 2008. Mutual paracrine effects of oral squamous cell carcinoma cells and normal oral fibroblasts: induction of fibroblast to myofibroblast transdifferentiation and modulation of tumor cell proliferation. ***Oral Oncol,*** **44, 509-17.**

KERN, S., EICHLER, H., STOEVE, J., KLUTER, H. & BIEBACK, K. 2006. Comparative analysis of mesenchymal stem cells from bone marrow, umbilical cord blood, or adipose tissue. ***Stem Cells,*** **24, 1294-301.**

KHAKOO, A. Y., PATI, S., ANDERSON, S. A., REID, W., ELSHAL, M. F., ROVIRA, II, NGUYEN, A. T., MALIDE, D., COMBS, C. A., HALL, G., ZHANG, J., RAFFELD, M., ROGERS, T. B., STETLER-STEVENSON, W., FRANK, J. A., REITZ, M. & FINKEL, T. 2006. Human mesenchymal stem cells exert potent antitumorigenic effects in a model of Kaposi's sarcoma. ***J Exp Med,*** **203, 1235-47.**

KHODAVIRDI, A. C., SONG, Z., YANG, S., ZHONG, C., WANG, S., WU, H., PRITCHARD, C., NELSON, P. S. & ROY-BURMAN, P. 2006. Increased expression of osteopontin contributes to the progression of prostate cancer. ***Cancer Res,*** **66, 883-8.**

KIDD, S., SPAETH, E., DEMBINSKI, J. L., DIETRICH, M., WATSON, K., KLOPP, A., BATTULA, V. L., WEIL, M., ANDREEFF, M. & MARINI, F. C. 2009. Direct Evidence of Mesenchymal Stem Cell Tropism for Tumor and Wounding Microenvironments Using In Vivo Bioluminescent Imaging. *Stem Cells,* 27, 2614-2623.

KIM, E. K., KIM, H. J., YANG, Y. I., KIM, J. T., CHOI, M. Y., CHOI, C. S., KIM, K. H., LEE, J. H., JANG, W. H. & CHEONG, S. H. 2013. Endogenous gastric-resident mesenchymal stem cells contribute to formation of cancer stroma and progression of gastric cancer. *Korean J Pathol,* 47, 507-18.

KIM, M. S., DAY, C. J. & MORRISON, N. A. 2005. MCP-1 is induced by receptor activator of nuclear factor-{kappa}B ligand, promotes human osteoclast fusion, and rescues granulocyte macrophage colony-stimulating factor suppression of osteoclast formation. *J Biol Chem,* 280, 16163-9.

KIM, S. J., UEHARA, H., KARASHIMA, T., MCCARTY, M., SHIH, N. & FIDLER, I. J. 2001. Expression of interleukin-8 correlates with angiogenesis, tumorigenicity, and metastasis of human prostate cancer cells implanted orthotopically in nude mice. *Neoplasia,* 3, 33-42.

KINNAIRD, T., STABILE, E., BURNETT, M. S., LEE, C. W., BARR, S., FUCHS, S. & EPSTEIN, S. E. 2004. Marrow-derived stromal cells express genes encoding a broad spectrum of arteriogenic cytokines and promote in vitro and in vivo arteriogenesis through paracrine mechanisms. *Circ Res,* 94, 678-85.

KLEIN-NULEND, J., ROELOFSEN, J., SEMEINS, C. M., BRONCKERS, A. L. & BURGER, E. H. 1997. Mechanical stimulation of osteopontin mRNA expression and synthesis in bone cell cultures. *J Cell Physiol,* 170, 174-81.

KLOPP, A. H., GUPTA, A., SPAETH, E., ANDREEFF, M. & MARINI, F., 3RD 2011. Concise review: Dissecting a discrepancy in the literature: do mesenchymal stem cells support or suppress tumor growth? *Stem Cells,* 29, 11-9.

KLOPP, A. H., SPAETH, E. L., DEMBINSKI, J. L., WOODWARD, W. A., MUNSHI, A., MEYN, R. E., COX, J. D., ANDREEFF, M. & MARINI, F. C. 2007. Tumor irradiation increases the recruitment of circulating mesenchymal stem cells into the tumor microenvironment. *Cancer Res,* 67, 11687-95.

KOJIMA, Y., ACAR, A., EATON, E. N., MELLODY, K. T., SCHEEL, C., BEN-PORATH, I., ONDER, T. T., WANG, Z. C., RICHARDSON, A. L., WEINBERG, R. A. & ORIMO, A. 2010. Autocrine TGF-beta and stromal cell-derived factor-1 (SDF-1) signaling drives the evolution of tumor-promoting mammary stromal myofibroblasts. *Proc Natl Acad Sci U S A,* 107, 20009-14.

KOPEN, G. C., PROCKOP, D. J. & PHINNEY, D. G. 1999. Marrow stromal cells migrate throughout forebrain and cerebellum, and they differentiate into astrocytes after injection into neonatal mouse brains. *Proc Natl Acad Sci U S A,* 96, 10711-6.

KRAMPERA, M., GLENNIE, S., DYSON, J., SCOTT, D., LAYLOR, R., SIMPSON, E. & DAZZI, F. 2003. Bone marrow mesenchymal stem cells inhibit the response of naive and memory antigen-specific T cells to their cognate peptide. *Blood,* 101, 3722-9.

KUCEROVA, L., ALTANEROVA, V., MATUSKOVA, M., TYCIAKOVA, S. & ALTANER, C. 2007. Adipose tissue-derived human mesenchymal stem cells mediated prodrug cancer gene therapy. *Cancer Res,* 67, 6304-13.

KUCEROVA, L., MATUSKOVA, M., HLUBINOVA, K., ALTANEROVA, V. & ALTANER, C. 2010. Tumor cell behaviour modulation by mesenchymal stromal cells. *Mol Cancer,* 9, 129.

LACERDA, L., DEBEB, B. G., SMITH, D., LARSON, R., SOLLEY, T., XU, W., KRISHNAMURTHY, S., GONG, Y., LEVY, L. B., BUCHHOLZ, T., UENO, N. T., KLOPP, A. & WOODWARD, W. A. 2015. Mesenchymal stem cells mediate the clinical phenotype of inflammatory breast cancer in a preclinical model. *Breast Cancer Res,* 17, 42.

LEE, M. J., HEO, S. C., SHIN, S. H., KWON, Y. W., DO, E. K., SUH, D. S., YOON, M. S. & KIM, J. H. 2013. Oncostatin M promotes mesenchymal stem cell-stimulated tumor growth through a paracrine mechanism involving periostin and TGFBI. *Int J Biochem Cell Biol,* 45, 1869-77.

LEE, R. H., KIM, B., CHOI, I., KIM, H., CHOI, H. S., SUH, K., BAE, Y. C. & JUNG, J. S. 2004. Characterization and expression analysis of mesenchymal stem cells from human bone marrow and adipose tissue. *Cell Physiol Biochem,* 14, 311-24.

LEHRER, S., DIAMOND, E. J., MAMKINE, B., STONE, N. N. & STOCK, R. G. 2004. Serum interleukin-8 is elevated in men with prostate cancer and bone metastases. *Technol Cancer Res Treat,* 3, 411.

LEVESQUE, J. P., HENDY, J., TAKAMATSU, Y., SIMMONS, P. J. & BENDALL, L. J. 2003. Disruption of the CXCR4/CXCL12 chemotactic interaction during hematopoietic stem cell mobilization induced by GCSF or cyclophosphamide. *J Clin Invest,* 111, 187-96.

LI, B., SHI, M., LI, J., ZHANG, H., CHEN, B., CHEN, L., GAO, W., GIULIANI, N. & ZHAO, R. C. 2007. Elevated tumor necrosis factor-alpha suppresses TAZ expression and impairs osteogenic potential of Flk-1+ mesenchymal stem cells in patients with multiple myeloma. *Stem Cells Dev,* 16, 921-30.

LI, W., ZHOU, Y., YANG, J., ZHANG, X., ZHANG, H., ZHANG, T., ZHAO, S., ZHENG, P., HUO, J. & WU, H. 2015. Gastric cancer-derived mesenchymal stem cells prompt gastric cancer progression through secretion of interleukin-8. *J Exp Clin Cancer Res,* 34, 52.

LI, X., LOBERG, R., LIAO, J., YING, C., SNYDER, L. A., PIENTA, K. J. & MCCAULEY, L. K. 2009. A destructive cascade mediated by CCL2 facilitates prostate cancer growth in bone. *Cancer Res,* 69, 1685-92.

LI, Z., WANG, Z., YANG, L., LI, X., SASAKI, Y., WANG, S., ARAKI, S., MEZAWA, M., TAKAI, H., NAKAYAMA, Y. & OGATA, Y. 2010. Fibroblast growth factor 2 regulates bone sialoprotein gene transcription in human breast cancer cells. *J Oral Sci,* 52, 125-32.

LIAW, L., SKINNER, M. P., RAINES, E. W., ROSS, R., CHERESH, D. A., SCHWARTZ, S. M. & GIACHELLI, C. M. 1995. The adhesive and migratory effects of osteopontin are mediated via distinct cell surface integrins. Role of alpha v beta 3 in smooth muscle cell migration to osteopontin in vitro. *J Clin Invest,* 95, 713-24.

LIN, P., SANKAR, S., SHAN, S., DEWHIRST, M. W., POLVERINI, P. J., QUINN, T. Q. & PETERS, K. G. 1998. Inhibition of tumor growth by targeting tumor endothelium using a soluble vascular endothelial growth factor receptor. *Cell Growth Differ,* 9, 49-58.

LIOTTA, L. A. 1986. Tumor invasion and metastases--role of the extracellular matrix: Rhoads Memorial Award lecture. *Cancer Res,* 46, 1-7.

LIU, H., CHEN, A., GUO, F. & YUAN, L. 2010. A short-hairpin RNA targeting osteopontin downregulates MMP-2 and MMP-9 expressions in prostate cancer PC-3 cells. *Cancer Lett,* 295, 27-37.

LIU, Y., HU, T., SHEN, J., LI, S. F., LIN, J. W., ZHENG, X. H., GAO, Q. H. & ZHOU, H. M. 2006. Separation, cultivation and biological characteristics of oral carcinoma-associated fibroblasts. *Oral Dis,* 12, 375-80.

LOBERG, R. D., DAY, L. L., HARWOOD, J., YING, C., ST JOHN, L. N., GILES, R., NEELEY, C. K. & PIENTA, K. J. 2006. CCL2 is a potent regulator of prostate cancer cell migration and proliferation. *Neoplasia,* 8, 578-86.

LOBERG, R. D., YING, C., CRAIG, M., DAY, L. L., SARGENT, E., NEELEY, C., WOJNO, K., SNYDER, L. A., YAN, L. & PIENTA, K. J. 2007a. Targeting CCL2 with systemic delivery of neutralizing antibodies induces prostate cancer tumor regression in vivo. *Cancer Res,* 67, 9417-24.

LOBERG, R. D., YING, C., CRAIG, M., YAN, L., SNYDER, L. A. & PIENTA, K. J. 2007b. CCL2 as an important mediator of prostate cancer growth in vivo through the regulation of macrophage infiltration. *Neoplasia,* 9, 556-62.

LOEBINGER, M. R., EDDAOUDI, A., DAVIES, D. & JANES, S. M. 2009a. Mesenchymal stem cell delivery of TRAIL can eliminate metastatic cancer. ***Cancer Res,*** **69, 4134-42.**

LOEBINGER, M. R., KYRTATOS, P. G., TURMAINE, M., PRICE, A. N., PANKHURST, Q., LYTHGOE, M. F. & JANES, S. M. 2009b. Magnetic resonance imaging of mesenchymal stem cells homing to pulmonary metastases using biocompatible magnetic nanoparticles. ***Cancer Res,*** **69, 8862-7.**

LOU, W., NI, Z., DYER, K., TWEARDY, D. J. & GAO, A. C. 2000. Interleukin-6 induces prostate cancer cell growth accompanied by activation of stat3 signaling pathway. ***Prostate,*** **42, 239-42.**

LU, Y., CAI, Z., GALSON, D. L., XIAO, G., LIU, Y., GEORGE, D. E., MELHEM, M. F., YAO, Z. & ZHANG, J. 2006. Monocyte chemotactic protein-1 (MCP-1) acts as a paracrine and autocrine factor for prostate cancer growth and invasion. ***Prostate,*** **66, 1311-8.**

LU, Y., CAI, Z., XIAO, G., KELLER, E. T., MIZOKAMI, A., YAO, Z., ROODMAN, G. D. & ZHANG, J. 2007a. Monocyte chemotactic protein-1 mediates prostate cancer-induced bone resorption. ***Cancer Res,*** **67, 3646-53.**

LU, Y., CHEN, Q., COREY, E., XIE, W., FAN, J., MIZOKAMI, A. & ZHANG, J. 2009. Activation of MCP-1/CCR2 axis promotes prostate cancer growth in bone. ***Clin Exp Metastasis,*** **26, 161-9.**

LU, Y., XIAO, G., GALSON, D. L., NISHIO, Y., MIZOKAMI, A., KELLER, E. T., YAO, Z. & ZHANG, J. 2007b. PTHrP-induced MCP-1 production by human bone marrow endothelial cells and osteoblasts promotes osteoclast differentiation and prostate cancer cell proliferation and invasion in vitro. ***Int J Cancer,*** **121, 724-33.**

LUO, J., OK LEE, S., LIANG, L., HUANG, C. K., LI, L., WEN, S. & CHANG, C. 2014. Infiltrating bone marrow mesenchymal stem cells increase prostate cancer stem cell population and metastatic ability via secreting cytokines to suppress androgen receptor signaling. ***Oncogene,*** **33, 2768-78.**

MADAR, S., BROSH, R., BUGANIM, Y., EZRA, O., GOLDSTEIN, I., SOLOMON, H., KOGAN, I., GOLDFINGER, N., KLOCKER, H. & ROTTER, V. 2009. Modulated expression of WFDC1 during carcinogenesis and cellular senescence. ***Carcinogenesis,*** **30, 20-7.**

MADIGAN, M. C., KINGSLEY, E. A., COZZI, P. J., DELPRADO, W. J., RUSSELL, P. J. & LI, Y. 2008. The role of extracellular matrix metalloproteinase inducer protein in prostate cancer progression. ***Cancer Immunol Immunother,*** **57, 1367-79.**

MAHMOOD, A., LU, D., LU, M. & CHOPP, M. 2003. Treatment of traumatic brain injury in adult rats with intravenous administration of human bone marrow stromal cells. ***Neurosurgery,*** **53, 697-702; discussion 702-3.**

MAITRA, B., SZEKELY, E., GJINI, K., LAUGHLIN, M. J., DENNIS, J., HAYNESWORTH, S. E. & KOC, O. N. 2004. Human mesenchymal stem cells support unrelated donor hematopoietic stem cells and suppress T-cell activation. ***Bone Marrow Transplant,*** **33, 597-604.**

MAJUMDAR, M. K., THIEDE, M. A., MOSCA, J. D., MOORMAN, M. & GERSON, S. L. 1998. Phenotypic and functional comparison of cultures of marrow-derived mesenchymal stem cells (MSCs) and stromal cells. ***J Cell Physiol,*** **176, 57-66.**

MANTOVANI, A., SOZZANI, S., LOCATI, M., ALLAVENA, P. & SICA, A. 2002. Macrophage polarization: tumor-associated macrophages as a paradigm for polarized M2 mononuclear phagocytes. ***Trends Immunol,*** **23, 549-55.**

MARTIN, F. T., DWYER, R. M., KELLY, J., KHAN, S., MURPHY, J. M., CURRAN, C., MILLER, N., HENNESSY, E., DOCKERY, P., BARRY, F. P., O'BRIEN, T. & KERIN, M. J. 2010. Potential role of mesenchymal stem cells (MSCs) in the breast tumour microenvironment: stimulation of epithelial to mesenchymal transition (EMT). ***Breast Cancer Res Treat,*** **124, 317-26.**

MATTERN, J., KOOMAGI, R. & VOLM, M. 1997. Coexpression of VEGF and bFGF in human epidermoid lung carcinoma is associated with increased vessel density. *Anticancer Res,* 17, 2249-52.

MAXWELL, P. J., NEISEN, J., MESSENGER, J. & WAUGH, D. J. 2014. Tumor-derived CXCL8 signaling augments stroma-derived CCL2-promoted proliferation and CXCL12-mediated invasion of PTEN-deficient prostate cancer cells. *Oncotarget,* 5, 4895-908.

MCINROY, L. & MAATTA, A. 2007. Down-regulation of vimentin expression inhibits carcinoma cell migration and adhesion. *Biochem Biophys Res Commun,* 360, 109-14.

MEADS, M. B., HAZLEHURST, L. A. & DALTON, W. S. 2008. The bone marrow microenvironment as a tumor sanctuary and contributor to drug resistance. *Clin Cancer Res,* 14, 2519-26.

MENON, L. G., PICINICH, S., KONERU, R., GAO, H., LIN, S. Y., KONERU, M., MAYER-KUCKUK, P., GLOD, J. & BANERJEE, D. 2007. Differential gene expression associated with migration of mesenchymal stem cells to conditioned medium from tumor cells or bone marrow cells. *Stem Cells,* 25, 520-8.

MEYER-SIEGLER, K. & HUDSON, P. B. 1996. Enhanced expression of macrophage migration inhibitory factor in prostatic adenocarcinoma metastases. *Urology,* 48, 448-52.

MEYER-SIEGLER, K. L., ICZKOWSKI, K. A., LENG, L., BUCALA, R. & VERA, P. L. 2006. Inhibition of macrophage migration inhibitory factor or its receptor (CD74) attenuates growth and invasion of DU-145 prostate cancer cells. *J Immunol,* 177, 8730-9.

MEYER-SIEGLER, K. L., ICZKOWSKI, K. A. & VERA, P. L. 2005. Further evidence for increased macrophage migration inhibitory factor expression in prostate cancer. *BMC Cancer,* 5, 73.

MI, Z., BHATTACHARYA, S. D., KIM, V. M., GUO, H., TALBOT, L. J. & KUO, P. C. 2011. Osteopontin promotes CCL5-mesenchymal stromal cell-mediated breast cancer metastasis. *Carcinogenesis,* 32, 477-87.

MI, Z., GUO, H., WAI, P. Y., GAO, C. & KUO, P. C. 2006. Integrin-linked kinase regulates osteopontin-dependent MMP-2 and uPA expression to convey metastatic function in murine mammary epithelial cancer cells. *Carcinogenesis,* 27, 1134-45.

MICHIGAMI, T., SHIMIZU, N., WILLIAMS, P. J., NIEWOLNA, M., DALLAS, S. L., MUNDY, G. R. & YONEDA, T. 2000. Cell-cell contact between marrow stromal cells and myeloma cells via VCAM-1 and alpha(4)beta(1)-integrin enhances production of osteoclast-stimulating activity. *Blood,* 96, 1953-60.

MISHRA, P. J., MISHRA, P. J., HUMENIUK, R., MEDINA, D. J., ALEXE, G., MESIROV, J. P., GANESAN, S., GLOD, J. W. & BANERJEE, D. 2008. Carcinoma-associated fibroblast-like differentiation of human mesenchymal stem cells. *Cancer Res,* 68, 4331-9.

MIZUTANI, K., SUD, S. & PIENTA, K. J. 2009. Prostate cancer promotes CD11b positive cells to differentiate into osteoclasts. *J Cell Biochem,* 106, 563-9.

MOHR, A., ALBARENQUE, S. M., DEEDIGAN, L., YU, R., REIDY, M., FULDA, S. & ZWACKA, R. M. 2010. Targeting of XIAP combined with systemic mesenchymal stem cell-mediated delivery of sTRAIL ligand inhibits metastatic growth of pancreatic carcinoma cells. *Stem Cells,* 28, 2109-20.

MONTAGUE, R., HART, C. A., GEORGE, N. J., RAMANI, V. A., BROWN, M. D. & CLARKE, N. W. 2004. Differential inhibition of invasion and proliferation by bisphosphonates: anti-metastatic potential of Zoledronic acid in prostate cancer. *Eur Urol,* 46, 389-401; discussion 401-2.

MONTERO, A., OKADA, Y., TOMITA, M., ITO, M., TSURUKAMI, H., NAKAMURA, T., DOETSCHMAN, T., COFFIN, J. D. & HURLEY, M. M. 2000. Disruption of the fibroblast growth factor-2 gene results in decreased bone mass and bone formation. *J Clin Invest,* 105, 1085-93.

MOORE, B. B., ARENBERG, D. A., STOY, K., MORGAN, T., ADDISON, C. L., MORRIS, S. B., GLASS, M., WILKE, C., XUE, Y. Y., SITTERDING, S., KUNKEL, S. L., BURDICK, M. D. & STRIETER, R. M. 1999. Distinct CXC chemokines mediate tumorigenicity of prostate cancer cells. ***Am J Pathol,*** **154, 1503-12.**

MORGIA, G., FALSAPERLA, M., MALAPONTE, G., MADONIA, M., INDELICATO, M., TRAVALI, S. & MAZZARINO, M. C. 2005. Matrix metalloproteinases as diagnostic (MMP-13) and prognostic (MMP-2, MMP-9) markers of prostate cancer. ***Urol Res,*** **33, 44-50.**

MORI, A., ARII, S., FURUTANI, M., MIZUMOTO, M., UCHIDA, S., FURUYAMA, H., KONDO, Y., GORRIN-RIVAS, M. J., FURUMOTO, K., KANEDA, Y. & IMAMURA, M. 2000. Soluble Flt-1 gene therapy for peritoneal metastases using HVJ-cationic liposomes. ***Gene Ther,*** **7, 1027-33.**

MORI, S., MURAKAMI-MORI, K. & BONAVIDA, B. 1999. Interleukin-6 induces G1 arrest through induction of p27(Kip1), a cyclin-dependent kinase inhibitor, and neuron-like morphology in LNCaP prostate tumor cells. ***Biochem Biophys Res Commun,*** **257, 609-14.**

MUEHLBERG, F. L., SONG, Y. H., KROHN, A., PINILLA, S. P., DROLL, L. H., LENG, X., SEIDENSTICKER, M., RICKE, J., ALTMAN, A. M., DEVARAJAN, E., LIU, W., ARLINGHAUS, R. B. & ALT, E. U. 2009. Tissue-resident stem cells promote breast cancer growth and metastasis. ***Carcinogenesis,*** **30, 589-97.**

MUERKOSTER, S., WEGEHENKEL, K., ARLT, A., WITT, M., SIPOS, B., KRUSE, M. L., SEBENS, T., KLOPPEL, G., KALTHOFF, H., FOLSCH, U. R. & SCHAFER, H. 2004. Tumor stroma interactions induce chemoresistance in pancreatic ductal carcinoma cells involving increased secretion and paracrine effects of nitric oxide and interleukin-1beta. ***Cancer Res,*** **64, 1331-7.**

MUNDY, G. R. & YONEDA, T. 1998. Bisphosphonates as anticancer drugs. ***N Engl J Med,*** **339, 398-400.**

MURPHY, C., MCGURK, M., PETTIGREW, J., SANTINELLI, A., MAZZUCCHELLI, R., JOHNSTON, P. G., MONTIRONI, R. & WAUGH, D. J. 2005. Nonapical and cytoplasmic expression of interleukin-8, CXCR1, and CXCR2 correlates with cell proliferation and microvessel density in prostate cancer. ***Clin Cancer Res,*** **11, 4117-27.**

MURRAY, M. M. & SPECTOR, M. 2001. The migration of cells from the ruptured human anterior cruciate ligament into collagen-glycosaminoglycan regeneration templates in vitro. ***Biomaterials,*** **22, 2393-402.**

NABHA, S. M., DOS SANTOS, E. B., YAMAMOTO, H. A., BELIZI, A., DONG, Z., MENG, H., SALIGANAN, A., SABBOTA, A., BONFIL, R. D. & CHER, M. L. 2008. Bone marrow stromal cells enhance prostate cancer cell invasion through type I collagen in an MMP-12 dependent manner. ***Int J Cancer,*** **122, 2482-90.**

NAKAMIZO, A., MARINI, F., AMANO, T., KHAN, A., STUDENY, M., GUMIN, J., CHEN, J., HENTSCHEL, S., VECIL, G., DEMBINSKI, J., ANDREEFF, M. & LANG, F. F. 2005. Human bone marrow-derived mesenchymal stem cells in the treatment of gliomas. ***Cancer Res,*** **65, 3307-18.**

NASH SMYTH, E., CONTI, I., WOOLDRIDGE, J. E., BOWMAN, L., LI, L., NELSON, D. R. & BALL, D. E. 2016. Frequency of skeletal-related events and associated healthcare resource use and costs in US patients with multiple myeloma. ***J Med Econ*****, 1-10.**

NAUTA, A. J., KRUISSELBRINK, A. B., LURVINK, E., WILLEMZE, R. & FIBBE, W. E. 2006. Mesenchymal stem cells inhibit generation and function of both CD34+-derived and monocyte-derived dendritic cells. ***J Immunol,*** **177, 2080-7.**

NCRI 2014. Cancer in Ireland 1994-2011: Annual report of the National Cancer Registry 2014. ***National Cancer Registry*****.**

NEMETH, J. A., YOUSIF, R., HERZOG, M., CHE, M., UPADHYAY, J., SHEKARRIZ, B., BHAGAT, S., MULLINS, C., FRIDMAN, R. & CHER, M. L. 2002. Matrix metalloproteinase

activity, bone matrix turnover, and tumor cell proliferation in prostate cancer bone metastasis. *J Natl Cancer Inst,* 94, 17-25.

NEMOTO, H., RITTLING, S. R., YOSHITAKE, H., FURUYA, K., AMAGASA, T., TSUJI, K., NIFUJI, A., DENHARDT, D. T. & NODA, M. 2001. Osteopontin deficiency reduces experimental tumor cell metastasis to bone and soft tissues. *J Bone Miner Res,* 16, 652-9.

NIEMINEN, M., HENTTINEN, T., MERINEN, M., MARTTILA-ICHIHARA, F., ERIKSSON, J. E. & JALKANEN, S. 2006. Vimentin function in lymphocyte adhesion and transcellular migration. *Nat Cell Biol,* 8, 156-62.

NISHIMORI, H., EHATA, S., SUZUKI, H. I., KATSUNO, Y. & MIYAZONO, K. 2012. Prostate cancer cells and bone stromal cells mutually interact with each other through bone morphogenetic protein-mediated signals. *J Biol Chem*.

NISSEN, L. J., CAO, R., HEDLUND, E. M., WANG, Z., ZHAO, X., WETTERSKOG, D., FUNA, K., BRAKENHIELM, E. & CAO, Y. 2007. Angiogenic factors FGF2 and PDGF-BB synergistically promote murine tumor neovascularization and metastasis. *J Clin Invest,* 117, 2766-77.

NOLL, J. E., WILLIAMS, S. A., TONG, C. M., WANG, H., QUACH, J. M., PURTON, L. E., PILKINGTON, K., TO, L. B., EVDOKIOU, A., GRONTHOS, S. & ZANNETTINO, A. C. 2014. Myeloma plasma cells alter the bone marrow microenvironment by stimulating the proliferation of mesenchymal stromal cells. *Haematologica,* 99, 163-71.

NTAMBI, J. M. & YOUNG-CHEUL, K. 2000. Adipocyte differentiation and gene expression. *J Nutr,* 130, 3122S-3126S.

OHTA, N., ISHIGURO, S., KAWABATA, A., UPPALAPATI, D., PYLE, M., TROYER, D., DE, S., ZHANG, Y., BECKER, K. G. & TAMURA, M. 2015. Human umbilical cord matrix mesenchymal stem cells suppress the growth of breast cancer by expression of tumor suppressor genes. *PLoS One,* 10, e0123756.

OKAMOTO, M., LEE, C. & OYASU, R. 1997. Interleukin-6 as a paracrine and autocrine growth factor in human prostatic carcinoma cells in vitro. *Cancer Res,* 57, 141-6.

OLUMI, A. F., GROSSFELD, G. D., HAYWARD, S. W., CARROLL, P. R., TLSTY, T. D. & CUNHA, G. R. 1999. Carcinoma-associated fibroblasts direct tumor progression of initiated human prostatic epithelium. *Cancer Res,* 59, 5002-11.

ORIMO, A., GUPTA, P. B., SGROI, D. C., ARENZANA-SEISDEDOS, F., DELAUNAY, T., NAEEM, R., CAREY, V. J., RICHARDSON, A. L. & WEINBERG, R. A. 2005. Stromal fibroblasts present in invasive human breast carcinomas promote tumor growth and angiogenesis through elevated SDF-1/CXCL12 secretion. *Cell,* 121, 335-48.

ORLIC, D., KAJSTURA, J., CHIMENTI, S., LIMANA, F., JAKONIUK, I., QUAINI, F., NADAL-GINARD, B., BODINE, D. M., LERI, A. & ANVERSA, P. 2001. Mobilized bone marrow cells repair the infarcted heart, improving function and survival. *Proc Natl Acad Sci U S A,* 98, 10344-9.

ORTIZ, L. A., GAMBELLI, F., MCBRIDE, C., GAUPP, D., BADDOO, M., KAMINSKI, N. & PHINNEY, D. G. 2003. Mesenchymal stem cell engraftment in lung is enhanced in response to bleomycin exposure and ameliorates its fibrotic effects. *Proc Natl Acad Sci U S A,* 100, 8407-8411.

OSWALD, J., BOXBERGER, S., JORGENSEN, B., FELDMANN, S., EHNINGER, G., BORNHAUSER, M. & WERNER, C. 2004. Mesenchymal stem cells can be differentiated into endothelial cells in vitro. *Stem Cells,* 22, 377-84.

OTSU, K., DAS, S., HOUSER, S. D., QUADRI, S. K., BHATTACHARYA, S. & BHATTACHARYA, J. 2009. Concentration-dependent inhibition of angiogenesis by mesenchymal stem cells. *Blood,* 113, 4197-205.

PAGET, S. 1989. The distribution of secondary growths in cancer of the breast. 1889. *Cancer Metastasis Rev,* 8, 98-101.

PARK, S. I., SOKI, F. N. & MCCAULEY, L. K. 2011. Roles of bone marrow cells in skeletal metastases: no longer bystanders. ***Cancer Microenviron,*** **4, 237-46.**

PASQUET, M., GOLZIO, M., MERY, E., RAFII, A., BENABBOU, N., MIRSHAHI, P., HENNEBELLE, I., BOURIN, P., ALLAL, B., TEISSIE, J., MIRSHAHI, M. & COUDERC, B. 2010. Hospicells (ascites-derived stromal cells) promote tumorigenicity and angiogenesis. ***Int J Cancer,*** **126, 2090-101.**

PAUNESCU, V., BOJIN, F. M., TATU, C. A., GAVRILIUC, O. I., ROSCA, A., GRUIA, A. T., TANASIE, G., BUNU, C., CRISNIC, D., GHERGHICEANU, M., TATU, F. R., TATU, C. S. & VERMESAN, S. 2011. Tumour-associated fibroblasts and mesenchymal stem cells: more similarities than differences. ***J Cell Mol Med,*** **15, 635-46.**

PENG, Y., LI, Z. & LI, Z. 2013. GRP78 secreted by tumor cells stimulates differentiation of bone marrow mesenchymal stem cells to cancer-associated fibroblasts. ***Biochem Biophys Res Commun,*** **440, 558-63.**

PEREIRA, R. F., HALFORD, K. W., O'HARA, M. D., LEEPER, D. B., SOKOLOV, B. P., POLLARD, M. D., BAGASRA, O. & PROCKOP, D. J. 1995. Cultured adherent cells from marrow can serve as long-lasting precursor cells for bone, cartilage, and lung in irradiated mice. ***Proc Natl Acad Sci U S A,*** **92, 4857-61.**

PERL, A. K., WILGENBUS, P., DAHL, U., SEMB, H. & CHRISTOFORI, G. 1998. A causal role for E-cadherin in the transition from adenoma to carcinoma. ***Nature,*** **392, 190-3.**

PESSINA, A., BONOMI, A., COCCE, V., INVERNICI, G., NAVONE, S., CAVICCHINI, L., SISTO, F., FERRARI, M., VIGANO, L., LOCATELLI, A., CIUSANI, E., CAPPELLETTI, G., CARTELLI, D., ARNALDO, C., PARATI, E., MARFIA, G., PALLINI, R., FALCHETTI, M. L. & ALESSANDRI, G. 2011. Mesenchymal stromal cells primed with paclitaxel provide a new approach for cancer therapy. ***PLoS One,*** **6, e28321.**

PETIT, I., SZYPER-KRAVITZ, M., NAGLER, A., LAHAV, M., PELED, A., HABLER, L., PONOMARYOV, T., TAICHMAN, R. S., ARENZANA-SEISDEDOS, F., FUJII, N., SANDBANK, J., ZIPORI, D. & LAPIDOT, T. 2002. G-CSF induces stem cell mobilization by decreasing bone marrow SDF-1 and up-regulating CXCR4. ***Nat Immunol,*** **3, 687-94.**

PETRYLAK, D. P., TANGEN, C. M., HUSSAIN, M. H., LARA, P. N., JR., JONES, J. A., TAPLIN, M. E., BURCH, P. A., BERRY, D., MOINPOUR, C., KOHLI, M., BENSON, M. C., SMALL, E. J., RAGHAVAN, D. & CRAWFORD, E. D. 2004. Docetaxel and estramustine compared with mitoxantrone and prednisone for advanced refractory prostate cancer. ***N Engl J Med,*** **351, 1513-20.**

PEUNOVA, N. & ENIKOLOPOV, G. 1995. Nitric oxide triggers a switch to growth arrest during differentiation of neuronal cells. ***Nature,*** **375, 68-73.**

PIETRAS, K. & OSTMAN, A. 2010. Hallmarks of cancer: interactions with the tumor stroma. ***Exp Cell Res,*** **316, 1324-31.**

PIETRAS, K., OSTMAN, A., SJOQUIST, M., BUCHDUNGER, E., REED, R. K., HELDIN, C. H. & RUBIN, K. 2001. Inhibition of platelet-derived growth factor receptors reduces interstitial hypertension and increases transcapillary transport in tumors. ***Cancer Res,*** **61, 2929-34.**

PIETRAS, K., RUBIN, K., SJOBLOM, T., BUCHDUNGER, E., SJOQUIST, M., HELDIN, C. H. & OSTMAN, A. 2002. Inhibition of PDGF receptor signaling in tumor stroma enhances antitumor effect of chemotherapy. ***Cancer Res,*** **62, 5476-84.**

PITTENGER, M. F., MACKAY, A. M., BECK, S. C., JAISWAL, R. K., DOUGLAS, R., MOSCA, J. D., MOORMAN, M. A., SIMONETTI, D. W., CRAIG, S. & MARSHAK, D. R. 1999. Multilineage potential of adult human mesenchymal stem cells. ***Science,*** **284, 143-7.**

PLUMAS, J., CHAPEROT, L., RICHARD, M. J., MOLENS, J. P., BENSA, J. C. & FAVROT, M. C. 2005. Mesenchymal stem cells induce apoptosis of activated T cells. ***Leukemia,*** **19, 1597-604.**

POLLARD, J. W. 2004. Tumour-educated macrophages promote tumour progression and metastasis. ***Nat Rev Cancer,*** **4, 71-8.**

PONTE, A. L., MARAIS, E., GALLAY, N., LANGONNE, A., DELORME, B., HERAULT, O., CHARBORD, P. & DOMENECH, J. 2007. The in vitro migration capacity of human bone marrow mesenchymal stem cells: comparison of chemokine and growth factor chemotactic activities. ***Stem Cells,*** **25, 1737-45.**

PRANTL, L., MUEHLBERG, F., NAVONE, N. M., SONG, Y. H., VYKOUKAL, J., LOGOTHETIS, C. J. & ALT, E. U. 2010. Adipose tissue-derived stem cells promote prostate tumor growth. ***Prostate,*** **70, 1709-15.**

QIAO, L., XU, Z., ZHAO, T., ZHAO, Z., SHI, M., ZHAO, R. C., YE, L. & ZHANG, X. 2008. Suppression of tumorigenesis by human mesenchymal stem cells in a hepatoma model. ***Cell Res,*** **18, 500-7.**

QUARTO, N. & LONGAKER, M. T. 2006. FGF-2 inhibits osteogenesis in mouse adipose tissue-derived stromal cells and sustains their proliferative and osteogenic potential state. ***Tissue Eng,*** **12, 1405-18.**

RAFII, A., MIRSHAHI, P., POUPOT, M., FAUSSAT, A. M., SIMON, A., DUCROS, E., MERY, E., COUDERC, B., LIS, R., CAPDET, J., BERGALET, J., QUERLEU, D., DAGONNET, F., FOURNIE, J. J., MARIE, J. P., PUJADE-LAURAINE, E., FAVRE, G., SORIA, J. & MIRSHAHI, M. 2008. Oncologic trogocytosis of an original stromal cells induces chemoresistance of ovarian tumours. ***PLoS One,*** **3, e3894.**

RAGGATT, L. J. & PARTRIDGE, N. C. 2010. Cellular and molecular mechanisms of bone remodeling. ***J Biol Chem,*** **285, 25103-8.**

RAJANTIE, I., ILMONEN, M., ALMINAITE, A., OZERDEM, U., ALITALO, K. & SALVEN, P. 2004. Adult bone marrow-derived cells recruited during angiogenesis comprise precursors for periendothelial vascular mural cells. ***Blood,*** **104, 2084-6.**

RAMANKULOV, A., LEIN, M., KRISTIANSEN, G., LOENING, S. A. & JUNG, K. 2007. Plasma osteopontin in comparison with bone markers as indicator of bone metastasis and survival outcome in patients with prostate cancer. ***Prostate,*** **67, 330-40.**

REAGAN, M. R., MISHIMA, Y., GLAVEY, S. V., ZHANG, Y., MANIER, S., LU, Z. N., MEMARZADEH, M., ZHANG, Y., SACCO, A., ALJAWAI, Y., SHI, J., TAI, Y. T., READY, J. E., KAPLAN, D. L., ROCCARO, A. M. & GHOBRIAL, I. M. 2014. Investigating osteogenic differentiation in multiple myeloma using a novel 3D bone marrow niche model. ***Blood,*** **124, 3250-9.**

REILAND, J., FURCHT, L. T. & MCCARTHY, J. B. 1999. CXC-chemokines stimulate invasion and chemotaxis in prostate carcinoma cells through the CXCR2 receptor. ***Prostate,*** **41, 78-88.**

REINHOLT, F. P., HULTENBY, K., OLDBERG, A. & HEINEGARD, D. 1990. Osteopontin--a possible anchor of osteoclasts to bone. ***Proc Natl Acad Sci U S A,*** **87, 4473-5.**

REN, G., LIU, Y., ZHAO, X., ZHANG, J., ZHENG, B., YUAN, Z. R., ZHANG, L., QU, X., TISCHFIELD, J. A., SHAO, C. & SHI, Y. 2014. Tumor resident mesenchymal stromal cells endow naive stromal cells with tumor-promoting properties. ***Oncogene,*** **33, 4016-20.**

REN, G., ZHANG, L., ZHAO, X., XU, G., ZHANG, Y., ROBERTS, A. I., ZHAO, R. C. & SHI, Y. 2008. Mesenchymal stem cell-mediated immunosuppression occurs via concerted action of chemokines and nitric oxide. ***Cell Stem Cell,*** **2, 141-50.**

RINGE, J., STRASSBURG, S., NEUMANN, K., ENDRES, M., NOTTER, M., BURMESTER, G. R., KAPS, C. & SITTINGER, M. 2007. Towards in situ tissue repair: human mesenchymal stem cells express chemokine receptors CXCR1, CXCR2 and CCR2, and migrate upon stimulation with CXCL8 but not CCL2. ***J Cell Biochem,*** **101, 135-46.**

ROMANOV, V. I. & GOLIGORSKY, M. S. 1999. RGD-recognizing integrins mediate interactions of human prostate carcinoma cells with endothelial cells in vitro. ***Prostate,*** **39, 108-18.**

ROODHART, J. M., DAENEN, L. G., STIGTER, E. C., PRINS, H. J., GERRITS, J., HOUTHUIJZEN, J. M., GERRITSEN, M. G., SCHIPPER, H. S., BACKER, M. J., VAN AMERSFOORT, M., VERMAAT, J. S., MOERER, P., ISHIHARA, K., KALKHOVEN, E., BEIJNEN, J. H., DERKSEN, P. W., MEDEMA, R. H., MARTENS, A. C., BRENKMAN, A. B. & VOEST, E. E. 2011. Mesenchymal stem cells induce resistance to chemotherapy through the release of platinum-induced fatty acids. *Cancer Cell,* 20, 370-83.

ROSS, F. P., CHAPPEL, J., ALVAREZ, J. I., SANDER, D., BUTLER, W. T., FARACH-CARSON, M. C., MINTZ, K. A., ROBEY, P. G., TEITELBAUM, S. L. & CHERESH, D. A. 1993. Interactions between the bone matrix proteins osteopontin and bone sialoprotein and the osteoclast integrin alpha v beta 3 potentiate bone resorption. *J Biol Chem,* 268, 9901-7.

RUSTAD, K. C. & GURTNER, G. C. 2012. Mesenchymal Stem Cells Home to Sites of Injury and Inflammation. *Adv Wound Care (New Rochelle),* 1, 147-152.

RYAN, J. M., BARRY, F. P., MURPHY, J. M. & MAHON, B. P. 2005. Mesenchymal stem cells avoid allogeneic rejection. *J Inflamm (Lond),* 2, 8.

SAAD, F., GLEASON, D. M., MURRAY, R., TCHEKMEDYIAN, S., VENNER, P., LACOMBE, L., CHIN, J. L., VINHOLES, J. J., GOAS, J. A., CHEN, B. & ZOLEDRONIC ACID PROSTATE CANCER STUDY, G. 2002. A randomized, placebo-controlled trial of zoledronic acid in patients with hormone-refractory metastatic prostate carcinoma. *J Natl Cancer Inst,* 94, 1458-68.

SADAT, S., GEHMERT, S., SONG, Y. H., YEN, Y., BAI, X., GAISER, S., KLEIN, H. & ALT, E. 2007. The cardioprotective effect of mesenchymal stem cells is mediated by IGF-I and VEGF. *Biochem Biophys Res Commun,* 363, 674-9.

SALCEDO, R., PONCE, M. L., YOUNG, H. A., WASSERMAN, K., WARD, J. M., KLEINMAN, H. K., OPPENHEIM, J. J. & MURPHY, W. J. 2000. Human endothelial cells express CCR2 and respond to MCP-1: direct role of MCP-1 in angiogenesis and tumor progression. *Blood,* 96, 34-40.

SASPORTAS, L. S., KASMIEH, R., WAKIMOTO, H., HINGTGEN, S., VAN DE WATER, J. A., MOHAPATRA, G., FIGUEIREDO, J. L., MARTUZA, R. L., WEISSLEDER, R. & SHAH, K. 2009. Assessment of therapeutic efficacy and fate of engineered human mesenchymal stem cells for cancer therapy. *Proc Natl Acad Sci U S A,* 106, 4822-7.

SATO, K., OZAKI, K., OH, I., MEGURO, A., HATANAKA, K., NAGAI, T., MUROI, K. & OZAWA, K. 2007. Nitric oxide plays a critical role in suppression of T-cell proliferation by mesenchymal stem cells. *Blood,* 109, 228-34.

SATO, T., SAKAI, T., NOGUCHI, Y., TAKITA, M., HIRAKAWA, S. & ITO, A. 2004. Tumor-stromal cell contact promotes invasion of human uterine cervical carcinoma cells by augmenting the expression and activation of stromal matrix metalloproteinases. *Gynecol Oncol,* 92, 47-56.

SATO, Y., ARAKI, H., KATO, J., NAKAMURA, K., KAWANO, Y., KOBUNE, M., SATO, T., MIYANISHI, K., TAKAYAMA, T., TAKAHASHI, M., TAKIMOTO, R., IYAMA, S., MATSUNAGA, T., OHTANI, S., MATSUURA, A., HAMADA, H. & NIITSU, Y. 2005. Human mesenchymal stem cells xenografted directly to rat liver are differentiated into human hepatocytes without fusion. *Blood,* 106, 756-63.

SCHRAUFSTATTER, I. U., CHUNG, J. & BURGER, M. 2001. IL-8 activates endothelial cell CXCR1 and CXCR2 through Rho and Rac signaling pathways. *Am J Physiol Lung Cell Mol Physiol,* 280, L1094-103.

SCHRODER, F. H., HUGOSSON, J., ROOBOL, M. J., TAMMELA, T. L., CIATTO, S., NELEN, V., KWIATKOWSKI, M., LUJAN, M., LILJA, H., ZAPPA, M., DENIS, L. J., RECKER, F., PAEZ, A., MAATTANEN, L., BANGMA, C. H., AUS, G., CARLSSON, S., VILLERS, A., REBILLARD, X., VAN DER KWAST, T., KUJALA, P. M., BLIJENBERG, B. G., STENMAN, U. H., HUBER, A., TAARI, K., HAKAMA, M., MOSS, S. M., DE KONING, H. J., AUVINEN,

A. & INVESTIGATORS, E. 2012. Prostate-cancer mortality at 11 years of follow-up. *N Engl J Med,* 366, 981-90.

SCOTT, R. E., FLORINE, D. L., WILLE, J. J., JR. & YUN, K. 1982. Coupling of growth arrest and differentiation at a distinct state in the G1 phase of the cell cycle: GD. *Proc Natl Acad Sci U S A,* 79, 845-9.

SERBINA, N. V. & PAMER, E. G. 2006. Monocyte emigration from bone marrow during bacterial infection requires signals mediated by chemokine receptor CCR2. *Nat Immunol,* 7, 311-7.

SHANGGUAN, L., TI, X., KRAUSE, U., HAI, B., ZHAO, Y., YANG, Z. & LIU, F. 2012. Inhibition of TGF-beta/Smad signaling by BAMBI blocks differentiation of human mesenchymal stem cells to carcinoma-associated fibroblasts and abolishes their protumor effects. *Stem Cells,* 30, 2810-9.

SHARON, Y., RAZ, Y., COHEN, N., BEN-SHMUEL, A., SCHWARTZ, H., GEIGER, T. & EREZ, N. 2015. Tumor-derived osteopontin reprograms normal mammary fibroblasts to promote inflammation and tumor growth in breast cancer. *Cancer Res,* 75, 963-73.

SHI, M., LI, J., LIAO, L., CHEN, B., LI, B., CHEN, L., JIA, H. & ZHAO, R. C. 2007. Regulation of CXCR4 expression in human mesenchymal stem cells by cytokine treatment: role in homing efficiency in NOD/SCID mice. *Haematologica,* 92, 897-904.

SHIBUYA, M. 2011. Involvement of Flt-1 (VEGF receptor-1) in cancer and preeclampsia. *Proc Jpn Acad Ser B Phys Biol Sci,* 87, 167-78.

SHINAGAWA, K., KITADAI, Y., TANAKA, M., SUMIDA, T., KODAMA, M., HIGASHI, Y., TANAKA, S., YASUI, W. & CHAYAMA, K. 2010. Mesenchymal stem cells enhance growth and metastasis of colon cancer. *Int J Cancer,* 127, 2323-33.

SICA, A., SACCANI, A. & MANTOVANI, A. 2002. Tumor-associated macrophages: a molecular perspective. *Int Immunopharmacol,* 2, 1045-54.

SICA, A., SCHIOPPA, T., MANTOVANI, A. & ALLAVENA, P. 2006. Tumour-associated macrophages are a distinct M2 polarised population promoting tumour progression: potential targets of anti-cancer therapy. *Eur J Cancer,* 42, 717-27.

SIEGEL, R. L., MILLER, K. D. & JEMAL, A. 2015. Cancer statistics, 2015. *CA Cancer J Clin,* 65, 5-29.

SINGH, S., SINGH, U. P., GRIZZLE, W. E. & LILLARD, J. W., JR. 2004. CXCL12-CXCR4 interactions modulate prostate cancer cell migration, metalloproteinase expression and invasion. *Lab Invest,* 84, 1666-76.

SKOLEKOVA, S., MATUSKOVA, M., BOHAC, M., TORO, L., DEMKOVA, L., GURSKY, J. & KUCEROVA, L. 2016. Cisplatin-induced mesenchymal stromal cells-mediated mechanism contributing to decreased antitumor effect in breast cancer cells. *Cell Commun Signal,* 14, 4.

SOLINAS, G., GERMANO, G., MANTOVANI, A. & ALLAVENA, P. 2009. Tumor-associated macrophages (TAM) as major players of the cancer-related inflammation. *J Leukoc Biol,* 86, 1065-73.

SORDI, V., MALOSIO, M. L., MARCHESI, F., MERCALLI, A., MELZI, R., GIORDANO, T., BELMONTE, N., FERRARI, G., LEONE, B. E., BERTUZZI, F., ZERBINI, G., ALLAVENA, P., BONIFACIO, E. & PIEMONTI, L. 2005. Bone marrow mesenchymal stem cells express a restricted set of functionally active chemokine receptors capable of promoting migration to pancreatic islets. *Blood,* 106, 419-27.

SOZZANI, S., MOLINO, M., LOCATI, M., LUINI, W., CERLETTI, C., VECCHI, A. & MANTOVANI, A. 1993. Receptor-activated calcium influx in human monocytes exposed to monocyte chemotactic protein-1 and related cytokines. *J Immunol,* 150, 1544-53.

SPAETH, E. L., DEMBINSKI, J. L., SASSER, A. K., WATSON, K., KLOPP, A., HALL, B., ANDREEFF, M. & MARINI, F. 2009. Mesenchymal stem cell transition to tumor-associated fibroblasts contributes to fibrovascular network expansion and tumor progression. *PLoS One,* 4, e4992.

STEEG, P. S. 2005. Cancer biology: emissaries set up new sites. ***Nature,*** **438, 750-1.**

STERNLICHT, M. D., LOCHTER, A., SYMPSON, C. J., HUEY, B., ROUGIER, J. P., GRAY, J. W., PINKEL, D., BISSELL, M. J. & WERB, Z. 1999. The stromal proteinase MMP3/stromelysin-1 promotes mammary carcinogenesis. ***Cell,*** **98, 137-46.**

STICH, S., HAAG, M., HAUPL, T., SEZER, O., NOTTER, M., KAPS, C., SITTINGER, M. & RINGE, J. 2009. Gene expression profiling of human mesenchymal stem cells chemotactically induced with CXCL12. ***Cell Tissue Res,*** **336, 225-36.**

STRAUSSMAN, R., MORIKAWA, T., SHEE, K., BARZILY-ROKNI, M., QIAN, Z. R., DU, J., DAVIS, A., MONGARE, M. M., GOULD, J., FREDERICK, D. T., COOPER, Z. A., CHAPMAN, P. B., SOLIT, D. B., RIBAS, A., LO, R. S., FLAHERTY, K. T., OGINO, S., WARGO, J. A. & GOLUB, T. R. 2012. Tumour micro-environment elicits innate resistance to RAF inhibitors through HGF secretion. ***Nature,*** **487, 500-4.**

SUBRAMANIAM, K. S., THAM, S. T., MOHAMED, Z., WOO, Y. L., MAT ADENAN, N. A. & CHUNG, I. 2013. Cancer-associated fibroblasts promote proliferation of endometrial cancer cells. ***PLoS One,*** **8, e68923.**

SUDA, T., TAKAHASHI, N., UDAGAWA, N., JIMI, E., GILLESPIE, M. T. & MARTIN, T. J. 1999. Modulation of osteoclast differentiation and function by the new members of the tumor necrosis factor receptor and ligand families. ***Endocr Rev,*** **20, 345-57.**

SUGIHARA, H., ISHIMOTO, T., YASUDA, T., IZUMI, D., ETO, K., SAWAYAMA, H., MIYAKE, K., KURASHIGE, J., IMAMURA, Y., HIYOSHI, Y., IWATSUKI, M., IWAGAMI, S., BABA, Y., SAKAMOTO, Y., MIYAMOTO, Y., YOSHIDA, N., WATANABE, M., TAKAMORI, H. & BABA, H. 2015. Cancer-associated fibroblast-derived CXCL12 causes tumor progression in adenocarcinoma of the esophagogastric junction. ***Med Oncol,*** **32, 618.**

SUGIMOTO, H., MUNDEL, T. M., KIERAN, M. W. & KALLURI, R. 2006. Identification of fibroblast heterogeneity in the tumor microenvironment. ***Cancer Biol Ther,*** **5, 1640-6.**

SUN, B., ROH, K. H., PARK, J. R., LEE, S. R., PARK, S. B., JUNG, J. W., KANG, S. K., LEE, Y. S. & KANG, K. S. 2009. Therapeutic potential of mesenchymal stromal cells in a mouse breast cancer metastasis model. ***Cytotherapy,*** **11, 289-98, 1 p following 298.**

SUN, Y. X., WANG, J., SHELBURNE, C. E., LOPATIN, D. E., CHINNAIYAN, A. M., RUBIN, M. A., PIENTA, K. J. & TAICHMAN, R. S. 2003. Expression of CXCR4 and CXCL12 (SDF-1) in human prostate cancers (PCa) in vivo. ***J Cell Biochem,*** **89, 462-73.**

SUNG, S. Y., HSIEH, C. L., LAW, A., ZHAU, H. E., PATHAK, S., MULTANI, A. S., LIM, S., COLEMAN, I. M., WU, L. C., FIGG, W. D., DAHUT, W. L., NELSON, P., LEE, J. K., AMIN, M. B., LYLES, R., JOHNSTONE, P. A., MARSHALL, F. F. & CHUNG, L. W. 2008. Coevolution of prostate cancer and bone stroma in three-dimensional coculture: implications for cancer growth and metastasis. ***Cancer Res,*** **68, 9996-10003.**

SUZUKI, K., SUN, R., ORIGUCHI, M., KANEHIRA, M., TAKAHATA, T., ITOH, J., UMEZAWA, A., KIJIMA, H., FUKUDA, S. & SAIJO, Y. 2011. Mesenchymal stromal cells promote tumor growth through the enhancement of neovascularization. ***Mol Med,*** **17, 579-87.**

TAICHMAN, R. S., COOPER, C., KELLER, E. T., PIENTA, K. J., TAICHMAN, N. S. & MCCAULEY, L. K. 2002. Use of the stromal cell-derived factor-1/CXCR4 pathway in prostate cancer metastasis to bone. ***Cancer Res,*** **62, 1832-7.**

TAKEICHI, M. 1991. Cadherin cell adhesion receptors as a morphogenetic regulator. ***Science,*** **251, 1451-5.**

TANG, D. G., CHEN, Y. Q., NEWMAN, P. J., SHI, L., GAO, X., DIGLIO, C. A. & HONN, K. V. 1993. Identification of PECAM-1 in solid tumor cells and its potential involvement in tumor cell adhesion to endothelium. ***J Biol Chem,*** **268, 22883-94.**

TANG, Y. L., ZHAO, Q., ZHANG, Y. C., CHENG, L., LIU, M., SHI, J., YANG, Y. Z., PAN, C., GE, J. & PHILLIPS, M. I. 2004. Autologous mesenchymal stem cell transplantation induce VEGF and neovascularization in ischemic myocardium. *Regul Pept,* 117, 3-10.

TANNOCK, I. F., DE WIT, R., BERRY, W. R., HORTI, J., PLUZANSKA, A., CHI, K. N., OUDARD, S., THEODORE, C., JAMES, N. D., TURESSON, I., ROSENTHAL, M. A., EISENBERGER, M. A. & INVESTIGATORS, T. A. X. 2004. Docetaxel plus prednisone or mitoxantrone plus prednisone for advanced prostate cancer. *N Engl J Med,* 351, 1502-12.

TAYLOR, S. T., HICKMAN, J. A. & DIVE, C. 2000. Epigenetic determinants of resistance to etoposide regulation of Bcl-X(L) and Bax by tumor microenvironmental factors. *J Natl Cancer Inst,* 92, 18-23.

THALMANN, G. N., SIKES, R. A., DEVOLL, R. E., KIEFER, J. A., MARKWALDER, R., KLIMA, I., FARACH-CARSON, C. M., STUDER, U. E. & CHUNG, L. W. 1999. Osteopontin: possible role in prostate cancer progression. *Clin Cancer Res,* 5, 2271-7.

THOMAS, X., ANGLARET, B., MAGAUD, J. P., EPSTEIN, J. & ARCHIMBAUD, E. 1998. Interdependence between cytokines and cell adhesion molecules to induce interleukin-6 production by stromal cells in myeloma. *Leuk Lymphoma,* 32, 107-19.

THUDI, N. K., MARTIN, C. K., MURAHARI, S., SHU, S. T., LANIGAN, L. G., WERBECK, J. L., KELLER, E. T., MCCAULEY, L. K., PINZONE, J. J. & ROSOL, T. J. 2011. Dickkopf-1 (DKK-1) stimulated prostate cancer growth and metastasis and inhibited bone formation in osteoblastic bone metastases. *Prostate,* 71, 615-25.

TILLI, T. M., MELLO, K. D., FERREIRA, L. B., MATOS, A. R., ACCIOLY, M. T., FARIA, P. A., BELLAHCENE, A., CASTRONOVO, V. & GIMBA, E. R. 2012. Both osteopontin-c and osteopontin-b splicing isoforms exert pro-tumorigenic roles in prostate cancer cells. *Prostate,* 72, 1688-99.

TOMASEK, J. J., GABBIANI, G., HINZ, B., CHAPONNIER, C. & BROWN, R. A. 2002. Myofibroblasts and mechano-regulation of connective tissue remodelling. *Nat Rev Mol Cell Biol,* 3, 349-63.

TOMIDA, A. & TSURUO, T. 1999. Drug resistance mediated by cellular stress response to the microenvironment of solid tumors. *Anticancer Drug Des,* 14, 169-77.

TSUTSUMI, S., SHIMAZU, A., MIYAZAKI, K., PAN, H., KOIKE, C., YOSHIDA, E., TAKAGISHI, K. & KATO, Y. 2001. Retention of multilineage differentiation potential of mesenchymal cells during proliferation in response to FGF. *Biochem Biophys Res Commun,* 288, 413-9.

TYAN, S. W., KUO, W. H., HUANG, C. K., PAN, C. C., SHEW, J. Y., CHANG, K. J., LEE, E. Y. & LEE, W. H. 2011. Breast cancer cells induce cancer-associated fibroblasts to secrete hepatocyte growth factor to enhance breast tumorigenesis. *PLoS One,* 6, e15313.

VANDERKERKEN, K., VANDE BROEK, I., EIZIRIK, D. L., VAN VALCKENBORGH, E., ASOSINGH, K., VAN RIET, I. & VAN CAMP, B. 2002. Monocyte chemoattractant protein-1 (MCP-1), secreted by bone marrow endothelial cells, induces chemoattraction of 5T multiple myeloma cells. *Clin Exp Metastasis,* 19, 87-90.

VASSALLI, J. D., SAPPINO, A. P. & BELIN, D. 1991. The plasminogen activator/plasmin system. *J Clin Invest,* 88, 1067-72.

VERWEIJ, J., CLAVEL, M. & CHEVALIER, B. 1994. Paclitaxel (Taxol) and docetaxel (Taxotere): not simply two of a kind. *Ann Oncol,* 5, 495-505.

VON LUTTICHAU, I., NOTOHAMIPRODJO, M., WECHSELBERGER, A., PETERS, C., HENGER, A., SELIGER, C., DJAFARZADEH, R., HUSS, R. & NELSON, P. J. 2005. Human adult CD34-progenitor cells functionally express the chemokine receptors CCR1, CCR4, CCR7, CXCR5, and CCR10 but not CXCR4. *Stem Cells Dev,* 14, 329-36.

WAGNER, W., HORN, P., CASTOLDI, M., DIEHLMANN, A., BORK, S., SAFFRICH, R., BENES, V., BLAKE, J., PFISTER, S., ECKSTEIN, V. & HO, A. D. 2008. Replicative senescence of mesenchymal stem cells: a continuous and organized process. *PLoS One,* 3, e2213.

WAGNER, W., WEIN, F., SECKINGER, A., FRANKHAUSER, M., WIRKNER, U., KRAUSE, U., BLAKE, J., SCHWAGER, C., ECKSTEIN, V., ANSORGE, W. & HO, A. D. 2005. Comparative characteristics of mesenchymal stem cells from human bone marrow, adipose tissue, and umbilical cord blood. *Exp Hematol,* 33, 1402-16.

WAKITANI, S., SAITO, T. & CAPLAN, A. I. 1995. Myogenic cells derived from rat bone marrow mesenchymal stem cells exposed to 5-azacytidine. *Muscle Nerve,* 18, 1417-26.

WANG, L., LI, Y., CHEN, X., CHEN, J., GAUTAM, S. C., XU, Y. & CHOPP, M. 2002. MCP-1, MIP-1, IL-8 and ischemic cerebral tissue enhance human bone marrow stromal cell migration in interface culture. *Hematology,* 7, 113-7.

WANG, W., LI, Q., YAMADA, T., MATSUMOTO, K., MATSUMOTO, I., ODA, M., WATANABE, G., KAYANO, Y., NISHIOKA, Y., SONE, S. & YANO, S. 2009. Crosstalk to stromal fibroblasts induces resistance of lung cancer to epidermal growth factor receptor tyrosine kinase inhibitors. *Clin Cancer Res,* 15, 6630-8.

WATERMAN, R. S., HENKLE, S. L. & BETANCOURT, A. M. 2012. Mesenchymal stem cell 1 (MSC1)-based therapy attenuates tumor growth whereas MSC2-treatment promotes tumor growth and metastasis. *PLoS One,* 7, e45590.

WATERMAN, R. S., TOMCHUCK, S. L., HENKLE, S. L. & BETANCOURT, A. M. 2010. A new mesenchymal stem cell (MSC) paradigm: polarization into a pro-inflammatory MSC1 or an Immunosuppressive MSC2 phenotype. *PLoS One,* 5, e10088.

WEBER, C. E., KOTHARI, A. N., WAI, P. Y., LI, N. Y., DRIVER, J., ZAPF, M. A., FRANZEN, C. A., GUPTA, G. N., OSIPO, C., ZLOBIN, A., SYN, W. K., ZHANG, J., KUO, P. C. & MI, Z. 2015. Osteopontin mediates an MZF1-TGF-beta1-dependent transformation of mesenchymal stem cells into cancer-associated fibroblasts in breast cancer. *Oncogene,* 34, 4821-33.

WU, G. D., NOLTA, J. A., JIN, Y. S., BARR, M. L., YU, H., STARNES, V. A. & CRAMER, D. V. 2003. Migration of mesenchymal stem cells to heart allografts during chronic rejection. *Transplantation,* 75, 679-85.

WU, K. J., ZENG, J., ZHU, G. D., ZHANG, L. L., ZHANG, D., LI, L., FAN, J. H., WANG, X. Y. & HE, D. L. 2009. Silibinin inhibits prostate cancer invasion, motility and migration by suppressing vimentin and MMP-2 expression. *Acta Pharmacol Sin,* 30, 1162-8.

WU, X., HU, J., ZHOU, L. F., MAO, Y., YANG, B., GAO, L., XIE, R., XU, F., ZHANG, D., LIU, J. & ZHU, J. H. 2008. In vivo tracking of superparamagnetic iron oxide nanoparticle-labeled mesenchymal stem cell tropism to malignant gliomas using magnetic resonance imaging. *Journal of Neurosurgery,* 108, 320-329.

WU, Y., CHEN, L., SCOTT, P. G. & TREDGET, E. E. 2007. Mesenchymal stem cells enhance wound healing through differentiation and angiogenesis. *Stem Cells,* 25, 2648-59.

WYNN, R. F., HART, C. A., CORRADI-PERINI, C., O'NEILL, L., EVANS, C. A., WRAITH, J. E., FAIRBAIRN, L. J. & BELLANTUONO, I. 2004. A small proportion of mesenchymal stem cells strongly expresses functionally active CXCR4 receptor capable of promoting migration to bone marrow. *Blood,* 104, 2643-5.

XIA, B., TIAN, C., GUO, S., ZHANG, L., ZHAO, D., QU, F., ZHAO, W., WANG, Y., WU, X., DA, W., WEI, S. & ZHANG, Y. 2015. c-Myc plays part in drug resistance mediated by bone marrow stromal cells in acute myeloid leukemia. *Leuk Res,* 39, 92-9.

XU, F., SHI, J., YU, B., NI, W., WU, X. & GU, Z. 2010. Chemokines mediate mesenchymal stem cell migration toward gliomas in vitro. *Oncol Rep,* 23, 1561-7.

XU, W. T., BIAN, Z. Y., FAN, Q. M., LI, G. & TANG, T. T. 2009. Human mesenchymal stem cells (hMSCs) target osteosarcoma and promote its growth and pulmonary metastasis. *Cancer Lett,* 281, 32-41.

XU, Y., TABE, Y., JIN, L., WATT, J., MCQUEEN, T., OHSAKA, A., ANDREEFF, M. & KONOPLEVA, M. 2008. TGF-beta receptor kinase inhibitor LY2109761 reverses the anti-apoptotic

effects of TGF-beta1 in myelo-monocytic leukaemic cells co-cultured with stromal cells. *Br J Haematol,* 142, 192-201.

XUE, Z., WU, X., CHEN, X., LIU, Y., WANG, X., WU, K., NIE, Y. & FAN, D. 2015. Mesenchymal stem cells promote epithelial to mesenchymal transition and metastasis in gastric cancer though paracrine cues and close physical contact. *J Cell Biochem,* 116, 618-27.

YAMAGUCHI, J., KUSANO, K. F., MASUO, O., KAWAMOTO, A., SILVER, M., MURASAWA, S., BOSCH-MARCE, M., MASUDA, H., LOSORDO, D. W., ISNER, J. M. & ASAHARA, T. 2003. Stromal cell-derived factor-1 effects on ex vivo expanded endothelial progenitor cell recruitment for ischemic neovascularization. *Circulation,* 107, 1322-8.

YAMATE, T., MOCHARLA, H., TAGUCHI, Y., IGIETSEME, J. U., MANOLAGAS, S. C. & ABE, E. 1997. Osteopontin expression by osteoclast and osteoblast progenitors in the murine bone marrow: demonstration of its requirement for osteoclastogenesis and its increase after ovariectomy. *Endocrinology,* 138, 3047-55.

YANG, F., STRAND, D. W. & ROWLEY, D. R. 2008. Fibroblast growth factor-2 mediates transforming growth factor-beta action in prostate cancer reactive stroma. *Oncogene,* 27, 450-9.

YE, H., CHENG, J., TANG, Y., LIU, Z., XU, C., LIU, Y. & SUN, Y. 2012. Human bone marrow-derived mesenchymal stem cells produced TGFbeta contributes to progression and metastasis of prostate cancer. *Cancer Invest,* 30, 513-8.

YIN, J. J., MOHAMMAD, K. S., KAKONEN, S. M., HARRIS, S., WU-WONG, J. R., WESSALE, J. L., PADLEY, R. J., GARRETT, I. R., CHIRGWIN, J. M. & GUISE, T. A. 2003. A causal role for endothelin-1 in the pathogenesis of osteoblastic bone metastases. *Proc Natl Acad Sci U S A,* 100, 10954-9.

YOKOSAKI, Y., MATSUURA, N., SASAKI, T., MURAKAMI, I., SCHNEIDER, H., HIGASHIYAMA, S., SAITOH, Y., YAMAKIDO, M., TAOOKA, Y. & SHEPPARD, D. 1999. The integrin alpha(9)beta(1) binds to a novel recognition sequence (SVVYGLR) in the thrombin-cleaved amino-terminal fragment of osteopontin. *J Biol Chem,* 274, 36328-34.

YOUNG, M. R. & WRIGHT, M. A. 1992. Myelopoiesis-associated immune suppressor cells in mice bearing metastatic Lewis lung carcinoma tumors: gamma interferon plus tumor necrosis factor alpha synergistically reduces immune suppressor and tumor growth-promoting activities of bone marrow cells and diminishes tumor recurrence and metastasis. *Cancer Res,* 52, 6335-40.

YOUNGS, S. J., ALI, S. A., TAUB, D. D. & REES, R. C. 1997. Chemokines induce migrational responses in human breast carcinoma cell lines. *Int J Cancer,* 71, 257-66.

YUAN, L., INOUE, S., SAITO, Y. & NAKAJIMA, O. 1993. An evaluation of the effects of cytokines on intracellular oxidative production in normal neutrophils by flow cytometry. *Exp Cell Res,* 209, 375-81.

ZARRILLI, R., PIGNATA, S., APICELLA, A., DI POPOLO, A., MEMOLI, A., RICCHI, P., SALZANO, S. & ACQUAVIVA, A. M. 1999. Cell cycle block at G1-S or G2-M phase correlates with differentiation of Caco-2 cells: effect of constitutive insulin-like growth factor II expression. *Gastroenterology,* 116, 1358-66.

ZDZISINSKA, B., BOJARSKA-JUNAK, A., DMOSZYNSKA, A. & KANDEFER-SZERSZEN, M. 2008. Abnormal cytokine production by bone marrow stromal cells of multiple myeloma patients in response to RPMI8226 myeloma cells. *Arch Immunol Ther Exp (Warsz),* 56, 207-21.

ZEISBERG, E. M., POTENTA, S., XIE, L., ZEISBERG, M. & KALLURI, R. 2007. Discovery of endothelial to mesenchymal transition as a source for carcinoma-associated fibroblasts. *Cancer Res,* 67, 10123-8.

ZENG, Z., SHI, Y. X., SAMUDIO, I. J., WANG, R. Y., LING, X., FROLOVA, O., LEVIS, M., RUBIN, J. B., NEGRIN, R. R., ESTEY, E. H., KONOPLEV, S., ANDREEFF, M. & KONOPLEVA, M.

2009. Targeting the leukemia microenvironment by CXCR4 inhibition overcomes resistance to kinase inhibitors and chemotherapy in AML. *Blood,* 113, 6215-24.

ZHANG, C., ZHAI, W., XIE, Y., CHEN, Q., ZHU, W. & SUN, X. 2013a. Mesenchymal stem cells derived from breast cancer tissue promote the proliferation and migration of the MCF-7 cell line. *Oncol Lett,* 6, 1577-1582.

ZHANG, F., TSAI, S., KATO, K., YAMANOUCHI, D., WANG, C., RAFII, S., LIU, B. & KENT, K. C. 2009. Transforming growth factor-beta promotes recruitment of bone marrow cells and bone marrow-derived mesenchymal stem cells through stimulation of MCP-1 production in vascular smooth muscle cells. *J Biol Chem,* 284, 17564-74.

ZHANG, J., PATEL, L. & PIENTA, K. J. 2010. CC chemokine ligand 2 (CCL2) promotes prostate cancer tumorigenesis and metastasis. *Cytokine Growth Factor Rev,* 21, 41-8.

ZHANG, W., GE, W., LI, C., YOU, S., LIAO, L., HAN, Q., DENG, W. & ZHAO, R. C. 2004. Effects of mesenchymal stem cells on differentiation, maturation, and function of human monocyte-derived dendritic cells. *Stem Cells Dev,* 13, 263-71.

ZHANG, X. H., JIN, X., MALLADI, S., ZOU, Y., WEN, Y. H., BROGI, E., SMID, M., FOEKENS, J. A. & MASSAGUE, J. 2013b. Selection of bone metastasis seeds by mesenchymal signals in the primary tumor stroma. *Cell,* 154, 1060-73.

ZHANG, Y., FUJITA, N., OH-HARA, T., MORINAGA, Y., NAKAGAWA, T., YAMADA, M. & TSURUO, T. 1998. Production of interleukin-11 in bone-derived endothelial cells and its role in the formation of osteolytic bone metastasis. *Oncogene,* 16, 693-703.

ZHENG, D. Q., WOODARD, A. S., TALLINI, G. & LANGUINO, L. R. 2000. Substrate specificity of alpha(v)beta(3) integrin-mediated cell migration and phosphatidylinositol 3-kinase/AKT pathway activation. *J Biol Chem,* 275, 24565-74.

ZHU, H., ZHAO, J., ZHU, B., COLLAZO, J., GAL, J., SHI, P., LIU, L., STROM, A. L., LU, X., MCCANN, R. O., TOBOREK, M. & KYPRIANOU, N. 2012. EMMPRIN regulates cytoskeleton reorganization and cell adhesion in prostate cancer. *Prostate,* 72, 72-81.

ZHU, W., XU, W., JIANG, R., QIAN, H., CHEN, M., HU, J., CAO, W., HAN, C. & CHEN, Y. 2006. Mesenchymal stem cells derived from bone marrow favor tumor cell growth in vivo. *Exp Mol Pathol,* 80, 267-74.

Appendix A

Donor	Donor ID	Expression of CD73, CD105 and CD90	Expression of CD14. CD34, CD45 and HLA-DR	Capacity for Osteogenesis	Capacity for Adipogenesis	Capacity for Chodrogenesis
1	054	+	-	+	+	+
2	112	+	-	+	+	+
3	069	+	-	+	+	+
4	054	+	-	+	+	+

Appendix Table 1. MSC Donor Characterisation

List of Publications

Oral Presentations

1. Ridge S, Shaw G, Sullivan FJ, Giles FJ, Glynn SA. Meeting: Irish Association for Cancer Research, Limerick, Ireland. The Education of MSCs by Prostate Cancer Cell Line Conditioned Media. 25th - 26th February 2015.
2. Ridge S, Shaw G, Sullivan FJ, Giles FJ, Glynn SA. Meeting: Irish Society of urology Annual Meeting, Killarney, Ireland. Bone Marrow Derived-Mesenchymal Stem Cell Reprogramming by Prostate Cancer Cells to Promote Prostate Cancer Progression. 25th September 2014.

Abstracts Published in Conference Proceedings

1. Title: Bone Marrow Derived-Mesenchymal Stem Cell Reprogramming by Prostate Cancer Cells to Promote Prostate Cancer Progression. Authors: Ridge S; O'Leary K; Shaw G; Murphy M; Walsh K, Durkan G, Rogers E, Sullivan FJ, Glynn SA. Conference: Annual Scientific Meeting of the Irish-Society-of-Urology Location: Killarney, IRELAND Date: SEP 25-26, 2014 Sponsor(s): Irish Soc Urol. BJU INTERNATIONAL Volume: 114 Special Issue: SI Supplement: 2 Pages: 18-19 Published: SEP 2014
2. Title: Prostate Cancer Mediated Differentiation of Bone-Marrow Derived Mesenchymal Stem Cells Facilitates Prostate Cancer Cell Invasive and Migratory Capacity. Author(s): SM Ridge, AE Ryan, S Finn, J O'Leary, FJ Giles, FJ Sullivan, SA Glynn. Source: BJU INTERNATIONAL Volume: 113 Pages 28-28. Published JUNE 2014.